Cryptosporidium and Particle Removal from Low Turbidity Water by Engineered Ceramic Media Filtration

by

David James Scott

A thesis

presented to the University of Waterloo

in fulfillment of the

thesis requirement for the degree of

Master of Applied Science

in

Civil Engineering

Waterloo, Ontario, Canada, 2008

AUTHOR'S DECLARATION

I hereby declare that I am the sole author of this thesis. This is a true copy of the thesis, including any required final revisions, as accepted by my examiners.

I understand that my thesis may be made electronically available to the public.

_____

David James Scott

Abstract

A series of pilot-scale granular media filtration experiments was conducted to examine the effect of media roughness on filter performance and to evaluate the applicability of spherical, rough engineered ceramic filter media for use in granular media filters used for drinking water treatment. Filter media performance was assessed using turbidity and particle count reductions, *Cryptosporidium* oocyst and oocyst-sized microsphere removal, head loss and stability of operation. Experiments were designed to allow related facets of current filtration research to be examined. These included: effect of loading rate, coagulant type and dosage, and suitability of latex microspheres as surrogates for *Cryptosporidium* oocyst removal by granular media filtration.

This study indicated that increased filter media roughness consistently improved turbidity and particle count reduction under the conditions investigated. As well, the engineered media also consistently achieved greater stability of operation during non-ideal operational periods (*e.g.* sudden change in filter influent turbidity).Oocyst removals were generally improved by media roughness, though this improvement was reliant on operating conditions, such as coagulant dose and type of coagulant used. The surrogate relationship between oocyst-sized latex microspheres and oocyst removal by filtration was also dependent on coagulant dose and type of coagulant. During trials with no coagulant addition, contrasts in oocyst removal were not significant, suggesting that neither surface roughness nor the size of media used were significant factors impacting oocyst removal by filtration during those periods of impaired operation. When pre-treating raw water with PACl, the engineered ceramic media achieved up to 1.25 $\log_{10}$ higher oocyst removals than conventional media. This improvement in oocyst removal relative to conventional media was not observed when alum was used as the primary coagulant, however. Future studies should directly compare engineered and conventional media filtration performance, using other raw water sources and different operating conditions. Biologically active filtration should also be included in future performance studies because the rough, highly porous surface of the engineered ceramic media is likely to provide excellent biofilm support.

Acknowledgements

As with all research, this was a collaborative effort which relied on a many people. I ran into a few obstacles now and then, and I am deeply grateful for the help from my colleagues and the pleasure of working with a very talented group. This project could not have been completed without the following people:

- First and foremost I thank my supervisors Dr. Monica B. Emelko and James Bolton for the opportunity to work on such a promising project. Your expertise, enthusiasm, patience and guidance were greatly appreciated.

- Lab Technicians Jenn Coxe, Garett Fierling, Makoto Kawano – Together we spent countless hours counting 4.7 micron dots and fluorescent *C. parvum* in the darkened micro lab. By my calculations, we collectively endured more than 700,000 clicks of those counters. Thank you for your good company and diligent work.

- The Staff at the Horgan Water Treatment Plant – Thank you for your hospitality and the use of your plant facilities.

- Fellow grad students Adam Arnold, Phil Schmidt, Katie Higgins and Ryan Snider: for your advice, help, wonderful banter, support and camaraderie, I thank you. Adam, I'm not sorry that the floc samples you processed for me were not helpful – I was glad to drag you out there. Katie, I'd like to say that I'm sorry for sabotaging your computer numerous times. And Phil, I couldn't have had friendlier stats help. Many thanks to all of you.

Dedication

To my parents.

Table of Contents

List of Figures

List of Tables

1. Introduction

The primary goal of drinking water treatment is to protect public health by removal or disinfection of chemical and biological contamination in drinking water supplies. The evolution of improved detection capabilities has resulted in the recognition of many emerging waterborne pathogens. Moreover, the implementation of increasingly stringent regulations requiring treatment of known waterborne pathogens continues. The waterborne pathogen *C. parvum*, which is ubiquitous in aquatic environments and present in the environmentally resilient oocyst form, poses particularly significant challenges to the protection of drinking water supplies because it is resistant to conventional chemical disinfection processes (Sunnotel et al., 2006).

Despite technological advances in water disinfection such as the demonstrated efficacy of UV irradiation for the disinfection of *C. parvum* oocysts, disease outbreaks due to waterborne pathogens remain a significant public health concern (Aboytes et al., 2004). As well, it is commonly recognized that to achieve proper performance, most disinfection technologies and alternative treatment technologies such as pressure-driven membranes require effective solids removal prior to their use. Accordingly, the costs and limitations associated with disinfection of pathogens such as *C. parvum* oocysts underscore the importance of multiple barrier strategies for their removal and/or disinfection from drinking water. Granular media filtration (GMF) is a conventional treatment process that has been demonstrated as an effective barrier against the passage of pathogens into drinking water. *C. parvum* oocyst reductions by GMF have been reported in ranges from 2 to over 5 $\log_{10}$ (Nieminski and Ongerth, 1995; Bustamente et al.; 2001, Harrington et al., 2003; Emelko et al., 2005).

The efficacy of GMF as a barrier to *C. parvum* oocyst passage into treated drinking water is greatly impacted by design and operational factors such as quality of pre-treatment (coagulation), point within the filter cycle, hydraulic loading rate, media type, and raw water quality (Bustamente, 2001; Huck et al., 2001; Emelko et al., 2003; Emelko, 2003; Harrington et al., 2003). Several studies to investigate the impacts of various aspects of filter operation (*i.e.* loading rate, backwash strategy, *etc.*) and design (*i.e.* media type, size, uniformity coefficients, depths, *etc.*) on the removal of *C. parvum* oocysts have been conducted. Most of these reported investigations have focused on the use of conventional media (sand, anthracite, or GAC) in a variety of configurations. Particle and *C. parvum* oocyst removals by other potential filtration media (*i.e.* pumice, crushed apricot stones, recycled glass, *etc.*) have also been investigated (Swertfeger et al., 1999; Farizoglu et al., 2003; Aksogan et al., 2003); however, most of the reported investigations are presented in case study

formats with limited performance comparison to conventional media and even less discussion and investigation of mechanisms contributing to that observed performance.

Whether considering inorganic colloids or biocolloids such as *C. parvum* oocysts, the development of filtration theory to describe colloid deposition within water-saturated porous media such as granular media filters has progressed considerably during the last several decades (Elimelech et al., 1994; Tufenkji and Elimelech 2004A; Bradford and Toride, 2007; Johnson et al., 2007A). Traditional colloid filtration theory (CFT) describes colloid deposition within ideal systems (composed of spherical collectors with smooth surfaces [*e.g.* glass beads]) well (Yao et al., 1971; Tufenkji et al., 2004). CFT does not account for non-idealities (grain shape [sphericity], surface roughness, *etc.*) inherent to natural porous media, however. Recent advances in colloid research applied to natural groundwater aquifer environments have demonstrated that non-spherical, rough media may offer increased colloid deposition capabilities (Saiers and Ryan, 2005; Bhattacharjee et al., 1998; Considine and Drummond, 2001B; Duval et al., 2004). CFT model development has also begun to address these parameters (Eichenlaub et al., 2004; Hoek and Agarwal, 2006). If media grain shape and roughness contribute to colloid deposition in natural environments, it is reasonable to hypothesize that these media characteristics may also play a role in colloid and specifically pathogen deposition (and removal) by granular media filtration (GMF) during drinking water treatment. The majority of media commonly used during GMF (*i.e.* anthracite, sand, GAC, garnet, ilmenite, *etc.*) are non-ideal with varying degrees of sphericity and roughness.

In recent years, engineered ceramic media have been developed for drinking water filtration applications. Unlike conventional filtration media, engineered filtration media can be manufactured with controllable and highly uniform properties such as: shape, size, sphericity, density, and composition. These qualities contribute to uniformity in filter bed porosity, bulk density, and macroscopic behaviour. Engineered media are typically designed to maximize available surface area within a granular filtration process. It has been suggested that the surfaces of engineered ceramic media are designed to have a porous texture and composition to promote colloidal attachment and that the sphericity and uniformity coefficient enhance contact opportunities between the filtration medium and colloids targeted for removal (*e.g.* pathogens). Anecdotal evidence from several pilot-scale studies indicates that the particle and pathogen removal performance of engineered ceramic filtration media are less dependent on chemical pre-treatment than conventional filtration media; a few of those studies have evaluated the effects of filter media porosity, sphericity, surface charge and composition on filtration performance (Media Process and Technology Inc., 1995, 1996). Since such properties are

controllable with manufactured media, their use represents an opportunity to further optimize and understand the filtration process.

1.1. Research Objectives

The overall goal of this research was to conduct a preliminary evaluation of the impacts of media surface characteristics on particle and *C. parvum* oocyst removal by GMF used in conventional drinking water treatment contexts to determine if 1) performance benefits could be associated with non-ideal (spherical, rough) media surfaces and 2) mechanistic models could be further developed or additional mechanistic investigations are justified. The following objectives were developed to address this goal:

- To conduct a preliminary investigation of the performance of various types of spherical, rough engineered ceramic media in a drinking water filtration context,
- To directly compare the performance of spherical, rough engineered ceramic media with conventional media at several operating conditions relevant to conventional drinking water filtration, and
- To evaluate the removal of potential surrogates (oocyst-sized polystyrene microspheres) for the removal of *C. parvum* oocysts by engineered ceramic media filtration.

1.2. Research Approach

The approach used for meeting the objectives specified above was based on conducting a direct comparison of pilot-scale conventional and spherical, rough engineered ceramic media filtration performance and quantitatively assessing that performance at various conditions relevant to typical drinking water filtration operations. Filtration performance was assessed by evaluating the following factors:

- conventional particle (turbidity, total particle counts) removal performance,
- *C. parvum* oocyst and potential surrogate (oocyst-sized latex microsphere) removal performance,
- conventional operational (filter run time and headloss build-up) performance, and

- stability of the above-mentioned performance factors at non-ideal operating conditions (*e.g.* sub-optimal coagulation, rapid change in filter influent turbidity, hydraulic surge, *etc.*).

Typical operational conditions that are relevant to higher rate conventional drinking water filtration were utilized during this study. They included:

- hydraulic loading rate (9.8 m/hr and 24.4 m/hr rates),
- coagulant type (alum and polyaluminum chloride),
- coagulant dosage (no coagulant, sub-optimal and optimal dosages),
- and raw water temperature (temperatures of approximately 5˚C and 20˚C).

Pilot-scale investigations were conducted to address each of the three research objectives specified above. These investigations were conducted in three phases, described as:

Phase 1: Preliminary, proof-of-concept investigations focused on engineered ceramic media screening and optimizing operation of pilot-scale filtration unit. These experiments were conducted using synthetic raw water.

Phase 2: Pilot-scale in-line filtration investigations focused on comparing conventional anthracite-sand and spherical, rough engineered ceramic media configurations optimized for the specific media (different media sizes and depths). The experiments were conducted using Lake Ontario raw water without chemical coagulant addition.

Phase 3: Pilot-scale in-line filtration investigations focused on directly comparing filtration performance achieved using conventional anthracite-sand and spherical, rough engineered ceramic media configurations (identical media sizes and depths). The experiments were conducted using Lake Ontario raw water at various temperatures and with varying levels and types of chemical coagulant addition.

1.3. Thesis organization

Chapter Two contains background information regarding the significance of the research and the theoretical concepts employed therein. Filtration processes and theory are briefly reviewed, with a focus on media characterization and media impacts on particle removal by filtration. A brief

discussion of the life cycle and occurrence of *Cryptosporidium* in water supplies and the challenges it poses to granular media filtration follows.

Chapter Three outlines the rationale behind the general research approach and design of experiments. The methods and materials used in this research are also presented.

Chapter Four contains the experimental results and Chapter Five is comprised of the conclusions and implications derived from this work. Recommendations for further work are also presented.

2. Background

Microorganisms are ubiquitous in the natural environment. It has been estimated that the contamination of drinking water with waterborne microbial contaminants such as *Cryptosporidium* oocysts and *E. coli* bacteria ultimately results in approximately 5 million deaths worldwide per year (Rochelle and Clancy, 2006). To combat waterborne diseases such as cholera, typhoid and cryptosporidiosis, a multi-barrier approach to water treatment is universally recommended as the preferred method for the removal and disinfection of particles and pathogens from surface waters (CCME, 2004). Well-operated rapid granular media filtration remains a critical component of that multi-barrier approach.

2.1. A Brief History of Granular Media Filtration and Filter Media

Since John Snow traced a cholera outbreak in London to an infected water pump in 1854, the potential contamination of drinking water supplies with microbial pathogens has been recognized as a critical public health concern (Rochelle and Clancy, 2006). Before municipal-scale water filtration was feasible in cities, aqueducts were used to divert water from cleaner sources to urban environments. The scale and engineering required for aqueducts in Roman cities made this solution an expensive one and beyond the capabilities of most societies at the time. After the fall of the Roman Empire and up to the 1600's, investment in clean water was generally low in the western hemisphere (Symons, 2006).

As Enlightenment theories evolved in the 1700's, access to clean water began being viewed as a human right (Symons, 2006). In response to changes in perceptions about public access to water, the first large-scale filters were installed in Europe in the early 1800's. This early style of slow sand filtration was eventually implemented in North America. The first drinking water filtration plant in the United States was built in Poughkeepsie, NY in 1872 (Symons, 2006). The first North American rapid sand filtration facility went into service in 1881 in Somerville, NJ. Subsequent operational and treated water quality improvements enabled by the use of coagulation made rapid sand filtration common in municipal water treatment.

Around the end of the 19th century, loading rates of 5 m/hr (or ~2 gpm/ft^2) became the standard for rapid sand filtration plants. At that time, typical filter beds consisted of 60-75 cm of 0.5 mm diameter sand over a graded gravel bed (Logsdon, 2006). Compared to typical modern filter operations, shorter filter run times were common with this mono-media configuration, especially if

the sand had a high uniformity coefficient (*i.e.* heterogeneous grain size distribution). In these situations, the smallest sand particles would be flushed to the top of the bed during backwash, and the resulting layer of very fine sand would prevent the storage capacity of the lower, coarser portion of the bed from being used. The cake of particles that accumulated on the surface would clog the upper layer of the filter in a short amount of time, thus requiring frequent back washing. This problem was somewhat mitigated by the use of sands with uniformity coefficients below 1.5 (MWH, 2005).

The next important step in the use and evolution of GMF occurred just after WWII, when the use of dual-media filters became more widespread (Logsdon, 2006). Dual media filters commonly consist of 45 cm of 1.0 to 1.5 mm diameter anthracite over a 30 to 40 cm layer of 0.5mm diameter sand. During backwash the anthracite grains, which have a specific gravity of about 1.5, remain above the sand grains which have a specific gravity of about 2.5. With the coarser material at the top of the filter, finer particles pass deeper into the filter, reducing the build-up of a filter cake. Compared to mono-media filters, dual media filters allow particles to pass into the depths of filter media and utilize more of the solids loading capacity of the filter bed; accordingly, this type of filtration is often referred to as "depth filtration". Dual media filters can operate at higher loading rates (around 4 to 12 m/hr) than typical mono-media filters (60-80 cm deep sand filter beds), which cannot operate successfully at rates much higher than 5 m/hr (Logsdon et al., 2006). To date, dual media filtration is the most common type of GMF used for the purposes of potable water production; accordingly, the dual-media configuration is commonly referred to as "conventional" filtration and both sand and anthracite are considered "conventional media".

To increase the removal of smaller particles from water by rapid GMF, tri-media filters, which incorporate a layer of finer media under the sand layer, were developed. The lower layer typically has a grain size between 0.3 and 0.6 mm, and has a specific gravity of 4 or slightly higher. Garnet or ilmenite is commonly used for the lower level due to their high specific gravity, durability and low cost. Comparisons of dual- and tri-media filters have shown that tri-media filters do not provide substantially greater pathogen removal over dual- or mono-media filters (Emelko, 2003; Harrington et al., 2003). Tri-media filter configurations are not as widespread as dual media filters, mainly because of increased head loss associated with the use of the finer media.

Since the development of the dual-media filter, many alternative filtration media have been evaluated. Although charcoal may have been in use in small water filters as early as 2000 BC, carbon was not put into use in large scale water filtration until the 1970's, when large quantities of activated carbon could be manufactured in granular form (Symons, 2006). Granular activated carbon (GAC) is

often used in place of anthracite due to its adsorptive capacity that removes many organic compounds from the water; that capacity is limited however, and the GAC must be regenerated periodically. GAC grains are much softer than anthracite, so loss of media due to attrition during backwash reduces the longevity of the media (Humby, 1996).

A summary of recently studied alternative filtration media is presented in Table 2-1. Though many of these materials showed promise for use in granular media filters, the bulk of the published research was not conducted in a manner that allowed the alternative materials to be directly compared to conventional filtration media. Direct comparisons of traditional filter performance parameters (*e.g.* turbidity and particle count reductions and filter run time) between different media are only possible when the filters treat the same water source and the filter media have the same effective size, uniformity coefficient and configuration (depths, relative stratification, *etc.*). Without such direct comparisons, it cannot be known if other filtration media perform better than, comparable to, or worse than conventional media because of the nature of the individual media grains themselves as opposed to other factors that impact filtration and describe the distribution of media in the filter (*e.g.* effective size (ES), uniformity coefficient (UC), depth, *etc.*). Unfortunately, many reported investigations of alternative filtration media performance have not included direct comparisons to conventional media filtration performance (*i.e.* Farizoglu et al., 2003; Melin et al., 2000; USEPA, 2001A, 2001B), though it must be noted that direct performance comparisons of conventional media with alternative media may not always be possible. Media with grain structures radically different from those of conventional media, cannot be made to have the same grain size (*i.e.* fibre filters). In such cases, it would be difficult to determine which differences in media characteristics (*i.e.* grain shape, surface chemistry, surface roughness, porosity, *etc.*) were responsible for contrasts in filter performance.

Table 2-1. Granular Filter Media Alternatives to Anthracite and Sand

Reference	Media	Key Findings Relative to Conventional Media/ Notes
Aksogan et al., 2003	Crushed apricot stones (CAS)	Good, comparable turbidity reduction by both anthracite and CAS. Different media grain sizes (anthracite was 0.85 mm, CAS was either 0.70 mm or 1.80 mm).
Biswas et al., 2003	Polyurethane foam filter (PFF)	Good reduction in turbidity due to higher surface area than conventional media. PFF filter media created lower head loss because granules had 95% porosity and larger granules than conventional media.
Caliskaner and Tchobanoglous, 2005	Compressible fibre balls	Fibre balls had high porosity and different sized granules relative to conventional media. Compressible filter allows medium properties to be adjusted to respond to variations in influent quality.
Chen et al., 1998; Lukasik et al., 1999	Sand with aluminum and iron hydroxide coatings	Turbidity reduction was comparable by coated and plain sand, but bacteria removal by coated sand was better by up to 4 $\log_{10} L/d$. Coating lasted 4 months or less depending on operational conditions.
CWC, 1998	Crushed glass	Glass media was effective for turbidity reduction, but the study compared 0.5mm glass to >0.6mm sand, so results do not indicate which material had better filter performance.
Eikebrokk and Saltnes, 2002	Crushed ceramic media	Ceramic grains were twice as large as anthracite grains, so observed poorer turbidity reduction by ceramic media was expected.
Farizoglu et al., 2003	Pumice	Pumice filtered well compared to sand media, but sand grain size was only reported as “0.5 to 1.0 mm“ while pumice was 0.59mm with a UC of 1.35
Fletcher et al., 1994	Fibre filter with applied electric field	Very low pressure drop due to 96% porosity and good particle reduction, but the filter tested was small (0.9 cm deep. 2cm dia.)
Gimbel and Nahrstedt, 1997	Plastic foam granules	Granules had higher porosity, and surface area than conventional media and achieved better particle reduction than conventional filter media.
Melin et al., 2000	pelletized ceramic media, marble and plastic cylinders	Media studied were used in upflow clarifiers, with only pelletized ceramic media being used in dual-media filter over sand. Experiments obtained acceptable particle reduction but no comparison was done with conventional media
USEPA, 2001A, 2001B	Spherical ceramic media	Ceramic media were investigated as part of a transportable, self-contained coagulation and pressure filtration system. *C. parvum* removals achieved by the system were between 2.6 to 3.6 $\log_{10}$. No other media were investigated during the studies.
Valdes and Liang, 2006	Compressible rubber granules	Proposed using rubber granulated media and compressing the filters when better filtration is required. Some good turbidity reduction results but no comparison to conventional media was conducted.

Anthropogenic materials that have been investigated for suitability as drinking water filtration media have included: polyurethane foam, rubber granules and ceramics. Early work on filtration with foam granules was promising due to the granules' high surface area (Gimbel and Nahrstedt, 1997), but this material has received little attention since then. Compressible foams (Biswas et al., 2003) and rubber media (Valdes and Liang, 2006) provide a variation on GMF. By compressing the filter bed, the pore sizes in the filter could be reduced to increase the retention of particles. The equipment required to compress the media adds complexity and cost to water treatment process. In addition, there may be concerns regarding the potential of the rubber to leach chemicals into the water. The use of rubber filter material is not recommended for the filtration of acidic waters because the rate of zinc leaching is accelerated (Valdes and Liang, 2006).

"Greensand" is made by coating natural sand in metal oxides. Greensand was developed in an effort to reduce iron and hydrogen sulphide concentrations in certain water sources. It can also be helpful for the removal of bacteria. Chen et al. (1998) suggested that improved bacterial removals by greensand (up to 4 $\log_{10}$ better than untreated sand) were due to increased electrostatic interactions. Under the conditions of that study, the metal hydroxide coating on these media wore off in approximately 4 months, or 3 months if biofilms were allowed to grow on the media (Chen et al., 1998). Other coatings including manganese, aluminum and ferric hydroxide coatings have also been investigated for use in granular media filters (Chen et al., 1998; Lukasik et al., 1998).

Ceramic engineered media have been installed in full scale municipal water works since the mid-1990's. There are two main types of commercially available ceramic media. In both cases the filter media are an inert, durable, kiln-fired ceramic material that has a high surface area per volume of material. Differences in the media arise from the manufacturing process. Some engineered ceramic media are manufactured by crushing pre-fired ceramic pellets, tumbling and finally sieving (Maxit Group, 2008); others are manufactured by prilling the clay material first, kiln firing the small spheres, followed by sieving (Kinetico, 2008). Because the ceramics are engineered materials, the size, density, roughness, and surface chemistry of the ceramics can be altered to optimize their performance for specific applications. In theory, the ability to adjust media properties may enable the development of better performing media; for example, adjustable media density may shorten backwash length or allow more effective backwashing because lighter media require less energy for fluidization during backwashing.

The high surface roughness of ceramic media enhances biofilm growth (Bolton et al., 2006); the additional surface area associated with that roughness may also be beneficial for particle capture (Kau

and Lawler, 1995). Although two "Environmental Technology Verification Reports" on the use of prilled, engineered ceramic media for drinking water treatment (USEPA, 2001A, 2001B) were published, neither study compared the filtration performance of the ceramic media to conventional media. The potential to use ceramic media for enhanced biofilm growth during biologically active filtration (BAF) in conjunction with ozonation has also not been explored relative to conventional anthracite and GAC BAF.

Some of the media listed in Table 2-1 have been investigated as alternatives to conventional filter media in response to local shortages of conventional media; crushed apricot stones, pumice, boiler clinker, crushed coconut shells, crushed glass from industrial off-cuts, pea gravel, and berry seeds are among those alternatives (CWC, 1998; Aksogan et al., 2003; Farizoglu et al., 2003). Promising filtration results were obtained from investigations of pumice media (Farizoglu et al., 2003), which reduced turbidity better than sand (turbidity removal was 98-99% as opposed to sand's 85-90%, with pumice also achieving longer filter run times than sand). Detailed descriptions of the pumice and sand media characteristics were not provided, however, so it is unknown if the better filtration performance observed with pumice was due to grain angularity or surface roughness or another media characteristic. It should be noted that while the ES and UC of the pumice were reported (0.59 mm and 1.35, respectively), the sand was only described as having a "grain size of 0.5 – 1.0mm". It is unclear whether the two materials were compared such that differences in filtration performance could be attributed to media properties and not media configuration, size and/or size distribution. Omissions of these types of key pieces of information are unfortunately common in the literature describing alternatives to conventional filter media.

2.2. Filtration Research

2.2.1 Filtration Processes

Filtration describes the removal of particles from a suspension and is generally considered to be a combination of 3 different particle capture processes: cake filtration, straining filtration and physicochemical attachment (Figure 2-1; McDowell-Boyer et al., 1986). Cake filtration (Figure 2-1A), sometimes referred to as size exclusion, is the most intuitively obvious example of filtration, during which particles larger the pores of a filter are excluded from passing through the filter. When considering spherical colloids and collectors, if the ratio of colloid/collector diameter is more than 0.154, the colloids will not be able to pass through the filter (Herzig et al., 1970); instead, the particle

will be captured at the top of the filter bed. During filtration, these large particles accumulate on the surface of the filter bed and form a cake which increases head loss dramatically.

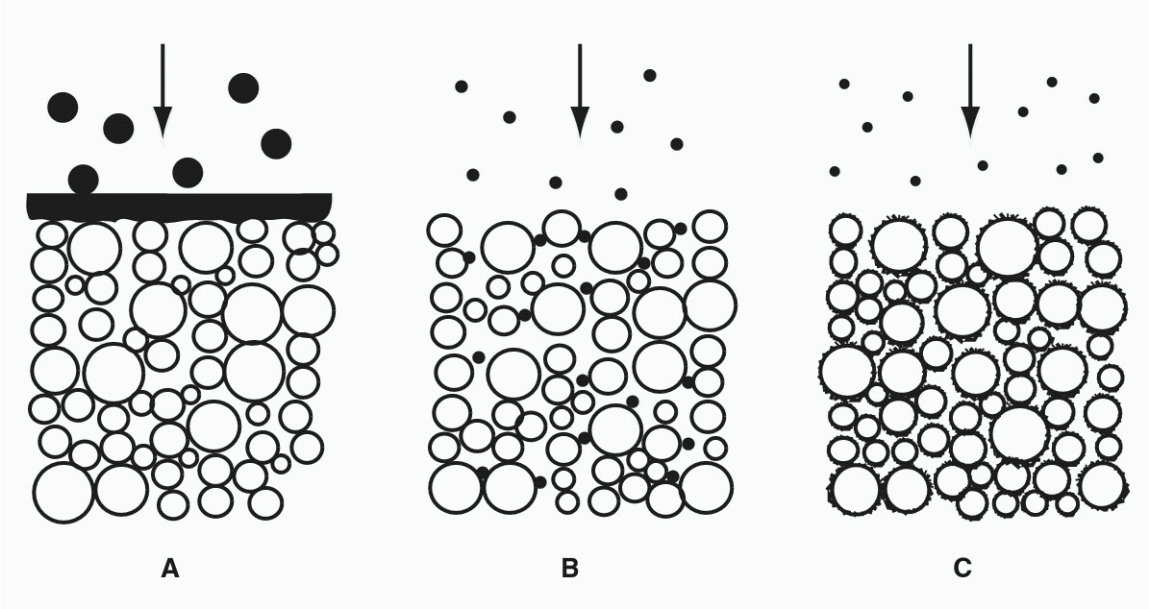

Figure 2-1. Filtration Mechanisms (Source: McDowell-Boyer et al., 1986)

The second filtration mechanism (Figure 2-1B) is often referred to as "straining filtration" (Lau et al., 2005). Straining filtration is defined as the retention of colloids in the smallest regions of pore spaces formed adjacent to grain-grain contact points (Bradford et al., 2007). Pore spaces directly adjacent to grain contacts provide optimal locations for colloids that are weakly attracted to the collector surfaces due to reduced hydrodynamic forces, pore size limitations and enhanced DLVO interactions. Straining filtration is sometimes used to explain why filters often remove some colloids even if CFT (colloid filtration theory) predicts that none should be captured. Under such conditions, it is thought that these low levels of particle removal are due solely to straining. Recent research suggests that straining filtration becomes significant when colloid diameter/collector diameter ratios are above 0.005 (Bradford et al., 2005A). Depending on such factors as collector packing structure, grain angularity, loading rate and IS (ionic strength), the threshold for significant straining filtration may be at a colloid/collector diameter ratio of 0.020 (Johnson et al., 2007) or as low as 0.002 (Li et al., 2007).

The mechanism of wedging, as described by Johnson et al. (2007) is a significant factor in straining filtration. "Wedging" describes colloid deposition along the upstream region of grain-to-grain contacts where particles have been brought into contact with both collectors by hydrodynamic

forces. Deposition occurs preferentially in these regions due to the lower fluid velocity and the fact that area of colloid/collector contact is doubled (Johnson et al., 2007).

The third type of filtration is commonly known as physicochemical attachment (Figure 2-1C); it is also sometimes referred to as adsorptive filtration. During conventional treatment, the addition of coagulant destabilizes suspended particles in the water. The destabilized particles that remain suspended in the water after clarification (*i.e.* sedimentation in most conventional water treatment plants) attach onto the surfaces of collectors as they flow through the filter media. The mechanism of physicochemical attachment dominates in rapid GMF facilities in which the majority of suspended particles reaching filters are much smaller than the filter media.

Generally speaking, colloids and natural organic matter (NOM) in untreated water have negative surface charges. Since like charges repel, these substances remain dispersed in the water and do not readily attach to other negatively charged particles or surfaces. During filter operation, filter media may accumulate a layer of NOM and acquire a negative surface charge as well. The negative charges on colloid surfaces inhibit sedimentation, flocculation and effective filtration. Accordingly, to be effective, rapid GMF must be preceded by effective coagulation. Coagulants, such as alum, ferric chloride, polyaluminum chloride, any of a number of commercially available polymers, *etc.* generally destabilize particles by the following mechanisms (MWH, 2005):

1. Compression of the electrical double layer,
2. Adsorption and charge neutralization,
3. Adsorption and inter-particle bridging, and
4. Enmeshment in a precipitate or “sweep floc”.

If filtration plant design incorporates sedimentation or some other clarification process prior to filtration, much of the solid material aggregated as floc will be removed before it reaches the filters. In situation without distinct clarification processes, the formation of smaller floc designed to penetrate the depth of filters will be targeted; this type of floc is not as likely to form a cake on the top of the filter media.

Filters generally progress through four operational stages illustrated in Figure 2-2:

1. ***Filter ripening*** - Ripening is a period of rapid improvement of filter effluent water quality that begins with newly "cleaned" (backwashed) filter beds and usually lasts less than 20 minutes, depending on how the endpoint of this period is defined. While they may overlap one another (and possibly be non-discernable from each other), it is generally accepted that there are two spikes in filter effluent turbidity associated with this phase of filter operation. The first spike in filter effluent turbidity is associated with backwash remnants and the second spike is associated with the clean filter media beginning to accumulate solids that then themselves act as additional collectors. As a result, filter effluent turbidity and particle counts are briefly elevated after which they rapidly decreased/improve. To prevent the use of filter effluent during ripening, many filters operate under "filter-to-waste" until filter effluent meets water quality requirements.
2. ***Stable filter operation*** – Granular media filters are generally operated from 6 hours to 4 days, depending on loading rate and raw water quality. This is the longest stage of the filtration process, during which time the filters accumulate solids and head loss increases as the solids loading capacity is diminished and pores within the filter become clogged. Turbidity and particle reductions are highest (and filter effluent turbidity and particle counts are lowest) during this period.
3. ***Breakthrough or excessive head loss*** –At the end of a filter cycle, filters either begin passing material into the effluent, resulting in increased filter effluent turbidity and particle counts, or the flow of water through the filters diminishes to the point where filter operation is no longer efficient. Either of these two events triggers the backwash stage. Figure 2-2 depicts breakthrough occurring at the end of the filter run, indicated by increasing effluent turbidity.
4. ***Backwash*** – Filtration is stopped to flush out the accumulated solids from the previous filter cycle. This is accomplished by reversing water flow through the filter bed, typically using previously filtered/treated water.

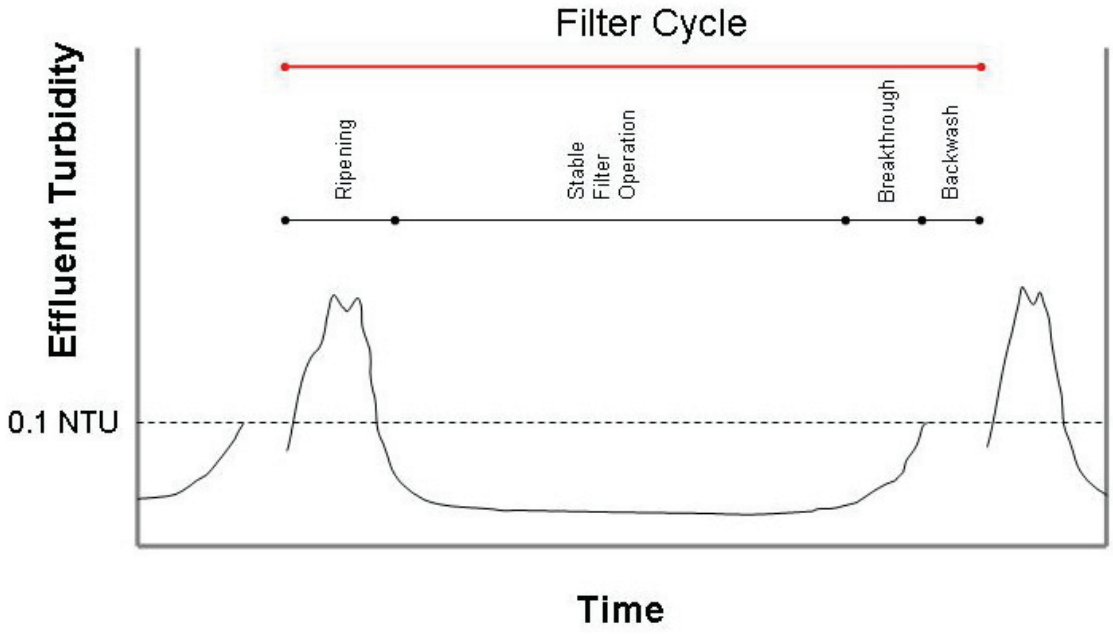

Figure 2-2. Conceptual Turbidity Profile During a Typical Filter Cycle

Filtration is often referred to as a polishing step and its goal is to remove as many colloids and remaining solids (and sometimes dissolved contaminants in the case of filtration with adsorptive media) as possible. The removal of suspended colloids reduces (1) the spread of waterborne disease such as typhoid, cholera and cryptosporidiosi*s*, (2) the post-filtration disinfection requirements of chlorination, ozonation or UV irradiation processes, (3) the disinfection by-product (DBP) formation potential of DBP's such as trihalomethanes, and (4) undesirable aesthetic characteristics such as cloudiness and colour.

2.2.2 Filtration Modelling

Filtration processes have generally been studied using two distinct approaches: modelling in conjunction with micro-scale experiments conducted at idealized conditions, or larger scale experiments conducted at more complex or "real" conditions. Common modelling approaches aim to elucidate individual factors or mechanisms responsible for colloid transport, deposition and detachment. In contrast, field-scale approaches are often more empirical in nature and focus on demonstrating filter performance in various operational contexts and providing regulatory guidance. Although field-scale studies have been relied upon for demonstrating filter performance, these types

of studies infrequently involve direct comparison between various media grain properties rather than media configuration, depth, size and/or size distribution.

The modelling approach with micro-scale experiments is often preferred for studying filtration from a research perspective because it allows reproducibility, has fewer confounding factors and enables the isolation of individual mechanisms and phenomena. Moreover, the need to produce potable water does not preclude the completion of laboratory-scale experiments. The ultimate goal of such modelling investigation is to develop sufficiently comprehensive models that will describe the essential physicochemical mechanisms of filtration processes. Then, once such conceptual model(s) are established, mathematical models can be further developed to predict various aspects of filter performance (particle reduction, pathogen reduction, head loss, run time, *etc.*). By individually understanding all of the factors impacting filtration, it is expected that specific mechanisms could be exploited to increase process performance by both engineered and natural filtration processes.

According to classical colloid filtration theory (CFT, Derjaguin et al., 1941; Verwey et al., 1948; McDowell-Boyer et al., 1986; Hunt et al., 1993), particles are removed from suspension by a two-step process whereby particles or colloids are transported to the vicinity of the surface of filter grains ("collectors") and then undergo physio-chemical attachment. Much of the published CFT modelling is based on an irreversible first-order kinetic attachment of colloids to a porous substrate. It predicts that the concentration of colloids will decrease exponentially with depth into the porous substrate (Bradford et al., 2003). The probability of attachment of a colloid to a collector is mathematically described as the product of two terms: the single-collector contact efficiency (η_T, or η_0 in some publications) and the deposition efficiency (α). Contact efficiency, η_T, quantifies the frequency of colloid collisions with the surface of a collector while deposition efficiency, α describes the probability of a colloid attaching to a collector should it come into contact with the collector (Elimelech, 1994).

The contact efficiency term, η_T is determined by processes that transport colloids to the surface of the collector: interception, diffusion or sedimentation (Yao et al., 1971). A more detailed examination of the underlying mathematical principles of CFT is given in Tufenkji and Elimelech, 2004A. Sedimentation and interception are the dominant processes for larger particles (>1 μm), while diffusion is the main process by which small particles (<1 μm) are transported to grain surfaces. For particles near 1-2 μm in diameter there is a minimum contact efficiency, which explains why particles approximately in this size range are generally the most difficult for granular media filters to remove

(Figure 2-3, Tufenkji and Elimelech, 2004A). Accordingly, filter performance can depend substantially on the size of colloids in the water being filtered.

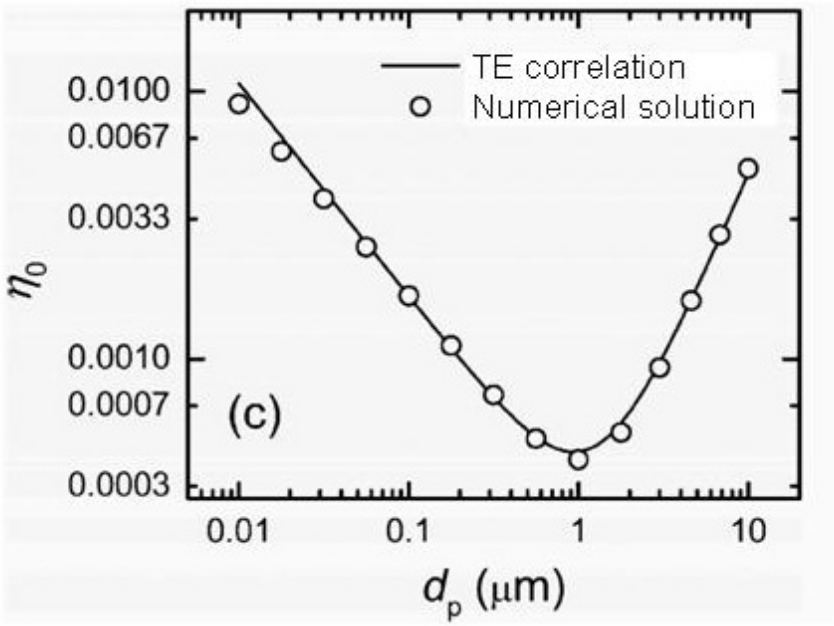

Figure 2-3. Comparison of predictions of single-collector contact efficiency (η_0) based on rigorous numerical solution of convective-diffusion equation (open circles) and the TE correlation (solid line), under conditions representing water treatment systems (Source: Tufenkji and Elimelech, 2004A)

The deposition efficiency term, α depends on the interaction energy between colloid and collector which is determined using DLVO (Derjaguin-Landau-Verwey-Overbeek) theory (Derjaguin and Landau, 1941; Verwey and Overbeek, 1948). DLVO theory combines the attractive Lifshitz-van der Waals (vdW) interaction and the electrostatic double layer interaction to determine whether colloid deposition is favourable. The surfaces of most colloids and grains in natural systems have a negative charge, resulting in a net repulsive force that is often stronger than the attractive vdW forces. The net negative surface charge arises predominantly from a coating of fulvic acids which cause an increase in the absolute surface potential (Wilkinson et al., 1997) The magnitude of the forces between colloids and collectors depends largely on the separation distance between a particular colloid and collector, so interaction energies between colloids and surfaces are generally depicted using interaction profiles that describe the interaction energy as a function of separation distance. The repulsive forces may be reduced or neutralized by an addition of coagulant, increase in ionic strength (IS) or reduction of pH.

Depending on the interaction profile, particles may be:

- repelled
- attracted into a primary minimum, or
- trapped in a secondary minimum

In some cases, there may be an energy barrier which must be overcome for a particle to attach to a collector, such as depicted in Figure 2-4a (Tufenkji and Elimelech, 2004B). Such an energy barrier may be due to steric repulsion or like surface charges. In the case depicted in Figure 2-4a, there is a secondary minimum in front of the barrier that can retain colloids at a distance from the surface of the collector. If the barrier to deposition is small enough, energy fluctuations may still allow the particle to cross the barrier and be retained in the primary energy minimum (Figure 2-4b). Under conditions favourable to attachment there are no barriers to attachment and it will occur if the particle comes close enough to the collector surface (Figure 2-4c).

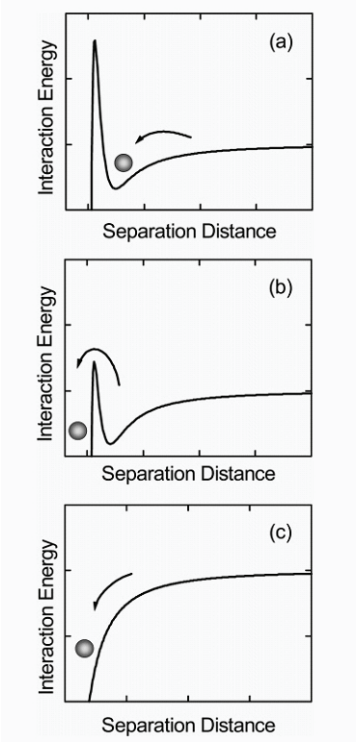

Figure 2-4. Colloid-Collector Interaction Scenarios (Source: Tufenkji and Elimelech, 2004B)

The first basic model of filtration in porous media was published by Yao et al. in 1971. The model adequately describes colloid deposition by clean filter beds at conditions favourable for deposition. The model is based on the accumulation of particles on a single collector that is assumed to be similar to all other collectors in the filter bed. This geometric simplicity is necessary due to the mathematical complexity of real systems. For example, the equation for the deposition efficiency (α) term in principle includes two empirical constants and functions for 11 different dimensionless parameters (Bai and Tien, 1999). As a result of this complexity, currently available computers are still not capable of processing the required computations for such complicated systems in a reasonable time frame. For example, Johnson et al., (2007) required 20 processors working simultaneously to compute particle trajectories in a simplified colloid deposition simulation that accounted for pore geometry under unfavourable attachment conditions.

Early approaches to filtration modelling almost exclusively determined interaction energies between microscopic particles by assuming perfectly smooth and geometrically regular surfaces (Bhattacharjee et al., 1998B). The inability to incorporate geometric and surface complexity affected the models' ability to describe non-idealized (*i.e.* real) filtration processes. Yao et al.'s (1971) model typically underestimates the number of collisions between particles and collectors, resulting in a corresponding underestimation of filter performance. Rajagopalan and Tien (1976) developed a fundamental depth filtration model using a "sphere-in-cell" model for granular media. Their model incorporated additional vdW forces as well as the effect of viscous resistance of the water that reduced particle-collector collisions at unfavourable conditions for colloid deposition. These improvements allowed the Rajagopalan and Tien (RT) model to better correspond with experimental data.

The drawback of the RT model is that it does not consider the influence of hydrodynamic interactions and vdW forces on deposition by diffusion (Tufenkji and Elimelech, 2005A). This leads to overestimation of the single-collector contact efficiency, η_T by as much as 60%. The RT model is not able to predict filter performance in full-scale filtration because it is based wholly on clean bed filtration, though in reality, collectors accumulate solids during filtration, changing pore geometry and collector surface properties. Such changes are too computationally complex to be modeled accurately by CFT models such as the RT model (MWH, 2005). The RT model also predicts a catastrophic decline in deposition rates with the onset of a repulsive force barrier, which is not typically experimentally observed (Bai and Tien, 1999). CFT modelling has continued to evolve nonetheless; at favourable attachment conditions, current CFT is in good agreement with particle attachment behaviour in situations that are similar to those of the model.

The most recent developments in CFT modelling are based on a modified version of the equation for single-collector contact efficiency referred to as the Tufenkji and Elimelech (TE) equation (Tufenkji and Elimelech, 2004A). The motivation for this advance was to include all physicochemical mechanisms governing particle deposition. Rajagopalan and Tien (2005) point out that the TE model still has severe shortcomings. The TE equation does not directly include the effects of electric double layer forces. Instead, the physics of colloid attachment are separated from the chemistry to avoid what Tufenkji and Elimelech (2005B) describe as a "breakdown of current theories to predict the actual deposition rate when considering electrostatic double-layer effects". Without this separation, "the theory predicts deposition rates that are several orders of magnitude smaller than the actual deposition rate" (Tufenkji and Elimelech 2005B).

It is well established that CFT in its current form does not accurately describe particle attachment at unfavourable conditions. Unfortunately, unfavourable deposition conditions are very common in aquifer research and during sub-optimal coagulation conditions in GMF. For CFT to better describe conditions in the natural environment and in water treatment systems, increased model complexity is required. Recent colloid deposition modelling investigations have included such factors as surface charge heterogeneity (Kemps and Bhattacharjee, 2005), pore geometry (Cushing and Lawler, 1998; Johnson et al., 2007), and surface roughness (Eichenlaub et al., 2004), to name a few. Straining, wedging and particle capture in secondary minima (Redman et al., 2004; Hahn et al., 2004; Xu et al., 2006) are also significant factors at unfavourable deposition conditions.

Modelling "bio-colloid" (virus, bacteria and protozoan) transport, deposition and re-entrainment presents additional modelling challenges because of the physical, chemical and biological heterogeneities inherent to these organisms. Albinger et al. (1994) found that monoclonal bacteria displayed significant differences in adhesion to collector surfaces, suggesting that despite efforts to use uniform bacteria, small differences in "bio-colloid affinity" may be just as important as size or intra-strain genetic variation. In response, Tufenkji (2007) proposed 3 modifications to CFT modelling:

1. A probability distribution function should be used to help describe microbial attachment. This would also be used in non-biological CFT models, where colloid population heterogeneity has been blamed for the breakdown of CFT (Tong and Johnson, 2007).

2. Straining should be incorporated as a removal mechanism. The process of straining is very different from physicochemical attachment and has been integrated into some models which have yielded better predictive capacity than those based exclusively on physicochemical attachment (Bradford et al., 2003). At conditions moderately favourable for colloid attachment, there may be some interaction between the two processes (Bergendahl and Grasso; 1998, Johnson et al. 2007)

3. Microbe motility needs to be accounted for within CFT models. While some bacteria can swim at great speeds, others can anchor themselves where tangential shear would normally preclude colloid attachment. Current models are overly simple and avoid much of the inherent complexity involved in microbial behaviour at non-steady-state conditions (Barton and Ford, 1997).

Regardless of the effective integration of these proposed additions to CFT modelling, the development of realistic, predictive filtration models will continue to prove challenging. Critical obstacles to predictive model development include the model dependency on quantities that and must be calculated indirectly because they cannot be measured directly in the laboratory or field (*e.g.* fraction of particles captured per unit particle path length) (Alvarez et al., 2007). This represents a significant obstacle for model verification. Another modelling challenge is that filtration itself is never a steady state process; for example, filtration models cannot account for increases colloid attachment during filter ripening (Tobiason and Vigneswaran, 1994), nor decreases in colloid attachment during particle breakthrough at the end of a filter cycle (Ko and Elimelech, 2000). Further examples of the breakdown of CFT at unfavourable conditions for deposition include:

- the spatial distribution of retained microorganisms is often inconsistent with modelled results (Elimelech et al., 2000),

- the theory generally underestimates real filtration efficiencies (Bai and Tien, 1999), and

- the theory best predicts clean bed deposition and is of little value for use in evaluating GMF performance after filter ripening (Hunt et al., 1993).

In light of the challenges presented to developing an accurate model of colloid deposition, it is understandable that comprehensive models for filtration are far from realized. Moreover, filtration performance depends on several often interrelated factors (many of which are difficult to measure or quantify). These include:

- ***Colloid/Floc Properties:*** shape, size, roughness, chemistry, strength, solubility, density, colloid population heterogeneity;

- ***Waterborne Microorganism Properties:*** species, metabolic rate, chemotaxis or motility, predation, decay, cell attachment/biofilm growth;

- ***Water Quality:*** pH, ionic strength, temperature, suspended solids, coagulant dose, humic substances, surfactants, biological oxygen demand, seasonal variations;

- ***Filter Media Characteristics:*** size, depth, configuration, uniformity coefficient, surface chemistry, density, porosity, grain shape, pore geometry; and

- ***Operational Parameters:*** loading rate, water pressure, water quality, backwash method, effectiveness of coagulation/flocculation/clarification, type and point of disinfection.

The task of developing realistic mathematical simulations of filter performance based on fundamental principles appears daunting. In response, empirical or phenomenological models of filter performance have been developed. Empirical models for filtration tend to be more relevant to drinking water treatment and may be used to predict filter performance by accounting for ripening and breakthrough and considering other processes such as particle re-entrainment (Tien, 1989). The drawback is that these models do not elucidate the mechanisms at work in colloid deposition and so provide little guidance to efforts for optimizing filter performance. They do not focus on the accumulation of individual particles on single collectors, but on the bulk increase of solids in a filter. The use of such empirical models requires three simplifying assumptions (MWH, 2005):

1. The accumulation of particles in the interstitial fluid is negligible compared to the mass of particles on media surfaces,

2. The number of particles entering or exiting the filter is negligible compared to the flux of water, and

3. The generation or loss of particles through reaction (*i.e.* production of biomass or consumption of particles via chemical or biological activity) can be ignored.

The resulting “models for deep bed filtration are based on two variables: filtration function (particles collected per length of path of particle) and formation damage (reduction in permeability). These quantities cannot be measured in the field or in the lab, so they have to be calculated indirectly"

(Alvarez et al., 2007). The general philosophy for empirical models has been to develop formulas that agree with the actual performance of the filtration system in question and leave concerns about individual mechanisms to researchers with access to supercomputers. The advantages of the empirical modelling approach are: a) the model can often predict filter performance from ripening through to breakthrough, and b) models can be adjusted to compensate for changes in water quality relatively easily.

There are a number of significant disadvantages to empirical modelling. These include:

- Each model is only applicable to the filter for which it was developed, and more specifically, under the conditions the model was created.

- The models are only as reliable as the data on which they are based. If experimental conditions (*i.e.* water quality, water source, treatment process, coagulant type) are not representative of typical operational conditions, the models may be of little use.

- Some models still require advanced mathematical solutions (simultaneous solution of 3 different equations in some cases, MWH, 2005). There are commonly-used assumptions to simplify the equations, but the utility of complex equations is questionable for actual filter operation.

2.2.3 Pilot and Full-Scale Filtration Experiments

Filtration studies have added greatly to understanding the filtration process, but not to the point where it is possible to design filter processes from fundamental principles. The actual design and operation of filters has remained largely empirical because once particles accumulate within pore spaces, there is limited fundamental understanding or predictive capacity of filter performance (Hunt et al., 1993). Accordingly, only experimentation at realistic conditions can produce results that are relevant to full scale operations. The general process by which full scale filtration facilities are typically designed is as follows:

- Characterize water and set performance criteria (*i.e.* effluent turbidity, available space, total plant capacity, source water, budget for infrastructure, *etc.*),

- Select process design (*i.e.* membrane or GMF, level of pre-treatment, backwash method), often based on budget and experiences at nearby filtration plants treating similar water ,

- Conduct pilot studies to evaluate basic design parameters: type of coagulant, flocculation/clarification conditions, media depth, filtration rate, *etc.*,

- Analyze differences in filter performance (effluent quality, head loss) as a response to the previous adjustments in order to optimize filtration (*i.e.* backwash protocol, media depth, coagulant type/dose, pH control),

- Re-pilot and further refine filter performance,

- Construct water treatment plant, and

- Continue adjusting WTP processes where possible to ensure optimal filter performance.

With regard to the scientific literature, there are numerous studies that have focused on various aspects of filtration to assist in filter design and operation. Some investigations have examined isolated aspects of filtration, while others have focused on performance improvements based on changes in filter options (media type, size, depth, configuration, *etc.*). Examples of the empirical approach to filtration research include:

- Amburgey and Amirtharajah (2005A) presented a modified backwash strategy (extended terminal subfluidization wash [ETSW]) that can (in some circumstances) shorten filter ripening and improve filter performance at the beginning of a filter cycle,

- Lang et al. (1993) established a minimum column to media diameter ratio for reliable pilot study design, and

- Tchio et al. (2005) completed a factorial design, 7-variable study into filter process and configuration design which isolated four main factors that control the design of filters (media size, media depth, flow rate and available head).

These are only a few examples of the commonly reported types of empirical approaches to optimizing filtration performance.

2.3. Effect of Media Properties on Colloid Removal

The impact of various media properties on filtration performance has been investigated with three general approaches:

1. experimenting with full scale or pilot scale filter operations,

2. experimenting with micro columns and particle to particle interactions, and

3. mathematical modelling of processes within filtration.

Generally a combination of all three approaches is required to understand filtration mechanisms. The more academic literature focus on the general topic of colloid transport and deposition as it is the fundamental underpinning of a number of areas of study (groundwater research, riverbank filtration, groundwater remediation, drinking water and wastewater treatment and a number of industrial and engineered systems). For this reason, a large portion of the research applies to the mechanisms in filtration, but often not at conditions relevant to water treatment plants. Many such investigations have indicated that specific media properties (size, uniformity coefficient, surface area, sphericity or angularity, shape, density and roughness) affect filter performance; however, the extent of their significance to GMF at a variety of operational conditions relevant to drinking water treatment remains poorly understood.

2.3.1 Size

Size is the most obvious media property that affects filter performance. Smaller diameter media give filters smaller pores and more surface area (Lang et al., 1993; Hunt et al., 2003). This results in more straining (Xu et al., 2006; Tufenkji et al., 2004A,) and more surface area for colloid adsorption (Kau and Lawler, 1995; Lawler and Nason, 2006). Under unfavourable deposition conditions, straining can be an important factor for colloids with diameters >0.005 times the media diameter (Bradford et al., 2005). For example, in 0.5 mm sand media, straining should therefore be significant for colloids larger than 2.5 μm. The drawbacks to using smaller media are increased head loss and shorter filter run time.

Montgomery (1985) proposed a filter design principle based on the ratio of filter media depth to grain size (*L/d*), and suggested that this ratio should be over 1000. This recommendation was arrived at empirically; almost all successfully operated filters at the time had *L/d* ratios above 850, and many of them were greater than 1000. This ratio does not take into account the effects of filtration velocity, bed porosity or characteristics of the influent water (Lawler and Nason, 2006); they proposed a formula that included some of these parameters, but was also based heavily on grain size and media depth.

Tchio et al., (2003) conducted a factorial design study that evaluated the effects of ES (0.4 *vs.* 1.0 mm media), bed depth (50 *vs.* 300 cm), filtration rate (5 *vs.* 30 m/hr), UC (1.3 *vs.* 1.5), media (sand *vs.* anthracite), raw water turbidity (1 *vs.* 5 NTU) and water head (50 *vs.* 300 cm). Under the conditions of that investigation, ES had the largest effect on turbidity reduction, and the second largest effect after media depth on particle reduction.

Stevenson (1997) conducted a modelling investigation that suggested that when interception is considered as the mechanism that brings particles to the vicinity of collector surfaces, the filtration coefficient varied with the inverse cube of the grain size. Similarly, modelling of the capture mechanisms of settlement and diffusion suggested that the filtration coefficient approximately also varied with the inverse of grain size. Because of the effect of grain size on filtration, Montgomery (1985) suggested that a filter bed depth of 40 cm consisting of 0.4 mm sand will achieve particle removal comparable to 100 cm of 1.0 mm sand. However, according to Lawler and Nason (2006), the relationship between filter performance and media grain size is affected by loading rate. The higher the loading rate, the greater the impact of media size on filter performance. Lawler and Nason (2006) suggested that once the effect of loading rate is considered, the contrast in particle capture caused by different grain size is even more significant. According to Lawler and Nason (2006), a filter consisting of 1.0 mm sand operated at a loading rate of 15 m/hr would require a bed depth of approximately 150 cm to equal the particle capture of a filter with a 25 cm deep bed of 0.4 mm sand.

Because the relationship between filter performance and media grain size, the smaller fraction of media in a filter has a disproportionately large influence on filter performance. For this reason the term most often used to describe filter media size is d_{10} (the media diameter which is larger than 10% of the media in the sample), not d_{50} (the mean media diameter). Thus the term d_{10} is also referred to as the "effective size" (ES) in filtration design.

2.3.2 Uniformity Coefficient

Uniformity coefficient (UC) is one descriptor of the range of grain sizes in a filter medium; that is, the media size heterogeneity. It is calculated by dividing d_{60} (grain diameter that is bigger than 60 percent of grains in the sample) by d_{10} (grain diameter that is bigger than 10 percent of grains in the sample). Lower uniformity coefficients indicate narrower media size distributions (*i.e.* more homogenously sized media). Media with high UC values have lower porosity since the media's smaller grains fit in the pore spaces between the larger grains. Lower porosities result in increased filter head loss and decreased filter solids holding capacity (Montgomery, 1985). Higher UC media

may also require more water pressure to initiate backwash due to media binding (Fitzpatrick, 1998). Actualized over a 20 year period, the use of low UC media could reduce filter operating costs substantially by extending filter run time and lowering backwash requirements (Tchio et al., 2003). Within the conditions studied by Tchio et al. (2003), differences in UC had only a minor effect on filter performance.

2.3.3 Shape

Two types of shape factor are described in the literature: prolate *vs.* oblate, and angular *vs.* round. For the purposes of this discussion, the former will be referred to as "shape" and the latter as "angularity". Oblate spheroids resemble pancakes while prolate spheroids are shaped more like rugby balls or footballs. The shape parameter is described by a "shape index" (S) which is calculated using the formula: S = c / a, where (a) is the length of the two perpendicular equal-length axes and (c) is the length of the remaining axis normal to the previous two axes (Saiers and Ryan, 2005). Shape indexes above one define "prolate-ness" while indexes between zero and one describe oblate spheroids. A shape index of one describes a perfect sphere.

Angularity is another shape-related factor which is usually described qualitatively (Figure 2-5). "Very angular" grains are produced by crushing stone or by the weathering out of resistant minerals from soft rock. Natural minerals become rounded as sharp edges are chipped away by prolonged abrasion with other grains, such as in river sediments, beaches and sand dunes. Backwash processes in filtration also tend to round media grains, especially softer materials such as GAC and anthracite.

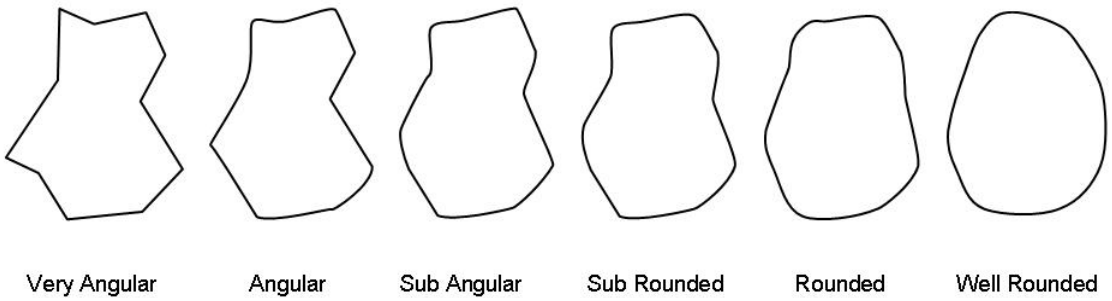

Figure 2-5. Grain angularity descriptions (modified from Walker and Cohen, 2006)

Saiers and Ryan (2005) incorporated shape (oblate *vs.* spherical *vs.* prolate) when modelling filtration in aquifers and demonstrated that single contact collector efficiency is highest for prolate ellipsoids when filtering sub-micron colloids. The same study found that oblate ellipsoids are best for

capturing larger colloids. The application of this research to drinking water treatment scenarios is limited for the following reasons:

- The modeled results were not validated.
- The model assumed that water flow was parallel to the collector axis (long axis for prolate collectors, short axis for oblate collectors). This is unrealistic for prolate collectors as they are unlikely to settle in perfectly vertical orientations after backwash.
- Collector surface area was not held constant. The study investigated collectors with identical cross-sectional area and varied the length of the collector's axis parallel to the flow of water. The resulting difference in surface area is substantial: the most prolate collector modelled had roughly 6 times the surface area of the most oblate collector. At favourable colloid deposition conditions, collectors with larger surface area can collect more particles than collectors with less surface area, thus the apparent advantage or prolate collectors may be due to their larger surface area in these simulations.
- The model tested single collectors in isolation, so pore geometry was not considered.

Torkzaban et al.'s (2007) modelling investigations found that collector shape advantages depended heavily on IS (ionic strength). Oblate collectors had larger flow stagnation zones that were more conducive to particle attachment under low IS/unfavourable conditions for deposition, while prolate collectors (assuming flow was parallel to collector axis) could collect more colloids at higher IS conditions. Similar to Saiers and Ryan (2005), experiments were not conducted to validate modeled results; moreover, the model still only consisted of singular collectors as opposed to "sphere-in-cell" models that would have accounted for collector-collector contacts and geometry. Of course, any modeled collector advantages might be unimportant in light of practical considerations. Relative to prolate collectors (media), highly oblate collectors are not generally used during GMF because of the higher head loss and lower porosity, resulting in shorter filter run and greater headloss build-up associated with their use (MWH, 2005).

It has recently been suggested that particle capture by sand grains is twice as high as by spherical glass beads (Tong and Johnson, 2006); however, it is critical to mention that the angularity of the sand was not described by Tong and Johnson. For example, fresh sand grains can be quite angular in contrast to well-abraded sand grains. At present, there are no full- nor pilot-scale investigations in the reported literature that have directly compared (*i.e.* keeping all other media characteristics constant)

particle or pathogen removals by highly angular media to those obtained by spherical glass beads. Tufenkji et al.(2004) suggest that "irregularity of grain shape contributes considerably to the straining potential of the porous medium". Similarly, Gaillard et al. (2007) concluded that colloid deposition is influenced by slight differences in pore geometry, suggesting that the pores between angular grains may be more conducive to colloid deposition than pores in well-rounded media.

In contrast to the above research, MP&T (1995) suggested that use of spherical filter media may positively affect colloid-collector contact opportunities, porosity and head loss build up. One published study (CWC, 1998) compared turbidity removal by sand and crushed recycled glass, but ES and UC of the two media were not the same, so it is unclear whether performance contrasts were due to grain angularity or other media size distribution characteristics. Overall, few published investigations have reported filtration performance outcomes (*e.g.* turbidity and/or particle reductions, pathogen reductions, head loss accumulation, maximum duration of filter cycle, *etc.*) from direct comparisons of various shaped media (*e.g.* crushed quartz compared to well-rounded quartz media).

2.3.4 Density

The use of different media densities allows the construction of reverse-graded filters such as the conventional dual-media filter, providing a marked improvement in filter loading rate and run time compared to rapid sand filters (Symons, 2006). The greater the density differences in a multi-media filter, the more defined the media interfaces will be. Anecdotal evidence suggests that the interface should be between 5 and 10 cm thick in a dual media filter to avoid accelerated head loss at the media interface (personal communication, J. Van den Oever, 2006).

Although media density does not directly affect filter performance, it can impact how well a filter is cleaned during backwashing and how it re-stratifies after backwashing. Heavier media have higher terminal velocities, as described by Stokes' Law (MWH, 2005). Because hydrodynamic shear stress is the dominant mechanism of filter media cleaning during backwashing, increases in media density promote better cleaning (Turan et al., 2003).

2.3.5 Roughness

For most academic fields of study, roughness is a qualitative term that describes the texture of an object's surface. It is a general descriptor that takes into account the number, shape, density and size of surface asperities relative to the scale of observation. Though asperities may vary in size, asperities responsible for surface roughness are small enough that they have no influence on the grain's overall

shape. Asperities which are large enough to affect grain shape are better described by terms of angularity.

The grains comprising sand and anthracite filter media are composed of either singular crystals or fragments of rock containing a number of crystals. In both cases the sand grains are solid, relatively homogenous substances with no internal porosity because mineral crystal structures are based on the repetition of atoms in a defined pattern. Because precipitation of atoms on smooth crystal faces results in the fewest bonds, precipitation preferentially fills in and completes all irregularities before nucleating a new surface. The lower free energy associated with completed crystal faces causes crystal growth to preferentially form smooth, regular crystal surfaces (Philpotts, 1990).

Apart from some microcrystalline forms of quartz (*i.e.* chert or flint), sand grains composed of multiple crystals are less resistant to weathering due to planes of weakness along crystal contacts within the grain. Natural deposits of sand are most commonly composed of quartz crystals (due to the attrition of other less refractory minerals), which are highly resistant to weathering. High energy impacts on mineral grains may break the grain along crystallographic planes of weakness or create a conchoidal fracture (a break forming a smooth, curved surface). Lower energy impacts may chip away sharp edges, abrade surface features and polish the surface of the grain until it is highly round and smooth. It is apparent that most forces acting on sand grains generally collaborate to reduce surface roughness.

Experimental deviations from CFT predictions at unfavourable filter conditions for deposition have been attributed to media surface roughness since the 1960's (Marshall and Kitchener, 1966; Nordin, 1967; Hull and Kitchener, 1969). Hull and Kitchener (1969) proposed that surface roughness provides additional surface area and sites with locally favourable geometry. Several mechanisms have been proposed to describe how surface roughness affects colloid attachment in porous media. These include:

- Roughness alters the geometry of colloid-collector interaction, causing: changes in the interaction energy, fluctuations in the interaction energy, and increases in tangential interaction forces,

- Asperities can shelter colloids from hydrodynamic shear forces, preventing particle re-entrainment, and

- Roughness prevents larger colloids from full contact with media surface by only allowing the colloid to contact the peaks of surface asperities.

Tamai et al. (1983) used latex spheres and smooth, grooved fibres to investigate how roughness affected the geometry of colloid-collector interactions and demonstrated that latex particle deposition occurred preferentially along the grooves on polyacrylonitrile fibre surfaces (Figure 2-6). Seeing that the deposition was affected by collector surface geometry, the authors accounted for this phenomenon by modelling the interaction energy between latex particles and a flat surface with a small cylindrical depression.

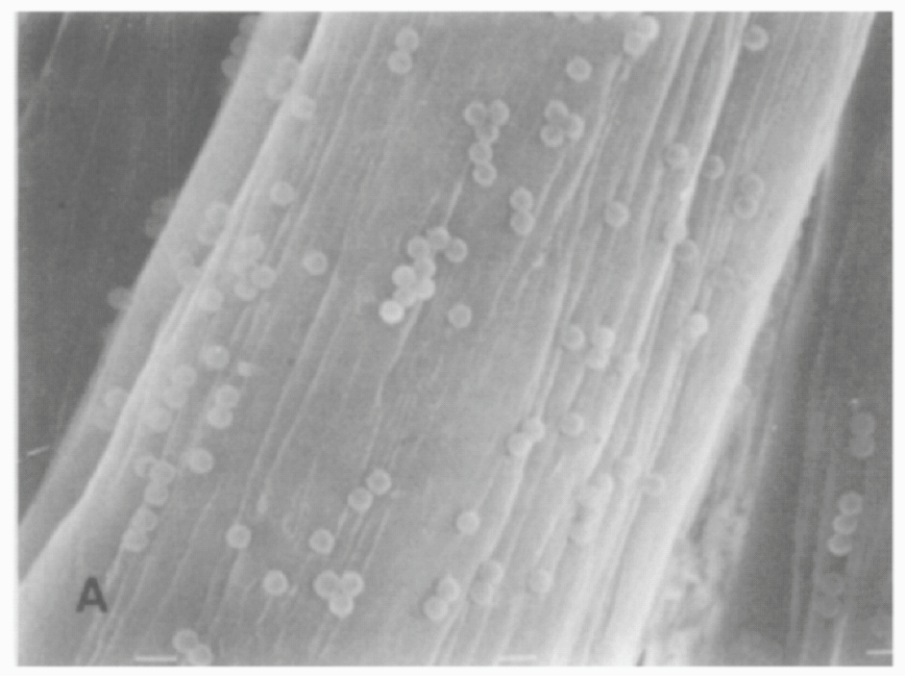

Figure 2-6. Polyacrylonitrile (Vonnel^{TM}) fibre with 0.6 micron latex spheres preferentially deposited along surface grooves (Source: Tamai et al., 1983)

The modelling investigations revealed a decrease in interaction energy along the groove (cylindrical depression), with lower interaction energy for holes closer to the diameter of the colloid. Figure 2-7 (Tamai et al., 1983) depicts interaction energy as a function of distance from the collector for different sized holes (cylinder diameters). Interaction energy profiles were calculated comparing the radius of a cylindrical hole (r) with the radius of latex particles (a), at ionic strength 10^{-3}M, pH 5.7 and 25˚C. In Figure 2-7, the solid line (Curve A, r=0) represents the interaction profile with a deep

primary minimum and a significant repulsive barrier to deposition. As the hole in the collector increases to ultimately ½ the diameter of the particle (progression of Curves B to D, calculated with the following depression dimensions: Curve B: r=a/6, Curve C: r=a/4, Curve D: r=a/2) the energy barrier to deposition diminishes until the hole provides a site that is entirely favourable (*i.e.* no energy barrier to overcome) for colloid deposition. The authors concluded that hemispherical roughness features on spherical colloids resulted in effectively larger separation distances. The increased separation enhanced colloid deposition by reducing the primary repulsive energy barrier and making the secondary energy minima shallower.

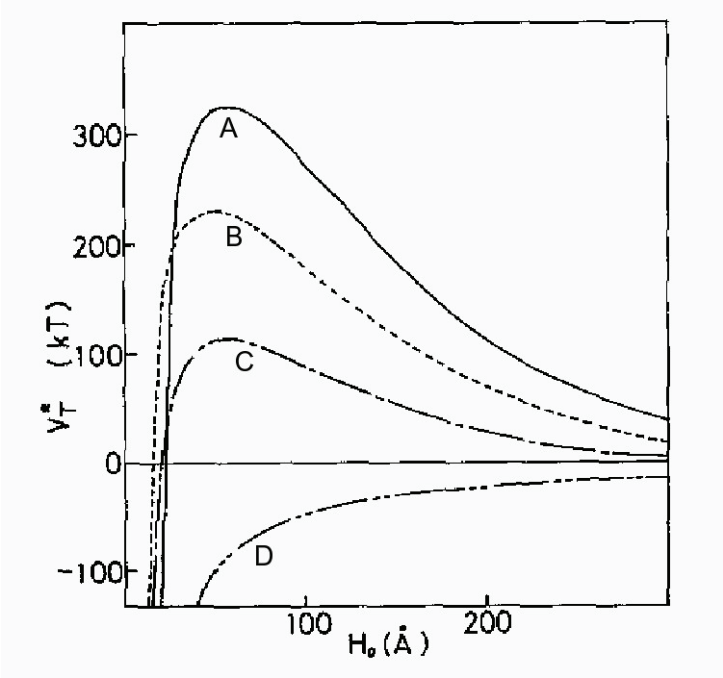

Figure 2-7. Total interaction energy between latex particles and polyacrylonitrile (Vonnel^{TM}) fibre (Source: Tamai et al., 1983)

Hoek and Agarwal (2006) comprehensively modeled surface roughness effects on colloid-collector interaction energy, taking into account the total "extended DLVO" (Derjaguin–Landau–Verwey–Overbeek) interaction energy by summing the unretarded Lifshitz-van der Waals, Lewis acid-base and the constant potential electrostatic double layer interaction energy. The authors modelled nano-scale surface roughness interactions with similarly-sized colloids to determine how surface/colloid geometry affects interaction energy. Their findings indicated that colloid-collector interactions between a colloid and a flat surface (Figure 2-8(a)) were the same as a colloid and a rough surface with widely-spaced asperities (Figure 2-8(c)) if the colloid contacted the collector

between asperities. Interaction forces between colloid and collector were much weaker if a colloid interacted with a positive asperity, producing interaction forces similar to those of two approaching spherical colloids (Figure 2-8(b)). In the opposite extreme, a colloid positioned in a similarly-sized depression, or negative asperity, experienced attractive interaction forces as much as 5 times greater than if it approached a flat surface (Figure 2-8, (d) versus (a) or (c)).

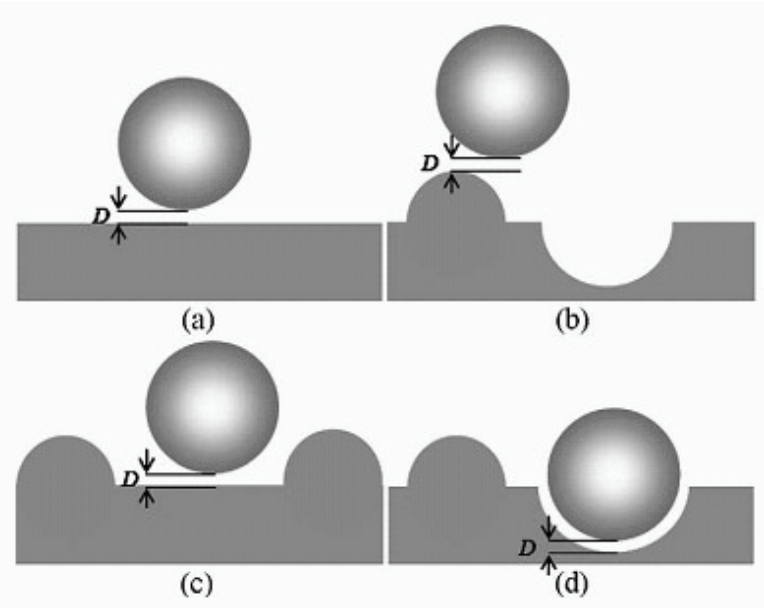

Figure 2-8. Colloid-collector geometries. D defines the minimum separation distance between a spherical nano-particle and a rough membrane surface. (Source: Hoek and Agarwal, 2006)

Modelling by Adamczyk et al. (1985) demonstrated that the interaction energy between particles and collectors fluctuated due to Brownian motion and surface roughness, despite the fact that most CFT models assumed interaction energy is constant. The authors demonstrated that slow energy fluctuations would result in minimum barrier level effective energy barriers as opposed to the mean barrier level of the interaction energy; thereby allowing more particles to cross the interaction energy barrier. Interaction fluctuations are caused by random fluctuations in the concentration of ions forming the electric double layer and in the volume between the interacting bodies. Rotary particle movement caused by fluid velocity gradients or Brownian motion can lead to fluctuations in the energy barrier height when aspects of surface roughness or charge heterogeneities are in different orientations.

Czarnecki et al. (1986) and Warszynski et al. (1988) found that surface roughness was responsible for increased tangential forces that had not been previously been accounted for. These tangential

forces could aid in particle deposition and retention. Kemps and Bhattacharjee (2005) came to similar conclusions when studying roughness and chemical surface heterogeneities. Their model of interactions between particles and heterogeneous collector surfaces demonstrated the importance of lateral DLVO interactions that were not typically accounted for in studies involving DLVO theory. Traditionally, colloidal systems were described assuming chemical as well as geometrical homogeneity (*i.e.* perfectly pure, smooth spheres). However, real surfaces are neither pure nor smooth, resulting in laterally directed force components (Kemps and Bhattacharjee, 2005) that can aid in directing and retaining colloids to attachments sites.

Bergendahl and Grasso (2003) found that larger colloids were easier to detach from collector surfaces because they were exposed to higher hydrodynamic shear forces, due to higher flow velocities towards the centre of flow channels. The results suggest that surface asperities reduce hydrodynamic shear forces on colloids if asperity spacing allows colloids to shelter between asperities. The higher tangential attractive forces and reduction of shear forces indicate that the use of rough filter media might improve filter performance. Ko and Elimelech (2000) reached a different conclusion, hypothesizing that "sand grain surface roughness" could create shadow zones downstream of surface protrusions where particle deposition is substantially hindered.

Surface roughness has also been used to explain lower than expected colloid deposition. According to Tabor (1977), increased surface roughness was responsible for decreasing colloid deposition. If the diameter of a colloid approaching a collector is larger than the distance between asperities, the colloid will only contact the collector surface at a few small points; the colloid will not be able to shelter between asperities. In this case, surface roughness is responsible for creating an "apparent" zero separation (Considine et al., 2001A). Despite a few small contact points, a layer of water remains between the colloid and the collector. The attractive force between the colloid and collector is reduced to that of colloid-colloid interaction forces or colloid-surface interactions at a distance. This lowering of attractive forces inhibits colloid deposition and increases the likelihood of removal by tangential fluid flow. However, Hoek and Agarwal (2006) concluded that this separation may be the reason that roughness is favourable for colloid deposition because the attractive vdW interactions are stronger at long range than either the acid-base or electrostatic interactions. In general, the majority though not all of the published literature suggests that increased media roughness should enhance colloid deposition by lowering interaction energy barriers (Adamczyk et al., 1985; Bergendahl and Grasso, 2003; Bhattacharjee et al., 1998; Considine et al., 2001A; Czarnecki, 1986; Duval et al., 2004; Eichenlaub et al., 2004; Herman et al., 1989; Kemps and

Bhattacharjee, 2005; Ko et al., 2000; Saiers and Ryan, 2005; Shellenberger and Logan, 2002; Song et al., 1994; Swanton, 1995; Warszynski et al., 1988; Zembla, 2004).

Several key questions regarding media grain surface roughness and its impacts on colloid deposition during GMF remained unanswered. These include:

- ***What is the best method for describing media grain surface roughness?*** Numerous methods for mathematically describing media grain surface roughness exist. Computer processing power practically limits the complexity of descriptive model terms. A full description of roughness requires many mathematical descriptors (shape, size of asperities, density of coverage, *etc.*). Since roughness occurs at numerous scales, asperities may be populated by other, smaller asperities, requiring additional terms or functions to describe asperity population/size/shape distributions. Presently, comprehensive tools for the mathematical analysis of asperities do not exist.

- ***Can effects of surface roughness on GMF performance be isolated from those of porosity and/or surface area?*** While rough media may be screened to the same size as smooth media, the individual grains of the rougher media have smaller volumes (Figure 2-11). Rough media have greater surface area compared to similarly-sized smooth media. Thus roughness effects on filtration performance may be confounded with porosity (both grain- and bulk-scale) and surface area effects.

- ***How does surface roughness affect the deposition of various sized colloids? Is there an optimal degree of roughness?*** There are a variety of geometries under which colloid/collector interaction energy has been studied (planar surfaces or spherical bodies, rough colloids or rough collectors, size of colloid, size of asperities on collector, *etc.*). These different geometries of interaction result in different conclusions for roughness regarding the deposition of colloids. For example, modelling rough plate/smooth plate interactions rather than rough particle/smooth plate interactions, leads to very different conclusions about colloid deposition. Bhattacharjee et al. (1998, Figure 2-9) compares the interaction energy between rough and smooth plates to that of two smooth plates. In this scenario, the interaction energy barrier is reduced by the use of one rough plate while the distance to the primary energy minimum remains unaffected. In contrast, Figure 2-10 (Bhattacharjee et al., 1998) depicts a situation between a rough 50 nm diameter particle and a smooth plate (Figure 2-10). In this case, the surface of the colloid was rough, but the effect was the same as if the colloid

was too large to fit between asperities: surface roughness prohibits close contact of large surface areas. The repulsive barrier is thus lowered by increasing numbers of colloid surface asperities, but there is no longer a primary minimum to promote colloidal attachment. Since the effect of roughness on colloid deposition depends on interaction geometry, it is possible that surface roughness may enhance the deposition of some sizes of colloids and lessen that of others.

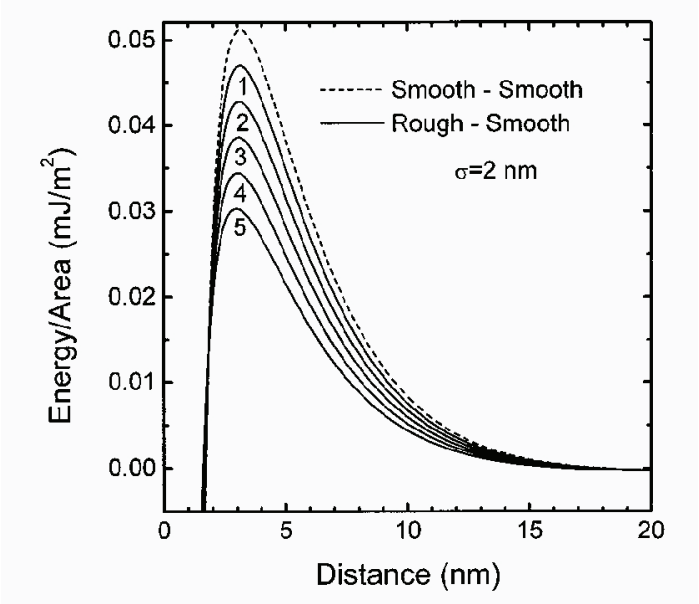

Figure 2-9. Variation of interaction energy per unit area for different values of surface asperity coverage. Solid lines represent the interaction energy between a rough and a smooth plate, lines 1 to 5 representing increasing surface coverage from 10% to 50% of surface. The dashed line represents the interaction energy between two smooth plates. (Source: Bhattacharjee et al., 1998)

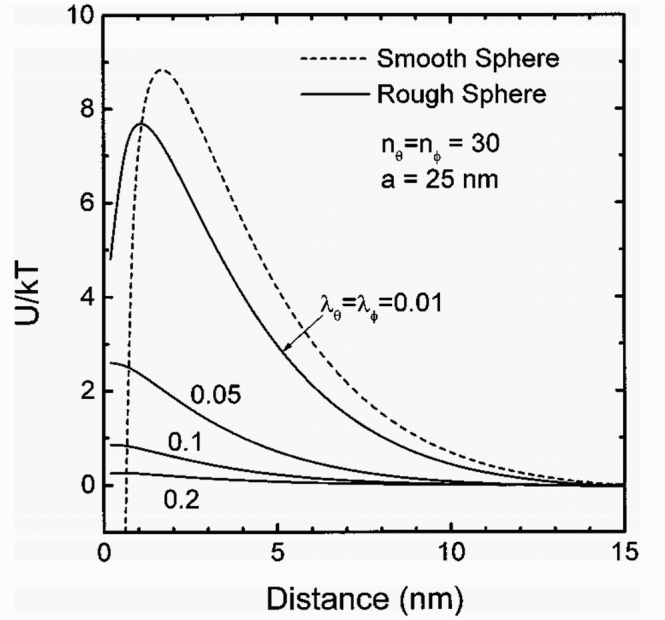

Figure 2-10. Variation of the interaction energy between a smooth plate and a rough spherical particle with varying asperity heights (Source: Bhattacharjee et al., 1998)

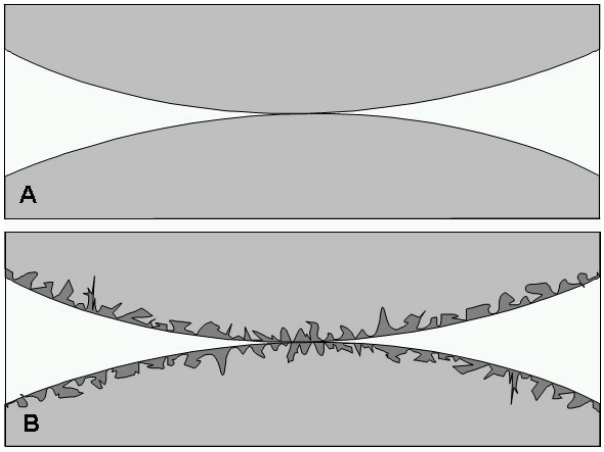

Figure 2-11. Comparison of rough and smooth media contacts. Dark grey areas in B represent additional voidage due to media roughness.

Despite the above uncertainties regarding the effect of media roughness on filtration, there is a general consensus that media roughness should enhance collector efficiency. Most research on the subject of media roughness has been in the form of modelling and micro-scale experiments. Of the few larger scale experiments that have compared the filter performance of different media, none have compared the performance of media with great differences in roughness. Kau and Lawler's 1995 study compared filter performance (evaluated by turbidity, particle counts and head loss) of glass

beads to sand with diameters of 0.39mm, 0.78 mm and 1.85 mm under identical conditions. All media were sieved though the same screens to give the media very similar media sizes. Two sieve sizes were used for each size of media tested to give very low uniformity coefficients: 0.355 mm and 0.425 mm sieves for 0.39mm media, 0.710 and 0.850 mm for the 0.78mm media, and 1.70 mm and 2.00 mm for the 1.85mm media). The resulting UC's were between 1.09 and 1.10. Loading rate was set at either 0.5 m/hr or 1.5 m/hr. The study found that the sand media had better initial turbidity removal, faster filter ripening and less extensive particle detachment at breakthrough. Differences in media performance were more pronounced for the larger, 1.85 mm media. Kau and Lawler (1995) suggest that differences in flow patterns between the two types of media are greater for the large size media than the small size media very near the surface. This result underscores the importance of conducting media comparisons using identically-sized media.

2.4. *Cryptosporidium*

Cryptosporidium is a 4-6 μm diameter waterborne parasite with a spherical to slightly ovoid shape. It is often found in the environment as an oocyst and contains 4 inner sporozoites surrounded by a thick shell wall. First discovered in the gastric glands of mice in 1907 (Tyzzer, 1908), *Cryptosporidium* was subsequently found in a variety of other animals (Angus, 1983). Rabbits, chickens, monkeys, deer, snakes, guinea pigs, turkeys, cats, cows, sheep, pigs and immunodifficient horses have all been found to harbour *Cryptosporidium*. Early *Cryptosporidium* outbreaks were of interest to researchers due to the widespread nature of the infections and their effects on the livestock farming industry. By 1983, livestock outbreaks of cryptosporidiosis had been documented in the U.S., Canada, the U.K., Hungary, Germany and Australia. The first case of human infection was documented in 1976 (Nime et al., 1976) and involved a 3-year-old girl with severe diarrhoea. *Cryptosporidium parvum* is perhaps the most common and least host-specific species of *Cryptosporidium*, which is now known to infect more than 155 different species (Fayer, 2004). The best known outbreak of human disease was the 1993 outbreak in Milwaukee, WI, during which 400,000 people were infected and 54 individuals died (Hoxie et al., 1997). Formerly thought to be a genotype of *C. parvum*, *C. hominis* is now considered a separate species of *C. parvum* that is more host-specific for humans.

2.4.1 Epidemiology and Life Cycle

Cryptosporidium is a faecally transmitted parasite and a cause of enteric disease in humans and livestock worldwide. The ingestion of contaminated food, water or direct contact with contaminated

animals is a risk factor for becoming infected. *Cryptosporidium* infection generally results in severe diarrhoea and is most prevalent for immunocompromised individuals (*e.g.* infants, the elderly, those undergoing chemotherapy and AIDS patients).

Cryptosporidium is thought to be closely related to coccidian parasites, but despite strong morphological similarities, no mitochondria-like organelle as found in coccidia has been seen in *Cryptosporidium* (Carreno et al., 1999). Angus (1983) states that "the life cycle of the parasite is direct and is essentially similar to other coccidia of the family *Eimeriidae*". Due to certain molecular evidence, Carreno (1999) suggests that *Cryptosporidium* is a relative of gregarines. There are 15 recognized species, with *C. parvum* being the most widespread, reported in over 150 different host species. There is some controversy as to whether or not there are more species-specific subtypes within *C. parvum* (Morgan-Ryan et al., 2002, Ruecker et al., 2007). Most species of *Cryptosporidium* appear to have some host specificity but are not strictly host specific. For example, *C. baileyi*, *canis*, *felis* and *muris* have all been found to infect humans despite being fairly host-specific (Caccio et al., 2002; Fayer, 2004). *C. hominis* has been isolated as a separate species of *Cryptosporidium*, but used to be referred to as "*C. parvum* genotype 1". *C. hominis* is primarily a human pathogen, though it has been detected in other primates, and cattle. To date, all outbreaks in the United States for which identification of *Cryptosporidium* to the species level was possible were associated with *C. hominis* and *C. parvum* (Bandyopadhyay et al., 2007).

The period of infection can last for one to several weeks in healthy humans, or several months in immunocompromised individuals. The period from ingestion to subsequent excretion of oocysts at the completion of one life-cycle can be as little as 3 to 5 days or as long as 2 weeks. The number of viable oocysts excreted by calves infected with 10^5 oocysts can be as high as 10^{10} over a period of 10 days (Fayer, 2004).

All species of *Cryptosporidium* are obligate intracellular parasites. They exhibit alternating cycles of sexual and asexual reproduction that are completed within the gastrointestinal tract of a single host (Ryan *et al.,* 1994). The only stage able to survive outside the host is the oocyst stage. The infective dose required for humans can be as low as 1 oocyst (Carey et al., 2004). After ingestion of the oocyst, the contents excyst, releasing 4 motile sporozites that invade the epithelial cells of the gastrointestinal tract and transform into trophozoites that subsequently go through merogony (asexual reproduction). The reproductive process involves multiple fission (schizogony) of the sporozoites to form schizonts containing eight daughter cells known as Type 1 merozoites. A second generation of Type 1

merozoites is produced when the daughter cells are released from the schizont, attach to further epithelial cells, and repeat schizogony. Figure 2-12 depicts the life cycle of *Cryptosporidium*.

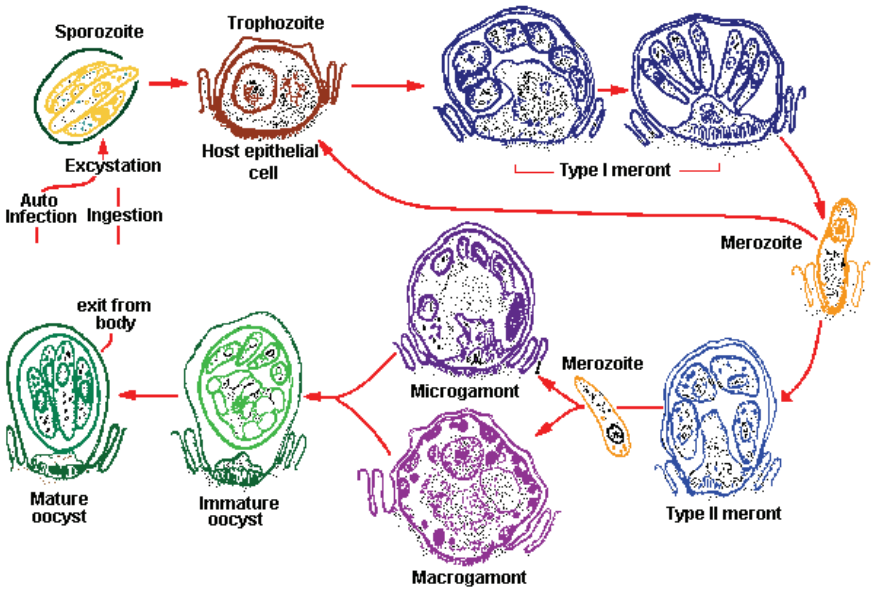

Figure 2-12. Life cycle of *Cryptosporidium* (Source: Fayer and Ungar, 1986)

2.4.2 Occurrence and Persistence

The oocyst stage can survive and remain viable for months in cool, damp environments (Dawson et al., 2004). Oocysts are constantly released into the environment since a large proportion of animals are infected and continually contaminate land and surface waters with fresh oocysts. In England, over 9% of 5000 fecal samples from wild and farmed animals tested positive for *Cryptosporidium* (Bodley-Tickell et al., 2002), while a study in Thailand, found that about 9.5% of cattle were infected at any one time (Jittapalapong et al., 2006). Rainfall and runoff events are major factors affecting the presence of total microbial load, including *Cryptosporidium* oocysts in surface and drinking water reservoirs (Kistemann et al., 2002).

The oocyst's thick outer membrane allows *Cryptosporidium* to survive outside its host for long periods. Oocysts can remain viable to mice after 6 months if stored below 20˚C in deionized water (Young and Komisar, 2005). *Cryptosporidium* can survive over 35 days in seawater at 4˚C. The number of freeze-thaw cycles seems to have little effect on oocyst survival (Fayer et al., 2004). Dehydration appears to be highly effective in killing oocysts. The presence of heterotrophic bacteria and other predatory microorganisms can reduce oocyst survival, so surface waters which appear clean can be the most hospitable to *Cryptosporidium*. Hancock et al., (1998) found that 9.5% to 22% of

U.S. groundwater samples tested positive for *Cryptosporidium*, while other studies of U.S. surface water have shown *Cryptosporidium* presence in 55% of samples evaluated (Sunnotel et al., 2006). In one Washington study, 34 out of 35 water sources were contaminated with *Cryptosporidum* oocysts (Hansen and Ongerth, 1991).

2.4.3 Water Treatment Processes for Disinfection/Removal of *Cryptosporidium*

Chlorination of drinking water is said to be one of the world's greatest inventions, having saved countless lives from waterborne diseases such as cholera (Rochelle and Clancy, 2006). Unfortunately, *Cryptosporidium* oocysts are poorly disinfected by chlorination because they are protected by a thick outer membrane. Thorough inactivation of *Cryptosporidium* by chlorination requires impractical concentrations of chlorine that could generate dangerous levels of disinfection by-products (DBP's). Disinfection of *C. parvum* by ozonation or UV irradiation can be effective, but requires specific operating conditions for optimal disinfection. For this reason, the removal of *Cryptosporidium* from the drinking water by filtration preceded by appropriate chemical pre-treatment before disinfection is recommended to ensure drinking water safety (CCME, 2004).

In addition to removing *Cryptosporidium* from the water, sedimentation and filtration improve the efficacy of disinfection measures such as ozonation and UV disinfection. Removal or inactivation of *Cryptosporidium* and other microorganisms by drinking water treatment processes is generally expressed as a $\log_{10}$ reduction. For example, a 1-$\log_{10}$ reduction represents a 90% removal and a 2-$\log_{10}$ reduction represents a 99% removal. Depending on filtration conditions, *Cryptosporidium* oocyst removal by filtration can range from just above 0 to greater than 5 $\log_{10}$ (Emelko et al., 2005). Near-zero $\log_{10}$ removals of microorganisms like *Cryptosporidium* oocysts are possible in the absence of coagulation, especially in cold waters.

Removal or inactivation of *Cryptosporidium* oocysts and other microorganisms by drinking water treatment processes is generally expressed as a $\log_{10}$ reduction. For example, a 1-$\log_{10}$ reduction represents 90% removal and a 2-$\log_{10}$ reduction represents 99% removal. Depending on filtration conditions, *Cryptosporidium* oocyst removal by filtration can range from just above 0 to greater than 5 $\log_{10}$ (Emelko et al., 2005). Near-zero $\log_{10}$ removals of microorganisms like *Cryptosporidium* oocysts are possible particularly at conditions of non-ideal operation, such as during the absence of coagulation, especially in cold waters.

Cryptosporidium oocyst removal by filtration can be challenging for the following reasons:

- The diameter of *Cryptosporidium* oocysts is close to that for the minimum depositional efficiency according to filtration theory (Tufenkji et al., 2006), and

- The "hairy" outer layer of *Cryptosporidium* oocysts creates a steric repulsive force that inhibits attachment (Nanduri et al., 1999; Considine et al., 2002; Kuznar and Elimelech, 2006; Byrd and Walz, 2007)

The difficulty in accurately enumerating *C. parvum* oocysts has made it impractical to suggest or reasonably enforce regulatory guidelines for this pathogen (Nieminski and Ongerth, 1995; Clancy et al., 1999). As a result, the United States Environmental Protection Agency (USEPA) Long-Term 2 Enhanced Surface Water Treatment Rule (LT2ESWTR) allows utilities that require additional treatment for pathogen removal/inactivation to choose from a variety of options; including "demonstration of system performance," which requires studies that reliably quantify pathogen removal (USEPA, 2000). Similar approaches have been implemented in parts of Canada; specifically, "treatment technologies in place should achieve at least a 3-$\log_{10}$ reduction in and/or inactivation of cysts and oocysts, unless source water quality requires a greater $\log_{10}$ reduction and/or inactivation" (CCME, 2004). Canadian federal guidelines require that WTP's treating surface water or groundwater under the direct influence of surface water (GWUDI) ensure by filtration and disinfection greater than:

- 3-$\log_{10}$ reduction of *Cryptosporidium*,

- 3-$\log_{10}$ reduction of *Giardia*, and

- 4-$\log_{10}$ reduction of viruses.

2.4.4 Surrogates for *Cryptosporidium* Oocyst Removal by GMF

Demonstrations of filter performance require reliable quantification of pathogen or surrogate removal. For organisms (or organism surrogates) present in relatively low concentrations (*e.g.* waterborne *Cryptosporidium* at indigenous levels or levels counted from treated water during filtration performance demonstrations), counting approximately ten or more organisms in a sample (or several replicates) substantially contributes to reducing uncertainty attributable to random sampling error (Emelko et al., 2008). As a result, high influent oocysts/surrogate concentrations are often required to reliably quantify oocyst removal. Seeding viable *Cryptosporidium* into operating municipal filters is not possible for obvious health concerns. Similar concerns can also preclude the

use of viable oocysts in pilot studies, especially if pilot columns are housed within a WTP; because the potential risk to the general public prohibits the use of high concentrations of viable *Cryptosporidium* in close proximity to public drinking water supplies.

To reduce the costs and risks associated with oocysts enumeration, various parameters have been investigated as surrogates for the removal *C. parvum* by water treatment processes. These include: turbidity measurements, particle counts, aerobic spores, *E. coli* bacteria and oocyst-sized polystyrene microspheres (Emelko et al., 2004; 2005). Many of these parameters, such as turbidity and particle counts are reliable indicators of treatment performance, but do not adequately aid in quantitatively assessing pathogen passage through various stages of the water treatment process (Nieminski & Ongerth, 1995; Ongerth & Pecoraro, 1995; Patania et al., 1995). Inactivated (non-viable) *C. parvum* oocysts have been used as surrogates for viable oocysts in many treatment performance evaluations (Nieminski & Ongerth, 1995; Huck et al., 2001). Chemically inactivated *C. parvum* oocysts have different surface charge characteristics (described by zeta potential) compared to live oocysts (Ongerth & Pecoraro, 1996); such differences in zeta potential might affect oocyst removal by filtration because zeta potential is indicative of the degree of particle destabilization (Amirtharajah & Mills, 1982). Emelko (2003) noted the zeta potential of *C. parvum* oocysts is affected by multiple factors such as water quality, coagulant type and dosage, and pH, in addition to chemical inactivation prior to treatment. While oocyst inactivation by heat treatment can damage cell membranes and affect oocyst filtration behaviour, oocyst inactivation using formalin has been shown to have only minor effects on membrane properties (Byrd and Walz, 2007). Bench-scale investigations of *C. parvum* removal during both optimal and vulnerable periods of filtration demonstrated that formalin-inactivated *C. parvum* oocysts were reliable surrogates for viable oocysts during filtration studies (Emelko, 2003). While the use of formalin-inactivated oocysts as a surrogate for live oocysts is desirable from a health and safety perspective, they remain non-ideal surrogates because they are expensive and subject to the same analytical uncertainty as live oocysts (Nieminski et al., 1995; Clancy et al., 1999).

Some of the challenges associated with oocyst enumeration include:

- many steps involved in sample preparation, which increase methodological variability,
- the fluorescent antibody stains and the oocysts themselves are expensive,
- depending on the concentration of suspended solids, enumeration can be hampered by interfering solids,

- staining of oocysts can be inconsistent, and

- despite chemical inactivation of oocysts, the possibility of infection must still be considered.

To date, the most consistently, somewhat predictive non-oocyst surrogate for viable *Cryptosporidium* oocyst removal by filtration has been similarly sized latex microspheres with a carboxylate coating (Emelko and Huck, 2004; Amburgey et al., 2001; Emelko et al., 2003). These microspheres contain a fluorescent dye which fluoresces with a far greater intensity than fluorescein isothiocyanate (FITC) -stained oocysts. Accordingly, they require no staining during sample preparation, are easy to visualize, and can be enumerated at lower magnifications than those required for oocysts enumeration. The distinctive and intense fluorescence of the microspheres makes them easily distinguishable from stained oocysts and other fluorescing material that may be present during analysis of samples obtained during filtration performance demonstrations.

Oocyst-sized microspheres are not consistently reliable as surrogates for the removal of viable *Cryptosporidium* oocysts by filtration, however. For example, they have some physical characteristics that are notably different from oocysts, such as rigidity, which may impact their retention in porous media. Moreover, the relative relationship between potential surrogate and oocyst removal by filtration must be established specifically for every different operational condition of interest. For example, while Emelko and Huck (2004) demonstrated an excellent correlation between microsphere and *C. parvum* removal by filtration preceded by alum coagulation, Emelko and Brown (2004) did not find microspheres to be a suitable surrogate for *C. parvum* removal by filtration preceded by chitosan coagulation, suggesting that different coagulation mechanisms may govern the removal of *C. parvum* and microspheres when chitosan was utilized. This result suggested that the reliability of oocyst-sized microspheres as surrogates for filtration of *C. parvum* may be coagulant (or pre-treatment) dependent. Moreover, because it is well established that oocyst removal varies during different phases or events encountered during a filter cycle, (Emelko et al., 2003; 2005; Huck et al., 2001; Patania et al., 1995), surrogate relationships for *C. parvum* removal by filtration must be established specifically within the context of operational conditions and filtration regimes.

3. Methods and Materials

3.1. Experimental Design

3.1.1 Rationale

Recent advances in colloid research applied to natural groundwater aquifer environments have demonstrated that non-spherical, rough media may offer increased colloid deposition capabilities (Kau and Lawler, 1995; Shellenberger and Logan, 2002; Tufenkji et al., 2004). CFT model development has also begun to address these media characteristics (Czarnecki and Dabros; 1980, Czarnecki, 1986; Eichenlaub et al., 2004; Duval et al., 2004; Saiers and Ryan, 2005; Hoek and Agarwal, 2006). If media grain sphericity and roughness contribute to colloid deposition in natural environments, it is reasonable to hypothesize that these media characteristics may also play a role in colloid and specifically pathogen deposition (and removal) by GMF during drinking water treatment. SEM images of microspheres on rough, ceramic media suggest that such surfaces could promote pathogen removal by providing additional attachment sites (Figure 3-1).

The majority of media commonly used during GMF (*i.e.* anthracite, sand, GAC, garnet, ilmenite, *etc.*) are non-ideal with varying degrees of sphericity and roughness. Although many studies have investigated various aspects of filtration performance achieved when comparing spherical glass beads to conventional media (Kau and Lawler, 1995), sand to anthracite (Tchio et al., 2003), or anthracite to GAC (Emelko et al., 2006), very few have directly compared conventional media to materials with much rougher surface textures.

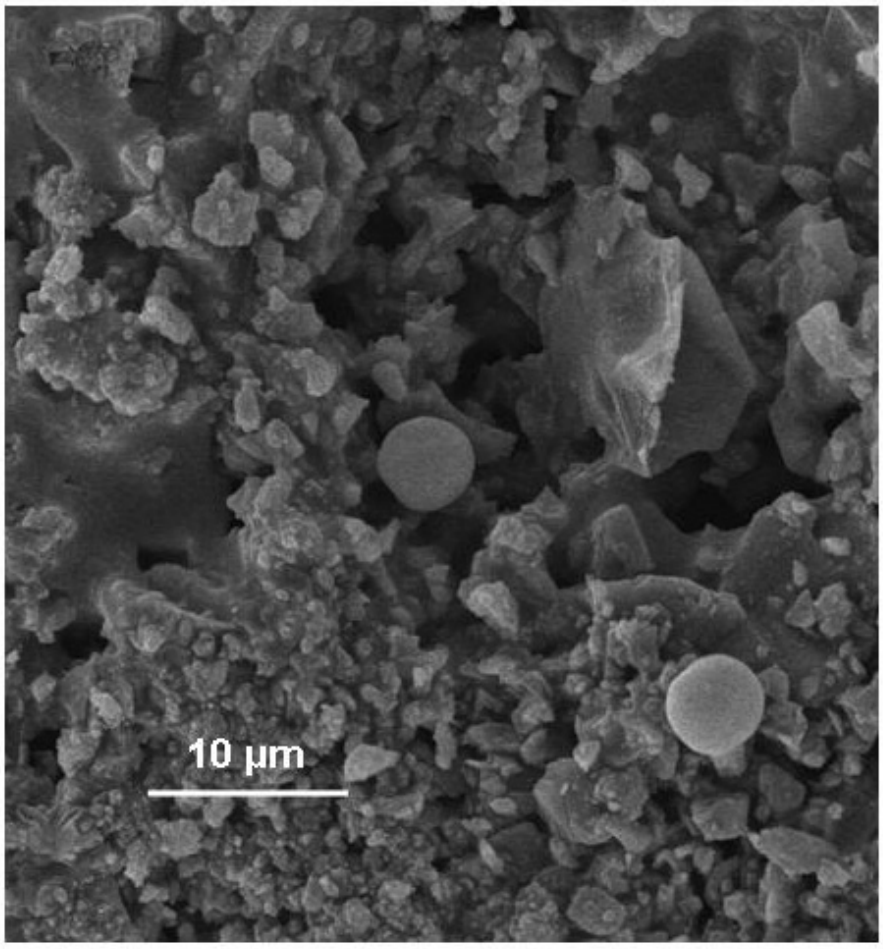

Figure 3-1. SEM image of two 4.5 µm latex microspheres on surface of ceramic media at 2000X magnification

In recent years, engineered ceramic media have been developed for drinking water filtration applications. Unlike conventional filtration media, engineered filtration media can be manufactured with controllable and highly uniform properties such as: shape, size, sphericity, density, and composition. These qualities contribute to uniformity in filter bed porosity, bulk density, and macroscopic behaviour. Engineered media are typically designed to maximize available surface area within a granular filtration process. The porous texture and composition of engineered ceramic media are designed to promote colloidal attachment, while the sphericity and uniformity coefficient enhance contact opportunities between the filtration medium and colloids targeted for removal (*e.g.* pathogens). Since these properties are controllable with manufactured media, their use represents an opportunity to further optimize and understand the filtration process. For example, anecdotal evidence from several pilot-scale studies indicates that the particle and pathogen removal performance of

engineered ceramic filtration media is less dependent on chemical pre-treatment than conventional filtration media performance. A few studies have evaluated the effects of filter media porosity, sphericity, surface charge and composition on filtration performance (MP&T, 1995, 1996), however the effects of media roughness on colloid deposition at typical GMF operational conditions are generally poorly understood. Moreover, such investigations must be conducted with both oocysts and potential surrogates for oocyst removal by filtration because several studies have clearly demonstrated that surrogate relationships for pathogen removal by filtration must be established specifically within the context of operational conditions and filtration regimes (Emelko and Brown, 2004; Emelko and Huck, 2004; Amburgey et al., 2001; Emelko et al., 2003).

3.1.2 Approach

To address knowledge gaps regarding the general performance of spherical, rough engineered ceramic media used during drinking water treatment applications of GMF and the impacts of media surface roughness on GMF performance, this investigation compared the performance of conventional and spherical, rough engineered ceramic media in a manner designed to contribute to both mechanistic filtration research and full-scale filter performance optimization. Specific knowledge gaps that were addressed included:

- Performance demonstration (filter effluent turbidity and particle counts, headloss build-up, *Cryptosporidium* oocyst and oocyst-sized microsphere removal, and stability of operation) of spherical, rough engineered ceramic media used during GMF,

- Performance comparison of spherical, rough engineered media to conventional anthracite-sand media used during GMF (same performance parameters as above),

- Assessment of operational conditions (temperature, coagulant type, coagulant dose, loading rate and water quality) on relative performance of spherical, rough engineered media and conventional anthracite-sand media used during GMF (same performance parameters as above), and

- Assessment of the effect of surface roughness on performance during GMF.

The ultimate goal of this investigation was to enable and conduct a direct comparison of conventional media and spherical, rough engineered ceramic media filtration performance and to quantitatively assess that performance at various conditions relevant to drinking water filtration. It was hypothesized that the ceramic media might achieve its optimal filter performance at different

filtration conditions from conventional media due to its contrasting surface properties, so a variety of operational conditions were investigated. They included:

- hydraulic loading rate (10 m/hr and 24 m/hr),
- coagulant type (alum and polyaluminum chloride),
- coagulant dosage (no coagulant, sub-optimal and optimal dosages), and
- raw water temperature (temperature of 5˚C and 20˚C).

The effects of the above variables were explored to: a) determine the degree to which differences in filter media performance were affected by changes in operating conditions, b) evaluate if the ceramic media offered more stable filter performance over conventional media, c) connect the results of this study to previous mechanistic findings and d) recommend optimal filtration conditions for future studies with engineered media.

Studying the effects of hydraulic loading rate on oocyst removal and general filter performance was a priority of this investigation. Since current high-rate filter designs attain loading rates up to 32 m/hr (Logsdon, 2006) while most dual media filters operate at loading rates near 10 m/hr, this study varied loading rate to provide results relevant to both current filter operations and to higher loading rate operations. There was also a gap in knowledge regarding whether or not engineered media would have greater oocyst removal at high loading rates. Lawler and Nason (2006) stated that loading rate has a direct impact on the performance of granular media filters while Harrington et al., (2003) found that there was no difference in oocyst removal by conventional media with increases in loading rate from 3.4 m/hr to 19.5 m/hr. Anecdotal evidence suggested that relative to conventional media, the rough, spherical engineered ceramic media could better maintain filter performance at higher loading rates. To determine if performance differences caused by filter media were influenced by loading rate, high and low loading rate trials were conducted for all operational conditions (24.4 m/hr (10 gpm/ft^2) and 10 m/h (4 gpm/ft^2)).

Oocyst removal by filtration is often highly dependent on both coagulant type and coagulant dose (Emelko and Brown, 2004; Xagoraraki and Harrington, 2004; Emelko et al., 2005). Despite demonstrated advantages of surface roughness on colloid deposition with increasing ionic strength (Bhattacharjee et al., 1998), the impacts of surface roughness on colloid removal from coagulated water have not been reported. It was therefore unknown if media roughness enhanced particle or

oocyst removal at conditions representative of GMF and if particle and oocyst removal by engineered ceramic media were affected by changes in coagulant dose and type. This concern was thus addressed by varying coagulant doses from zero to optimal and above optimal and by testing filter performance with the use of other coagulants.

Water temperature was an important variable in this study since many WTP's alter operational processes in response to water temperature changes (*i.e.* the Horgan WTP switches coagulant type from alum to PACl during cold water conditions). Biological matter (both detrital and living) forms a significant portion of particulate matter in natural surface waters and biological activity (growth, metabolic processes, abundance) is greatly affected by water temperature. Water temperature also affects coagulation, flocculation and filtration processes and changes in filter performance brought about by seasonal differences in water temperature are important to evaluations of filter media performance.

Pilot-scale investigations were conducted to address each of the three research objectives specified above. These investigations were conducted in three phases, described as:

Phase 1: Preliminary, proof-of-concept investigations focused on engineered ceramic media screening and optimizing operation of the pilot-scale filtration unit. These experiments were conducted using synthetic raw water.

Phase 2: Pilot-scale investigations focused on comparing conventional and spherical, rough engineered ceramic media configurations optimized for the specific media (different media sizes and depths). The experiments were conducted using Lake Ontario raw water without chemical coagulant addition.

Phase 3: Pilot-scale investigations focused on directly comparing filtration performance achieved using conventional and spherical, rough engineered ceramic media configurations (identical media sizes and depths). The experiments were conducted using Lake Ontario raw water at various temperatures and with varying levels and types of chemical coagulant addition.

A summary of the experimental objectives, operational conditions and filter configurations can be found in Table 3-1, Table 3-2 and Table 3-3. The Phase 1 trials were conducted at the University of Waterloo using synthetic water (tap water with kaolin addition to achieve filter influent turbidities of approximately 1.2 NTU). These experiments were preliminary proof-of-concept experiments focused on engineered ceramic media screening and optimizing operation of the pilot-scale filtration unit. The

removal of oocyst-sized fluorescent polystyrene microspheres and turbidity and particle reductions at 24.4 m/h (10 gpm/ft^2) and 9.8 m/h (4 gpm/ft^2) by three filtration media configurations (fine and coarse spherical, rough engineered ceramic media and conventional anthracite and sand media) were investigated. These experiments were conducted without any chemical pre-treatment, representing complete coagulation failure. Expected reductions of *C. parvum* oocysts and oocyst-sized microspheres by the various media were not known *a priori*; accordingly, these investigations were critical for establishing the concentrations of *C. parvum* oocysts and oocyst-sized microspheres that would need to be added/seeded into the pilot filter column influent water during subsequent performance demonstration investigations. Summarized in Table 3-2, several filter bed configurations were evaluated to determine which media configurations would be utilized during subsequent experiments. Filters in Phase 1 experiments contained either graded gravel or crushed garnet to support the filter media. These preliminary investigations also enabled the refinement of laboratory/analytical methods and operational techniques associated with the use of the pilot scale filtration unit, the design of which is presented in Section 3.2.

The Phase 2 trials were conducted at the Municipality of Toronto's Horgan Water Treatment Plant (HWTP) in Scarborough Ontario, Canada, which enabled the use of natural, low turbidity source water. Details regarding the Lake Ontario source water quality are provided in Section 3.2.8. Given anecdotal evidence from several pilot-scale investigations that suggested that the particle and pathogen removal performance of engineered ceramic filtration media are less dependent on chemical pre-treatment than conventional filtration media, non-chlorinated, non-coagulated water from Lake Ontario was processed through the pilot filters during this phase of experiments. These operational conditions are analogous to a worst-case scenario of complete failure of coagulant addition. Two preliminary trials were conducted with oocyst-sized microspheres to evaluate the required seeding concentrations of *C. parvum* oocysts and microspheres for the four subsequent trials. Phase 2 trials compared filter performance of 3 different filter configurations as specified in Table 3-2 (fine, dense ceramic media; fine, less dense ceramic media; and conventional media). These media configurations were optimized for the specific media (different media sizes and depths) and represented a preliminary assessment of what was believed to be a best-case scenario for media configurations. These trials were conducted to provide a preliminary indication of whether or not an appreciable particle and/or oocysts reduction performance benefit, such as less dependence on chemical pre-treatment, could be achieved from low turbidity source waters such as Lake Ontario.

The Phase 3 trials were also conducted at the HWTP in Scarborough Ontario, Canada. These investigations focused on directly comparing filtration performance achieved using conventional and

spherical, rough engineered ceramic media configurations. These experiments were designed to provide a fair, direct comparison of particle, oocyst, and oocyst-sized microsphere reductions by spherical, rough engineered ceramic and conventional anthracite and sand media filters. As specified above in Table 3-2, one of the filter configurations used during the Phase 2 trials was replaced with a ceramic media configuration that had the same ES (effective size) and UC (uniformity coefficient) as the conventional anthracite and sand media configuration that was used during the Phase 2 pilot scale trials. The first trial in Phase 3 was conducted with a much lower seeded oocyst concentration (1,000 oocysts/L as compared to 50,000 oocysts/L) than used during the Phase 2 trials to briefly assess the impacts of seeded oocyst concentration on observed oocyst removal by the utilized filtration configurations. Only one such trial was conducted because more extensive studies using a similar experimental set-up with conventional media had not indicated notable differences in observed oocyst and oocyst-sized microsphere reductions when different seeded concentrations of these organisms and surrogates were used at operational conditions similar to those utilized herein (Emelko et al., 2001). The subsequent pilot trials conducted during Phase 3 utilized Lake Ontario raw water at various temperatures and with varying levels and types of chemical coagulant addition. The coagulant type and dose were those utilized by the HWTP during the time of the trials because they were optimized for the raw water conditions encountered at the time the trials were conducted.

Table 3-1. Summary of Experimental Objectives

Experiment	Objectives	Operational Conditions			
		Microsphere and/or *Cryptosporidium* Oocyst Removal Evaluated	**Water source**	**Coagulant**	**Temperature (C^0)**
Phase 1					
1A, 1B	Test operational capabilities of apparatus, develop method, proof of engineered media performance	Microsphere	Waterloo Municipality tap water	no	14
Phase 2					
2A. 2B	Test capabilities of media under conditions representing coagulation failure, further refine method for HWTP location	Microsphere	Lake Ontario	No	22
2C, 2D, 2E, 2F	Evaluate performance capabilities of conventional *vs.* ceramic media	Microsphere and ***Cryptosporidium***	Lake Ontario	No	22 to 9
Phase 3					
3A	Determine if spike dose influenced pathogen reduction	Microsphere and ***Cryptosporidium***	Lake Ontario	No	9
3B to 3K	Evaluate performance capabilities of conventional *vs.* ceramic media with optimal and sub-optimal coagulation	Microsphere and ***Cryptosporidium***	Lake Ontario	PACl	5.5 to 7.5
3L and 3M	Evaluate performance capabilities of conventional *vs.* ceramic media with different coagulant	Microsphere and ***Cryptosporidium***	Lake Ontario	Alum	22

Table 3-2. Summary of Operational Conditions Utilized During Experimental Phases

Experiment	Temperature (˚C)	Loading Rate (GPM/ft^2)	Description
Phase 1			Initial testing at University of Waterloo. Tap water with approx 1NTU kaolin dust addition. See Table 3-7 for media configurations.
1A	14	10	30 minute spike duration.
1B	13	4	Low loading rate variation of Trial 1A
Phase 2			"No coagulant" testing on Lake Ontario water at HWTP. 60 minute spike duration. See Table 3-8 for column configurations.
2A	21	10	Microsphere test only.
2B	22	4	Microsphere test only.
2C	20	10	First of 4 microsphere and *Cryptosporidium* experiments, similar to Trial 2A.
2D	21	4	Second of 4 microsphere and *Cryptosporidium* experiments, similar to Trial 2B.
2E	20	10	Repeat of Trial 2C.
2F	9	4	Repeat of Trial 2D.
Phase 3			Continuation of testing at HWTP. "Dense" ceramic media switched out for "matched" ceramic configuration. See Table 3-9 for column configurations.
3A	4	10	Low spike concentration test to determine if spike concentration affected filter performance. No coagulant.
3B	2	10	Excess coagulant trial.
3C	5.5	10	"Optimal" coagulant dose spike test
3D	5.5	4	Low loading rate version of Trial 3C
3E	6.5	4	Duplicate of Trial 3D
3F	6.5	10	Duplicate of Trial 3C
3G	7	4	Duplicate of Trial 3C, but with no microspheres in spike suspension
3H	6	10	"Sub-optimal" coagulant dose spike test
3I	6	4	Low loading rate variation of Trial 3H
3J	7	4	Duplicate of Trial 3I
3K	7	10	Duplicate of Trial 3H
3L	22	10	Warm water, alum coagulant spike trial
3M	22	4	Low loading rate variation of Trial 3L

Table 3-3. Summary of Media Configurations used During Experimental Phases

Trial	Column 1	Column 2	Column 3
Phase 1 Experiments 1A, 1B	45 cm 0.45 mm ceramic 5 cm 0.22 mm ceramic 5 cm 0.34 mm garnet	50 cm 0.94 mm anthracite 30 cm 0.44 mm sand 12 cm graded gravel	45 cm 0.96 mm ceramic 15 cm 0.22 mm ceramic 5 cm 0.34 mm garnet
Phase 2 Experiments	45 cm 0.64 mm ceramic 15 cm 0.22 mm ceramic 20 cm graded gravel	45 cm 0.96 mm ceramic 15 cm 0.21 mm ceramic 20 cm graded gravel	45 cm 0.89 mm anthracite 30 cm 0.47 mm sand 20 cm graded gravel
Phase 3 Experiments	45 cm 0.89 mm ceramic 30 cm 0.47 mm ceramic 20 cm graded gravel	45 cm 0.96 mm ceramic 15 cm 0.21 mm ceramic 20 cm graded gravel	45 cm 0.89 mm anthracite 30 cm 0.47 mm sand 20 cm graded gravel

3.2. Column Experiments

3.2.1 Design Criteria

The successful completion of the experimental objectives described in Section 3.1.1 required a suitable pilot filter apparatus that could meet the following criteria:

- provided performance assessments at conditions (*e.g.* filter run times, hydraulic loading rates, *etc.*) as representative of full-scale operation as possible,
- enabled concurrent evaluation of multiple media types and configurations,
- provided continuous online headloss and filter influent and effluent turbidity and total particle count (>2 μm) data at a frequency comparable to that utilized in full-scale drinking water treatment plants, and
- consisted of a safe and portable design that could be easily modified to investigate various operational scenarios.

To achieve realistic filter run times comparable to those that could be expected during full-scale filtration, the individual filter columns had to be at least as tall as conventional filter tanks are deep. A modular column design was employed, so column heights could be configured as necessary.

Wall effects are created by higher porosity grain arrangements along the inside walls of filter columns which reduce filter performance in small column filters (McWhirter et al., 1997). Porosity at the wall face approaches unity and declines to a steady value in an oscillatory manner away from the wall. This steady value is generally reached within 5 media grain diameters from the column wall (de Klerk, 2003, Figure 3-2), so if the ratio of column diameter (*D)* to media diameter (*d*) is low, the reduction in porosity can allow short circuiting in the column to occur. The difference in bulk porosity and filter performance is negligible above *D/d* ratios of 20 to 30 (McWhirter et al., 1997, Lang et al., 1993), though variability in filter performance between filter cycles can be significant for ratios below 26 (Lang et al., 1993). To ensure that wall effects were negligible during this study, the ratio of filter column diameter to media diameter was designed to exceed a 50:1 ratio. This ratio was determined by theoretical analysis and experimentation (Ergun, 1952; Mehta and Hawley, 1969; Lang et al., 1993; McWhirter et al., 1996; Sodré and Parise, 1998). For this reason, Lang et al. (1993) recommended using columns of a large enough diameter to maintain a *D/d* ratio over 50. Since the largest media used in the present investigation had an ES (effective size) of approximately 1 mm, the interior diameter of the pilot columns had to be at least 50 mm; the columns use for this study had an interior diameter of 75 mm.

The pilot scale filtration unit design utilized herein permitted the use of realistic hydraulic loading rates typical of full scale conventional direct filtration operations such as those utilized at the HWTP. For example, the HWTP typically operates at loading rates between 4 to 14 m/hr. Accordingly, the pilot scale filtration unit was designed to enable these and even higher hydraulic loading rates.

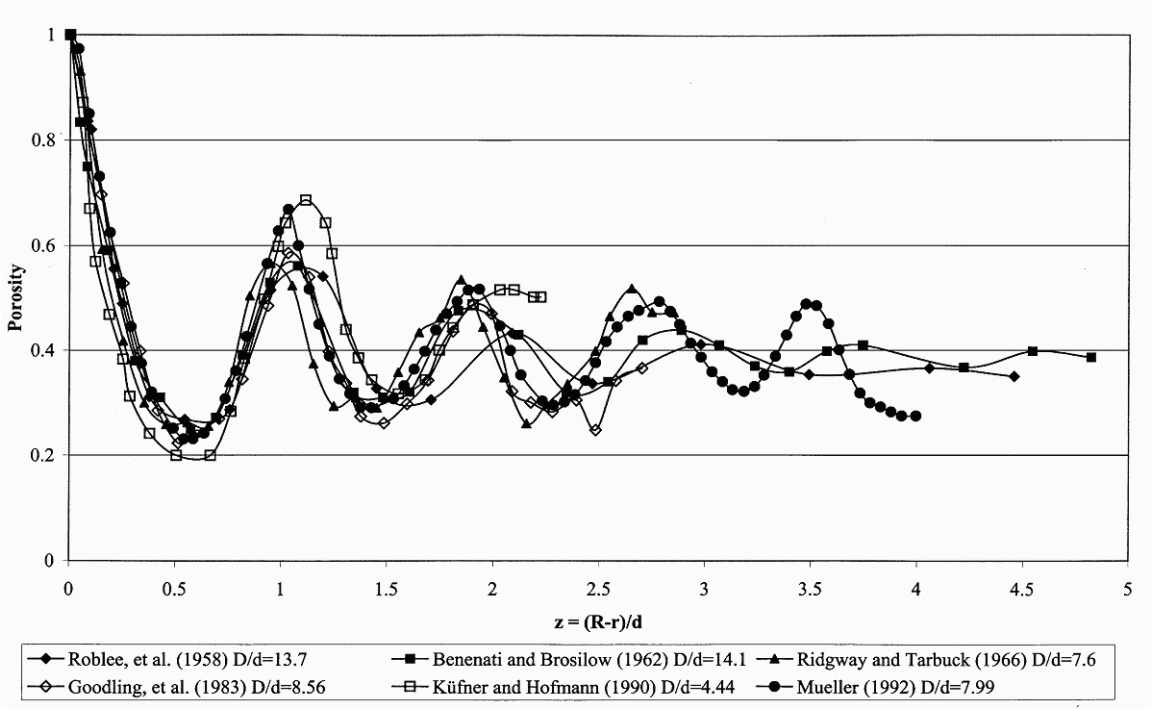

Figure 3-2. Porosity oscillations caused by wall effects. (Source: de Klerk, 2003)

3.2.2 Equipment

The pilot-scale filtration unit utilized during the present investigation is shown in Figure 3-3. It consisted of three clear PVC columns supported on a stainless steel frame. Each column consisted of 3 flanged sections for a total column height of 3.96 m. Overflow drainage was installed 31 cm from the top of each column, giving the filters 3.65m of available head. The upper sections of the filters were covered but not sealed to ensure that the filters operated under constant head.

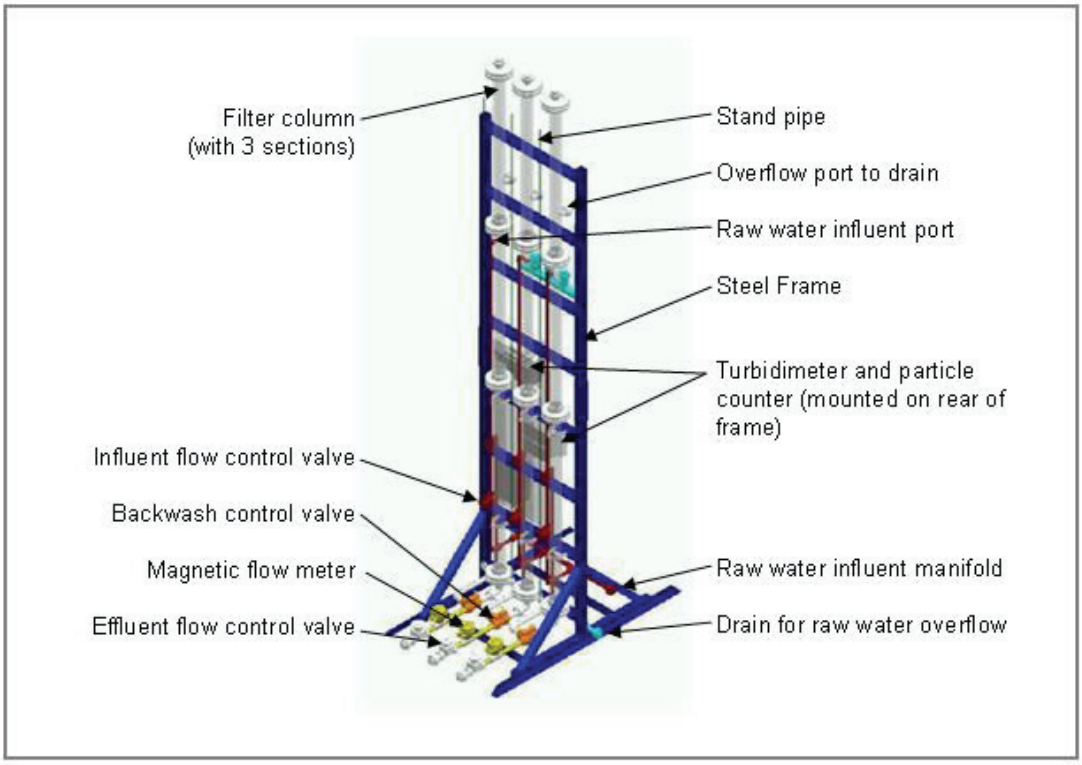

Figure 3-3. Diagram of pilot-scale filtration unit

Each column was equipped with the following fittings, listed from top to bottom (Figure 3-4): overflow to drain, influent port, primary port to pressure gauge, spike injection port, influent sample line, effluent sample line, port to stand pipe, effluent lines to turbidimeters, particle counters and drain. The bottom of each column was fitted with wedgewire to prevent media loss. Each column was equipped with its own dedicated turbidimeter, particle counter, pressure gauge and flow meter. An additional turbidimeter and particle counter enabled the influent turbidity and particle counts to be compared to the effluent from the filter columns. Figure 3-5 shows the pilot filters on location at the HWTP.

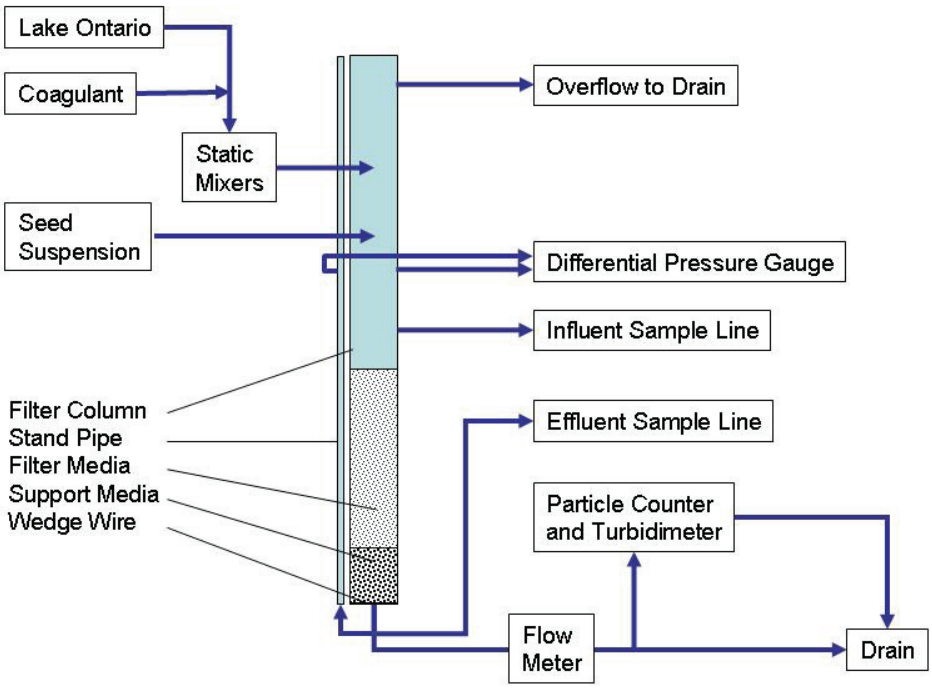

Figure 3-4. Schematic of pilot-scale filter column

Figure 3-5. Photograph of pilot-scale filtration unit at HWTP

3.2.3 Source Water

Phase 1 trials were conducted using the Region of Waterloo's chlorinated municipal tap water directly from faucets at a laboratory in the University of Waterloo. Little variation in water quality

parameters was observed during the short period of Phase 1 experiments (Table 3-4). The bulk of experiments during the study were conducted as part of Phases 2 and 3, both of which were conducted at the HWTP. The HWTP is a conventional direct filtration plant with a plant capacity of 455 million litres per day. It operates 8 granular media filters: 4 with sand and anthracite, 4 with sand and GAC. Loading rates in its filters range from 4 to 14 m/hr, depending on seasonal requirements. The water temperature at HWTP during the study period ranged from 1˚C in the winter to 24˚C in late summer. The source water for the plant entered through a 3.3 m diameter pipe extending 2.96 km offshore. The inlet for the plant's raw water sample line is at the same location as the plant's main intake. During Phase 2 and 3 experiments, raw water for the pilot filters was taken from the HWTP's raw water sample line in Lake Ontario, which provided the filter columns with uncoagulated, unchlorinated water directly from the lake. Raw water temperature for the pilot plant during the winter was 1.5˚C warmer than the HWTP's raw water due to exposure to heated interior areas. Table 3-5 provides further raw water quality information.

Table 3-4. Tap water quality during Phase 1

Water Quality Parameters (without kaolin addition):	**Mean:**	**Maximum:**	**Minimum:**
Temperature (˚C)	13.5	14.5	13
pH	7.4	7.6	7.3
Turbidity (NTU)	0.04	0.06	0.03
Alkalinity (mg/L as $CaCO_3$):	300	325	280
Total Organic Carbon (mg/L)	1.8	1.8	1.8

Table 3-5. HWTP Raw water quality during Phase 2 and 3

Water Quality Parameter:	**Mean:**	**Maximum:**	**Minimum:**
Temperature (˚C)	7.4	24.3	0.5
pH	8.1	7.6	8.5
Turbidity (NTU)	0.29	2.97	0.06
Alkalinity (mg/L of $CaCO_3$):	92	96	87
Hardness (mg/L of $CaCO_3$):	123	132	118
Nitrogen (N as total ammonia, mg/L):	0.12	0.40	0.02
Nitrogen (N as Nitrate, mg/L):	0.43	0.56	0.20
Organic Nitrogen (mg/L)	0.22	0.43	0.13
Total Organic Carbon (mg/L)	2.56	3.12	2.1

After diversion from the HWPT raw water sample line, raw water was fed to the pilot-scale filters through a pressure regulator at a rate of 9 L/min. For trials requiring coagulation, coagulant was injected into the line via a positive displacement chemical injection pump (Model Gala 1601 PPE, ProMinent Fluid Controls Ltd., Guelph ON). The coagulant solution was diluted to the appropriate concentration with distilled water before being added to the raw water. The coagulated water then passed through 4 static mixers (models ½-, 1-, and 2-40C-4-12-2, Koflo Corp., Cary IL) that were designed to mimic full-scale flocculation and contact time. The first static mixer, which represented rapid mixing, had an internal diameter of 1.25 cm and a length of 35 cm. The next, larger static mixer had in internal diameter of 2.5 cm and was 45 cm in length. Because it was larger than the first mixer, the water velocity within it was slower, resulting in lower shear forces that were less likely to break up newly formed floc. The subsequent two static mixers were 5 cm in diameter and 90 cm long.

Before entering the influent manifold at the base of the filter apparatus, 300 mL/min of raw water flow was diverted to the influent turbidimeter and particle counter. The remaining influent water fed into the pilot apparatus through the manifold at the base of the apparatus. Each column received water from the manifold through a rotameter (Model F-400, Blue-White Industries Inc., Huntington Beach, CA) and diaphragm valve. Raw water entered the filter columns via an influent port 1.52 m from the top of the filter column.

During seeding trials, each column received raw water at 3 L/min which passed through the filter by gravity flow. Flow through the column was controlled by a diaphragm valve on the effluent. Depending on the loading rate utilized, flow was either 0.745 L/min (10 m/h loading rate) or 1.86 L/min (24.4 m/h loading rate). Excess water exited the top of the filter through the overflow drain. Seed suspensions of oocysts and microspheres were pumped via peristaltic pump (Model 7553-70, Cole-Parmer Instrument Canada Inc., Montreal QC) into the filter column from a 2.5 L glass container on a magnetic stir plate. The seed suspension injection port was 61 cm above the upper surface of the filter media and was fitted with a distributor nozzle that released the seed suspension into the centre of the column through 6 radial openings.

Influent samples were collected from a port 46 cm below the seed injection port and stored in 250 mL glass sample containers pre-rinsed with a buffered surfactant solution (1× phosphate buffered saline [PBS] with final concentrations of: 0.1% sodium dodecyl sulphate, 0.1% Tween 80, and 0.01% Sigma Antifoam A and final pH of 7.4). At the base of each filter, 100 mL/min of filter effluent was diverted to an effluent sample collection line for the duration of each experiment. Effluent samples

were collected in 1 L glass bottles pre-rinsed with the buffered surfactant solution. Control samples were collected before the start of each experiment from all influent and effluent sample ports.

The majority of filter effluent flowed through an insertion magnetic flow meter (Model FMG 3001-PP, Omega Engineering Inc., Stanford CT). Downstream of the flow meter, approximately 300 mL/min was fed by peristaltic pump to the column's respective turbidimeter (Model 1720E, Hach Inc., Loveland CO) and particle counter (Model PCX2200, Hach Inc., Loveland CO). Head loss was measured using a differential pressure gauge (Model PX771A-100WCDI, Omega Engineering Inc., Stanford CT). The pressure gauge compared the water head in the column to that of the stand pipe attached to the bottom of the filter, such that changes in head loss caused by the filter media could be quantified. The measurements from the pressure gauges, turbidimeters and flow meters were recorded by 2 dataloggers (Model DI-710, DATAQ Instruments Inc., Akron OH) contained in an enclosure attached to the steel frame. Signals from the particle counters were fed through an RS 232 to RS 485 converter (Model RS 485, B&B Electronics Manufacturing Company, Ottawa IL), which allowed the data to be processed and recorded by a particle counter program (WinDaq, DATAQ Instruments Inc., Akron OH) running on a dedicated desktop computer.

Table 3-6. Filter Column Equipment

Equipment	Model	Manufacturer	Location
Turbidimeter	1720E	Hach Inc.	Loveland, CO
Particle counter	PCX 2200	Hach Inc.	Loveland, CO
Insertion magnetic flowmeter	FMG 3001-PP	Omega Engineering Inc.	Stanford, CT
Differential pressure gauge	PX771A-100WCDI	Omega Engineering Inc.	Stanford, CT
Rotameter	F-400	Blue-White Industries Inc.	Huntington Beach, CA
Static mixers (1/2, 1 and 2" in diameter)	½-40C-4-12-2, 1-40C-4-12-2, 2-40C-4-12-2	Koflo Corp.	Cary, IL
Overhead stirrer	RZR-50	Brinkmann Instruments Inc.	Westbury, NY
Injection Pump	Gala 1601 PPE	ProMinent Fluid Controls Ltd.	Guelph, ON
Data logger	DI-710	DATAQ Instruments Inc.	Akron, OH
RS-232-485 converter	RS 485	B&B Electronics Manufacturing Company	Ottawa, IL
Peristaltic pumps	7553-70, 7553-71, 7553-80, 7554-90	Cole-Parmer Instrument Canada Inc.	Montreal, QC

3.2.4 Filter Media

Standard sieve analyses were performed on all filter media using a standard sieve shaker (Oscillatap model ML 4330OST, M&L Testing Equipment, Dundas, ON) according to ASTM # C-136. Sieve data including effective size and uniformity coefficient are provided in Appendix B.

3.2.5 Conventional Media

The media used in most conventional (dual-media) filters generally consists of approximately 1.0 mm diameter anthracite over 0.5 mm diameter sand (MWH, 2005). For Phase 1 of the study, the conventional filter column was filled with angular to sub-angular sand with an ES of 0.44 mm and a UC of 1.52. The anthracite used was also angular, with an ES of 0.94 and a UC of 1.65. For Phases 2 and 3, the media in the conventional filter column were replaced with rounded to sub-angular sand (Figure 3-6 A) and sub-angular anthracite (Figure 3-6 C) obtained from one of the HWTP filters. This study's sieve analysis determined that the sand obtained from HWTP had an ES of 0.47mm, with a UC of 1.53. The anthracite had an ES of 0.89mm, with a UC of 1.70.

SEM images of the HWTP media demonstrate that both the sand and anthracite had relatively smooth surfaces (Figure 3-6 B and D, respectively). The surfaces of the sand grains showed more pitting than the anthracite. Neither media displayed any visible porosity.

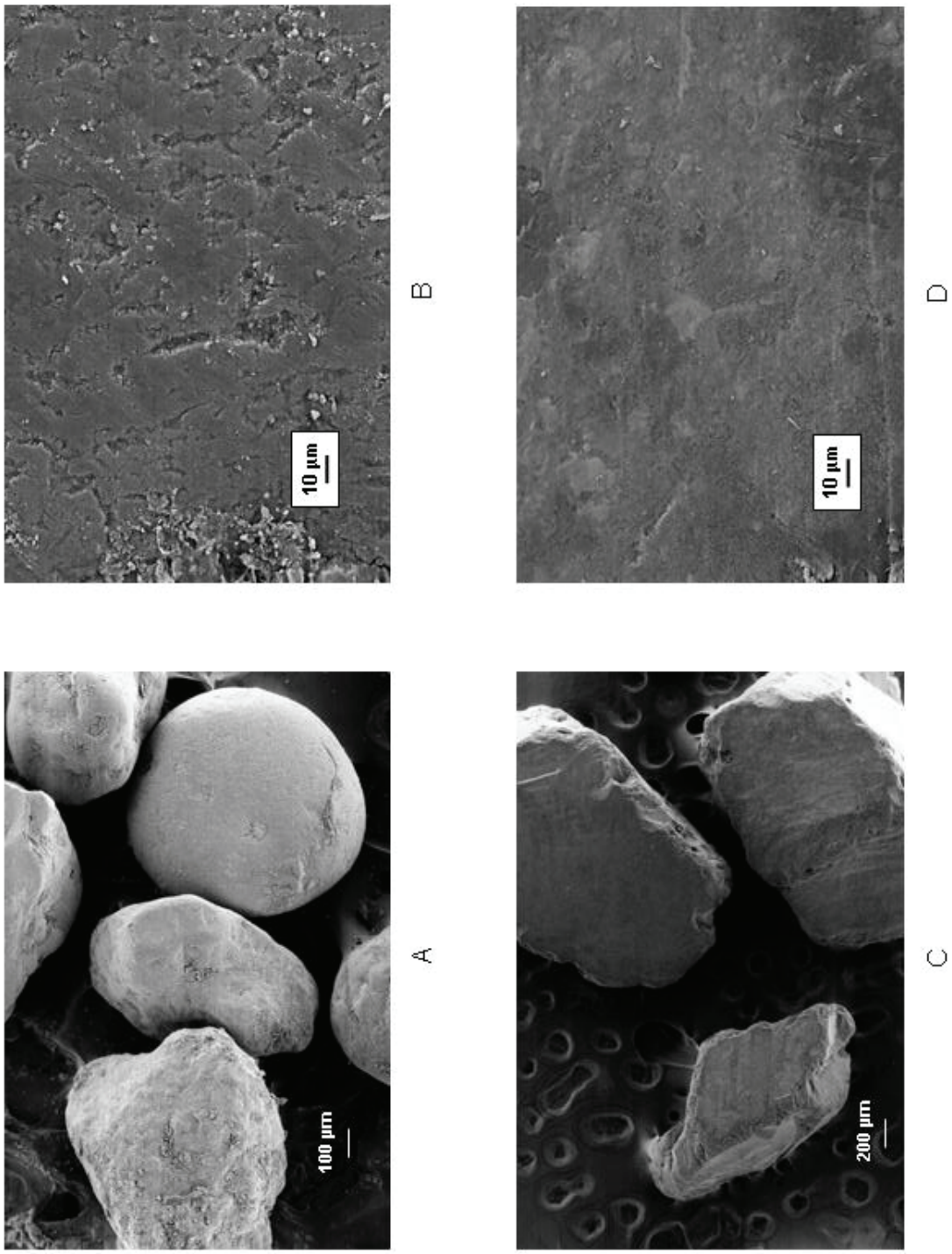

Figure 3-6. SEM image of conventional media obtained from HWTP filter (A) sand at 100X magnification, (B) sand surface at 2000X magnification, (C) anthracite at 50X magnification, and (D) anthracite surface at 2000X magnification

3.2.6 Engineered Ceramic Media

The rough engineered ceramic media used during all experimental phases of the present investigations were inert kiln-fired clay aggregates generally spherical in shape (Figure 3-7). The ceramic material used in this study is commercially known as "Macrolite™" and is composed primarily of nepheline syenite (approximately 90% by weight), with minor amounts of aluminum oxide, bentonite and silicon carbide (Kinetico, 1994). Standard sieve analyses indicated that the material had UC's generally between 1.12 and 1.60. SEM images of the ceramic media used in the "very fine", "fine" and "matched" media configurations displayed media surfaces that were densely covered with highly irregular asperities of all sizes (Figure 3-7 B). Asperities ranged from less than 0.5 μm to over 20 μm. Coarse ceramic media, with grains larger than 0.6 mm, could display larger "topographical" roughness features, which included crevices up to 50 μm wide and 300 μm long, and deep pores over 20 μm in diameter. The specific gravity (S_g) of these ceramic media is typically between 1.2 and 2.6.

Engineered media may exhibit more surface roughness than conventional media due to the processes involved in their manufacture. The ceramic media in this study are kiln-fired aggregates composed primarily of finely ground crystals of nepheline syenite aluminum oxide and bentonite. The high temperatures of the kiln act to remove all interstitial and bonded water and fuse the individual crystals to each other. The resultant ceramic material is porous and composed of randomly-oriented crystals of many sizes. Just as a section through the middle of a sponge will be as rough as its outside, abrasion of the ceramic media only serves to expose more surface texture (roughness).

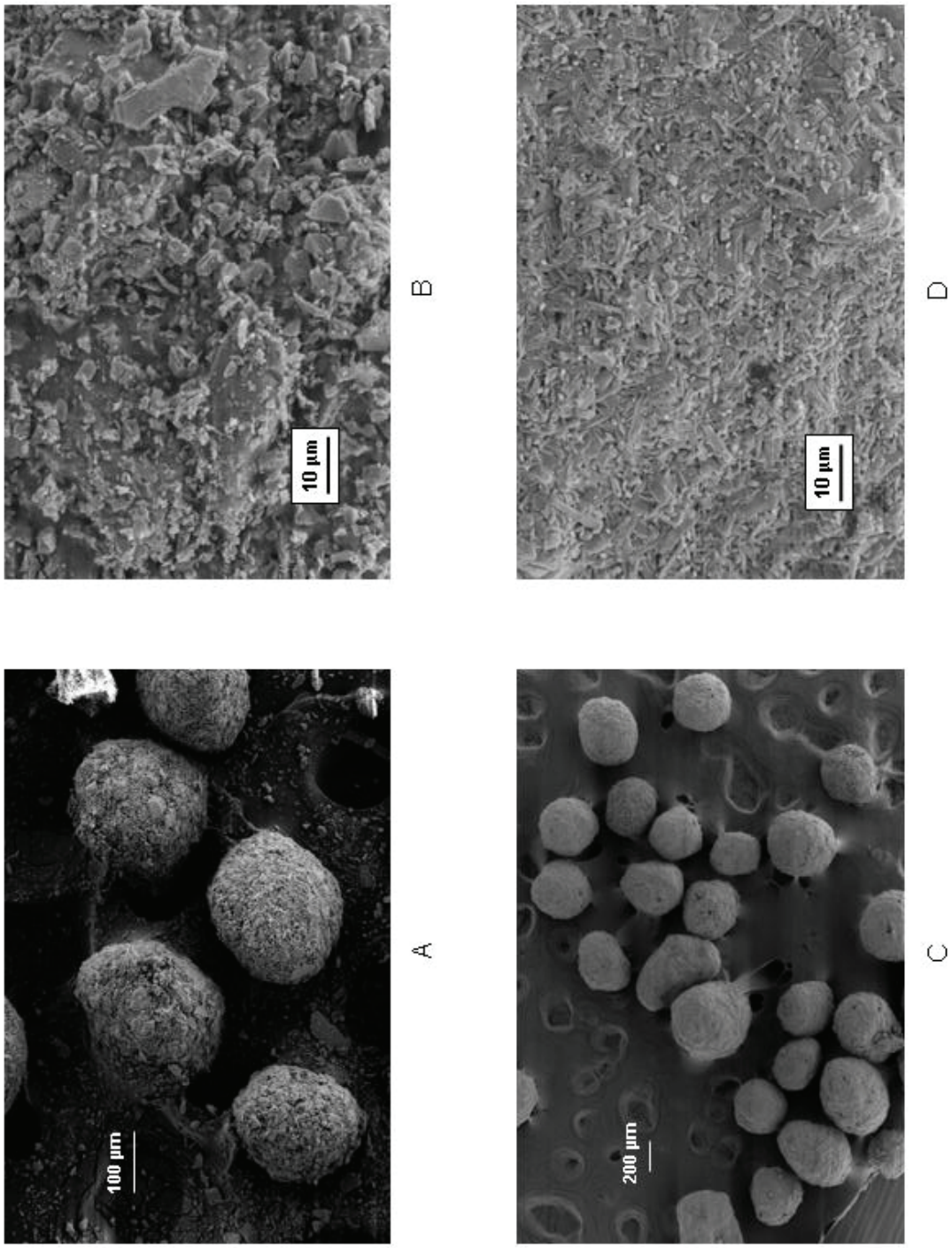

Figure 3-7. SEM Images of Ceramic Media, (A) fine ceramic at 200X magnification, (B) fine ceramic surface at 2000X magnification, (C) dense ceramic at 50X magnification, and (D) dense ceramic at 2000X magnification

The ceramic medium utilized in the lower layer of the "dense" media configuration (Phase 2 trials, Column 1) was a ceramic product being developed at the time (Figure 3-7, C) which had a S_g of 3.3. The denser minerals comprising the filter grains had a less angular, rod-shaped morphology visible in SEM images of the media surface (Figure 3-7 D). The resulting media surface had fewer pores, smoother features and a more consistent surface texture compared to the previously described, less dense ceramic media.

The use of engineered media, such those described herein, in drinking water filters may potentially result in particle and pathogen removal performance differences relative to conventional anthracite and sand media for the following reasons:

- ***Greater surface roughness.*** It has been suggested that filters with greater surface area are able to capture more particles (Stevenson, 1997; Kau and Lawler, 1995). Media with rough surfaces have greater surface areas than similarly sized smooth media. The use of rough media could thus increase the surface area of a filter without requiring greater media bed depth.

- ***Higher sphericity.*** Though colloid deposition modelling and laboratory experiments conducted using glass spheres or very small filters have suggested that "irregularity of grain shape contributes considerably to the straining potential" of a porous medium (Tufenkji, 2004), pilot filtration studies (MP&T, 1995; Kau and Lawler, 1995) suggest that spherical grain shapes may increase colloid capture.

- ***Adjustable properties.*** If it can be demonstrated that a particular level of surface roughness improves filtration, additional ceramic media may be manufactured to meet specifications. Size, density and chemical composition can also be adjusted to meet requirements.

3.2.7 Column Preparation

After full assembly of the pilot scale filtration columns, the bottom sections of the PVC columns were removed and filled with the desired amounts of media. Once the sections were re-attached, the media were backwashed for 2 hours, one column at a time. The ceramic media usually had a small proportion (0 to 10% of total media added) of low density particles that would wash out during media preparation, so sieves were placed over the floor drain to capture lost media. The volume of washed-out material was then measured and an equal amount ceramic media were added to the column to

ensure that design filter media depths were maintained. This loss of media only occurred during initial column preparation and not during subsequent backwashes.

3.2.8 Phase 1: Synthetic Water Experiments

The filter media configurations utilized during the Phase 1 preliminary investigations were based on filter bed configurations commonly used in full scale plants (MWH, 2005). The "conventional" media filter consisted of a graded gravel bed that supported the sand and anthracite (Table 3-7). This conventional configuration (configurations similar to 45 cm of anthracite over 35 cm of sand) is common in GMF facilities in North America (MWH, 2005; Bolton, 2005; Lawler, 2006). The "fine" ceramic media configuration was recommended by the manufacturer. It was the manufacturer's experience that a thin layer of support media was beneficial for filter run time. Accordingly, an 8 cm layer of garnet was used as the support medium for the ceramic media filters instead of the 20 cm graded gravel support medium that was used for the conventional configuration. The "very fine" configuration included a finer upper layer of ceramic media (0.45 mm ES), as part of a filter configuration that had been in use in municipal pressure filtration applications.

Table 3-7. Media Configurations and Characteristics Utilized During Phase 1 Experiments

	Column 1 **Very Fine Ceramic**	**Column 2** **Conventional**	**Column 3** **Fine Ceramic**
Upper layer	45 cm of ceramic, 0.45 mm ES, 1.39 UC	45 cm of anthracite, 0.94 mm ES, 1.65 UC	45 cm of ceramic, 0.96 mm ES, 1.60 UC
Lower layer	15 cm of ceramic, 0.21 mm ES, 1.12 UC	35 cm of sand 0.44 mm ES, 1.52 UC	15 cm of ceramic, 0.21 mm ES, 1.12 UC
Support media	8 cm of garnet, 0.34 mm ES, 1.44 UC	20 graded gravel 1 to 25 mm ES	8 cm of garnet, 0.34 mm ES, 1.44 UC
***L/d* ratio**	1704	1274	1193

The water source utilized during Phase 1 trials was tap water with kaolin induced turbidity (JT Baker Analytical, Phillipsburg, NJ). Nominal raw water quality data (prior to kaolin addition) were provided in Table 3-4. Water temperature remained between 13 and 14˚C during these trials. The turbidity was generally maintained at approximately 1 NTU (after kaolin addition) to simulate typical raw water turbidity influent to direct filtration processes. As specified previously, the Phase 1 trials were conducted at a loadings rate of 24.4 m/hr (10 gpm/ft^2) and 9.8 m/hr (4 gpm/ft^2).

Microsphere spike suspensions were prepared using tap water and a microsphere suspension (4.5 μm Fluoresbrite® carboxylate YG fluorescent polystyrene microspheres, Polysciences, Warrington, PA). They were mixed on a magnetic stir plate for at least 30 minutes before being introduced into the filter influent. From a 2.5 L container, the spike suspension was added for 30 minutes into each of the columns using a peristaltic pump with 3 pump heads (Model 7553-70 6-600 RPM, Cole-Parmer Instrument Canada Inc., Montreal QC). The spike suspension entered the filter influent approximately 61 cm above the individual filter beds, 46 cm above the influent sample ports (Figure 3-4). The microsphere spike concentration was selected to achieve effluent sample concentrations that were approximately 10^4 to 10^5 microspheres/L.

To ensure no carryover of microspheres or oocysts between experimental trails, negative control samples were collected from both the influent and effluent sample ports before the start of each spike experiment. For the first trial, influent and effluent samples were collected at 0, 15, 30, 45, 60, 120, 180, 300 and 420 minutes after spike addition commenced. During subsequent trials, samples were collected every 10 minutes during the spike injection. All collected samples were stored in the dark at 4˚C until analysis. Samples were processed within approximately 2 weeks (or less) of collection.

3.2.9 Phase 2: Lake Ontario Water Experiments without Coagulant Addition

After the initial spike experiments in Waterloo, all subsequent spike experiments were conducted at the HWTP, which is operated by the City of Toronto. All testing at the HWTP used the plant's raw water sample line, which provided the filter columns with uncoagulated, unchlorinated water directly from Lake Ontario.

In preparation for Phase 2 testing, a number of changes were made to the filter configurations. The media characteristics and configurations used during the Phase 2 experimental period are presented in Table 3-8. All filter columns were given identical graded gravel support media. As mentioned earlier in the section regarding media size, the *L/d* ratio has been used as a benchmark for filter design (Montgomery, 1985). The *L/d* ratios of ceramic media filters in Phase 1 of the study were significantly higher if the support media was included in the calculations. The graded gravel bed raised the *L/d* ratio for the conventional media 54 to 1329, while the garnet support media contributed 235 to the ratios of the ceramic media configurations. To ensure that differences in filtration performance between the ceramic and conventional media were not influenced by support media, Phase 2 experiments used the same graded gravel support media in all 3 columns. The graded gravel bed used in all columns for Phase 2 and 3 trials was made with the following sizes of gravel:

- 2 cm of 10-14 mesh sand (grain size approx. 1.5 mm), screened from "Red Flint™," fine gravel,
- 6.5 cm of "Red Flint™" fine gravel (grain size approx. 2.5 mm),
- 6.5 cm of pea gravel (grain size approx. 5 mm), and
- 5 cm of coarse gravel (grain size approx. 15 mm).

In addition to changing the support media, Column 1 was filled with a dense ceramic medium (Table 3-8), which had a density of approximately 3 g/cm^3. The configuration was similar to that of the "fine" ceramic media configuration used during Phase 1. Column 2 had the same "fine" ceramic configuration as was used in Column 3 during Phase 1. This configuration maintained continuity between phases and, based on the manufacturer's experience, represented an optimized ceramic media configuration.

Table 3-8. Media Configurations and Characteristics Utilized During Phase 2 Experiments

	Column 1 **Dense Fine Ceramic**	**Column 2** **Fine Ceramic**	**Column 3** **Conventional**
Upper layer	45 cm of ceramic, 0.64 mm ES, 2.11 UC	45 cm of ceramic, 0.96 mm ES, 1.60 UC	45 cm of anthracite, 0.89 mm ES, 1.70 UC
Lower layer	15 cm of ceramic, 0.22 mm ES, 1.23 UC	15 cm of ceramic 0.21 mm ES, 1.12 UC	30 cm of sand, 0.47 mm ES, 1.53 UC
Support media	20 graded gravel 1 to 25 mm ES	20 graded gravel 1 to 25 mm ES	20 graded gravel 1 to 25 mm ES
***L/d* ratio**	1401	1193	1144

A conventional filter configuration comprised of media collected directly from HWTP filters was installed in Column 3 with the same filter configuration as the HWTP filters. By utilizing the same media and configuration as the plant, it was hoped that performance of the conventional media in this pilot investigation would match the HWTP filter performance. If so, the findings of this study would likely be applicable to full scale GMF operations

All of the Phase 2 trials at the HWTP consisted of:

- backwash with combined water and air scour,

- a period of filter ripening of at least 4 hours,
- a 1-hour spike with influent and effluent samples collected every 10 minutes, and
- an additional 5-hour monitoring phase after the spike injection, with less frequent sampling.

The preliminary trials of Phase 2 (2A and 2B) at the HWTP occurred in August 2006. These two spike trials were conducted with only microspheres in the seed suspension to confirm the methods to be used in the subsequent trials, all of which were conducted with the addition of both latex microspheres and *Cryptosporidium parvum* oocysts. Spike concentrations were used such that filter influents would contain between 10^4 and 10^5 microspheres and *Cryptosporidium* oocysts per litre. All trials in this group of experiments were conducted without coagulant, representing filter performance under a complete coagulation failure. This represented a worst case scenario for water filtration.

3.2.10 Phase 3: Lake Ontario Water Experiments with Coagulant Addition

Due to lower turbidity reduction from Column 1 during Phase 2 experiments, it was evident that the "dense" media configuration was not optimal at the filtration conditions investigated. This presented an opportunity to begin filter performance experiments that would directly compare conventional and rough engineered ceramic media performance during GMF. The media characteristics and configurations used during the Phase 2 experimental period are presented in Table 3-9.

A detailed sieve analysis of the conventional media obtained from one of HWTP's filters was used to create a filter containing rough engineered ceramic media with a configuration as close to that of the conventional filter as possible. Three different sizes of light-weight ceramic media were screened and combined so that the final media had the same proportion of grain sizes as the anthracite from the HWTP filter. The same process of sieving and mixing was conducted on 3 different sizes of denser ceramic media in order to match the sand from the HWTP filter. The bulk density ratio between the light and heavy ceramic media was similar to that of anthracite and sand. The media were combined to create a ceramic filter with the same ES and UC, as well as a similar media interface between heavy and light materials (Table 3-9). By matching the conventional media, the two columns had approximately the same number of collectors, the same configuration, bed depth, media size, uniformity coefficient and *L/d* ratio. A comparison between Columns 1 and 3 would therefore indicate whether or not the rough engineered ceramic media's surface properties were the cause of any observed difference in filter performance.

Table 3-9. Media Configurations and Characteristics Utilized During Phase 3 Experiments

	Column 1 **Matched Ceramic**	**Column 2** **Fine Ceramic**	**Column 3** **Conventional**
Upper layer	45 cm of ceramic, 0.89 mm ES, 1.70 UC	45 cm of ceramic, 0.96 mm ES, 1.60 UC	45 cm of anthracite, 0.89 mm ES, 1.70 UC
Lower layer	30 cm of ceramic, 0.47 mm ES, 1.53 UC	15 cm of ceramic 0.21 mm ES, 1.12 UC	30 cm of sand, 0.47 mm ES, 1.53 UC
Support media	20 graded gravel 1 to 25 mm ES	20 graded gravel 1 to 25 mm ES	20 graded gravel 1 to 25 mm ES
***L/d* ratio**	1144	1193	1144

The first of Phase 3's thirteen trials (3A) was conducted to determine if spike concentrations affected *Cryptosporidium* oocyst and oocyst-sized microsphere removals by GMF. It was hypothesized that the high dose of *Cryptosporidium* oocysts in the spike suspension may affect the filter performance by creating what Ko and Elimelech (2000) termed "shadow effects". All trials subsequent to Trial 3A were conducted using coagulated raw water to simulate full scale operation.

Before commencing Phase 3's coagulant trials, the pilot filters were conditioned by operating with coagulation for 3 weeks because the ceramic media are more porous and might require more time to reach stable operation (relative to conventional filtration media). Operators at the HWPT commonly noted that when the plant switched coagulants, a phenomenon called "blue-water" could occur, during which time the combination of alum and PACl coagulants interfered with each other. At these times, HWTP filter operation could be significantly impaired. Accordingly, this conditioning period was also necessary because alum coagulant had been used in the pilot filters during the Phase 1 trials and PACl was going to be used during the Phase 2 trials.

Trial 3B was the first of the trials conducted with coagulant addition. The plant's effluent turbidity was matched by increasing the coagulant dosage to the pilot unit until the conventional filter column had effluent turbidity similar to that of the full-scale filters. The effluent turbidity was eventually matched by using a coagulant dose more than 5 times higher than that used by the plant. Terminal head loss in the conventional media was reached after 5 hours of operation, while the plant's filter run time was more than 48 hours (the loading rate to the full-scale filters was also much lower, at 4 m/hr as opposed to 24.4 m/hr in the pilot filters). To get sufficiently long filter runs, it was decided that subsequent trials would receive the same coagulant dose as the full-scale plant, with the recognition that the pilot- and full-scale conventional filter turbidities may not be matched. Trials 3C to 3G were

conducted with these "optimal" coagulant doses that were equal to those being applied at the full-scale the plant (0.6 mg/L PACl).

Sub-optimal coagulation trials (3H to 3K) used PACl coagulant concentrations that were 50% (0.3 mg/L PACl) of the full-scale plant's applied dosage. These experiments were conducted to investigate how filter performance was affected by sub-optimal coagulant dosing. Trials 3L and 3M were conducted during the summer of 2007 to investigate whether the use of a different coagulant type (alum) and higher water temperatures (20˚C as opposed to less than 8˚C) affected the ceramic media's filter performance differently from the conventional media.

3.3. Water Quality and Filter Performance Analyses

3.3.1 *Cryptosporidium* Oocyst and Microsphere Enumeration

The *C. parvum* oocysts used during the seeding experiments were bovine in origin, and were provided in a clean, purified form (Sterling Parasitology Laboratory, University of Arizona, Tucson, AZ). They were inactivated with 5% formalin (final concentration) in 1× PBS with 0.01% Tween 20 to prevent clumping. All microorganism stocks were refrigerated at 4°C in the dark until use.

All samples collected at HWTP for microsphere and oocyst enumeration were kept in coolers on ice and transferred as quickly as possible (typically within 3 hours of the completion of an experiment) to refrigerated storage at 4˚C. Samples collected at the beginning of a 6-hour trial would thus wait roughly 9 hours before being refrigerated. Ambient temperatures in the testing location were generally the same as the water temperature in the summer months and 13˚C to 16˚C during winter months. Once refrigerated, all samples remained in storage at 4˚C in the dark until removed for analysis. The sample storage period was typically less than 2 months, but reached as much to 3-4 months in a few instances. Differences in enumeration results were not observed with regard to storage duration.

C. parvum oocyst analysis was performed using a direct membrane filtration and a standard immunofluorescence assay (IFA) method similar to that reported by Emelko (2001) and Watling (2004). A detailed methodological protocol is provided in Table 3-11. All samples were vigorously mixed before being filtered through 25mm, 0.4µm nominal porosity polycarbonate filter membranes (Whatman Inc., Clifton NJ). These membranes were supported by 25mm, 8.0µm nitrocellulose membranes (Millipore Canada Inc., Nepean ON), which were placed directly on a manifold (model FH225VM, Hoefer Scientific, San Francisco CA). The membranes were kept in place with stainless

steel filter weights having approximately 20 mL volumes. When filtering volumes larger than 100 mL, PVC riser tubes were attached to the filter weights which had a capacity of approximately 250 mL. Phosphate buffered solution (PBS), DABCO-glycerol mounting medium, bovine serum albumin (BSA) reagents were prepared as outlined in the literature included in the Hydorfluor™ Combo *Cryptosporidium* and *Giardia* Kit. NoFade™ Mounting Medium (Waterborne Inc., New Orleans, LA) was used instead of the DABCO-glycerol for the analyses of Trial 3C and thereafter. Eluting solution (buffered detergent solution) was prepared by mixing 100 mL of 1% sodium dodecyl sulfate (SDS), 100 mL 1% polyoxyethylenesorbitan monooleate 80 (Tween 80), 100 mL 10X PBS, and 0.1 mL Sigma Antifoam A (Sigma Chemical Co., Cat. No. A5758) with 500 mL of distilled water. The pH was adjusted to 7.4 using 0.1 N HCl or 0.1 N NaOH, and the final volume adjusted to 1 L with additional distilled water.

Due to the time and cost requirements of the *C. parvum* analysis, only a subset of the collected samples were enumerated (influent samples times at 25, 35, 45, 55 minutes after start of spike injection and effluent sample times 20, 30, 40 and 50 minutes after spike injection). Volumes to be filtered through the membranes were chosen to ideally yield 200 to 500 oocysts/microspheres per membrane (Emelko et al., 2008). *C. parvum* identification during trials 2C to 2E was conducted using the Strategic Diagnostics (Newark DE) HydrofluorTM stain. The quality of that stain changed (due to changes in its production). As a result, all subsequent *C. parvum* analyses were conducted using Waterborne Inc.'s (New Orleans. LA) Crypt-a-Glo™ stain. When using the Hydrofluor™ stain, enumeration of *C. parvum* oocysts was performed at 400X magnification. Most samples prepared using the Crypt-a-Glo™ stain were enumerated at 200X magnification. All samples were enumerated using a Zeiss Axioskop 2 Plus (Carl Zeiss Canada Inc., Toronto, ON), fitted with an HBO 100 UV lamp and appropriate UV filters for fluorescein isothiocyanate (FITC) fluorescence.

Carboxylated fluorescent-dyed polystyrene microspheres (Fluoresbrite® carboxylated YG microspheres, Polysciences, Warrington, PA) were used as non-biological surrogate indicators for *C. parvum* oocyst removal by filtration. The oocyst-sized microspheres had a mean diameter of 4.889 ± 0.208 μm and a density of 1.045 g/mL. The dye contained in the microspheres is a proprietary chemical that has maximum excitation at 458 nm and maximum emission at 540 nm, which allows their concurrent enumeration with FITC-stained oocysts. In general, microspheres were enumerated concurrently with *C. parvum* oocysts. When analyzing samples solely to enumerate microspheres, the same filtration protocol was used without the inclusion of the IFA staining steps and microspheres were enumerated at 100X magnification.

3.3.2 Turbidity and Total Particle Counts

A standard protocol was used to verify the calibration of the particle counters. It involved using commercially available, calibrated, mono-disperse polymer microspheres (Duke Scientific Corporation, Palo Alto, CA.). Each particle counting instrument was calibrated by the manufacturer. The particle counters (Hach 2200 PCX Particle Counter, Hach Co., Loveland, CO.) measured total particles from 2-750 μm, with the data reported as total number of particles ≥2 μm. Filter influent and effluent particle counts were monitored. Turbidity was monitored using on-line turbidimeters (Hach Model 1720C, Hach Co., Loveland, CO.) that were calibrated using dilute formazin solutions as specified by the manufacturer. Turbidimeters were also used at the filter influent and effluent locations.

3.3.3 pH

Sample pH was measured with grab samples analyzed by a pH meter that was calibrated daily, using pH 7.00 and 9.18 buffer solutions.

3.3.4 Headloss

Differential pressure gauges (Model PX771A-100WCDI, Omega Engineering Inc. Stanford, CT) continuously measured headloss during all trials.

3.3.5 Calculation of *C. parvum* Oocyst and Microsphere Removals by Filtration

Cryptosporidium oocyst and microsphere removals were calculated as the $\log_{10}$ of the ratio of the influent and effluent concentrations. In the event that the microspheres or *Cryptosporidium* oocysts on a microscope slide were too numerous to count, the sample would be reprocessed with a smaller volume of water and a correspondingly lower number of oocysts and microspheres on the slide. A recovery study and system losses study were conducted after Trial 3M was completed. Details of both experiments are described in Appendix B.2. Analysis of the recovery study determined that the variability in results was over-disperse and that system losses for both microspheres and oocysts were minimal. For this reason, all microsphere and oocyst data presented herein are unadjusted.

3.3.6 Example Data

To illustrate the mathematical approach used to assess the difference in removals between different filter media, microsphere data from Trial 3E are shown below (Table 3-10). To calculate the

log_{10} removal of microspheres at time 40 min, the influent data at time 45 (which represents the concentration of microspheres in the influent at 45 minutes after the spike experiment began) and effluent data at time 40 (which represents the mean microsphere concentration from 40 minutes to 50 minutes after the spike experiment began) were used. The log_{10} of the ratio of the influent and effluent concentrations yields the log_{10} removal of 1.79 at this time. The log_{10} removal for the entire spike is calculated from 20 minutes to 60 minutes after the start of spike injection. Starting the enumeration 20 minutes after the start of spike injection allowed *Cryptosporidium* oocysts time to pass through the filter and for effluent concentrations to stabilize. To calculate the mean *Cryptosporidium* oocyst removal achieved during the trial, the influent *Cryptosporidium* oocyst concentrations were summed and divided by the sum of effluent concentrations. The log_{10} of this ratio produced the mean log_{10} removal achieved by the filter during a particular seeding experiment.

Table 3-10. Example of Calculations

Total *Cryptosporidium* counted in influent at time 45:	784
Volume of sample:	1.25 mL
Concentration of *Cryptosporidium* in influent at time 45:	784 X 1000 mL/L ÷1.25mL = 627,200 ***Cryptosporidium***/L
Total *Cryptosporidium* counted in effluent at time 40:	205
Volume of sample passed through membrane:	20 mL
Concentration of *Cryptosporidium* in influent, at time 40:	205 X 1000 mL/L ÷ 20 mL = 10,250 ***Cryptosporidium***/L
Ratio of influent to effluent concentrations:	627,200÷ 10250 = 61.2
Log_{10} removal of *Cryptosporidium* at time 40:	$Log_{10}(61.2) = 1.79$
Sum of influent concentrations (time 25 to 55 minutes):	268,800 + 680,800 + 627,200 + 561,600 = 2,138,400
Sum of effluent concentrations (time 20-60 minutes):	4,000 + 6,100 + 10,250 + 45,500 = 65,900
Mean log_{10} removal for Trial 3E:	$Log_{10}(2,138,400 \div 65.900) = 1.45$

Table 3-11. Summary of Modified *Cryptosporidium* IFA Method

1. Rinse all graduated cylinders, pipette tips, and riser tubes with eluting solution
2. Prepare stains and reagents according to the instructions provided in the Hydrofluor Combo Kit and store all reagents in the dark at 4˚C
3. Ensure that vacuum chamber under filter manifold is empty and drain clamp is firmly closed. Close filter ports and wet with PBS
4. Place 25 mm diameter 8.0 µm support membrane in filter port with forceps
5. Place 25 mm diameter 0.4 µm filter membrane in port with forceps, holding the membrane by the outer edge.
6. Open valve on filter port to let PBS drain. If membranes are not centred after draining, close port, re-wet filter, adjust membranes and drain again. Be careful to only contact

the outer edge of the membrane to ensure that the membrane is never punctured. Repeat these steps as necessary until filter membranes properly centered in the port.

7. Place filter weight (with attached riser tube if filtering more than 50 mL) over membrane and pour in approximately 10mL into the filter well. Inspect the bottom of the filter weight for PBS seeping from the bottom.
8. Repeat steps 3 to 7 for all additional samples and positive and negative controls, keeping at least one filter port empty to allow for vacuum control
9. Open empty filter port and turn on vacuum pump. Adjust port valve so that vacuum in chamber is between 5 and 10 inches Hg.
10. Open filter ports to drain PBS.
11. Close ports, add 2 mL of BSA solution and drain.
12. Close ports and add PBS to keep filter membranes wet.
13. Shake all sample bottles before measuring out volume to be sampled. For larger volumes, weigh sample bottles before and after pouring sample directly into riser tube. For sample volumes between 50 and 100 mL, use graduated cylinders and for smaller volumes, use appropriately sized pipettes and pipette tips.
14. Open filter port.
15. Carefully filter samples through the appropriate filter membranes.
16. Rinse each riser tube and graduated cylinder twice with eluting solution and filter the eluting solution through the membrane between rinses.
17. For the negative control, add 2 mL of PBS. The negative control is to test the cleanliness of the apparatus and the effectiveness of washing methods. Other types of negative control can include such things as filtrate from the vacuum tank which would determine if oocysts were passing through the membranes.
18. Ensure all ports are closed and vacuum pump is detached from the filter manifold
19. If using riser tubes, replace filter weight and attached riser tube with a clean filter weight.
20. Add 0.5 mL of antibody stain to each filter weight and cover with foil for 40 minutes.
21. Reconnect vacuum pump and rinse each membrane 5 times with 2 mL of 1 X PBS, draining filter ports between each rinse.
22. Remove filter weights from the manifold.
23. Label microscope slides and add one small drop of mounting medium to each slide in the location that the filter membrane will be placed.
24. With rinsed and flamed forceps, place the 0. 4 μm filter membrane on the appropriate slide and place one more drop of mounting medium onto the middle of the membrane. Rinse and flame forceps. Repeat for each membrane.
25. Cover each membrane with a coverslip and seal the coverslip with clear nail polish after air bubbles have been removed from under the coverslip.
26. Enumerate at 200X magnification. Use 400X magnification where necessary (in case of clumping, interfering matter, *etc.*).

4. Results and Discussion

During the course of this research, 21 pilot-scale seeding trials were conducted to examine the impact of media roughness on filter performance and to evaluate the applicability of spherical, rough engineered ceramic filter media for use in conventional granular media filters used during drinking water treatment. This work was comprised of three research phases conducted at two research platforms: the University of Waterloo (2 preliminary trials comprising Phase 1 of experimentation) and the Horgan Water Treatment Plant in Scarborough, Ontario, Canada (19 trials comprising Phases 2 and 3 of experimentation). Details regarding the experimental approach and research platforms were provided in Chapter 3.

The detailed results from all of the conducted experimental trials are summarized in Appendix C. The effect of loading rate, coagulant type and dosage, as well as the suitability of latex microspheres as surrogates for *Cryptosporidium* oocyst removal by granular media filtration were examined. Filter media performance during the pilot-scale investigations was mainly assessed by filter effluent turbidity and particle counts, *Cryptosporidium* oocyst and microsphere removal and head loss. Additionally, stability of operation was evaluated. Disinfection processes are operated based on the lower limits of filter performance to ensure that during periods of least optimal filter performance (*i.e.* highest filter effluent turbidity), the treated water remains potable. For this reason, it can sometimes be preferable to operate a filter with good but stable performance over a filter with excellent quality effluent but occasional filtration "failures" (*i.e.* spikes in filter effluent turbidity), particularly when those failures are sustained over some period of time. For the purposes of this study, differences in stability of operation between filters were compared qualitatively, without specific quantification of "stability" because variations in raw water conditions did not allow for meaningful quantitative comparisons between trial conditions and because the development of a quantitative measure of filtration process "stability" was beyond the scope of this thesis research.

4.1. Phase 1 Results

During the Phase 1 pilot-scale studies, preliminary, proof-of-concept investigations focused on engineered ceramic media screening and optimizing operation of the pilot-scale filtration unit. These experiments were conducted using synthetic raw water. Specifically, two oocyst-sized microsphere seeding experiments were performed at the University of Waterloo to compare microsphere, turbidity,

and particle count reductions by conventional and various spherical, rough engineered ceramic filtration media.

The spike suspensions used in Phase 1 contained fluorescent oocyst-sized microspheres but no *Cryptosporidium* oocysts. They were added to synthetic raw water that was comprised of tap water with approximately 1.0 NTU of kaolin-induced turbidity. The loading rates used during the trials were 24.4 m/hr during Trial 1A and 9.8 m/hr during Trial 1B. Further operational and experimental details were provided in Section 3.2. Table 4-1 summarizes the filter effluent turbidities and total particle counts, oocyst-sized microsphere reductions and head loss observed during the Phase 1 filtration experiments; mean values obtained over the duration of each trial are presented.

Table 4-1. Summary of Mean Filter Effluent Turbidities and Total Particle Counts, Oocyst-Sized Microsphere Reductions and Head Loss During Phase 1 Filtration Experiments

Experimental Details & Performance Measures	Influent	Very Fine Ceramic	Conventional	Fine Ceramic
Trial 1A (9.8 m/hr)				
Turbidity (NTU)	1.119	0.067	0.365	0.145
Particle counts (total >2µm/mL)	11569	264	2295	855
Microsphere Removal (log_{10})	-	2.81	0.71	1.86
Clean Bed Head Loss (cm)	-	144	71	143
Trial 1B (24.4 m/hr)				
Turbidity (NTU)	1.125	0.050	0.253	0.086
Particle counts (total >2µm/mL)	11690	86	1016	245
Microsphere Removal (log_{10})	-	3.71	1.56	3.62
Clean Bed Head Loss (cm)	-	82	28	78

From the data in Table 4-1, it is clear that the ceramic media were more effective than conventional media in removing particles and lowering turbidity. During both trials, the "fine" engineered ceramic media consistently achieved better microsphere removals than the conventional media by approximately 1 log_{10}, whereas the "very fine" engineered ceramic media removed approximately 2 log_{10} more microspheres than the conventional media.

As is evidenced by turbidity results from Trial 1A (Figure 4-1), compared to the conventional media, the engineered ceramic media offered more operational stability; that is, filter effluent turbidity was more stable in response to variations in filter influent water quality. During Trial 1A there was a cyclical variation in filter influent turbidity resulting from the mode of turbidity injection

into the filter influent. Comparison of the influent and effluent turbidity data obtained during this experiment demonstrates that the effluent turbidity from the conventional media filter fluctuated consistently with the influent turbidity; the amplitude of the cyclical turbidity variation in the filter effluent was dampened, however. This effect raw water turbidity on effluent turbidity was particularly evident at 150 minutes after the start of the microsphere seeding period, at which point the influent turbidity increased and remained elevated throughout the remainder of the experiment. Although the response in the filter effluent from the conventional filter was offset (as would be expected), the filter effluent turbidity also increased and remained elevated. In contrast, neither of the engineered ceramic media filters appeared to be affected by either the periodic variation or the later elevation in influent water turbidity; that is, the filter effluent turbidity from these filters remained consistent and stable. Comparison of particle count data from the three columns revealed similar differences in filter performance as well as operational stability.

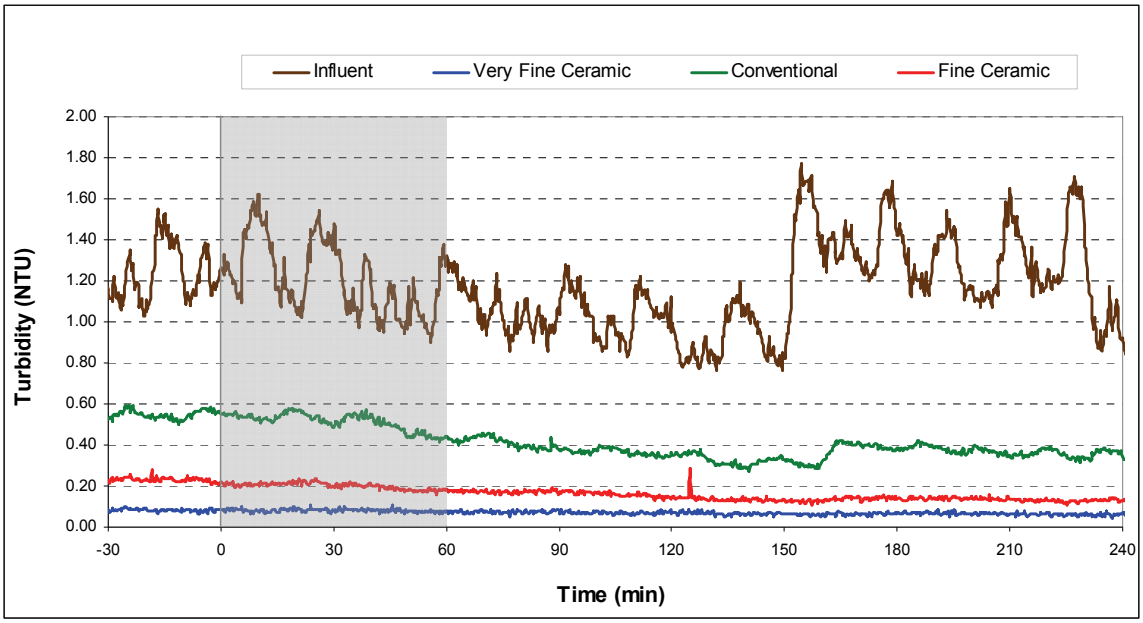

Figure 4-1. Filter Influent and Effluent Turbidity During Trial 1A. The grey shaded section represents the 60 minute period of microsphere injection.

In granular media filtration, the diameter of media grains (*d*) is often compared to the depth of the media in the filter (*L*) as described in Section 2.3.1. During the present investigation, the *L/d* ratio for the very fine ceramic media configuration was substantially different from that of the conventional filter because the media were smaller and the filter configuration included different support media. Including the gravel support media, the conventional column had an *L/d* ratio of 1329, while the very

fine ceramic media had an *L/d* ratio of 1939. The fine ceramic column had an *L/d* ratio of 1429, which was 7% higher than the conventional column. Despite this small difference in *L/d* ratios between the conventional and fine ceramic filters, it is clear that these two filter columns did not perform similarly, as indicated by filter effluent turbidity and particle count data. This suggested that the *L/d* ratio alone is not an ideal predictor of filter performance. The main differences between the ceramic and conventional media filter configurations were: a) the ceramic media had a much finer lower layer than the sand layer in the conventional filter, and b) the surface textures of the ceramic media was much rougher than the conventional media. Since the filter configurations were tested in parallel and simultaneously, all other variables were held as close to constant as possible. Results from the Phase 1 experiments therefore suggested that the observed difference in performance was due to differences in both media properties and media sizes between the columns.

It should be noted that the enhanced particle, turbidity, and pathogen surrogate removal performance of the ceramic media did come at an operational price: the ceramic media filters had higher head losses that limited filter run length. For example, during Trial 1A, which was conducted at a loading rate of 24.4 m/hr, the clean bed head loss in both the filters containing engineered ceramic media was approximately 143 cm; 71 cm greater than that observed in the conventional media filter. The differences in head loss were smaller in Trial 1B during which a lower loading rate of 9.8 m/hr was utilized. In Trial 1B, the head loss in the ceramic and conventional media filters was approximately 80 and 29 cm respectively. The two filter columns containing engineered ceramic media had similar head losses throughout all observed filter cycles, suggesting that the measured increase in head loss relative to conventional media was caused predominantly by the fine 0.21 mm ES media. Headloss build up during Phase 1 trials was negligible for all filter media, resulting in 0 to 4 cm of additional headloss over 6 hours of filtration.

The Phase 1 trials also indicated that filter performance was adversely affected by increased loading rates at the conditions investigated. While both of the engineered ceramic media filters achieved better than 3.5 $\log_{10}$ reductions of microspheres when filter loading was 9.8 m/hr, microsphere removal by the very fine and the fine engineered ceramic media dropped to 2.8 and 1.9 $\log_{10}$ respectively when the loading rate was increased to 24.4 m/hr. Similarly, microsphere removal by the conventional media filter dropped from 1.6 $\log_{10}$ to 0.7 $\log_{10}$ when the filter loading rate was increased. The increase in loading rate was also accompanied by decreases in filter effluent turbidity and particle count reductions (*i.e.* higher filter effluent turbidities and particle counts) (Table 4-2). The decline in turbidity reduction due to increased loading rate was the greatest for the conventional media, while the very fine ceramic media was the least affected.

The RT model has been used to demonstrate the value of having a fine lower media under poor coagulation conditions (O'Melia and Shin, 2001, from MWH, 2005). When raw water is not properly conditioned for filtration (*i.e.* due to insufficient coagulant addition) the attachment efficiency decreases. The use of finer filter media facilitates better colloid/collector contacts, lessening the decline in turbidity and particle count reductions during poor raw water pre-treatment. It is therefore not surprising to observe that the finer media was less affected by changes in loading rate (MWH, 2005).

4.1.1 Key Findings from Phase 1

- During Phase 1 trials using synthetic water with kaolin-induced turbidity, filters with engineered ceramic media configurations consistently produced better effluent water quality and were less affected by perturbations in influent water quality, as measured by particle counts, turbidity and microsphere removal.

- The engineered ceramic media had 50 cm to 75 cm higher clean bed head losses relative to conventional media configurations, especially at the higher loading rates investigated,

- Differences in filter performance were possibly due contrasts in media surface characteristics but differences in filter configuration (specifically size of media) confounded any mechanistic interpretation of the data.

- Filter performance was impaired at higher loading rates (24.4 m/h as compared to 9.8 m/hr). The particle and turbidity reductions of the filter configurations using smaller media were less affected by the increased loading rates.

4.2. Phase 2

Experiments conducted during Phase 1 indicated that improvements in filter performance might be associated with the surface characteristics of the engineered ceramic media. Accordingly, the pilot-scale filtration unit was relocated for further investigation at a site where the filters could process a "real" source water that was used by a full scale filtration plant producing potable water. The filtration plant chosen was the Horgan Water Treatment Plant (HWTP), which is a direct filtration plant situated on the north shore of Lake Ontario, east of Toronto, Ontario. The plant's raw water sample line supplied the pilot-scale filters with raw, uncoagulated, unchlorinated water. Details regarding HWTP operations and the nominal raw water quality were provided in Table 3-5.

The Phase 2 pilot-scale investigations continued comparing conventional and spherical, rough engineered ceramic media configurations optimized for the specific media (different media sizes and depths). Similar to Phase 1, the experiments were conducted without chemical coagulant addition; however, the source water was from Lake Ontario rather than the synthetic source water used during phase 1. Two of the filter configurations were changed from those used during Phase 1. Sand and anthracite were collected from the full scale filters at the HWTP replaced the conventional media configuration used during Phase 1. The anthracite and sand depths used were identical to those used in the HWTP's full-scale filters. In addition, the "very fine" engineered ceramic media used during Phase 1 were replaced by a "dense" engineered ceramic configuration that was similar in grain size and configuration to the "fine" ceramic media. The "fine" ceramic media configuration used during Phase 1 was also used during Phase 2; however, it was transferred from Column 3 into Column 2. Details regarding the conventional and engineered ceramic filtration media and experimental conditions utilized during Phase 2 are provided in section 3.2.

Phase 2 consisted of six seeding trials. Oocyst-sized microspheres were seeded into the filter influent during the first two trials. Both oocyst-sized microspheres and formalin-inactivated *Cryptosporidium* oocysts were seeded into the filter influents during the subsequent four seeding trials. The results obtained from the seeding trials conducted during Phase 2 are summarized below (Table 4-2).

Table 4-2. Summary of Mean Filter Effluent Turbidities and Total Particle Counts, *Cryptosporidium* Oocyst and Oocyst-Sized Microsphere Reductions Phase 2 Filtration Experiments

	Influent	**Dense Ceramic**	**Fine Ceramic**	**Conventional**
Turbidity (NTU)	0.484	0.292	0.278	0.356
Turbidity reduction (% of influent turbidity)	-	39	42	26
Particle Counts (total ≥2 µm/mL)	3257	1439	901	1502
***Cryptosporidium* Oocyst Removal** (log_{10}, mean of Trials 2C to 2F)	-	0.54	0.39	0.50
Microsphere removal (log_{10}, mean of Trials 2A to 2F)	-	0.91	1.26	0.49
Microsphere removal (log_{10} mean of Trials 2C to 2F)	-	0.65	0.92	0.53

Similar to the results observed during Phase 1, it is evident that during Phase 2, use of the rough, spherical engineered ceramic media resulted in improved turbidity and particle reductions by

filtration relative to conventional media (Table 4-2). Influent turbidity varied between the trials from a minimum of 0.186 to 0.730 NTU. Filters in Phase 2 lowered turbidity from a minimum of 12 % to a maximum of 51%. Despite changes in influent turbidity between trials, the fine ceramic filter consistently achieved 10% to 20% better turbidity reduction compared to the conventional filter.

Relative to the conventional media; however, neither the dense engineered ceramic nor the fine engineered ceramic media enhanced *C. parvum* oocyst removal significantly. It would appear that at conditions that are not favourable for oocyst deposition (*i.e.* complete coagulation failure), neither media surface roughness nor finer media enable more effective oocysts removal from raw water. At these same conditions; however, the engineered ceramic media configurations did enhance oocyst-sized microsphere removals. The fine engineered ceramic media achieved 0.77 $\log_{10}$ (or 83%) lower microsphere concentrations in the filter effluent compared to the conventional media. The dense ceramic media did not achieve substantially higher oocyst or microsphere removals than the conventional media.

Figure 4-2 provides a summary of the mean *Cryptosporidium* oocyst removals observed during the Phase 2 filtration experiments. This figure demonstrates the variability in oocyst removals observed during the various trials conducted during Phase 2. During these trials, *Cryptosporidium* oocyst reductions were as low as no oocyst removed by filtration (*e.g.* during Trial 2E, the fine ceramic media yielded a mean of -0.04 $\log_{10}$ oocyst removal, which was essentially no removal, which appeared to be negative due to the variability inherent to the oocyst enumeration method). *Cryptosporidium* oocyst removals were similarly low during Trial 2F, during which the observed mean oocyst removals by the fine engineered ceramic and conventional media filters were 0.13 (25%) and 0.07 (15%) $\log_{10}$ respectively. Within the 4 trials of Phase 2 during which *Cryptosporidium* oocysts were seeded into the filter influents, there appeared to be no appreciable differences in oocyst removal between the three filter configurations evaluated. Mean oocyst removals achieved by the dense engineered ceramic, fine engineered ceramic and conventional media during Phase 2 were: 0.54, 0.39 and 0.50 $\log_{10}$ respectively. Given the considerable variation observed in oocyst reductions by all of the filters between trials, it is uncertain if the differences in oocyst removals observed between the filters during any given trial are meaningful or merely a product of random error associated with the *Cryptosporidium* enumeration method and/or variations in filtration conditions. In contrast to the Phase 1 investigations, there appeared to be no correlation between filter performance and loading rate during this phase of testing.

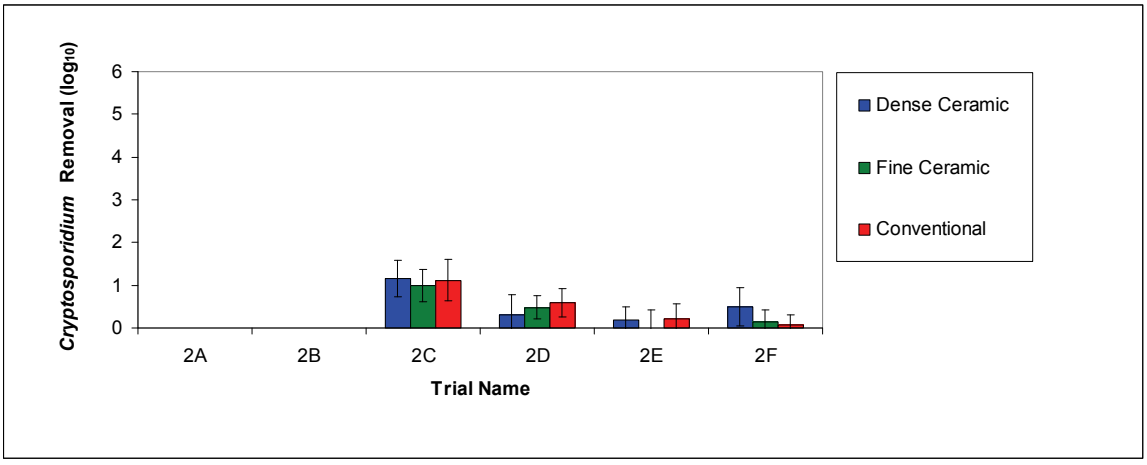

Figure 4-2. Mean *Cryptosporidium* Oocyst Removals and Turbidity Reductions During Phase 2 Filtration Experiments. Black bars represent ± one standard deviation from mean results.

The ≥2 $\log_{10}$ levels of *Cryptosporidium* oocyst reduction that would be expected from well-operated filters (CCME, 2004; Harrington et al., 2003) were not achieved during any of the trials conducted during Phase 2, which was not surprising given that filtration was not preceded by coagulation. These results also suggest that media roughness did not significantly enhance oocyst removal by filtration at conditions that were not favourable for oocyst deposition. It also appeared that straining was also insignificant because *Cryptosporidium* oocyst removals by the fine engineered ceramic media and the conventional media were comparable; accordingly, these results suggest that even with media as fine as 0.21mm, and at the conditions investigated, straining is not a significant colloid deposition mechanism when filtration conditions are unfavourable (*i.e.* complete lack of coagulant addition) during GMF.

Figure 4-3 provides a summary of the mean oocyst-sized microsphere removals observed during the Phase 2 filtration experiments. It demonstrates the variability in microsphere removals observed during the various trials conducted during Phase 2. The microsphere removals observed during the last four trials of Phase 2 were similar to the oocyst removals achieved by the dense ceramic and the conventional filters. At the conditions investigated during the Phase 2 experiments, the observed microsphere removals slightly overestimated *Cryptosporidium* oocyst removals by these two filters. The difference between mean *Cryptosporidium* oocyst and microsphere removals achieved by the fine engineered ceramic media filter was even greater (0.39 $\log_{10}$ removal of oocysts and 0.92 $\log_{10}$ removal of microspheres). A simple evaluation of the mean turbidity reduction (based on the percent of mean influent and effluent turbidities observed over the full 6 hour duration of each trial) was not indicative of either *Cryptosporidium* oocyst nor oocyst-sized microsphere removal by filtration at the

conditions investigated (Figure 4-2 and Figure 4-3, respectively). Similarly, filter effluent turbidities were also not indicative of either *Cryptosporidium* oocyst nor oocyst-sized microsphere removal by filtration.

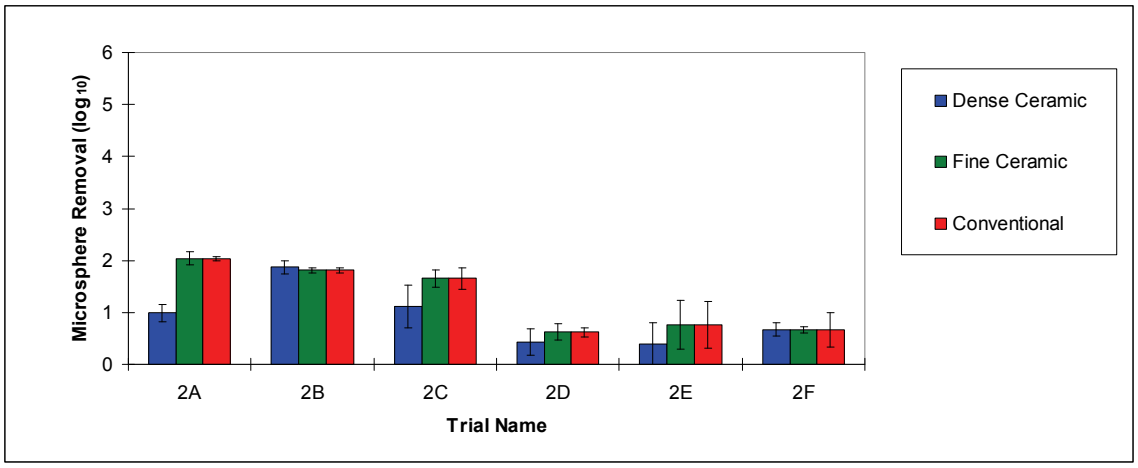

Figure 4-3. Mean Oocyst-Sized Microsphere Removals and Turbidity Reductions During Phase 2 Filtration Experiments. Black bars represent ± one standard deviation from mean results.

As demonstrated in Figure 4-3, oocyst-sized microsphere reductions by all of the filters declined from Trial 2A to 2F. It could be hypothesized that these changes may be associated with temporal changes in water quality and associated treatment performance (*e.g.* seasonal changes in parameters such as temperature). The observed differences in oocyst and microsphere reductions are not easily related to changes in water quality, however. During Phase 2, there were no significant storm events or changes in wind direction that affected source water quality and HWTP raw water quality data indicated no substantive changes in water quality. Some additional water quality analyses were conducted to evaluate the presence of surfactants in the raw water. A modified Methylene Blue Active Substances method (MBAS, ASTM method 512A, Chitikela, 1995) was used to assess the presence of anionic surfactants in the raw water. Although these analyses indicated that there were differences in anionic surfactant levels between trials, these differences could not be correlated with the changes in oocyst and oocyst-sized microsphere reductions by filtration that were observed between trials. The detailed MBAS analyses and data are provided in Appendix B. Notably, full-scale performance at the HWTP remained consistent during the Phase 2 investigations.

In contrast to the generally similar oocyst and microsphere reductions that were observed by the various filters during Phase 2, the different media configurations did yield appreciable differences in

the stability of the filter effluent turbidity and particle counts in response to sudden changes in raw water quality. The filter influent and effluent turbidity data obtained during Trial 2D (Figure 4-4) are useful for demonstrating these observed differences in the stability of operation or process robustness. Approximately 73 minutes into Trial 2D, a sudden change in filter influent turbidity was observed. This rapid increase in turbidity was due to a HWTP scheduled sample line flush event that caused the plant's raw water sample pump to shut down temporarily. The reduction in water pressure allowed backflow of water into the pilot-scale filter columns, which were located 6 floors underground. The turbidity of the filter influent rapidly increased from approximately 0.55 NTU to approximately 13 NTU within 2 minutes; as a result, filter effluent turbidities also spiked. In response to the rapid increase in filter influent turbidity, the peak turbidity of the conventional media filter effluent was 2.29 NTU, while the peak effluent turbidities from the dense and fine engineered ceramic media filters were 1.03 and 0.91 NTU respectively. In addition to having a smaller amplitude, the ephemeral increases in filter effluent turbidity from the engineered ceramic media had the same duration, indicating that the relatively lower turbidity spike responses from these media were not just a product of hydrodynamic retardation in the filters due to the use of finer media. If simple retardation was the cause for the dampened turbidity spike, the duration of the spike response from the ceramic media would be longer than that observed from the conventional filter media. Accordingly, as during the Phase 1 trials, it appears that the roughness of the engineered ceramic media contributed to more stable filtration as well as improved effluent turbidity and particle counts relative to conventional filtration.

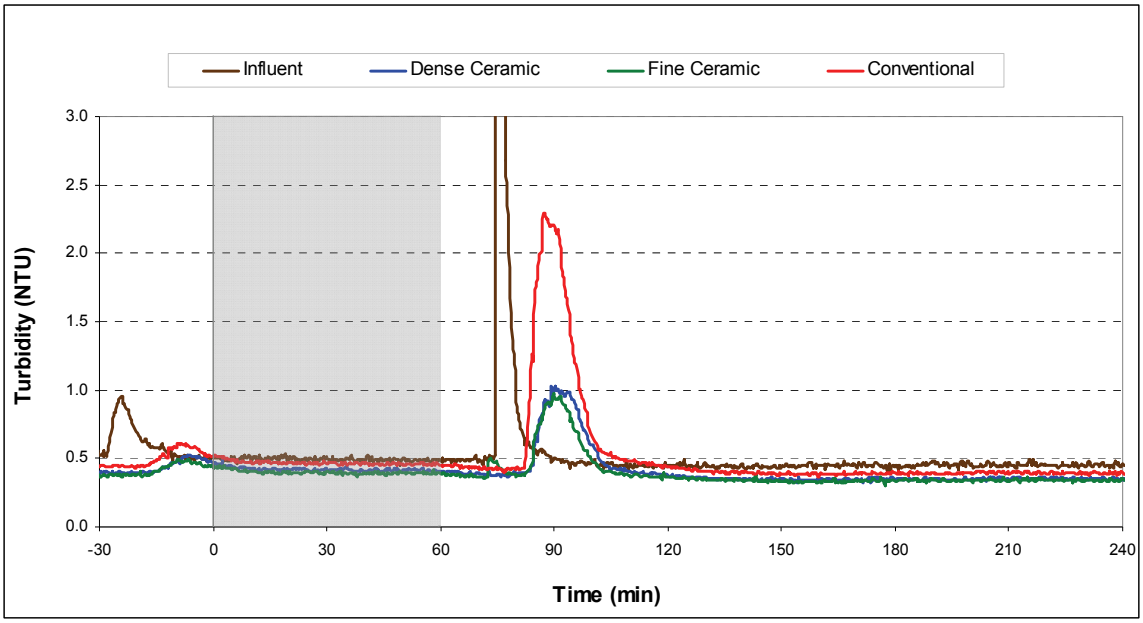

Figure 4-4. Filter Influent and Effluent Turbidity During Trial 2D. The grey shaded section represents the 60 minute seeding period.

The engineered ceramic media filters achieved higher oocyst-sized microsphere removals than the conventional media filters during each trial, with the fine ceramic media performing better in this regard than the dense ceramic media in most cases. This result is interesting given that the dense engineered ceramic media filter had a higher *L/d* ratio than the fine ceramic media filter and the same ES media in the lower layer. The main differences between the media and media configurations in these two filters were: UC, media size of the upper layer, and surface texture. The UC of the upper layer in the dense engineered ceramic media filter was 2.11 as compared to 1.60 in the upper layer of the fine engineered ceramic media. The difference in UC between the lower layers of media in the fine and dense engineered ceramic media filters was substantially smaller (1.12 *vs.* 1.23 respectively). The higher UC and finer grain size of the upper layer of media in the dense engineered ceramic media filter was likely the reason for the higher head loss that was observed relative to that in the fine engineered ceramic media filter. Despite the finer size of media and higher UC used in the dense engineered ceramic media filter, the microsphere, turbidity, and particle count reductions and head loss observed from the dense engineered ceramic media filter were all poorer than those observed from the fine engineered ceramic media filter.

While differences in UC and ES should favour the dense ceramic media in microspheres and turbidity reduction, it appeared that surface texture was a more important factor in filter performance.

As discussed in Section 3.2.6, the dense ceramic media's surfaces were much smoother than the fine ceramic media. As well, the morphology of the crystals covering the surface of the dense media is less angular than those of the fine ceramic media. It is possible that the dense ceramic media had surface properties that were not as suited for filtration as the fine ceramic media.

4.2.1 Key Findings from Phase 2

- Filters with engineered ceramic media configurations consistently produced better effluent water quality (turbidity and total particle counts) and were less affected by perturbations in influent water quality.

- Specifically, the mean turbidity reduction achieved by the fine ceramic filter was 16% higher than the conventional media. The dense ceramic filter's turbidity reduction was 13% better than the conventional filter.

- The engineered ceramic media demonstrated higher head losses relative to conventional media configurations, likely because of the smaller size of the ceramic media. The dense engineered ceramic media configuration demonstrated higher head losses than the fine engineered ceramic media configuration, likely due to higher UC and smaller diameter media in upper layer.

- The dense ceramic media configuration was not optimal at the conditions investigated because it yielded the highest clean bed head loss and, despite having smaller diameter media, it yielded higher filter effluent turbidity than the fine ceramic media.

- The difference in filter effluent turbidity and total particle counts between the dense and fine engineered ceramic media filters suggests that the rougher surface of the fine media enhanced turbidity and particle count reduction.

- Differences in loading rate did not appear to have a definitive effect on filter performance, regardless of media type.

- Oocyst-sized microsphere reductions by the fine engineered ceramic media were higher than those obtained by either the conventional or the dense engineered ceramic media filters.

- *Cryptosporidium* oocysts reductions by the fine and dense engineered ceramic and conventional media filters were similar.

- At no coagulant conditions, utilizing finer filter media did not appear to provide additional *Cryptosporidium* oocyst removal capacity from low turbidity source water, suggesting that straining was not a significant oocyst removal mechanism at the conditions investigated during Phase 2.

- Similar to the use of finer media, the use of rougher media did not appear to improve *Cryptosporidium* oocyst removal at no-coagulant conditions.

4.3. Phase 3

Phase 3 Results are summarized in Table 4-3, Figure 4-5 and Figure 4-6. The results of specific sections of Phase 3 are discussed in greater detail in the following sections.

Table 4-3 Summary of Phase 3 Results

	Influent	**Matched Ceramic**	**Fine Ceramic**	**Conventional**
Trial 3A				
Turbidity (NTU)	0.194	0.206	0.153	0.190
Particle counts (total # >2µm/mL)	NA	722	395	695
Cryptosporidium Oocyst Removal (log_{10})	-	-0.03	0.53	0.42
Microsphere Removal (log_{10})	-	0.28	0.33	0.39
Trial 3B				
Turbidity (NTU)	0.211	0.055	0.045	0.062
Particle counts (total # >2µm/mL)	827	302	408	684
Cryptosporidium Oocyst Removal (log_{10})	-	5.13	4.82	4.64
Microsphere Removal (log_{10})	-	0.38	0.59	0.53
Trials 3C to 3K				
Mean Turbidity (NTU)	0.192	0.097	0.087	0.117
Mean Particle counts (total # >2µm/mL)	1220	816	915	1009
Mean *Cryptosporidium* Oocyst Removal (log_{10})	-	1.46	1.78	1.29
Mean Microsphere Removal (log_{10})	-	0.84	1.00	0.71
Trials 3L and 3M				
Mean Turbidity (NTU)	0.281	0.071	0.086	0.120
Mean Particle counts (total # >2µm/mL)	1129	505	487	681
Mean *Cryptosporidium* Oocyst Removal (log_{10})	-	2.34	2.48	1.72
Mean Microsphere Removal (log_{10})	-	2.43	2.82	1.80

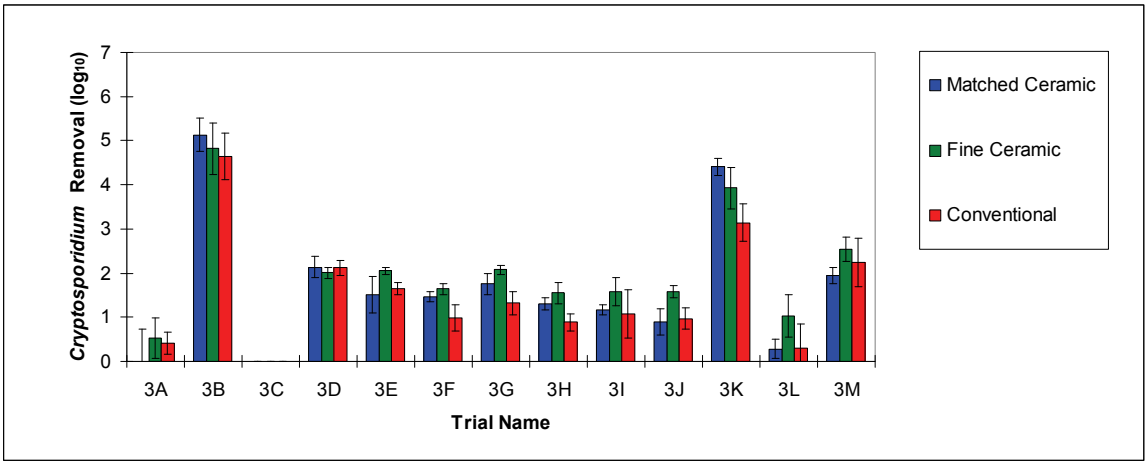

Figure 4-5 Summary of Phase 3 *Cryptosporidium* Oocyst Removals. Black lines represent ± one standard deviation from mean.

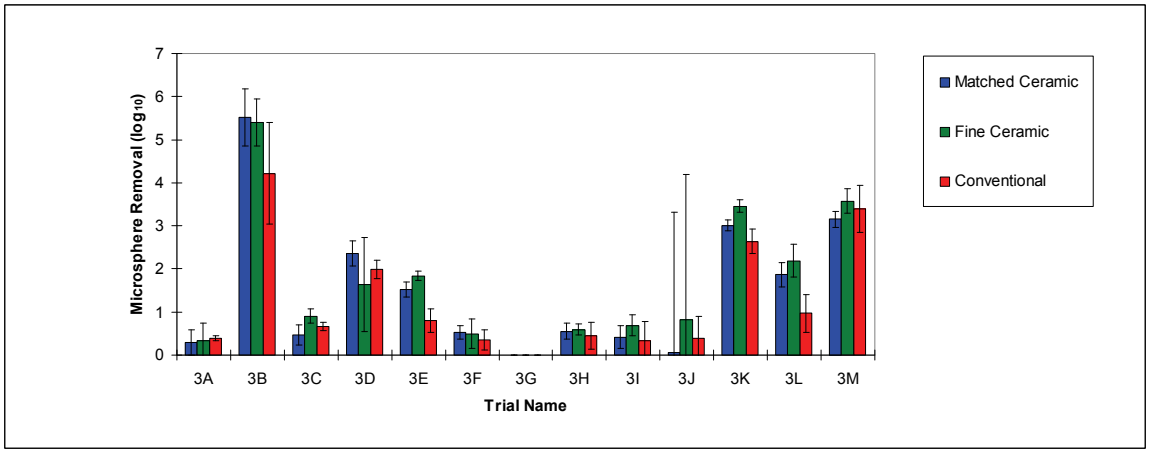

Figure 4-6 Summary of Phase 3 Microsphere Removals. Black lines represent ± one standard deviation from mean.

4.3.1 Trial 3A

One of the experimental considerations unexplored to this point in the research program concerned the use of seeded *Cryptosporidium* oocyst concentrations that were much higher than those that would be found in the natural environment. It is well known that, relative to other waterborne pathogens such as *Giardia* cysts (which are about twice the size of oocysts), because of their size *Cryptosporidium* oocysts can be difficult to remove by conventional GMF processes. During filtration investigations it is conceptually possible for filter media to become covered with oocysts (if high enough seeded concentrations of oocysts are utilized), ultimately having a negative impact on filter performance. This phenomenon was described by Ko and Elimelech (2000) and was termed the

"shadow effect". To evaluate whether *Cryptosporidium* oocyst concentrations utilized during the present investigation affected oocyst removal by filtration, a trial was conducted utilizing *Cryptosporidium* oocyst and microsphere concentrations that were lower than those utilized during Phases 1 and 2. The previous seeding trials utilized influent *Cryptosporidium* oocyst and microsphere concentrations in the range of 25,000-50,000 oocysts/spheres per litre. Trial 3A utilized influent microsphere and *Cryptosporidium* oocyst concentrations just above 1,000 oocysts/spheres per litre. Trial 3A was conducted at a loading rate of 24.4 m/hr with a water temperature of 4˚C. The previous experiment, Trial 2F had been conducted with water at 9˚C and a loading rate of 9.8 m/hr. A comparison of Trials 2F and 3A is provided in Table 4-4.

Table 4-4. Summary of Mean Filter Effluent Turbidities and Total Particle Counts, *Cryptosporidium* Oocyst and Oocyst-Sized Microsphere Reductions, and Head Loss During Trials 2F and 3A

Trial 2F	**Influent**	**Dense Ceramic**	**Fine Ceramic**	**Conventional**
Turbidity (NTU)	0.186	0.102	0.095	0.135
Particle counts (total # >2µm/mL)	1211	495	358	600
Cryptosporidium Oocyst Removal (log_{10})	-	0.50	0.13	0.07
Microsphere Removal (log_{10})	-	0.67	0.66	0.40
Clean Bed Head Loss (cm)	-	98	85	34
Trial 3A	**Influent**	**Matched Ceramic**	**Fine Ceramic**	**Conventional**
Turbidity (NTU)	0.194	0.206	0.153	0.190
Particle counts (total # >2µm/mL)	NA	722	395	695
Cryptosporidium Oocyst Removal (log_{10})	-	-0.03	0.53	0.42
Microsphere Removal (log_{10})	-	0.28	0.33	0.39
Clean Bed Head Loss (cm)	-	100	206	100

A comparison of results from Trials 2F and 3A did not conclusively indicate if spike concentrations affected *Cryptosporidium* oocyst removal. The *Cryptosporidium* oocyst removals did improve when lower oocyst seed concentrations were utilized; however, other performance indicators suggest that direct comparisons may not be possible between the two trials. For example, compared to Trial 2F, Trial 3A had poorer turbidity reductions, despite similar filter influent turbidities between the two trials. Microsphere removal results between the two trials were also inconsistent: while the conventional media achieved almost identical microsphere removals between the two trials,

microsphere removals by the fine engineered ceramic media dropped by 0.33 $\log_{10}$ (53%). Given the uncertainty regarding the impact of seed concentration, efforts were made in all subsequent trials to use the lowest possible *Cryptosporidium* oocyst spike concentrations that would allow for reliably countable and statistically significant numbers of oocysts to be present in the filter effluents (Emelko et al., 2008).

Interestingly, during this first trial the matched engineered ceramic filter did not perform as well as the conventional media filter in all performance aspects except head loss. The matched ceramic filter generally achieved better filter performance in subsequent trials however, suggesting that there may have been some filter conditioning effect. Clean bed head loss and rate of head loss accumulation data during Phase 3 indicated that the matched engineered ceramic media filter configuration was comparable to that of the conventional media filter.

4.3.2 Trial 3B

The coagulant dose in Trial 3B was set higher than that utilized by the full-scale plant to achieve filter effluent turbidities comparable to those achieved by the full-scale filters. At the increased coagulant doses, the pilot filters produced good quality effluent with turbidities similar to those achieved by the full scale filters (approximately 0.05 NTU on average). As a result, the pilot filter run times were noticeably decreased, especially for the fine engineered ceramic media, which reached terminal head loss after 3 hours, while the matched engineered ceramic and conventional media filters could be operated for 6 hours. Another factor that undoubtedly impacted the observed differences in filter run times was the applied hydraulic loading rates: the full-scale plant utilized loading rates of approximately 4 m/hr, whereas Trial 3B was conducted at 24 m/hr. Full scale filter cycles were approximately 48 hours and backwashes were not due to head loss as they were during warmer water conditions.

Despite only minor differences in effluent turbidities between the matched engineered ceramic and conventional filters (mean values of 0.055 NTU and 0.062 NTU respectively), the total particle counts were markedly different. Total counts of particles >2 μm from the conventional media filter were twice as high as those from the matched engineered ceramic media filter. Moreover, whereas the matched ceramic effluent contained almost no particles greater than 7μm in size, it was common for the conventional media to pass particles greater than this size. The higher particle counts in the conventional media filter effluent were largely due to the passage of 2-3 μm and 3-5 μm sized particles.

Comparisons of *Cryptosporidium* oocyst and microsphere removals achieved by the matched engineered ceramic and conventional media are difficult. One of the 12 effluent samples collected from the matched ceramic effluent had far higher oocyst and microsphere concentrations than other samples collected subsequently. It is unclear if this sample should be considered an outlier, possibly due to a sudden release of deposits within the filter effluent tubing, or if these data are simply indicative of the variability in normal filter operation. In light of the fact that no matching spikes were seen in either the effluent turbidity or particle count data for the matched ceramic filter at that time, the extreme data point in effluent oocyst concentration was noted and considered an outlier (Table 4-5). Given this consideration, the matched engineered ceramic media filter achieved 0.49 $\log_{10}$ higher *Cryptosporidium* oocyst removal than the conventional media filter; microsphere removal by the matched engineered ceramic media filter was also higher (approximately 0.31 $\log_{10}$ higher relative to the conventional media filter).

Table 4-5. Trial 3B *Cryptosporidium* Oocyst and Oocyst-Sized Microsphere Removal by Filtration During Trial 3B

	Matched Ceramic	Fine Ceramic	Conventional
***Cryptosporidium* $\log_{10}$ reduction, (With extreme data point)**	5.18 (2.63)	4.82	4.64
Microsphere $\log_{10}$ reduction, (With extreme data point)	5.52 (3.57)	5.40	4.22

During Trial 3B, clean bed head losses in the matched ceramic and conventional media were similar (114 cm and 112 cm, respectively). Head loss with time was higher in the matched ceramic media (224 cm and 193 cm, respectively).

4.3.3 Trials 3C to 3K

Trials 3C to 3K were conducted during winter when raw water temperatures were 5-8˚C. Due to the low water temperatures, the HWTP used PACl for coagulation during this period. Filter effluent turbidities during Phase 3 were always lower from the matched engineered ceramic media filter than from the conventional filter, though the magnitude of these observed differences varied and was occasionally small. The mean difference in filter effluent turbidities achieved by the matched and conventional media filters was 0.021 NTU (Table 4-6). It should be noted that the conventional media's filter effluent turbidities were never as low as those achieved by the HWTP's full-scale filters, which were consistently between 0.05 and 0.06 NTU. The fine engineered ceramic media generally achieved lower filter effluent turbidities than the matched engineered ceramic filter, though

there were occasional exceptions (Trials 3D, 3E). These results underscore the differences in filter influent quality between the pilot- and full-scale filtration processes and the difficulty in matching pilot- and full-scale coagulation performance, which is known to be critical for effective conventional GMF.

Notable differences in total particle counts were also observed between the effluents of the three pilot filters (Table 4-6), though it must be stated that the particle counter for the matched engineered ceramic media under-reported particle counts during all of the experiments conducted during the present experimental phase (despite calibration by the manufacturer prior to the trials. This particle counter ultimately required subsequent recalibration.). A comparison of particle counter measurements on a single, well-mixed water source demonstrated that filter effluent particle counts from the matched ceramic media filter were in actuality between the levels observed from the fine engineered ceramic and conventional media filters.

Table 4-6. Summary Mean Filter Effluent Turbidities and Total Particle Counts, *Cryptosporidium* Oocyst and Oocyst-Sized Microsphere Reductions, and Head Loss During Trials 3C to 3K

	Influent	Matched Ceramic	Fine Ceramic	Conventional
Turbidity (NTU)	0.194	0.098	0.088	0.119
Particle counts (total # ≥2µm/mL)	1217	804	897	997
***Cryptosporidium* Oocyst Removal (log_{10})**	-	1.83	2.05	1.52
Microsphere Removal (log_{10})	-	1.11	1.30	0.95
Clean Bed Head Loss (cm)	-	79	160	73

During the course of the nine experimental trials conducted during Phase 3, the matched engineered ceramic media filter generally achieved higher *Cryptosporidium* oocyst removals than the conventional media filter (Table 4-6), averaging 0.31 log_{10} (50%) better oocyst removal. The fine engineered ceramic media filter achieved the highest *Cryptosporidium* oocyst removals observed during Phase 3, averaging 0.53 log_{10} (70%) better than those achieved by the conventional media filter during Trials 3C through 3K.

The variability within the oocyst removal results is illustrated by the fact that the conventional media filter achieved better oocyst removals than the matched engineered ceramic filter during three trials (3D, 3E, 3J) and better than the fine engineered ceramic media filter during one trial (3D).

Despite conducting Trials 3C through 3K at very similar conditions (as similar as is practically possible when treating real raw water), *Cryptosporidium* oocyst reductions achieved by the matched engineered ceramic media filter ranged from 1.17 to 4.40 $\log_{10}$; similarly, the conventional media filter achieved oocyst removals that ranged from 0.97 to 3.14 $\log_{10}$. With the exception of Trial 3K, differences in *Cryptosporidium* oocyst removals achieved during "optimal" and "sub-optimal" coagulation conditions were approximately 0.5 $\log_{10}$. The oocyst removal differences between filter media were not consistent between trials and were not attributable to any one variable. Filter loading rate did not appear to affect oocyst removals appreciably. Regardless of filter media type and consistent with the published literature, neither filter effluent turbidities nor turbidity reductions correlated with *Cryptosporidium* oocyst reductions achieved by filtration.

The cause of the noticeably higher *Cryptosporidium* oocyst removals achieved during Trial 3K remains unexplained. Trial 3K was conducted only 2 days after Trial 3J, with no notable changes in raw water quality parameters measured at the HWTP. This level of *Cryptosporidium* oocyst removal was unexpected, especially since Trial 3K involved using a high filter loading rate during sub-optimal coagulation.

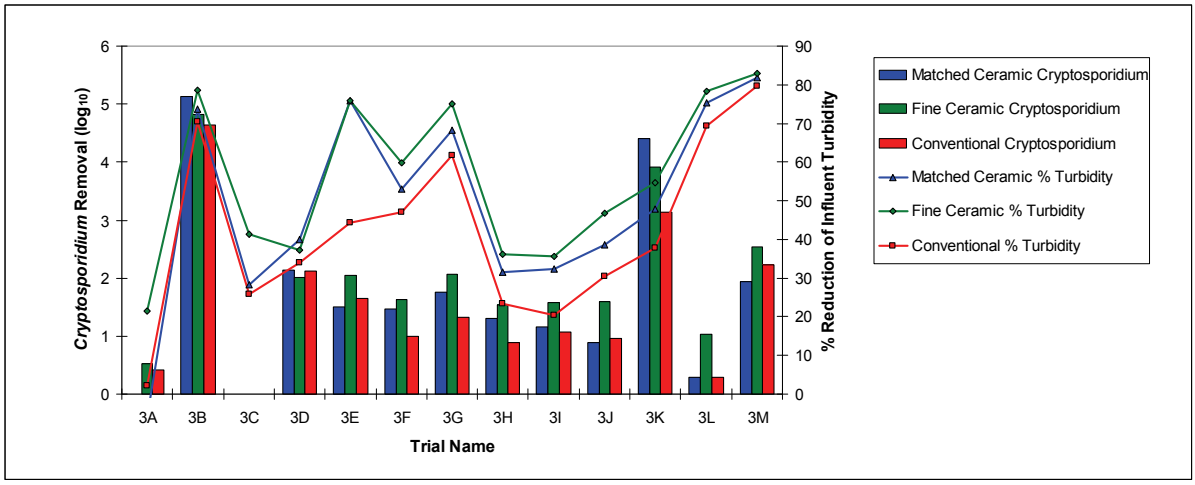

Figure 4-7. Mean *Cryptosporidium* Oocyst Removals and Turbidity Reductions During Phase 3 Filtration Experiments (Lines are connecting turbidity reductions are included to illustrate overall trends, not to suggest a functional relationship.)

Oocyst-sized microsphere removals were generally consistent with the *Cryptosporidium* oocyst removals observed during Trials 3C through 3K (Table 4-8). Regardless of filter media configuration, microsphere removals were consistently lower than *Cryptosporidium* oocyst removals, indicating that microsphere removals at the conditions investigated during Phase 3 were a conservative indicator of

Cryptosporidium oocyst removals by filtration. On average, *Cryptosporidium* oocyst removals were more than 0.5 $\log_{10}$ higher than microsphere removals during this course of testing. The differences in mean microsphere and *Cryptosporidium* oocyst removals achieved by matched ceramic, fine ceramic and conventional filters were 0.71, 0.75 and 0.57 log, respectively. The relationship between oocyst-sized microsphere and *Cryptosporidium* oocyst reductions by filtration was variable; however, it appeared that this variability was not related to any of the factors investigated during Phase 3.

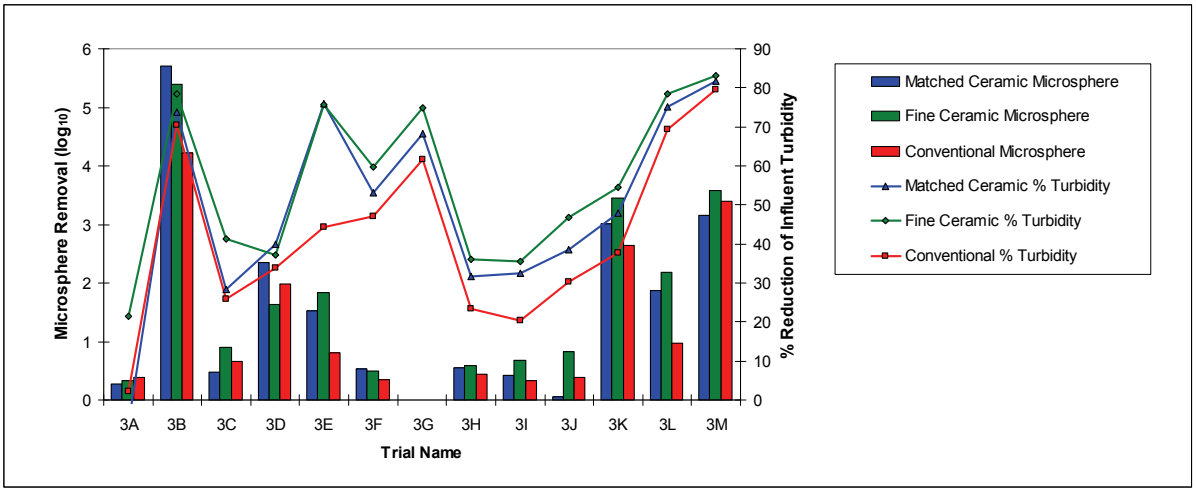

Figure 4-8. Mean Oocyst-sized Microsphere Removals and Turbidity Reductions During Phase 3 Filtration Experiments (Lines are connecting turbidity reductions are included to illustrate overall trends, not to suggest a functional relationship.)

Consistent with experiments conducted during Phase 2, relative to conventional media filters, the engineered ceramic media filters produced more stable effluent turbidities in response to sudden increases in filter influent turbidity. This was most evident in Trial 3E (Figure 4-9), during which there filter influent turbidity increased suddenly, rising from 0.13 NTU to almost 11 NTU. In response, the filter effluent turbidity from the conventional filter increased from 0.12 NTU to 0.25 NTU. After the brief increase in filter influent turbidity, the conventional filter effluent turbidity remained elevated, just below 0.15 NTU. During the same period, the filer effluent turbidity from the matched engineered ceramic filter increased from 0.06 NTU to 0.126 NTU; however, it promptly decreased back to 0.06 NTU shortly after the spike in filter influent turbidity passed. The fine engineered ceramic media showed no response to the increase in filter influent turbidity, maintaining a mean filter effluent turbidity of 0.061 NTU throughout the trial.

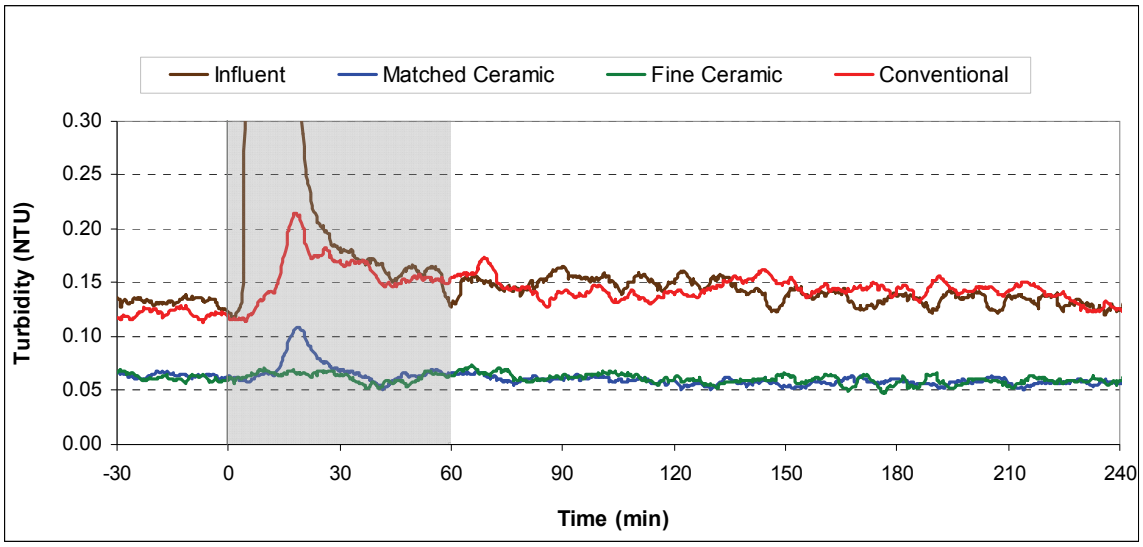

Figure 4-9. Filter Influent and Effluent Turbidities During Trial 3E. Turbidity results were smoothed with a 3-minute time-averaging method to reduce analytical noise. Grey shaded area indicates 60-minute seeding period.

Similar operational robustness was observed in filter effluent total particle counts during Phase 3, demonstrated by results from Trial 3E (Figure 4-10). The particle count profiles in this figure are similar to the turbidity profile presented in Figure 4-9. Specifically, the filter influent concentration of total particle counts suddenly increased and the conventional and matched engineered ceramic media filters responded with increases in filter effluent total particle counts. The increase in filter effluent total particle counts from the matched engineered ceramic media was notably smaller than that observed from the conventional media filter. In contrast, there was no visible increase in filter effluent total particle counts from the fine ceramic media filter.

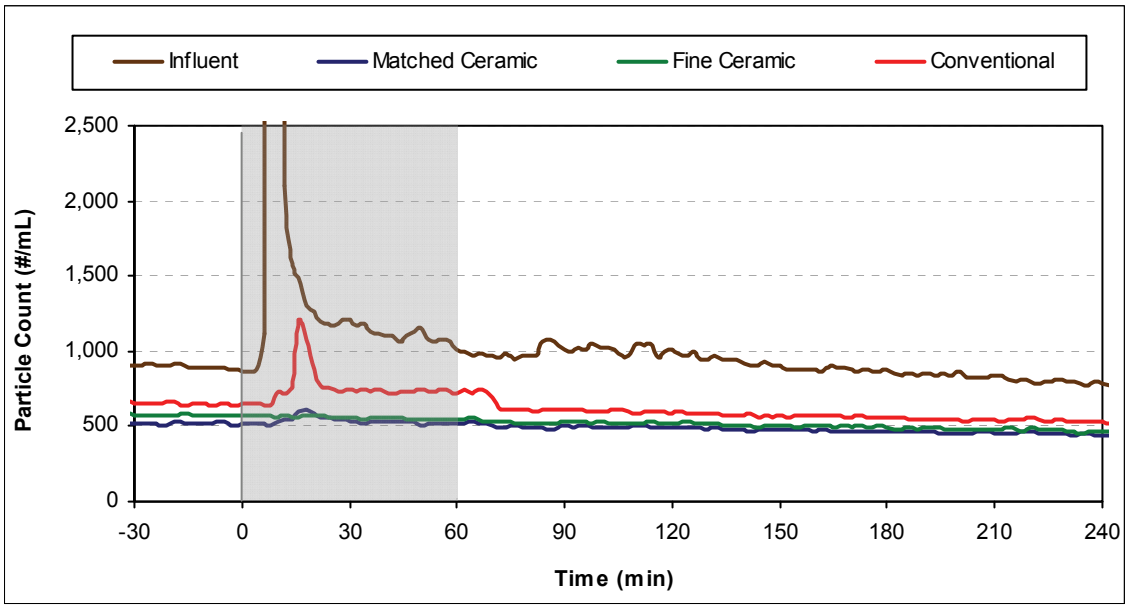

Figure 4-10. Filter Influent and Effluent Total Particle Counts ≥ 2µm/mL During Trial 3E. Grey shaded area indicates 60-minute seeding period.

In contrast to the turbidity data obtained during Trial 3E, the filter effluent total particle counts for the conventional media show a response to both the filter influent water quality change (sudden in crease in filter influent turbidity) and the introduction of the oocyst and microsphere seeding suspension; the latter response appears as a 60 minute plateau of elevated effluent particle counts in the conventional media effluent. Though the oocyst suspension did not affect the filter effluent total particle counts from either of the engineered ceramic media filters during Trial 3E, addition of the seed suspension did affect filter effluent total particle counts from the ceramic media filters during other trials, particularly Trial 3H.

It should be noted that though the matched engineered ceramic media appeared to have lower filter effluent total particle counts than the fine engineered ceramic media in general, this was not actually the case. Problems with particle counter calibrations resulted in slight under-reporting of total particle counts from Column 1. Additional evaluations examining particle counter performance revealed that the matched ceramic media had mean filter effluent total particle counts that were generally slightly higher than those observed in the effluent from the fine engineered ceramic media filter during this trial, but lower than those observed from the effluent of the conventional media filter.

Head loss profiles obtained from the matched ceramic and conventional media filters were similar (Table 4-7). When using PACl coagulation, the matched engineered ceramic media filter experienced

a similar rate of head loss accumulation, despite achieving better turbidity and total particle count removals. Results from trials conducted with alum coagulation differed from those obtained from trials conducted with PACl coagulation in that head loss in the matched engineered ceramic filter increased more than in the conventional media filter during 6 hours of filter operation. In general, these results indicate that the engineered ceramic media had a higher capacity for solids retention at some of the conditions investigated. As expected, clean bed head loss and the rate of head loss accumulation in the fine engineered ceramic filter was higher than in the other filters during all of the trials comprising Phase 3 (Table 4-7).

Table 4-7. Summary Head Loss Results During Phase 3 Filtration Experiments

	Matched Ceramic	Fine Ceramic	Conventional
Mean clean bed head loss for 10 m/hr trials (cm)	49.0	119.2	51.9
Mean clean bed head loss for 24 m/hr trials (cm)	105.2	209.6	99.1
Mean change in head loss for all 10 m/hr trials (cm)	8.9	16.1	8.5
Mean change in head loss for all 24 m/hr trials (cm)	70.1	111.4	65.4
Mean change in head loss for PACl trials (cm)	15.2	65.8	18.8
Mean change in head loss for Alum trials (cm)	91.0	65.7	72.9

4.3.4 Trial 3J

It was hypothesized that if surface roughness was responsible for improved filter performance, this advantage would diminish as a filter run progressed due to the burial of roughness features under accumulated solids. To evaluate this theory, Trial 3J was extended beyond the usual 6 hours period of operation so that the filters would be subjected to a sudden increase in filter influent turbidity 48 hours after the start of filtration (Figure 4-11). The turbidity spike was achieved by injecting a kaolin suspension through an injection port located immediately downstream of the coagulant addition port.

The turbidity reduction provided by the engineered ceramic media was consistently greater than that achieved by the conventional media throughout the trial. This performance difference is evidenced by both consistently lower filter effluent turbidities during stable operation and the different filter effluent turbidities observed in response to suddent increases in filter influent turbidity (Figure 4-11). Over the duration of a filter cycle, the performance advantage (i.e. relative difference in filter effluent turbidities) during stable operation diminished over time. For example, early in Trial 3J filter effluent turbidity from the matched ceramic media was 0.014 NTU lower than that from the

conventional filter; however, by the end of the filter cycle this difference was only 0.005 NTU. Similarly, the ability of the fine ceramic media to effectively "dampen" the effect of sudden increases in filter influent turbidity (i.e. continue producing filter effluent of consistently or near to consistenly good quality) diminished over time. This effect is illustrated in Figure 4-11. During the kaolin-induced turbidity spike at 48 hours, the influent turbidity increased to above 20 NTU, which was the maximum turbidity that the turbidimeters were calibrated to read. The responses to this rapid increase in turbidity by the matched engineered ceramic and conventional media filters were similar, both in maximum effluent turbidity and duration of spike response. The fine ceramic filter yielded a relatively more dampened response to the sudden increase in filter influent turbidity, though it was a larger response than had been observed during other such events evaluated during previous trials.

These results suggest that once the engineered ceramic filter media in the columns were covered by enough captured particles, their surface properties were altered such that filter performance became less affected by media surface properties and more affected by the solids attached to the media. Both the decrease in observed differences in filter effluent turbidities during 1) stable operation and 2) in response to sudden changes in filter influent turbidity are consistent with media roughness causing the performance differences observed between the matched engineered ceramic and conventional media filters.

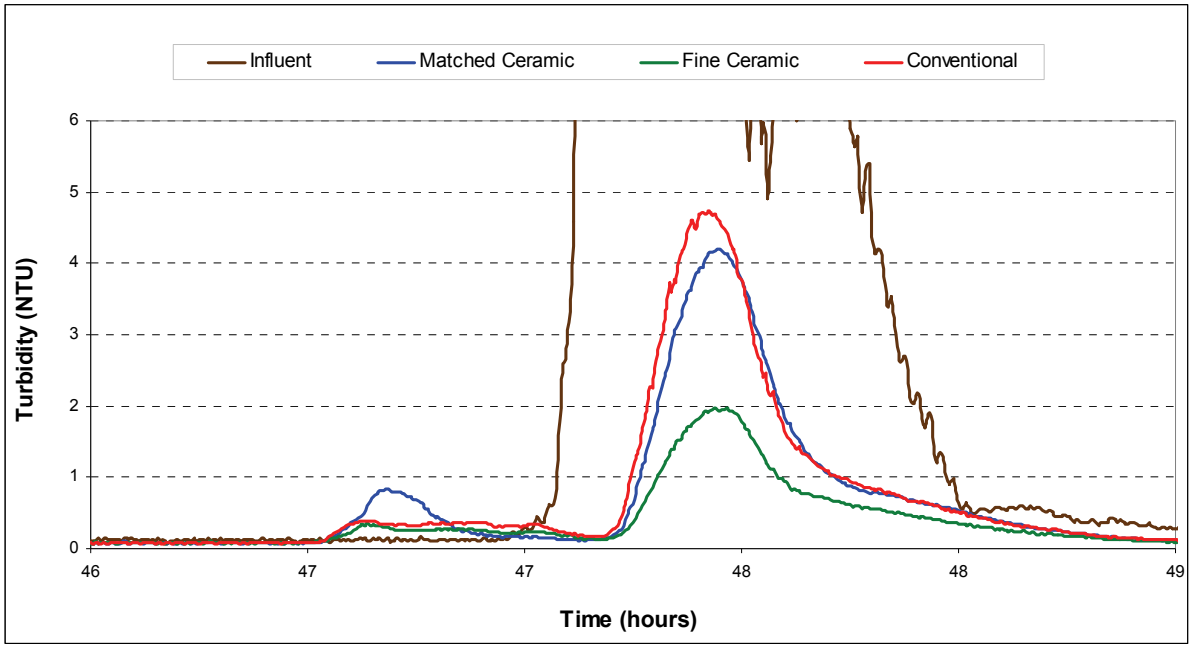

Figure 4-11. Filter influent and effluent turbidities during sudden increase in filter influent turbidity at end of Trial 3J

4.3.5 Trial 3K

Some of the highest *Cryptosporidium* oocyst reductions observed during Phase 3 were achieved at "sub-optimal" coagulation conditions (0.3 mg/L PACl) and high (24.4 m/hr) loading rates. The relatively high levels of *Cryptosporidium* oocyst reduction that were observed during Trial K could not be attributed to any single factor. Due to the size of Lake Ontario, bulk chemical water quality parameters generally do not change quickly. Temperature and turbidity variations occur at times, but none were noted in this case. As well, Trials 3J and 3K were conducted only 2 days apart, but yielded very different oocyst removal performance. As with the performance deterioration during trials conducted without coagulant during Phase 2, the performance of the HWTP's full-scale filters did change during this period of time. Accordingly, it appears that the filtration performance of the low-turbidity, un-chlorinated Lake Ontario water was highly sensitive to small changes in filter conditions and coagulant dosage. The decline in oocyst removal after Trial 2C, and the increase in oocyst removal between Trials 3J and 3K remain unexplained.

It should be noted that despite the low coagulant dose, Trial 3K was the only trial during which coagulated oocyst and microsphere seed suspension produced easily visible pinpoint floc. Specifically, 3 mm to 4 mm diameter aggregates were clearly visible until the mixing intensity was increased. Consistent with this result, head loss in all of the filters was considerably higher during this trial than during any previous trial.

The mean filter influent turbidity during Trial 3K was similar to that observed during Trial 3F. The higher coagulant dose during Trial 3F (0.6 mg/L PACl as compared to 0.3 mg/L PACl) allowed all 3 filters to achieve better turbidity reduction than during Trial 3K, yet the *Cryptosporidium* oocyst removals achieved by the filters during Trial 3K were 2 to 3 $\log_{10}$ higher than those achieved during Trial F. Microsphere removals were also 2 to 3 $\log_{10}$ higher during Trial 3K.

4.3.6 Trials 3L and 3M

Trials 3L and 3M were conducted to impact of difference coagulants on filter performance. Other investigations have indicated that *Cryptosporidium* oocyst and oocyst-sized microsphere removal by granular media filtration can be affected not only by coagulant dose but type of coagulant used (Emelko and Brown, 2004). Since the full scale operations at the HWTP switched from PACl to alum during warmer water conditions, it was important to investigate filter performance at both of these coagulant conditions.

Coagulation was a challenge during Trial 3L. This trial was conducted at a loading rate of 24.4 m/hr, so head loss was higher than in the full scale filters, which were operated at 14 m/hr at the time. In addition, filter performance varied significantly between preliminary experiments conducted using alum filtration, despite having the same coagulant dosage. For this reason determining the optimum coagulant dose for the seeding studies was challenging. For the high-loading rate experiment (Trial 3L), a compromise between low head loss and good turbidity reduction was reached at an applied alum dose of 5 mg/L. For the lower loading rate trial (Trial 3M), a coagulant dose of 3.7 mg/L was sufficient to bring pilot-scale filter effluent turbidities down to levels that were comparable to those achieved by the full-scale filters. The full-scale plant utilized a coagulant dose of 3 mg/L of alum to coagulate their pre-chlorinated raw water at that time.

All of the filters achieved higher turbidity reductions during Trials 3L and 3M than during most previous trials during which PACl coagulation was utilized. Filter effluent turbidities during Trial 3M were lower than during any of the other trials conducted during Phases 2 and 3 and were similar to the filter effluent turbidities achieved by the HWTP's full-scale filters. The differences observed in mean filter effluent turbidities between the various filters during Trials 3L and 3M were similar to those observed during previous trials: the fine engineered ceramic media yielded the lowest filter effluent turbidity (mean of 0.064 NTU), followed by the matched engineered ceramic media (mean of 0.071 NTU) and the conventional media filters (mean of 0.085 NTU). In contrast to the noticeably lower filter effluent turbidities relative to previous trials, total particle count reductions were not noticeably different.

Due to a malfunction in one of the particle counters, total particle counts in only two of the filter effluents were measured during this trial (matched engineered ceramic and conventional). As during previous trials, the matched engineered ceramic media filter yielded filter effluent total particle counts that were lower less affected by the injection of the seed suspension than the conventional media.

Cryptosporidium oocyst removals by all of the pilot filters during the trials utilizing alum coagulation were lower than expected; in fact, the oocyst removals during Trial 3Lwere the lowest observed during Phase 3 and were similar to those achieved during Phase 2 trials without the use of coagulant. *Cryptosporidium* oocyst removals during Trial 3M were only slightly higher than those observed during Trial 3D, despite achieving appreciably lower filter effluent turbidities. It is generally assumed that filter performance improves with warmer water temperatures (MWH, 2005), so the decrease in *Cryptosporidium* oocyst removals was not expected; particularly when accompanied by excellent filter effluent turbidities.

While operating the pilot filters with alum coagulation, mean microsphere removals were higher than oocyst removals by more than 1.2 $\log_{10}$. When coagulating with PACl, mean microsphere removals were 0.61 $\log_{10}$ lower than *Cryptosporidium* oocyst removals. This fact emphasizes the importance of evaluating the *Cryptosporidium*–microsphere surrogate relationship at conditions relevant to those being utilized. Microsphere removals over-estimated oocyst removal by filtration during Phase 2 trials and trials using alum coagulation; however, they under-estimated oocyst removal by filtration when PACl was used for coagulation.

Clean bed head loss results during the trials conducted with alum coagulant were similar to those observed during the trials utilizing PACl coagulation. Changes in head loss were much higher during the trials utilizing alum coagulation, however.

4.3.7 Key Findings from Phase 3

- Based on clean bed head loss and rate of head loss accumulation, the matched engineered ceramic and conventional media filter configurations were essentially identical.

- Mean filter effluent turbidities during the trials utilizing PACl coagulant were 0.021 lower in the effluent from the matched engineered ceramic media filter as compared to the conventional media filter. Mean turbidities for the matched, fine and conventional media were 0.98, 0.88 and 0.119 NTU, respectively.

- Total particle counts during the trials utilizing PACl coagulant were also lower in the effluent from the matched engineered ceramic media filter as compared to the conventional media filter.

- The matched ceramic filter's better turbidity and particle count reduction combined with similar head loss suggests that the matched engineered ceramic media filter had higher solids loading capacity at the operating conditions investigated.

- Filter effluent turbidities and total particle counts were lowest in the effluent from the fine engineered ceramic media filter during normal operation and in response to sudden increases in filter influent turbidity; however, this configuration also had the highest head loss.

- The matched engineered ceramic media achieved slightly higher *Cryptosporidium* oocyst removals (approximately 0.2 $\log_{10}$ difference in mean oocyst removals from all Phase 3 trials)

as compared to the conventional media filter. In some instances the difference in oocyst reductions by these different media configurations was as high as 1.25 $\log_{10}$.

- Regardless of media configuration, *Cryptosporidium* oocyst removals by filtration at sub-optimal coagulation conditions were generally lower than those observed during optimal coagulation conditions.

- The enhanced oocyst removal achieved by the matched engineered ceramic media filter relative to the conventional media filter was dependant on coagulant type.

- The difference in roughness between the matched engineered ceramic and conventional media may have been responsible for the better stability of operation and lower filter effluent turbidities observed from the matched engineered ceramic media filter in response to the sudden increase in filter influent turbidity during Trial 3J.

- Loading rate did not appear to significantly impact *Cryptosporidium* oocyst removal by granular media filtration while using PACl coagulant at the conditions investigated. In contrast, higher loading rates appeared to contribute to lower *Cryptosporidium* oocyst removals when alum coagulation was utilized.

- Regardless of media configuration, neither filter effluent turbidity nor total particle counts were reliable indicators of oocyst removal by filtration.

- Oocyst-sized microsphere reduction was generally consistent with *Cryptosporidium* oocyst reduction; however, relative to oocyst removals by filtration, microsphere removals were slightly higher during alum coagulation and lower during PACl coagulation.

4.4. Synthesis of Results

4.4.1 Filter Performance

Filter performance was assessed by evaluating the following parameters: filter effluent turbidity and total particle counts, *C. parvum* oocyst and potential surrogate (oocyst-sized microsphere) removal, filter run time, and head loss. The stability of these performance factors at non-ideal operating conditions (*e.g.* sub-optimal coagulation, rapid change in filter influent turbidity, hydraulic surge, *etc.*) was also assessed.

4.4.2 Filter Effluent Turbidity

Effluent turbidities from the engineered ceramic media filters were consistently lower than those from the conventional media filters. Given the smaller effective grain size of the very fine, fine and dense engineered ceramic media configurations, it was not surprising that the use of these ceramic media during filtration enhanced turbidity reductions. For these fine-grained media configurations, better turbidity reduction came at a price; their clean bed head loss was higher, especially at higher hydraulic loading rates. In contrast, the matched engineered ceramic media filter enhanced turbidity reduction relative to conventional media filtration with essentially the same initial head loss and rate of head loss increase. This indicated that the engineered ceramic media's surface properties were responsible for the improved turbidity reduction , and that it was not solely media size that was the cause of the better turbidity reduction achieved by the finer engineered ceramic media filter configurations.

The engineered ceramic media filters not only produced water with lower effluent turbidities, they produced effluent with more consistent/stable turbidity levels. More difficult to quantify, this performance benefit was particularly evident during periods of sudden increases in raw water turbidity. Without exception, relative to conventional media, the engineered ceramic media yielded lower amplitude spikes in filter effluent turbidity in response to sudden increases in raw water turbidity. This observed difference in filter effluent stability diminished near the end of filter cycles, indicating that this performance benefit was associated with to the greater surface roughness of the engineered ceramic filter media and the associated solids loading capacity.

Pilot-scale filter influent turbidity measurements were consistent with those observed at the full-scale plant. In general, the pilot-scale filter influent turbidity readings were within 10% of the HWTP's measured raw water turbidities. Filter effluent turbidities from the pilot-scale filters were not generally representative of those observed at the HWTP. For example, the full-scale filter effluent turbidities rarely exceeded 0.065 NTU; in contrast, the pilot-scale conventional filter effluent turbidities during the experiments conducted using "optimal" coagulant dosing ranged from 0.101 to 0.151 NTU and were similar to the full-scale filter effluent turbidities during only 2 of the 12 trials that investigated filtration of optimally coagulated water (Trials 3B and 3M). Of these pilot-scale trials with low effluent turbidity, 3B used coagulant doses well above those used prior to full-scale filtration. It was only during Trial 3M that the pilot-scale filter effluent turbidities were similar to those observed from the full-scale filters while using similar coagulant doses.

Three possible reasons for the observed discrepancies between pilot- and full-scale filter effluent turbidities are:

1. The un-chlorinated raw water used during the pilot-scale investigations did not flocculate in the same way that the full-scale plant's chlorinated raw water flocculated. It is commonly recognized that pre-oxidation of raw water impacts subsequent flocculation and filtration processes,

2. The static mixer and in-line flocculation process in the pilot plant did not accurately mimic full-scale coagulation and flocculation. Both visual and microscopic evaluation of both full- and pilot-scale flocs confirmed this and indicated the formation of much larger flocs at full-scale, and/or

3. The full-scale coagulation process utilized undiluted coagulant addition prior to flocculation whereas diluted coagulant was added at pilot-scale.

4.4.3 Filter Effluent Total Particle Counts

The filter effluent total particle count results and trends observed during the investigations reported herein were generally similar to those observed by comparing full- and pilot-scale filter effluent turbidity results. Direct comparisons between filter effluent total particle counts obtained from the various filter media are limited; however, because of several instrumentation difficulties that resulted in poor calibrations and low instrument reliability. Several general conclusions were possible, however. They are:

- The matched engineered ceramic media achieved lower filter effluent total particle counts ≥2 μm than the conventional media,

- The matched engineered ceramic media's response to filter influent spikes in total particle counts ≥2 μm was smaller (*i.e.* smaller spike in filter effluent total particle counts ≥2 μm) than the conventional media's response,

- The period during which oocysts and oocyst-sized microspheres were seeded into the filter influent was more frequently accompanied by a noticeable increase in filter effluent total particle counts ≥2 μm than a noticeable increase filter effluent turbidity (as is commonly observed during these types of low raw water turbidity filtration investigations), and

- The filter effluent total particle counts ≥2 μm were not reliably indicative of *Cryptosporidium* oocyst or oocyst-sized microsphere passage into filter effluents, though elevated total particle counts during oocyst and microsphere seeding periods were typically in the 3-5 μm channel.

4.4.4 *Cryptosporidium* Oocyst Removal

Cryptosporidium oocyst removals varied considerably throughout the investigated reported herein. The cause for this variability is at least partly associated with the variability inherent to the enumeration methodology; however, the observed variability in oocyst removals between trials suggests that other factors also contributed to this observed variability in oocyst removals by filtration. Given differences in raw water chlorination and performance factors such as filter effluent turbidities achieved by the pilot-scale conventional filtration media, it is uncertain and unlikely that the *Cryptosporidium* oocyst removals achieved by the pilot-scale filters are representative of those that would be achieved by full-scale filtration because of the same factors that may have resulted in the difference between full- and pilot-scale filter effluent turbidities.

Phase 2 *Cryptosporidium* oocyst removals were low for all three filters investigated, indicating that neither media surface properties nor grain size were significant factors impacting *Cryptosporidium* oocyst removal by filtration at the operational conditions investigated. Because grain size was not a significant factor during trials resulting in low oocyst removals, it can be inferred from Phase 2 results that straining is not an important removal mechanism for oocysts when colloid attachment is impaired.

It appears that at conditions that resulted in poor overall filter performance, all three pilot filters had poor *Cryptosporidium* oocyst removals. The matched ceramic media achieved only slightly better oocyst removals than the conventional media at such conditions (Table 4-8). For trials during which both the matched and conventional filters achieved less than 2 $\log_{10}$ *Cryptosporidium* oocyst removals (Trials 3E to 3J, and Trial 3M), the mean difference in oocyst removals was 0.11 $\log_{10}$ higher for the matched ceramic media filter as compared to the conventional filter. During Trial 3L, for example, the *Cryptosporidium* oocyst removals achieved by the conventional and matched media filters were almost identical at 0.28 and 0.29 $\log_{10}$, respectively. Phase 3 results support the conclusion that at poor filtration conditions, the surface properties of the media do not have a large impact on *Cryptosporidium* oocyst removal by filtration, though they may still be a significant factor influencing the removal of other colloids from suspension, as measured by turbidity and particle count reductions.

Table 4-8. Summary of Mean *Cryptosporidium* Oocyst and Oocyst –Sized Microsphere Removal by Filtration

	Matched Ceramic Media	Conventional Media	Log_{10} Difference between Matched and Conventional
***Cryptosporidium* Oocyst Removals:**			
Mean oocyst removal (log_{10}) of trials with ≥2 log_{10} oocyst removals (Trials 3E to 3J, and 3M)	1.29	1.18	0.11
Mean oocyst removal (log_{10}) of trials with ≥2 log_{10} oocyst removals (Trials 3B, 3D and 3K)	3.91	3.30	0.61
Microsphere Removals:			
Mean oocyst removal (log_{10}) of trials with ≥2 log_{10} oocyst removals (Trials 3E to 3J, and 3M)	1.16	0.95	0.21
Mean oocyst removal (log_{10}) of trials with ≥2 log_{10} oocyst removals (Trials 3B, 3D and 3K)	2.98	2.95	0.03

At conditions favourable for filtration, the matched ceramic filter removed more *Cryptosporidium* oocysts than the conventional media filter. The mean difference between *Cryptosporidium* oocyst removals by the matched and conventional media filters during Trials 3B, 3D, and 3K was 0.59 log_{10} (74%). Accordingly, it appears that media surface properties exert more influence on *Cryptosporidium* oocyst removal at conditions that favour the attachment of *Cryptosporidium* oocysts to filter media. For example, with the use of PACl coagulation, the matched ceramic media achieved oocyst removals by filtration that were as much as 1.25 log_{10} higher than those achieved by the conventional media. It should be noted that the trends seen in microsphere removals indicated precisely the opposite effect: differences in oocyst-sized microsphere removals were the lowest during trials that achieved high oocyst removals. For trials with high oocyst removals, the difference in oocyst removal between matched and conventional media filters was 0.61 log_{10} (a 75% difference), while differences in microsphere removal was only 0.03 log_{10} (Table 4-8). It is unclear why surface roughness would be more important to the removal of oocysts than microspheres when coagulation is improved.

It has been previously suggested that the type of coagulant used may affect *Cryptosporidium* oocyst removal by filtration (Emelko and Brown, 2004). Though the use of alum in Trial 3L and 3M allowed the filters to produce low turbidity effluent (mean effluent turbidities of 0.085 NTU and

0.071 NTU from the conventional and matched ceramic media filters respectively), *Cryptosporidium* oocyst removals were lower during these trials than previous experience with PACl-coagulated experiments would predict (means of 1.27 and 1.11 $\log_{10}$ oocyst removal by the conventional and matched ceramic media filters respectively). These observations suggest that coagulant type affects *Cryptosporidium* oocyst removal and turbidity reduction differently. These observations are also consistent with numerous studies in the literature that have concluded that filter effluent turbidity is not necessarily indicative *Cryptosporidium* oocyst passage through filters (Nieminski et al., 1994; Nieminski and Ongerth, 1995; Patania et al., 1995; Dugan et al., 1999; Swertfeger et al., 1999).

4.4.5 Potential Surrogates for *Cryptosporidium* Oocyst Removal by Filtration

As stated above, the experiments reported herein are consistent with numerous studies in the literature that have concluded that filter effluent turbidity is not indicative *Cryptosporidium* oocyst passage through filters. This is especially well illustrated by comparing Trials 3J and 3K, during which filter influent turbidities were 0.17 NTU and 0.21 NTU, respectively. Microsphere and oocyst removals were 2 to 3 $\log_{10}$ higher in Trial 3K, however filter effluent turbidities from all three filters were virtually identical between the two trials. It is clear that filter effluent turbidity values are not dependable predictors of *Cryptosporidium* oocyst removals by filtration.

Turbidity reduction correlates to oocyst removal better than effluent turbidity (Figure 4-12). The graph shows a general increase in turbidity reduction with increasing oocyst removal, though there are several instances where good turbidity reduction was achieved during very poor oocyst removal. It is apparent from the graph that no high oocyst removals were achieved during poor turbidity reduction in this study, suggesting that while good turbidity reductions do not guarantee good oocyst removal, *low* turbidity reduction can indicate that the filter is at greater risk of poor oocyst removal.

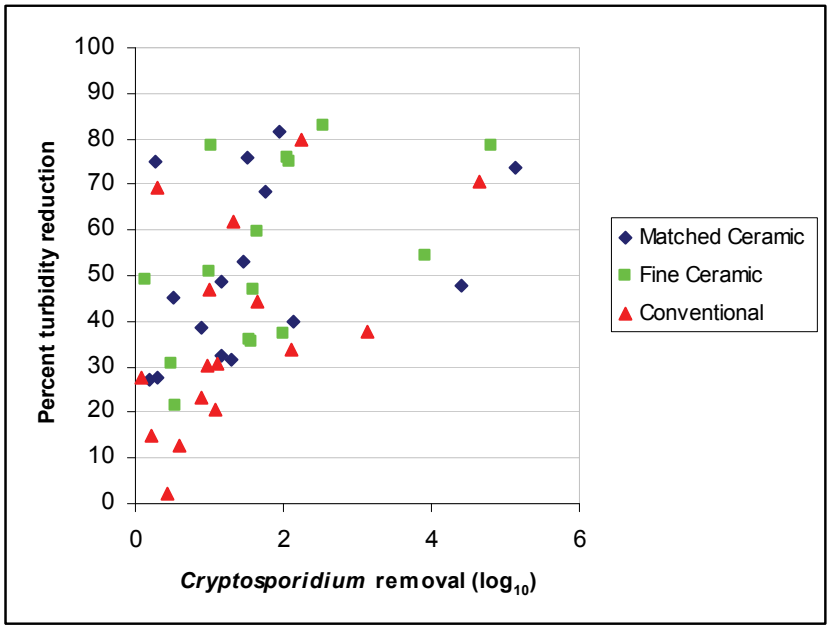

Figure 4-12. *Cryptosporidium* Oocyst Removals and Turbidity Reductions by Various Filtration Media During Phase 3 Experiments

Though there were discrepancies, oocyst-sized microsphere removal was the best indicator of *Cryptosporidium* oocyst removal investigated during the present study (Figure 4-13). The coefficient of determination for the oocyst-microsphere removal relationship was 0.76, which indicates that there is a relatively robust surrogate relationship. A comparison of *Cryptosporidium* oocyst and oocyst-sized microsphere removals by the different filter configurations did not uncover any systematic bias based on filter media type (Figure 4-14), suggesting that oocyst-sized microsphere removal was impacted by media properties in a similar manner as *Cryptosporidium* oocysts. Figure 4-13 and Figure 4-14 clearly illustrate the difference in minimum oocyst and microsphere removals. Only one of the microsphere removals is below 0.3 $\log_{10}$, and there are enough low microsphere removal results to almost form a line at approximately 0.4 $\log_{10}$, from 0 to 1 $\log_{10}$ on the oocyst removal axis. In contrast, there does not appear to be a minimum removal for oocysts.

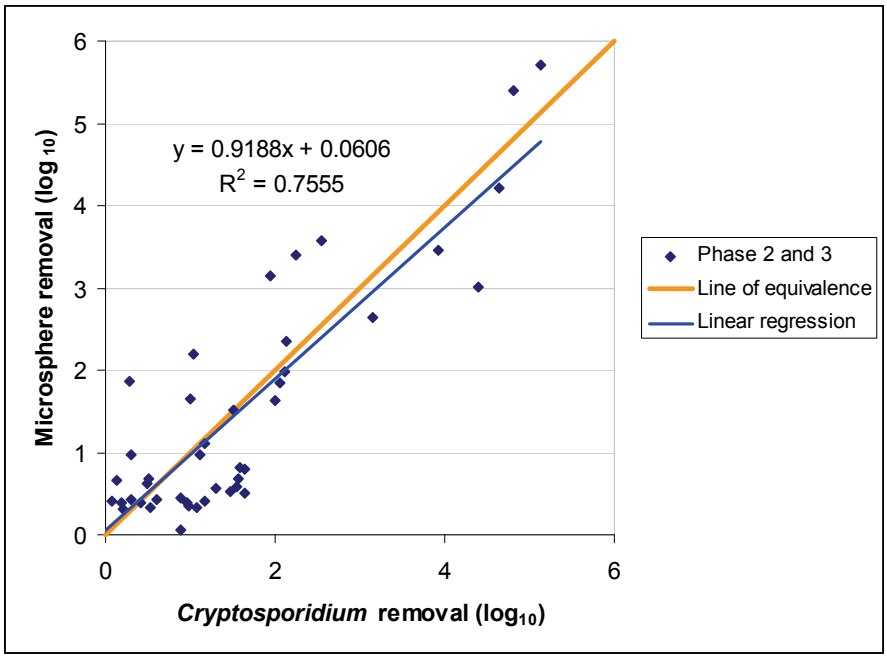

Figure 4-13. *Cryptosporidium* Oocyst and Oocyst-Sized Microsphere Removals by Filtration During Phase 2 and 3 Experiments

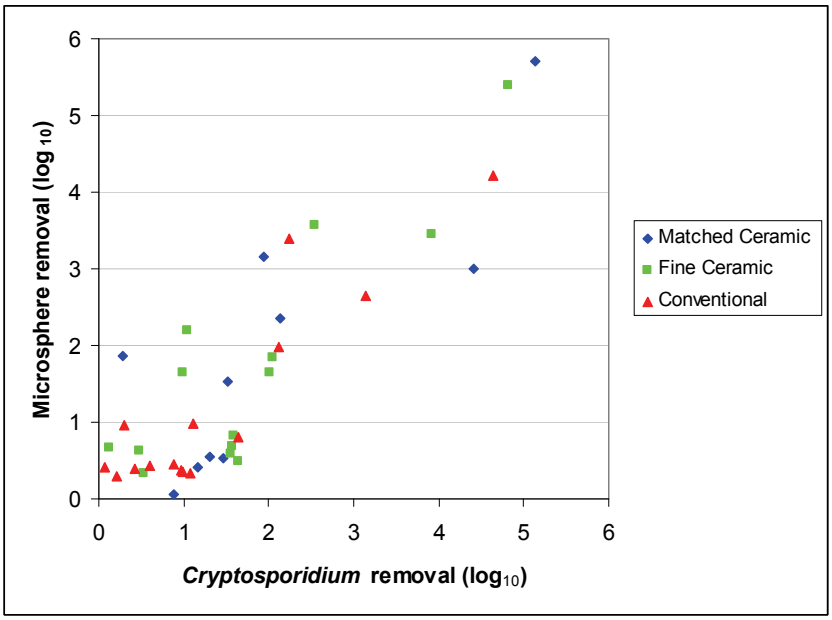

Figure 4-14. *Cryptosporidium* Oocyst and Oocyst-Sized Microsphere Removals by Various Filtration Media During Phase 3 Experiments

The impact of chemical pre-treatment, and more specifically coagulant type, on the reliability of oocyst-sized microspheres as surrogates for *Cryptosporidium* oocyst removal by filtration is presented in Figure 4-15. During the investigations reported herein, microsphere removal by filtration was generally higher than oocyst removal when alum coagulation was utilized. In contrast, microsphere removals were consistently lower than *Cryptosporidium* oocyst removals by filtration when raw water was coagulated with PACl. Specifically, oocyst-sized microsphere removals by filtration preceded by alum coagulation were 1.14 $\log_{10}$ higher than oocyst removals on average; however, when filtration was preceded by PACl coagulation, microsphere removals were on average 0.61 $\log_{10}$ lower than oocyst removals. The slopes of the regression lines for alum and PACl coagulated trials are not far from 1 (0.990 and 0.851, respectively) and the coefficients of determination are reasonable (0.918 and 0.854 for the alum and PACL trials, respectively). The reasonably high values for both the regression slopes and coefficients of determination indicate that it might be possible to account for the discrepancy between oocyst-sized microsphere and *Cryptosporidium* oocyst removals by adding a simple correction constant (specific to the type of coagulant used) to the correlation equation. In such as way microsphere removals might be adjusted to be more representative of oocyst removals GMF.

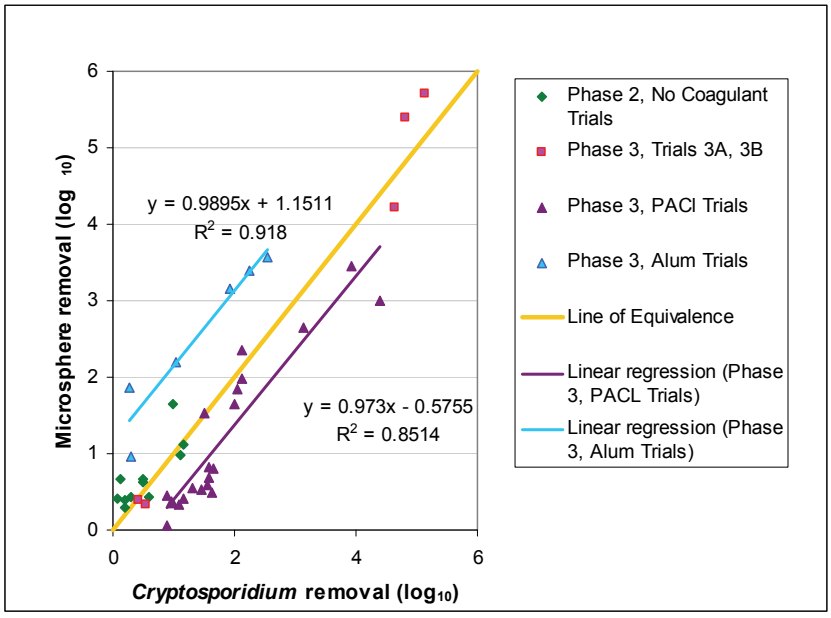

Figure 4-15. *Cryptosporidium* Oocyst and Oocyst-Sized Microsphere Removals Observed During Phase 2 and 3 Experiments When Various Coagulants Were Utilized (regression equations shown are for alum- and PACl-coagulated trials)

The minimum *Cryptosporidium* oocyst reductions observed during the present study were effectively zero, while the lowest microsphere removals were approximately 0.25 $\log_{10}$ (44%). In microsphere results from Phase 2 and 3, there appears to be a minimum microsphere reduction of approximately 0.3 $\log_{10}$ for the conventional media. The minimum microsphere removal for the fine ceramic media appeared to be closer to 0.50 $\log_{10}$. Because the matched ceramic and conventional media achieved similar minimum microsphere removals, these microsphere results suggest that the dominant microsphere removal mechanism during these lower microsphere removals was straining. Since oocysts were close to the same size as the microspheres, straining rates would be expected to be similar. The fact that oocyst removal results from Phase 2 trials were substantially lower than microsphere removals suggests that straining is not an effective filtration mechanism at the operational conditions used during the present investigation. The oocyst's deformable surface may be responsible for the difference in minimum removals, allowing it to be forced through pores smaller than its outer diameter; however, further work on this facet of filtration is beyond the scope of this thesis research.

4.4.6 Head loss

Head loss measurements demonstrated that the fine ceramic filter had consistently higher head loss than the conventional filter during all of the trials conducted (Table 4-9). The matched ceramic filter had slightly higher clean bed head loss than the conventional filter. It is unclear if the slightly higher rate of head loss increase in the matched filter is due to differences in filter configuration, better particle capture, or a combination of both these factors.

Table 4-9. Phase 3 Head Loss

	Matched Ceramic	Fine Ceramic	Conventional
Clean Bed Head Loss (High Loading Rate)	105	210	99
Clean Bed Head Loss (Low Loading Rate)	49	119	52
Mean Head Loss (High Loading Rate)	134	250	125
Mean Head Loss (Low Loading Rate)	54	127	55
Change in Head Loss (High Loading Rate)	70	97	65
Change in Head Loss (Low Loading Rate)	9	16	9

4.5. Mechanistic Aspects

4.5.1 Straining

Filtration models often disregard straining in favour of physicochemical attachment processes (Tufenkji, 2004). During conventional filtration, the addition of coagulant destabilized suspended colloids such that physicochemical attachment of colloids to filter media is favoured. Unfortunately, classical CFT models are often inaccurate in the presence of an energy barrier to colloid deposition, and such models generally underestimate the number of particles captured by filters. When physicochemical attachment is minimized, it is believed that straining is the dominant particle capture mechanism responsible for the minimum observed levels of particle removal.

It has been suggested that straining becomes an important colloid filtration mechanism for colloid/collector diameter ratios as low as 0.008 (Xu, 2006) or even 0.002[1] (Li, 2004). In this study, the lower layer in the fine ceramic media filter (ES: 0.22 mm), had a microsphere (4.8 μm) to collector diameter ratio of 0.02. The colloid/collector diameter ratio for the lower layer in both the conventional and matched engineered ceramic filters was 0.01. Both of these ratios were well above the 0.005 value that Bradford et al. (2004) suggested as the value below which straining becomes important.

According to Bradford et al. (2005), straining was responsible for 68% of the retention of *Cryptosporidium* oocysts in a filter consisting of 15 cm of 0.71 mm diameter sand. Since total oocyst removal was estimated at 58% during Bradford's investigations, straining was apparently responsible for the removal of 39% (0.22 $\log_{10}$) of the oocysts in suspension. Assuming that the mechanism of straining operates constantly through such a filter and that the portion of attachment sites remains relatively unchanged, a 30 cm deep filter of 0.71 mm sand should remove the equivalent of 2 beds of 15 cm deep 0.71 mm sand filters plumbed in series. If this was true, the second filter would remove 39% of the oocysts passed by the first filter, resulting in a cumulative oocyst removal by straining of 63% (0.43 $\log_{10}$). Bradford conducted similar experiments on 0.36 mm and 0.15 diameter sands (Table 4-10)

[1] Please note that this ratio was obtained under very low pore water velocities

Table 4-10. Removal of *Cryptosporidium* Oocysts by Straining (based on Bradford et al., 2005)

Media (L=15 cm)	Total Removal of *Cryptosporidium* Oocysts	Percent of Total Removal due to Straining	Total Removal due to Straining	Equivalent log_{10} Removal due to Straining
0.71 mm Sand	58%	68%	39%	0.22
0.36 mm Sand	75%	79%	59%	0.39
0.15 mm Sand	89%	87%	77%	0.65

Assuming that no straining took place in the coarser upper layer of the dual-media filters utilized during the present investigation, Bradford et al.'s (2005) analysis can be compared to the *Cryptosporidium* oocyst removal results obtained for granular media filtration processes reported herein. Because the lower media in both the conventional and matched ceramic filters consisted of 30 cm of 0.47 mm grains, the minimum observed *Cryptosporidium* oocyst removal should be between the minimum oocyst removals found and reported by Bradford (2005) for the 0.71 mm and 0.36 mm sands; those values were 0.43 log_{10} and 0.78 log_{10} respectively. This was not the case, however. For the conventional media from HWTP, 4 out of 16 oocyst seeding studies yielded oocyst removals between 0.07 and 0.42 log_{10}. 8 out of 19 trials with HWTP's conventional media yielded microsphere removals between 0.30 and 0.42 log_{10}. The minimum oocyst removals achieved by the matched ceramic media filter were also lower than those that would have been expected given Bradford's (2005) work, though there were fewer of these results because the matched ceramic filter configuration was installed after most of the un-coagulated trials were complete. Nevertheless, 2 of the 12 *Cryptosporidium* oocyst removal results (-0.03 and 0.28 log_{10}) were well below the minimum oocyst removal suggested by Bradford (2005).

Based on Bradford et al.'s (2005) study, the fine ceramic media should have yielded oocyst removals between those found for 0.36 mm sand and 0.15 mm sand. Accordingly, minimum *Cryptosporidium* oocyst removals would be between 0.39 log_{10} and 0.65 log_{10} (Table 4-10). Though the *Cryptosporidium* oocyst removals by the fine ceramic media were generally 0.50 log_{10} higher than those observed by the conventional configuration, it is unclear if there was actually a minimum oocyst removal due purely to straining. During Trials I and J, the fine ceramic media removed 0 and 0.13 log_{10}, respectively. These results are far less than the minimum removals suggested by Bradford (2005). The low *Cryptosporidium* oocyst removals achieved by filtration and reported herein indicate that straining filtration is a complex mechanism that does not depends solely on the geometry of pores and colloids. If the straining process was simple, the *Cryptosporidium* oocyst removals achieved

during the present investigation would have been more similar to those reported by Bradford et al. (2005). Two factors that may contribute to the differences between oocyst removal by filtration reported herein and by Bradford et al (2005) are:

- The loading rate used by Bradford was 0.07 m/hr, whereas loading rates of either 9.8 or 24.4 m/hr were utilized herein. At the higher loading rate of 24.4 m/hr the greater tangential velocities and turbulence could prevent some oocysts from remaining attached to collectors. Elevated pressures might aid in colloid passage by forcing colloids through pore restrictions.

- Colloid properties may affect straining. *Cryptosporidium* oocysts have soft, deformable outer membranes. The greater the loading rate, the more likely oocysts could be squeezed through pore restrictions. The steric repulsion caused by the oocysts' "hairy" outer layer may also help the oocysts slide past pore restrictions.

The combination of higher flow rate and deformable colloids may account for the differences in minimum oocyst removals observed between this study and Bradford et al. (2005). The importance of these considerations is supported by the fact that even the fine ceramic medium did not appear to have a minimum oocyst removal capability, despite the fact that the oocyst/media diameter ratio was 0.02 – well above the 0.005 mentioned by Bradford et al. (2005) and others. To further support the importance of colloid deformability, it must be noted that there *was* actually a minimum microsphere removal for all three pilot filters. Accordingly, the higher minimum removals of microspheres may have been due to their hard surfaces, which prevented them from passing through pores.

The Bradford et al. (2005) oocyst straining results can also be used to evaluate the oocyst-sized microsphere removal data obtained during the present investigation. Disregarding Trial 3J (there are 2 microsphere results in this data set which are extreme values that appear to be anomalous. The reason for the extreme values remains undetermined.), the minimum microsphere $\log_{10}$ removals calculated from means of the 4 lowest results in Phase 2 and 3 experiments were 0.34 $\log_{10}$ (54%) by the conventional media and 0.52 $\log_{10}$ (70%) by the fine ceramic media. If these results do represent the minimum possible microsphere removals, then straining was likely the major filtration mechanism contributing to microsphere removal during the trials with poor filter performance.

According to the data presented by Bradford et al. (2005), the minimum possible microsphere removal by the fine ceramic media should have been between those found for the 0.36 mm and 0.15 mm sand (0.39 $\log_{10}$ and 0.65 $\log_{10}$, respectively). The results from this study indicate that the minimum microsphere removal by the fine ceramic media was 0.54 $\log_{10}$, which is consistent with

Bradford et al.'s (2005). If the conventional and matched ceramic media behaved similarly to Bradford et al.'s (2005) media, minimum microsphere removals between those of the 0.71 mm and 0.36 mm sand (0.43 $\log_{10}$ and 0.78 $\log_{10}$, respectively) would be expected. The observed microsphere reductions the matched ceramic and conventional media filters were below those values, at approximately 0.34 $\log_{10}$ however. A more detailed evaluation of straining in rapid granular media filtration applications and by the conventional and engineered ceramic media specifically is warranted but beyond the scope of this research, however.

4.5.2 Key Findings Regarding Straining

- During trials that resulted in low levels of *Cryptosporidium* oocyst removal, reducing media grain size by half did not increase the minimum *Cryptosporidium* oocyst reduction levels. Within this study as a whole, the use of smaller sized media resulted in increased head loss, without increasing the minimum level of observed *Cryptosporidium* oocyst removal.

- Because minimum *Cryptosporidium* oocyst removals were not observed by any of the filter configurations (minimum oocyst removals were essentially zero), it is possible that straining was not a significant mechanism for *Cryptosporidium* oocyst removal at the operational conditions investigated; accordingly, although recent CFT model developments have demonstrated that straining can be an important mechanism for colloid deposition in some porous media systems (regardless of the presence of coagulant), it should not be regarded as an effective mechanism for *Cryptosporidium* oocyst removal by rapid GMF at impaired coagulation conditions.

- The potential straining of *Cryptosporidium* oocysts and oocyst-sized microspheres must be further investigated. It appears that at unfavourable conditions for physicochemical attachment, the differences in surface roughness between the ceramic and conventional media did not affect the removal of *Cryptosporidium* oocysts or microspheres, though greater media surface roughness appeared to enhance turbidity and particle count reductions.

- Oocyst-sized microspheres exhibited a minimum level of removal that appeared to be influenced by media size. Consistent with straining theory, the matched ceramic and conventional media yielded similar minimum levels of microsphere removal, while the fine ceramic media yielded a relatively higher minimum level of microsphere removals.

- Straining appears to be affected by hydraulic loading rate and colloid characteristics and is not a purely geometrically defined phenomenon.

5. Conclusions and Recommendations

5.1. Conclusions

A series of seeding experiments were conducted to examine the impacts of media roughness on filter performance and to evaluate engineered ceramic filter media for use in granular media filters. Filter media performance was assessed based on turbidity and particle count reductions, *Cryptosporidium* oocyst and oocyst-sized microsphere removals, head loss and stability of operation. Experiments were designed to allow related facets of current filtration research to be examined: effect of loading rate, coagulant type and dosage, and suitability of latex microspheres as surrogates for *Cryptosporidium* oocyst removal by filtration. Conclusions derived from the analysis of experimental results can be divided into 3 main categories: general filter performance, *Cryptosporidium* oocyst removals and mechanistic findings.

5.1.1 General Filter Performance

The matched ceramic filter media performed achieved better filter effluent turbidity and particle counts than the conventional media filter at all conditions investigated, while maintaining similar filter run times. The matched ceramic media also provided more stable operation when exposed to changing influent water quality.

- The fine ceramic configuration consistently demonstrated lower filter effluent turbidities and particle counts than the matched ceramic media, likely due to differences in media grain size. The magnitude of this improved performance varied depending on the operational conditions investigated.

- The matched ceramic media generally achieved higher oocyst removals on average relative to the conventional media at all conditions investigated except alum coagulation, during which essentially comparable oocyst removals were observed. Depending on the operational conditions, oocyst removal was as much as 1.25 $\log_{10}$ higher in the matched ceramic media filter.

- The matched ceramic media produced higher quality effluent with filter run times similar to the conventional filter, suggesting that the ceramic media may have a higher solids loading capacity than the conventional media.

5.1.2 *Cryptosporidium* Oocyst Removals

- *Cryptosporidium* oocyst removals achieved by the matched ceramic media were generally higher than those achieved by the conventional media, though the magnitude of this difference depended on operational conditions, especially coagulant type and coagulant dose. On average, the difference for eight PACl trials was 0.31 $\log_{10}$; however, the mean difference during the two alum-coagulated trials was -0.16 $\log_{10}$.

- It appears that the ceramic and conventional media responded differently to changes in coagulant type. Specifically, alum coagulation did not appear to be an optimal coagulation regime for oocyst removal by ceramic media filters at the operational conditions investigated.

- Increased loading rates only appeared to have an effect on oocyst removal during trials with alum coagulation.

- When using PACl for coagulation, differences in *Cryptosporidium* oocyst removal between the various media configurations were most pronounced at conditions closer to optimal coagulation. Stated simply: the higher the *Cryptosporidium* reductions were, the greater the difference in oocyst removals between ceramic and conventional media.

- Filter effluent turbidity and turbidity reduction were poor predictors of oocyst removal. However, turbidity reduction may be valuable for indicating when filters are at risk of pathogen passage since high oocyst removals were only achieved when turbidity reduction was higher.

- Microsphere removal provided the most accurate surrogate for oocyst removal in this study, though there were several non-idealities:

    - Microsphere removals were higher than oocyst removals during trials conducted with alum coagulant,

    - Microsphere removals were lower than oocyst removals during trials conducted with PACl coagulant, and

- At conditions of highly impaired colloid attachment, microspheres appeared to be removed by straining filtration more significantly than oocysts.

- Contrasts in oocyst removals due to the use of alternative media were most pronounced when oocyst removals were at the highest levels observed; however, differences in microsphere removals were highest when oocyst removals were at the lowest levels observed.

5.1.3 Mechanistic Findings

- The matching of the conventional media configuration with engineered ceramic media allowed media surface properties to be isolated as the cause for the ceramic media's improved filtration.

- Results from the investigations of sudden filter influent quality changes (*i.e.* turbidity spikes) near the end of filter cycles support the conclusion that filter performance advantages provided by the ceramic media were due principally to its greater surface roughness. Comparison of the "dense" and "fine" ceramic media performance during these investigations also indicated that surface roughness resulted in the observed differences in effluent water quality from these media.

- Surface roughness contributed to improved filter effluent turbidities and particle counts at all conditions investigated. Roughness did not provide any considerable advantage in oocyst removal when oocyst deposition was severely impaired by either lack of coagulant addition or by poor coagulation conditions.

- Straining by itself, was not a major mechanism contributing to *Cryptosporidium* oocyst removal under the experimental conditions investigated. The use of granular filter media finer than those utilized herein is unlikely to provide a practical advantage in oocyst removal by filtration because of the dramatic decrease in filter run time it would likely cause. The best strategy for removal of *Cryptosporidium* oocysts utilizes the optimization of physicochemical filtration through careful media selection, coagulant dosing and flocculation.

- Straining was an important microsphere removal mechanism at unfavourable deposition conditions, suggesting that microspheres should not be used as surrogates for *Cryptosporidium* oocyst filtration at conditions during which oocyst removal is severely compromised.

5.2. Significance of Results

The results of this study helped to fill a gap in knowledge regarding 1) the impacts of media roughness on overall filtration performance and 2) the utility of using engineered ceramic media in rapid gravity granular media filtration applications while also comparing the performance of engineered media to conventional filtration media. This investigation found that WTP's may be able to significantly improve both filter effluent quality and treatment robustness through the use of rough, spherical filtration media such as the engineered ceramic media, without drastic alterations to existing GMF processes. Specifically, engineered media that are optimized for granular media filtration have the potential to improve all aspects of granular media filter performance, including pathogen removal, without decreasing filter run time.

If future pilot or full scale experiments demonstrate that engineered media reliably provide significant improvements in pathogen removal relative to conventional filtration media, requirements for disinfection could plausibly be lowered; thereby resulting in potential cost savings and decreases in disinfection by-products formation. Accordingly, further investigation of rough, spherical media such as the engineered ceramic media is worthwhile for its potential to improve filter effluent quality and operational stability while lowering the potential for disinfection by-product formation.

The contrasts in filter performance between media in response to various operating conditions underscore the importance of tailoring filtration process for specific media. When replacing filter media in favour of different materials, WTP's may not be able to simply replace media and continue operating exactly as before. Changes in filter media likely require process alterations in order to optimize performance for the alternate media (*i.e.* changes in coagulant type, dose, flocculation system) even if media size and configuration are held constant. Similarly, pilot studies that compare the filter performance of different media should test numerous experimental conditions to determine each media's optimal operating conditions before finalizing media choices. Piloting filter performance for an entire year is recommended if there are major seasonal variations in water conditions (temperature, turbidity, algae blooms) and operating conditions (water demand, coagulant type, water source).

There were important gaps in knowledge regarding the effect of media surface roughness on GMF which were addressed by this investigation. Previous work on the subject generally lacked one or more of the following:

- Direct comparison with conventional media of the same size and configuration,

- Comparison of conventional media with media that was significantly rougher,
- Conditions which were representative of full-scale water treatment, and/or
- Experiments larger than bench-scale.

The present study's pilot-scale experimentation was conducted without any of the above shortcomings to ensure that this mechanistic research into colloid filtration provided a link between CFT and full-scale drinking water filtration. Analysis of oocyst and microsphere removals under a variety of conditions shed light on straining filtration as a pathogen removal mechanism in GMF.

5.3. Recommendations

This research demonstrated that the surface texture of filter media has a significant impact on filter performance and that the use of optimized engineered filter media can improve filter performance in granular media filtration. The results suggest that further testing of this ceramic media should be pursued and that optimizing media properties will yield important gains in filter performance and drinking water safety. This research also shed light on the mechanism of straining and how colloid properties affect straining filtration under realistic filtration conditions. In light of the results of this study, a number of recommendations for further research are proposed:

- This study compared the performance of ceramic and conventional media using low turbidity source water. It is worthwhile to compare the media using other surface waters to explore how the media respond to different water matrices. Using the pilot filters on high turbidity river water may provide further insight into media properties and media optimization. Such experiments will also assist municipalities with decision making regarding the value of piloting alternative media in filter upgrades.
- Biologically Active Filtration (BAF) is increasingly popular as disinfection by ozonation is installed in more WTP's. Since the rough surface of the ceramic media is advantageous for biofilm growth (Bolton et al., 2006), testing of this media should be pursued under BAF conditions.
- The continuation of mechanistic studies may be useful in determining how various media properties affect filtration. The results of such experimentation may prove invaluable for

future attempts to model filtration. Since the many variables in filtration tend to interact, a factorial design experiment is recommended which would compare:

- ceramic media *vs.* sand *vs.* glass,
- spherical *vs.* angular (*i.e.* crushed glass/ceramics *vs.* glass spheres/ceramic spheres),
- large *vs.* small media (*i.e.* 1 mm *vs.* 0.5 mm),
- high loading rate *vs.* low loading rate (24.4 or 9.8 m/hr), and
- different coagulation regimes (Alum, PACl, ferric chloride, *etc.*).

Appendix A List of Abbreviations

ASTM	American Society for Testing and Materials
BAF	Biologically active filtration
CCME	Canadian Council of Ministers of the Environment
CFT	Colloid filtration theory
CWC	Clean Washington Center
d	Diameter of media grain
D	Interior diameter of pilot column
DBP	Disinfection by-product
ES	Effective Size
GAC	Granular activated carbon
GPM/ft^2	gallons per minute per square foot
GWUDI	Groundwater under the influence of surface water
HWTP	Horgan Water Treatment Plant
IFA	Immuno-fluorescence Assay
L	Depth of filter media
LT22ESWTR	Long Term 2 Enhanced Surface Water Treatment Rule
MBAS	Methylene Blue active substances
MP&T	Media Process and Technology Incorporated
MWH	Montgomery Watson Harza Incorporated
NOM	Natural Organic Matter
PACl	Polyaluminum chloride
RT	Rajagopalan and Tien
TE	Tufenkji and Elimelech
UC	Uniformity coefficient
vdW	van der Waal
WTP	Water treatment plant
η_T	single-collector contact efficiency
α	deposition efficiency

Appendix B Auxiliary Experiments

The following experiments were conducted to provide further information for various aspects of the main testing. These supplementary experiments include:

- Sieve analysis of filter media
- Recovery and system losses studies
- Plant and pilot floc analysis
- MBAS (methylene blue active substances) testing
- Zeta potential measurements of raw and coagulated waters

B.1. Sieve Analysis

All engineered ceramic media were supplied by Kinetico Canada Inc. Conventional media were supplied by the University of Waterloo, City of Toronto and Kinetico Canada Inc.

Standard sieve analyses were performed on all filter media using a standard sieve shaker (Oscillatap model ML 4330OST, M&L Testing Equipment, Dundas, ON) according to ASTM # C 136. Number 4, 10, 20, 30, 40, 50, 60, 70, 100, 200 sieve sizes were used. These numbers correlate to nominal sieve openings of 4.76 mm, 2.00 mm, 0.841 mm, 0.595 mm, 0.420 mm, 0.297 mm, 0.250 mm, 0.210 mm, 0.149 mm and 0.074 mm, respectively. Please see Table B-1 and Table B-2 for the raw sieve data as well as information on d_{10}, d_{60}, uniformity coefficient and usage. Dates noted for material descriptions in Table B-2 denote the date the material was delivered to the project.

The graded gravel bed used in all columns in Phase 2 and 3 trials was made with the following sizes of gravel:

- 2 cm of 10-14 mesh sand (grain size approx. 1.5 mm), screened from "Red Flint™" fine gravel
- 6.5 cm of "Red Flint™" fine gravel (grain size approx. 2.5 mm)
- 6.5 cm of pea gravel (grain size approx. 5 mm)
- 5 cm of coarse gravel (grain size approx. 15 mm)

Table B-1. Raw Sieve Analysis Data

	Percent of Total, by mass										
Sieve Mesh Number	4	10	20	30	40	50	60	70	100	200	tray dust
Nominal Sieve Opening (mm)	4.75	2.00	0.85	0.60	0.43	0.30	0.25	0.21	0.15	0.08	<0.08
Material											
Phase 1 Anthracite	0	5.00	91.03	3.46	0.51	0	0	0	0	0	0
Phase 1 Sand	0	0	7.34	43.89	43.54	4.55	0.35	0.18	0.11	0.04	0
"Red Flint", uncut fine gravel (support media)	0	78.01	21.99	0	0	0	0	0	0	0	0
"Best Sand" pea gravel (support media)	31.34	68.64	0.02	0	0	0	0	0	0	0	0
Phase 1 garnet (support media)	0	0	0	1.63	60.29	37.08	0.76	0.20	0.04	0	0
HWTP Anthracite, filter #5	0	0.58	93.09	2.72	2.51	1.11	0	0	0	0	0
HWTP Sand, filter # 5	0.42	3.46	10.05	52.53	32.41	1.14	0	0	0	0	0
Ceramic 70/80 (Oct, 2005)	0	0	0	0	0	0.28	5.88	83.47	10.22	0	0.14
Ceramic 70/80 (Oct, 2005) heavy fraction	0	0	1.11	0	0.22	0.89	10.89	81.00	5.78	0	0.11
Ceramic "M9" (Oct, 2005)	0	0	0	0	21.85	71.06	5.58	1.20	0.30	0	0
Ceramic 20/40 (Oct, 2005)	0	0	0	44.34	54.16	1.39	0	0	0	0	0.11
Ceramic 14/30 (Oct, 2005)	0	0	99.85	0.15	0	0	0	0	0	0	0
Ceramic 14/30 (Oct, 2005) light fraction	0	0	99.89	0.05	0.05	0	0	0	0	0	0
Ceramic "M6" (July, 2006)	0	0.21	70.79	22.71	6.09	0.21	0	0	0	0	0
Ceramic "M9" (July, 2006)	0	0	0	0	0.12	9.40	50.64	36.54	3.25	0	0.06
Ceramic matched to HWTP Anthracite	0	5.00	91.03	3.46	0.51	0	0	0	0	0	0
Ceramic matched to HWTP Sand	0	0	7.34	43.89	43.54	4.55	0.35	0.18	0.11	0.04	0

Table B-2. Media Analysis Results

Material	E.S. (d10)	d60	Uniformity Coefficient	Used In:
	(mm)	(mm)	(d60/d10)	Column # (Trial or Phase)
UW anthracite	0.94	1.55	1.65	2 (1A, 1B)
UW sand	0.44	0.67	1.52	2 (1A, 1B)
"Red Flint", uncut fine gravel	1.36	3.35	2.46	2 (1A, 1B), 1, 2, 3 (Phase 2, 3)
"Best Sand" pea gravel	2.41	4.4	1.83	2 (1A, 1B), 1, 2, 3 (Phase 2, 3)
Garnet	0.34	0.49	1.44	1, 3 (1A, 1B) 1, 2, 3 (1C, 1D)
HWTP Anthracite, filter #5	0.89	1.51	1.70	3 (Phase 2, 3)
HWTP Sand, filter # 5	0.47	0.72	1.53	3 (Phase 2, 3)
Ceramic 70/80 (Oct, 2005)	0.21	0.235	1.12	2 (Phase 2, 3)
Ceramic 70/80 (Oct, 2005) heavy fraction	0.22	0.235	1.07	1, 3 (1A, 1B)
Ceramic "M9" (Oct, 2005)	0.30	0.39	1.30	1, 2, 3 (1C, 1D)
Ceramic 20/40 (Oct, 2005)	0.45	0.625	1.39	1 (1A, 1B)
Ceramic 14/30 (Oct, 2005)	0.96	1.54	1.60	1, 2, 3 (1C, 1D), 2 (Phase 2, 3)
Ceramic 14/30 (Oct, 2005) light fraction	0.96	1.54	1.60	3 (1A, 1B)
Ceramic "M6" (July, 2006)	0.64	1.35	2.11	1 (Phase 2)
Ceramic "M9" (July, 2006)	0.22	0.27	1.23	1 (Phase 2)
Ceramic matched to Horgan Anthracite	0.89	1.51	1.70	2 (Phase 3)
Ceramic matched to Horgan Sand	0.47	0.72	1.63	2 (Phase 3)

B.2. Recovery Study and System Losses

A recovery study was conducted at the University of Waterloo to compare haemocytometer counts with IFA counts. IFA counts were used for all *Cryptosporidium* enumeration in Trials 2 and 3. One microsphere and one *Cryptosporidium* oocyst suspension were prepared from stock suspensions. The stock suspensions were diluted such that haemocytometer counts would be well above 50 counts per 1/50,000 mL (Table B-3). After enumeration by haemocytometer, equal amounts of the two suspensions were combined and further diluted by serial dilution until *Cryptosporidium* oocysts and microsphere concentrations were similar to that of influent concentrations during previous trials. Using sample volumes of 0.5 mL, *Cryptosporidium* oocyst and microsphere concentrations in the suspension were then enumerated by the same method as was used to enumerate influent samples

during seeding trials. A portion of this suspension was further diluted until *Cryptosporidium* oocyst and microsphere concentrations were similar to those commonly found in effluent samples during previous trials. Utilizing sample volumes of 50 mL, *Cryptosporidium* oocyst and microsphere concentrations in this suspension were enumerated using the same method as was used to enumerate influent samples.

To ensure that all *Cryptosporidium* oocysts in the samples were being effectively stained, a pre-stained suspension of *Cryptosporidium* oocysts was prepared for enumeration by haemocytometer. Enumeration by haemocytometer under UV and visible light yielded identical results. Comparison of UV and visible light images of the same field of view showed that all *Cryptosporidium* oocysts in suspension were effectively stained and that all visible particles in the oocyst stock suspensions were *C. parvum* oocysts.

After Trial 3M, the contents of Column 1 (the matched ceramic media) were emptied into a container for later re-use and the empty column was prepared for a study of system losses. The test was conducted at a loading rate of 10 m/hr with the same coagulant dose as in Trial 3M: 3.7 mg/L alum. The spike concentration was diluted to approximately 1% of the previous spike. To prepare for this test, the filter column was backwashed thoroughly and run for 10 minutes at high rate, approximately 50 m/hr. The loading rate was reduced to 10 m/hr and run for 10 minutes to limit eddy currents from the previous, higher loading rate. The spike was injected for 60 minutes, during which time influent and effluent samples were collected every 10 minutes using the same method as in all other trials.

The results obtained during the study of system losses indicate that these losses were minimal. Effluent concentrations of *Cryptosporidium* oocysts were 13% (0.06 $\log_{10}$) lower than influent measurements, while effluent microsphere concentrations were close to 100% of influent (Table B-4). Because of variability in the results, it is not possible to determine if the observed 13% loss of *C. parvum* oocysts to the system was significant. As a result, all *C. parvum* and microsphere data reported in this study are un-adjusted. Statistical analyses revealed that the variability in both the haemocytometer and IFA results was over-disperse. Due to the variability, it is not possible to determine confidence intervals for either of the two enumeration methods.

Table B-3. Summary of Recovery Study Results

	Haemocytometer results		IFA results, "Influent" Concentrations		IFA results, "Effluent" Concentrations	
	Microsphere Concentration (per mL)	*C. parvum* Concentration (per mL)	Microsphere Concentration (per L)	*C. parvum* Concentration (per L)	Microsphere Concentration (per L)	*C. parvum* Concentration (per L)
1	8,950,000	12,900,000	380,000	794,000	3,020	2,980
2	7,600,000	13,150,000	672,000	1,572,000	1,060	4,280
3	3,700,000	19,250,000	424,000	748,000	1,260	4,080
4	9,000,000	8,850,000	382,000	790,000	1,100	4,360
5	10,750,000	11,200,000	436,000	766,000	1,000	2,680
6	7,100,000	11,000,000	376,000	748,000	1,140	4,560
7	8,400,000	10,000,000	328,000	698,000	600	3,920
8	8,900,000	11,250,000	392,000	882,000	840	3,600
9	3,850,000	10,350,000	-	-	-	-
10	6,200,000	8,750,000	-	-	-	-
Mean	7,445,000	11,670,000	423,750	874,750	1,253	3,808

Table B-4. Summary of System Loss Data

Time (minutes)	Microsphere Concentrations (per L)		*C. parvum* Concentrations (per L)	
	Influent	Effluent	Influent	Effluent
0	520	140	140	380
10	39550	33950	60600	41150
20	49500	44200	64550	52800
30	50867	30600	73133	55733
40	45600	33467	81333	59667
50	6133	63867	67467	83200
Mean (10 to 50 minutes)	38330	41217	69417	58510
Percent of Influent recovered:	-	107.5	-	84.3

B.3. Floc Analysis

Flocculation is the process whereby suspended particles in the filter influent are carefully mixed after coagulation in order to promote particle collisions. The destabilized particles adhere to each other and eventually form aggregates called floc. In conventional filtration systems with sedimentation, flocculation creates large, dense floc so that they settle out in sedimentation tanks before the raw water proceeds to the filters. In direct filtration flocculation processes are designed such that small flocs are created. The smaller flocs can penetrate deeper into the filter allowing more of the filter capacity to be used. The cleaner source waters are, the more difficult flocculation becomes because the frequency of colloid collisions is low because of the low concentration of suspended particles. In addition, flocculation of low turbidity water can be more sensitive to small changes in water quality, requiring closer monitoring of raw water and coagulant dosing conditions.

Since the HWTP's source water is the generally low turbidity water from Lake Ontario (raw water turbidity levels are generally below 0.5 NTU), the HWTP is a direct filtration plant in which the chemical pre-treatment process (coagulation and flocculation) results in the formation of relatively small flocs.

During the winter of 2007, Mr. Adam Arnold (an M.A.Sc. candidate at the University of Waterloo) collected floc samples from both HWTP filter influent and from the pilot apparatus utilized during the present investigation when PACl coagulation was being utilized. Analysis of the HWTP samples revealed that floc concentrations measurable by conventional floc characterization techniques (de Boer et al., 2000) were very low and that the majority of visible particles were not floc but rather detritus and other natural substances. Similar results were found for the pilot filters. Because of these limitations, floc characterization and comparison were not possible.

It is worth noting that samples from HWTP took much longer to filter through the sample membranes. This suggests that flocculation was more effective in full-scale operations. The fact that the effluent turbidity from the pilot's conventional media never matched the full scale operation's effluent turbidity also indicates that chemical pre-treatment by the pilot scale treatment process was not adequate. Despite adjustments in the operation of the pilot flocculator and coagulant dosage, full-

scale filter performance (filter effluent turbidities and filter run times) could not be matched at pilot-scale. It is possible that the lack of pre-chlorination may have been responsible for these observed differences in filter performance. Continued efforts to match full scale flocculation were beyond the scope of this project.

B.4. MBAS Experiments

After a significant drop in filter performance (as measured by *C. parvum* removals during Trials 2C to 2F) occurred in September of 2006, a number of hypotheses emerged proposing mechanisms that might account for this change.

Due to lack of significant changes in influent water quality, temperature or weather conditions, the possibility of the presence of natural surfactants contributing to filtration performance was investigated. This possibility was proposed since no measurable change had occurred in any of the plant's daily measurements of water quality (turbidity, temperature, pH, alkalinity, hardness, DO, TOC, colour, aluminum, fluoride, iron, nitrogen, etc.) that could be correlated to changes in *C. parvum* removals. If filter performance was dramatically affected despite there being no measurable change in the water's chemistry, it was possible that a surface active substance was responsible. Surfactants have been shown to enhance microbe passage through porous media (Li and Logan 1999; Brown and Jaffe 2001, 2006). In some cases, *C. parvum* uptake of surfactants can have significant effects on surface potential at surfactant concentrations as low as 2×10^{-8} M (Karaman et al., 1998). Czarnecki (1991) concluded that the absorption of surfactant to latex particles would increase their hydrodynamic radius and as a result, alter the particle's diffusion coefficient. The increase in hydrodynamic radius would likely increase particle re-entrainment (Li et al., 2005; Bergendahl and Grasso, 2003) without increasing particle capture by straining.

Unfortunately surfactants are extremely difficult to detect in low concentrations in natural water matrices (Youssef et al., 2004). Full scale operations showed no similar decline in filter performance

of increase in coagulant requirements, suggesting that pre-chlorination of raw water prevented the surfactant from interfering with filtration.[2]

It was proposed that algae in the lake had responded to seasonal changes (shortening of daylight hours, cooling of lake water) either by producing natural surfactants, or by dying and releasing surfactants upon decomposition. There are a number of analyses available to check for the presence of surfactants, but because surfactant behaviour is highly dependant on the individual water matrix, there are no quick tests for surfactant concentration. To test if there were changes in anionic surfactant levels, a modified MBAS (Methylene Blue Active Substances, Chitikela, 2001) test was conducted on various water samples collected during Phase 2 and early Phase 3 trials. This method only detected qualitative differences in anionic surfactant concentrations; nonionic and cationic surfactants were not measured. The results indicate that there were changes in the concentration of anionic surfactants during the course of these trials, though the measured changes did not correlate to changes in filter performance (Table B-5).

While the surfactant test results did indicate that there were differences in anionic surfactant levels, they provided no indication of what the surfactants were (or what their source was) or if the surfactants were the cause of the changes in filter performance.

Between trials 3J and 3K (less than 2 days) the pilot filter's *C. parvum* oocyst removals increased suddenly for all 3 filter configurations by 2 to 3 $\log_{10}$ - perhaps the reversal of the change that occurred in September of the previous year. As in September, the HWTP measured no obvious changes in raw water chemistry (temperature, TOC, pH, alkalinity, turbidity, particle counts, nitrogen, HPC) that might explain the difference in observed *C. parvum* oocyst removals. Again, this difference in filter performance was not observed in the full scale operations, possibly because the full scale

[2] A speculative proposal by the author suggests that the performance difference might be related to changes in biofilm community. Turbidity and particle count reductions were not affected by whatever resulted in the observed differences of *Cryptosporidium* oocyst removals by filtration, so perhaps the reason for the change in *C. parvum* removals was biological. Due to the pre-chlorination of the HWTP raw water, the full scale filters would not be able to grow a biofilm. If seasonal changes favoured one biofilm microorganism over another, backwashing during this change might allow for the new organism to populate the surfaces of the filter. Could it be that different biofilm communities might be more or less beneficial for *C. parvum* removal?

filters were receiving pre-chlorinated raw water. Other hypotheses were proposed, but though interesting, they were outside the scope of the present work.

Table B-5. MBAS Results

Trial (Date)	UV Absorbance
2B (August 11th, 2006)	0.0141
2C (September 6th, 2006)	0.0237
2F (September 25th, 2006)	0.00798
3A (December 11th, 2006)	0.00478

B.5. Zeta Potential Testing

It was proposed that electrophoretic mobility measurements and subsequent calculations of zeta potential might help elucidate the mechanism(s) contributing to the observed differences in filter performance between Trials 3J and 3K. Zeta potentials (ZP) were analyzed using a Malvern Zetasizer by Stefan Liedtke and Prof. Nathalie Tufenkji (Department of Chemical Engineering, McGill University, Montreal, Quebec). Water samples (including raw, coagulated, spiked and spiked coagulated water) containing approximately 10^5 *C. parvum* oocysts/L were analyzed in June of 2007. ZP results presented in Table B-6 are means of 3 readings.

ZP results obtained for the various water samples (including raw, coagulated, spiked and spiked coagulated water) were variable and yielded no obvious trends. Moreover, changes in ZP did not correlate to the observed changes in filter performance.

Table B-6. Zeta Potential Results

Description of Sample (Date sample taken)	Zeta Potential (mV)[3]
Trial F Raw Water (August 11, 2006)	-9.06
Trial G Raw water (September 6, 2006)	-7.33
Trial J Raw Water (September 25, 2006)	-6.55
Trial L Raw Water (December 11, 2006)	-7.72
Trial O Raw Water (April 2, 2007)	-6.43
Trial P Raw Water (April 6, 2007)	-4.30
Trial Q Raw Water (April 11, 2007)	-5.27
Trial S,T[4] Raw Water (April 20, 2007)	-6.17
Trial V Raw Water (April 26, 2007)	-7.38
Trial T Coagulated Water (April 21, 2007)[5]	-6.60
Trial T Coagulated and Spiked Water (April 21, 2007)[6]	-5.17
Trial U Coagulated Water (April 24, 2007)	-5.26
Trial U Coagulated and Spiked Water (April 24, 2007)	-6.30
Trial V Coagulated Water (April 26, 2007)	-6.99
Trial V Coagulated and Spiked Water (April 26, 2007)	-6.29

[3] Results shown are means of 3 readings

[4] Trial S and T were performed consecutively - raw water sample taken between the experiments

[5] Coagulant for these trials was PACl, and was between 0.3 and 0.6mg/L for these trials

[6] The spike for these experiments was a mix of microsphere and *C. parvum* in coagulated water resulting in a concentration of about $1.5X10^6$ *C. parvum* and MS combined per litre.

Appendix C Summary of Trial Results

Summary Information for: Trial 1A

Trial Conditions:	
Trial Date	March 16, 2006
Location	University of Waterloo
Water Source	Tap water with Kaolin Dust
Loading Rate	10 GPM/ft2 (24.4 m/hr)
Coagulation	No Coagulant
Water Temperature	14^0C

Filter Media Configuration:

	Column 1	**Column 2**	**Column 3**
	Very Fine Ceramic	Conventional	Fine Ceramic
Top Layer	45 cm ceramic, ES 0.45 mm	45 cm anthracite, ES 0.4 mm	45 cm ceramic, ES 0.96 mm
Bottom Layer	15 cm ceramic, ES 0.22 mm	35 cm sand, ES 0.44 mm	15 cm ceramic, ES 0.22 mm
Support Media	8 cm garnet , ES 0.34 mm	20 cm graded gravel bed	8 cm garnet , ES 0.34 mm

Parameter:	**Influent**	**Very Fine Ceramic**	**Conventional**	**Fine Ceramic**
Log reductions:				
Cryptosporidium		0.00	0.00	0.00
Microspheres		2.81	0.71	1.86
Other Parameters[1]:				
Average turbidity (NTU)	1.119	0.067	0.365	0.145
Turbidity reduction (%)		94	67	87
Average total particle count (#/mL)	11569	264	2295	855
Particle reduction (%)		98	80	93
Average flow (mL/min)		1825	1832	1839
Clean bed headloss		144	71	143
Average headloss (cm)		143	72	143
Change in headloss (cm)		0	3	0

[1] *Data calculated from time 0 (start of spike injection) to 360 elapsed minutes*

***Cryptosporidium* and Microsphere Removal Summary:** **Trial 1A**

***Cryptosporidium* Log Removal**

Time	Col 1	Col 2	Col 3
10 min			
20 min	0.00	0.00	0.00
30 min	0.00	0.00	0.00
40 min	0.00	0.00	0.00
50 min	0.00	0.00	0.00
60 min			
70 min			
Avg.[1]	**0.00**	**0.00**	**0.00**

[1]*Avgerage denotes time interval from 15 min to 30 min*

Microsphere Log Removal

Time	Col 1	Col 2	Col 3
0 min	2.98	0.81	2.01
15 min	2.63	0.53	1.51
30 min	1.91	0.57	1.07
45 min	0.88	-0.13	0.28
60 min	0.97	-1.01	-0.21
120 min	0.74	-1.11	-0.65
180 min	-2.74	-1.33	-0.54
Avg.[1]	**2.81**	**0.71**	**1.86**

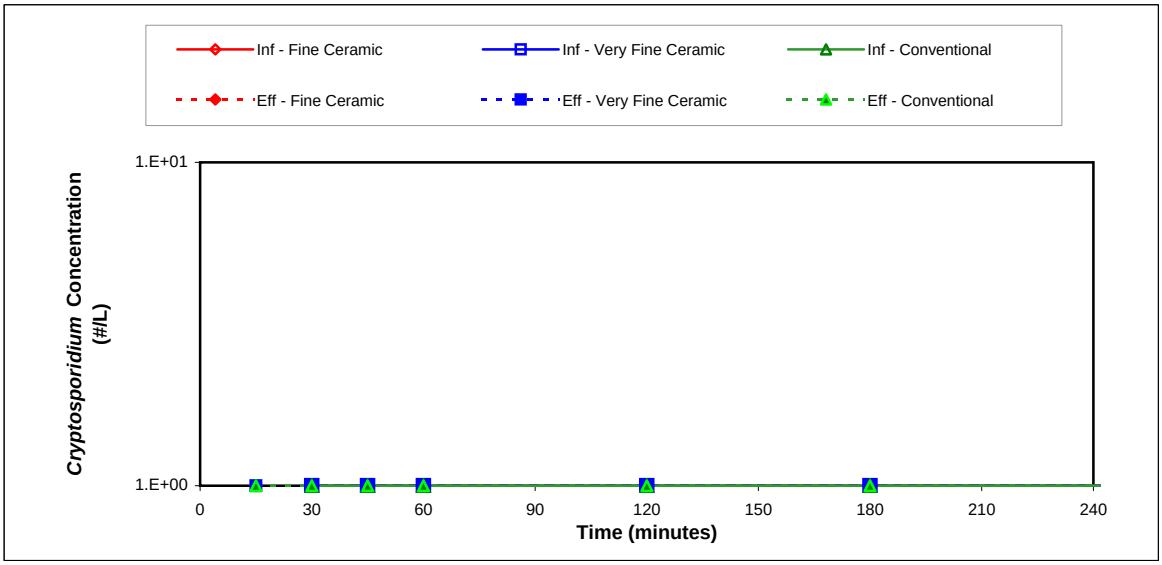

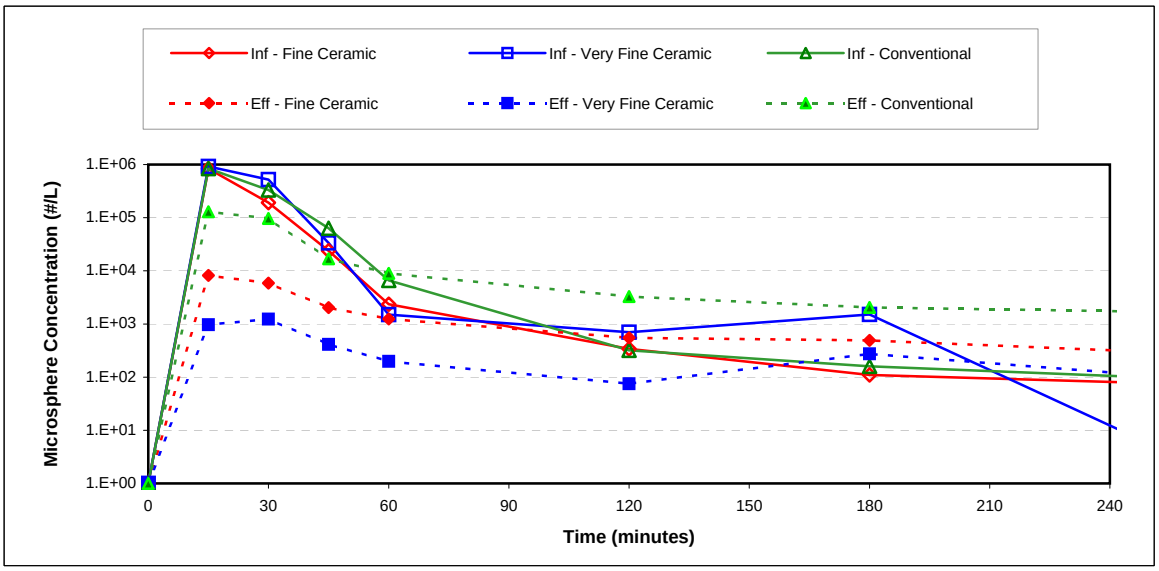

Turbidity Summary: Trial 1A

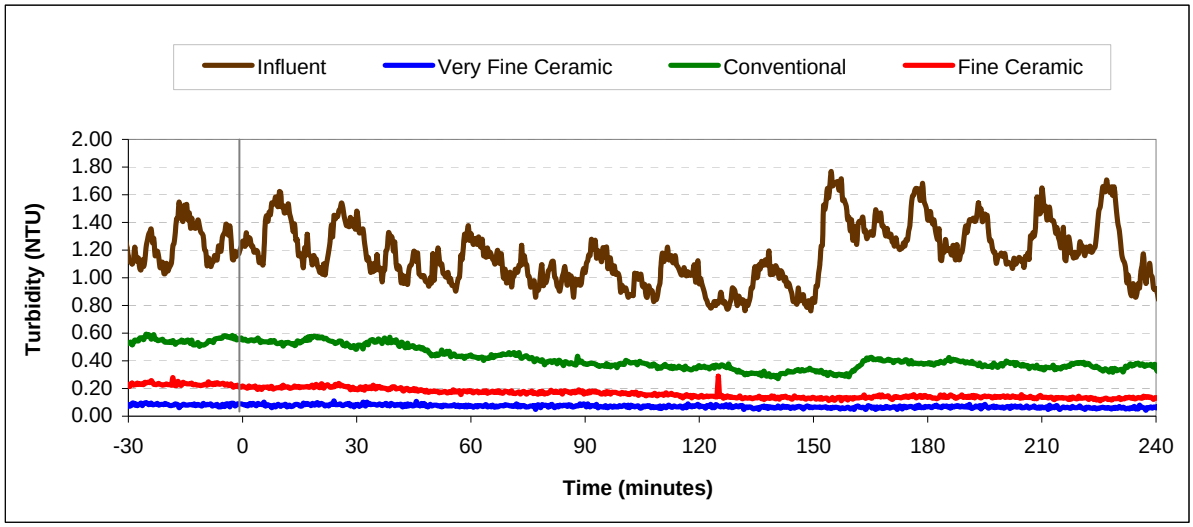

Turbidity Box and Whisker Plots

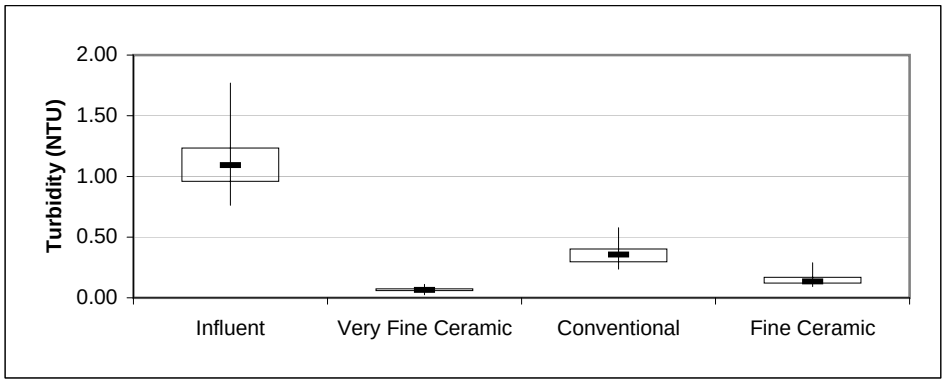

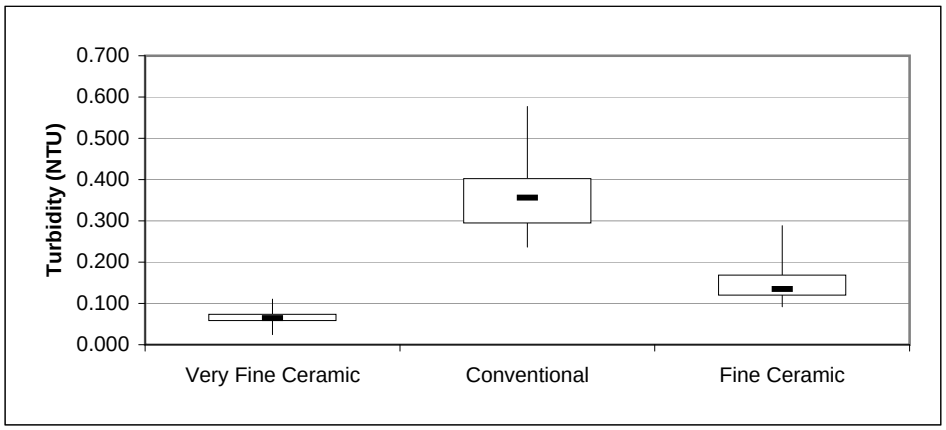

Vertical lines represent maximum and minimum turbidity range. Top and bottom of boxes represent 75th and 25th percentiles of turbidity data. Centre dash represents median turbidity measurement during seeding study.

Particle Count Summary: **Trial 1A**

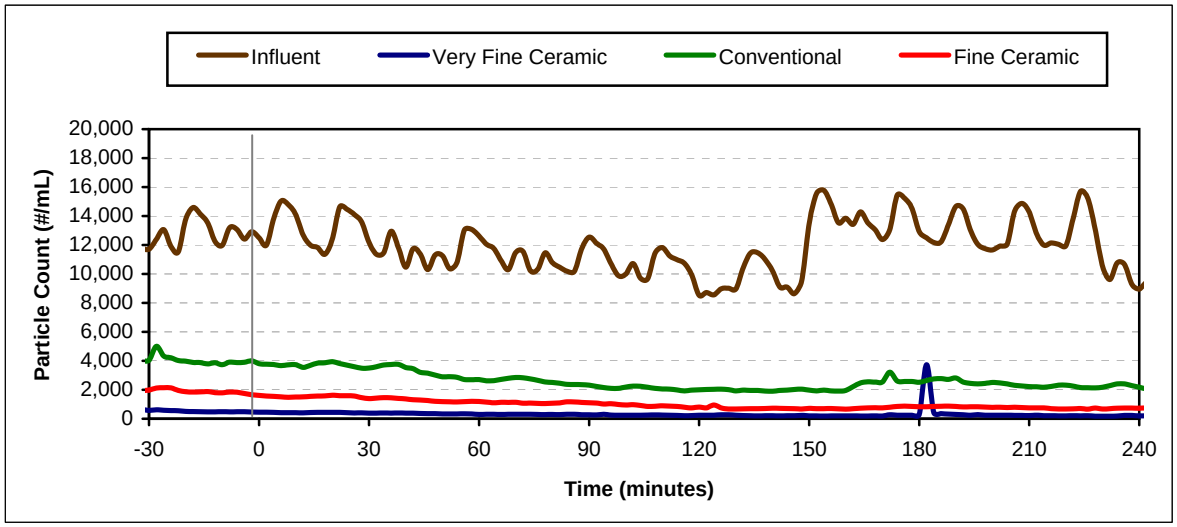

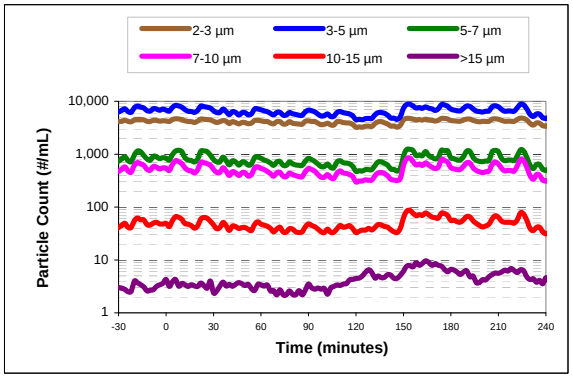

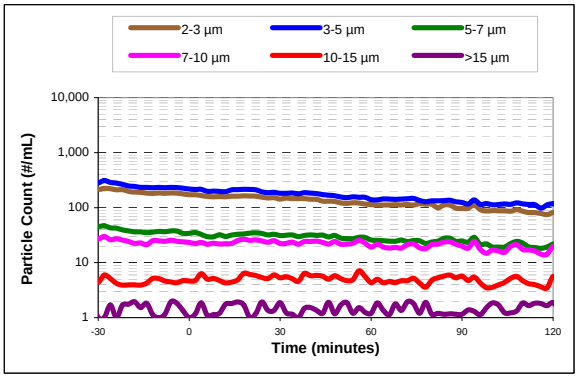

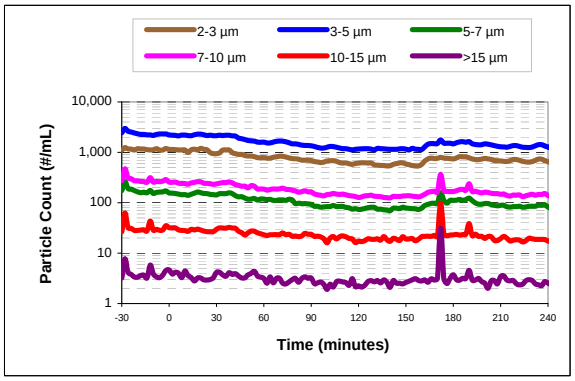

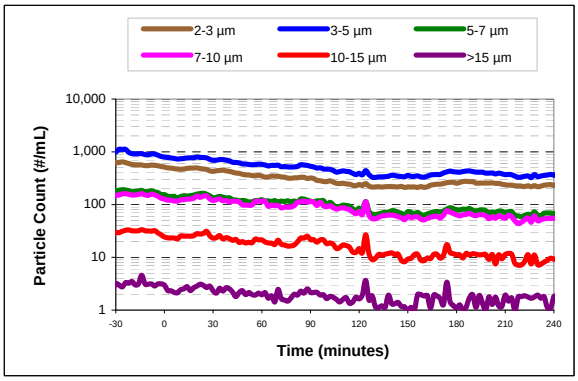

Flow and Headloss Summary: Trial 1A

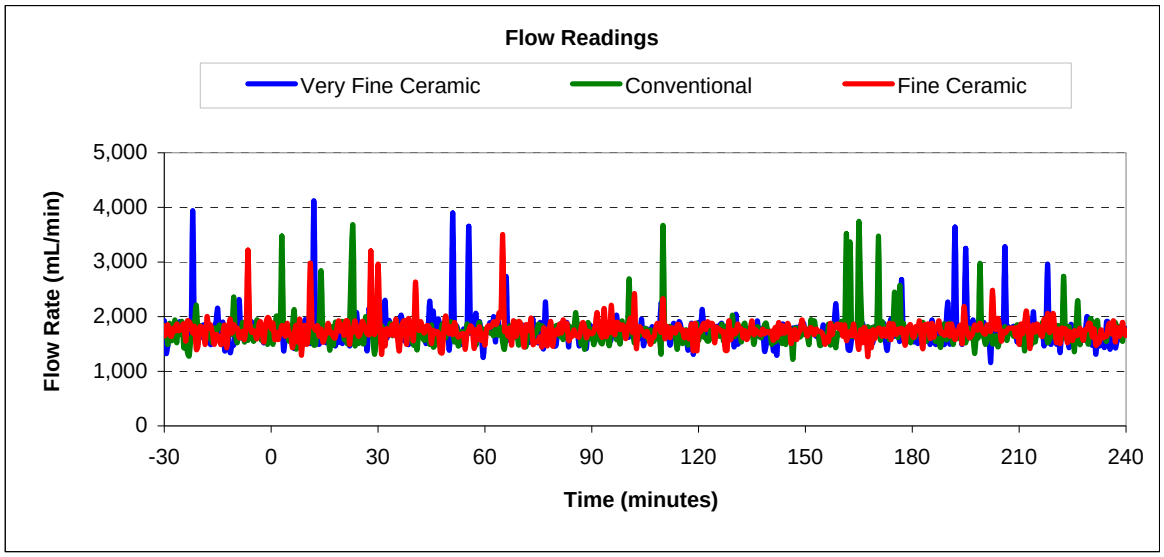

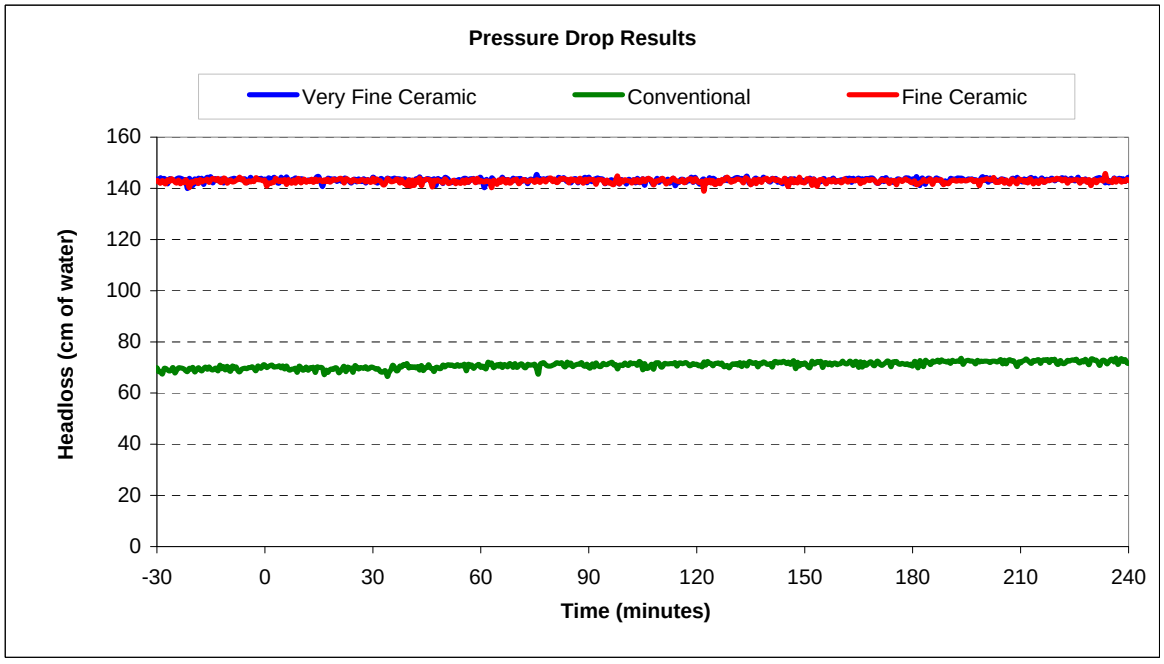

Summary Information for: Trial 1B

Trial Conditions:	
Trial Date	May 18, 2006
Location	University of Waterloo
Water Source	Tap water with Kaolin Dust
Loading Rate	4 GPM/ft2 (9.8 m/hr)
Coagulation	No Coagulant
Water Temperature	13^0C

Filter Media Configuration:

	Column 1	**Column 2**	**Column 3**
	Very Fine Ceramic	Conventional	Fine Ceramic
Top Layer	45 cm ceramic, ES 0.45 mm	45 cm anthracite, ES 0.4 mm	45 cm ceramic, ES 0.96 mm
Bottom Layer	15 cm ceramic, ES 0.22 mm	35 cm sand, ES 0.44 mm	15 cm ceramic, ES 0.22 mm
Support Media	8 cm garnet , ES 0.34 mm	20 cm graded gravel bed	8 cm garnet , ES 0.34 mm

Parameter:	**Influent**	**Very Fine Ceramic**	**Conventional**	**Fine Ceramic**
Log reductions:				
Cryptosporidium		0.00	0.00	0.00
Microspheres		3.71	1.56	3.62
Other Parameters[1]:				
Average turbidity (NTU)	1.125	0.050	0.253	0.086
Turbidity reduction (%)		96	77	92
Average total particle count (#/mL)	11690	86	1016	245
Particle reduction (%)		99	91	98
Average flow (mL/min)		748	708	825
Clean bed headloss		82	28	78
Average headloss (cm)		83	29	79
Change in headloss (cm)		1	2	2

[1] *Data calculated from time 0 (start of spike injection) to 360 elapsed minutes*

***Cryptosporidium* and Microsphere Removal Summary:** **Trial 1B**

***Cryptosporidium* Log Removal**

Time	Col 1	Col 2	Col 3
10 min			
20 min	0.00	0.00	0.00
30 min	0.00	0.00	0.00
40 min	0.00	0.00	0.00
50 min	0.00	0.00	0.00
60 min			
120 min			
Avg.[1]	**0.00**	**0.00**	**0.00**

[1]*Avgerage denotes time interval from 10 min to 30 min*

Microsphere Log Removal

Time	Col 1	Col 2	Col 3
10 min	3.80	1.76	4.45
20 min	4.05	1.69	3.53
30 min	3.91	1.93	3.50
40 min	3.39	1.35	3.02
50 min	2.82	1.19	2.33
60 min	1.10	-0.63	0.92
120 min	0.90	-1.36	0.85
Avg.[1]	**3.71**	**1.56**	**3.62**

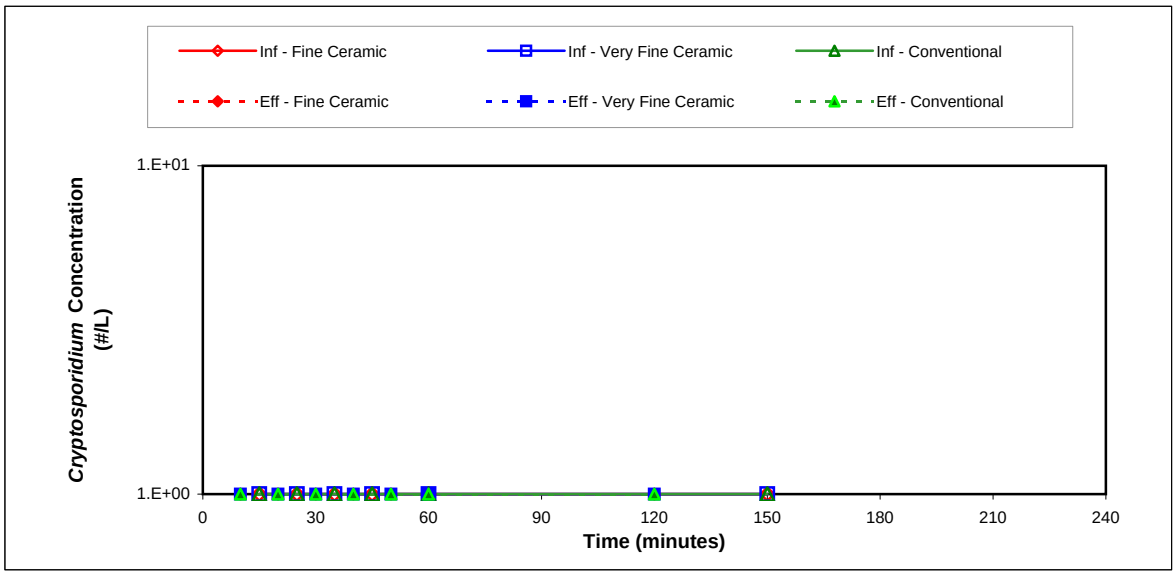

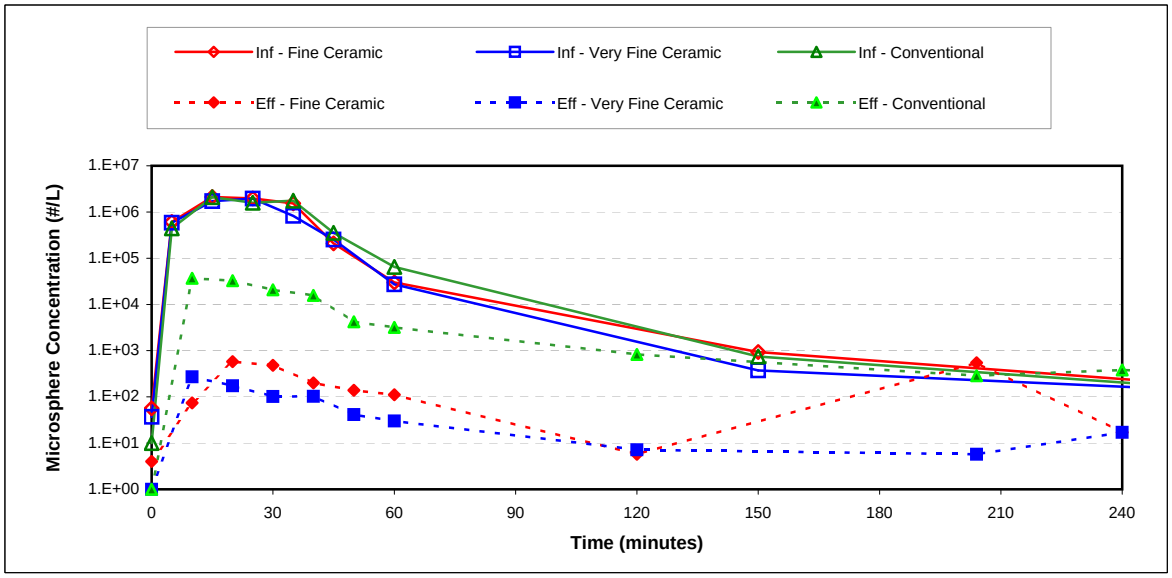

Turbidity Summary: Trial 1B

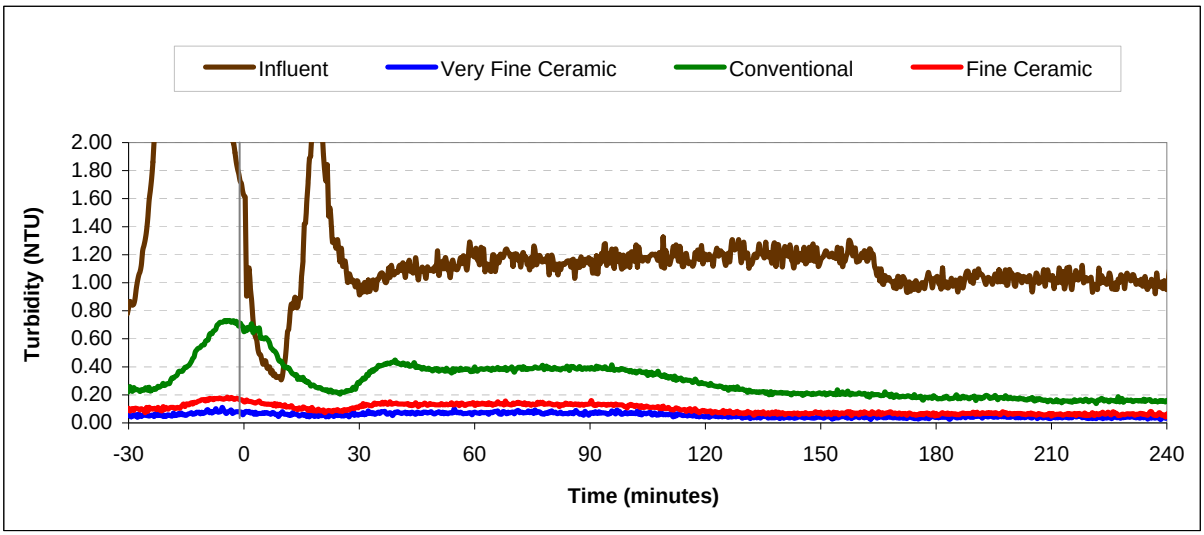

Turbidity Box and Whisker Plots

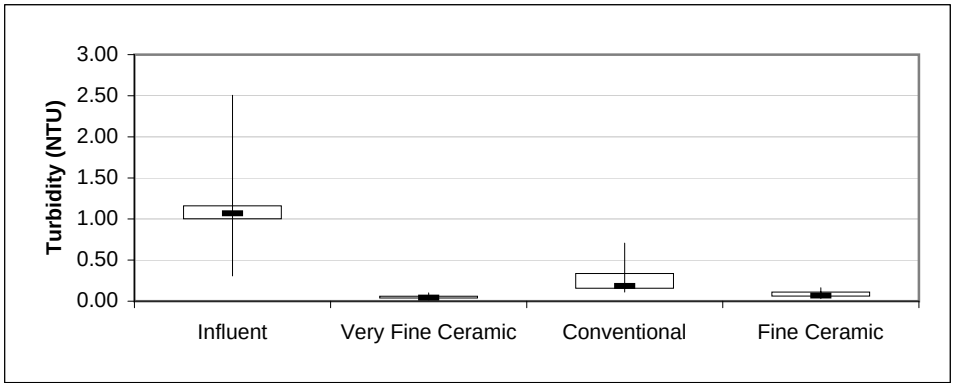

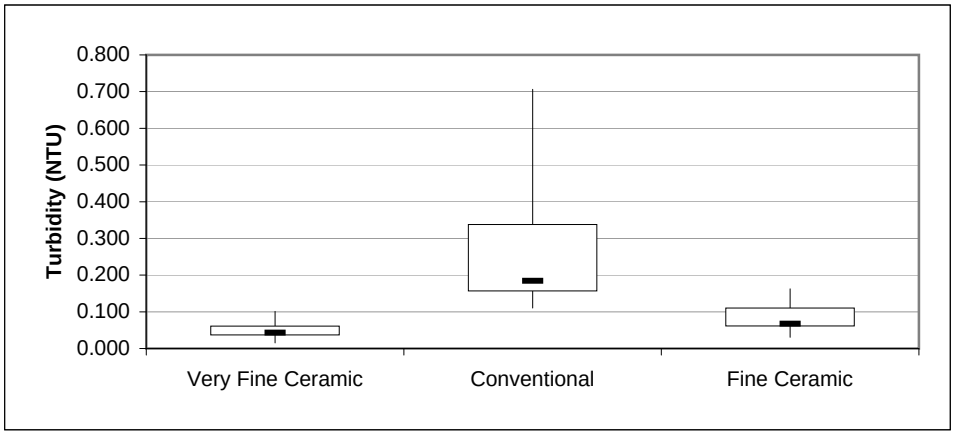

Vertical lines represent maximum and minimum turbidity range. Top and bottom of boxes represent 75th and 25th percentiles of turbidity data. Centre dash represents median turbidity measurement during seeding study.

Particle Count Summary: **Trial 1B**

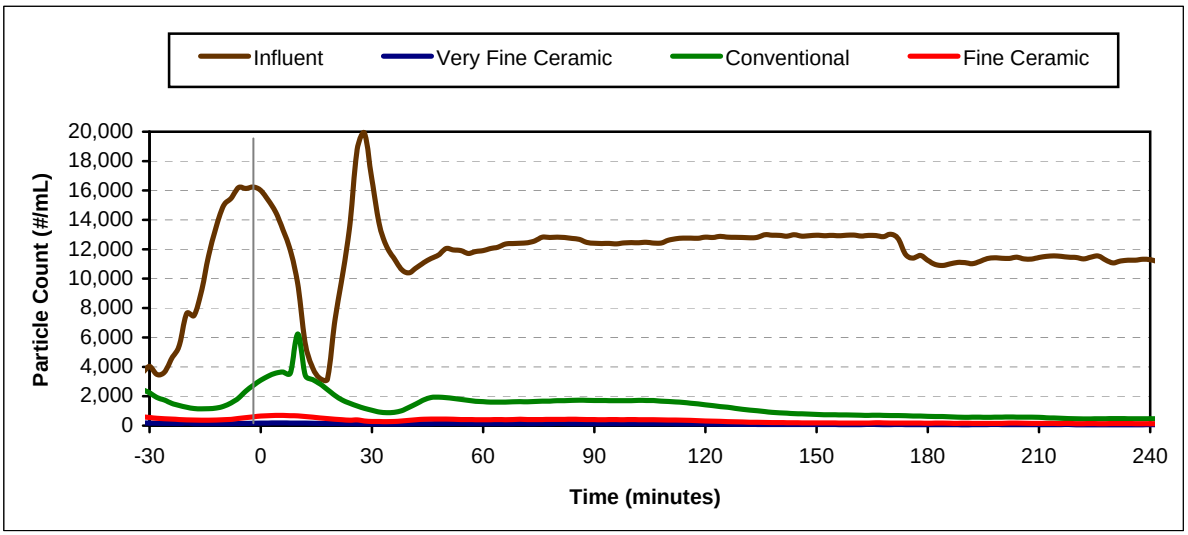

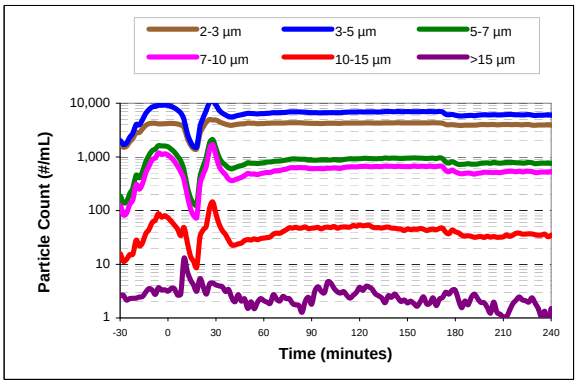

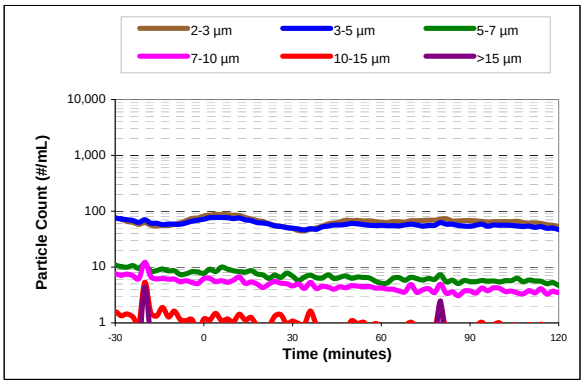

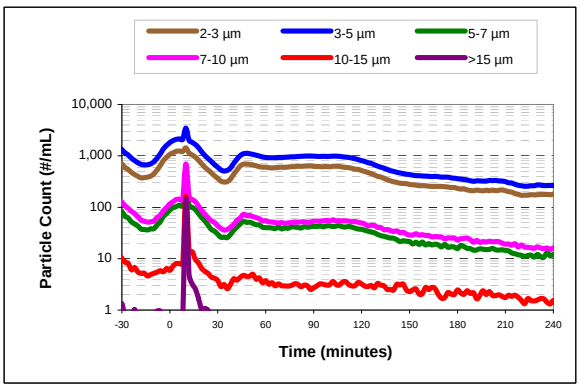

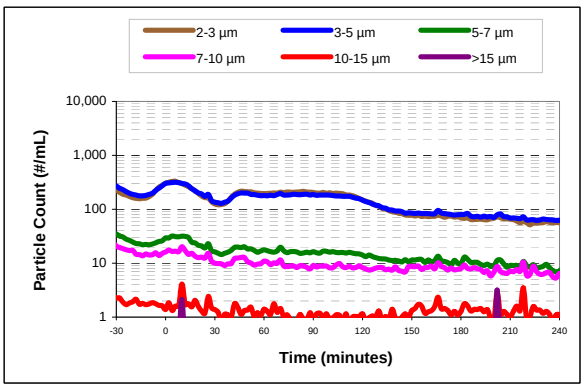

Flow and Headloss Summary: Trial 1B

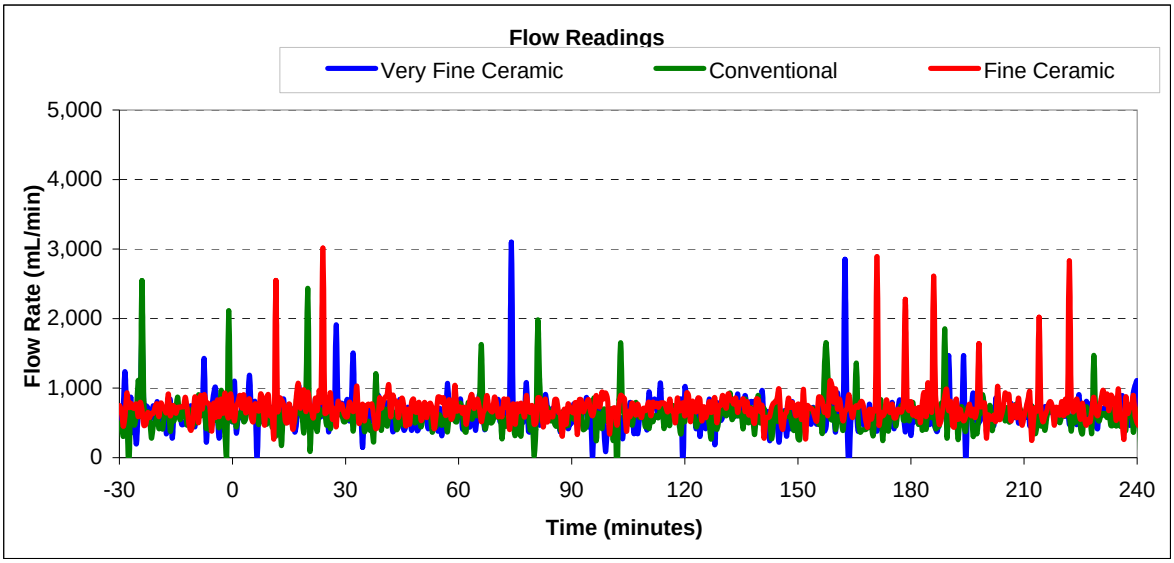

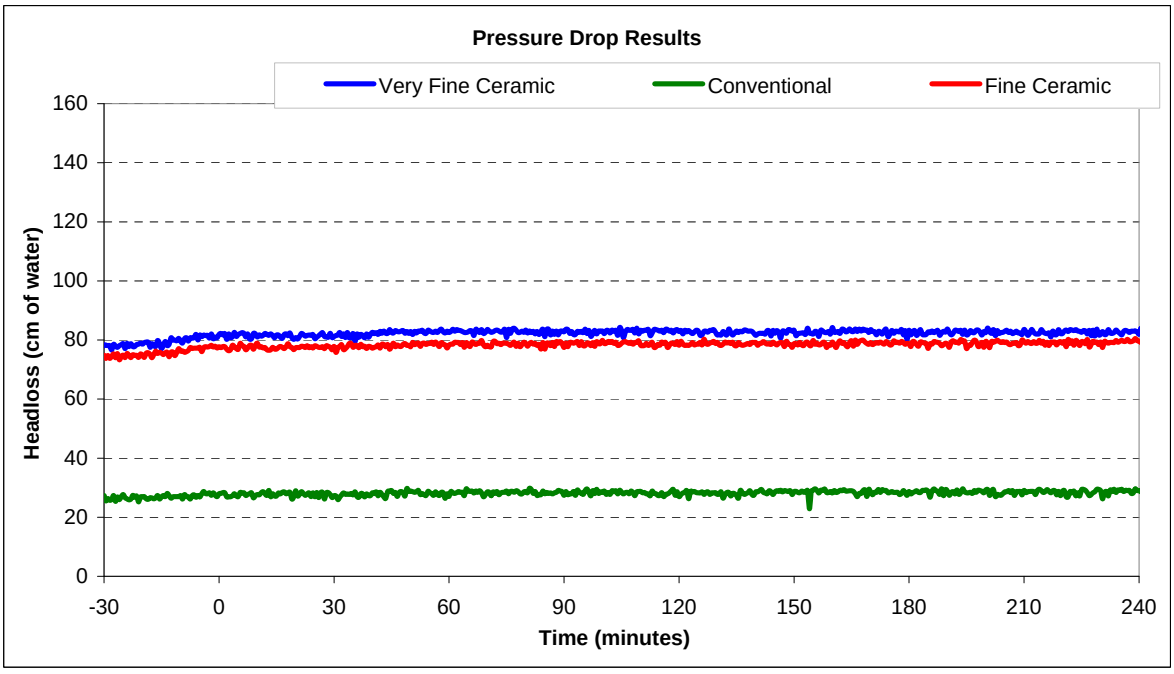

Summary Information for: Trial 2A

Trial Conditions:	
Trial Date	August 8, 2006
Location	Horgan WTP
Water Source	Lake Ontario
Loading Rate	10 GPM/ft^2 (24.4 m/hr)
Coagulation	No Coagulant
Water Temperature	21^{0}C

Filter Media Configuration:

	Column 1	**Column 2**	**Column 3**
	Dense Ceramic	Fine Ceramic	Conventional
Top Layer	45 cm ceramic, ES 0.64 mm	45 cm ceramic, ES 0.96 mm	45 cm anthracite, ES 0.89 mm
Bottom Layer	15 cm ceramic, ES 0.22mm	15 cm ceramic, ES 0.21mm	30 cm sand, ES 0.47 mm
Support Media	20 cm graded gravel bed	20 cm graded gravel bed	20 cm graded gravel bed

Parameter:	**Influent**	**Dense Ceramic**	**Fine Ceramic**	**Conventional**
Log reductions:				
Cryptosporidium		0.00	0.00	0.00
Microspheres		0.99	2.03	0.38
Other Parameters[1]:				
Average turbidity (NTU)	0.487	0.311	0.286	0.336
Turbidity reduction (%)		36	41	31
Average total particle count (#/mL)	na	na	na	na
Particle reduction (%)				
Average flow (mL/min)		2161	1968	2145
Clean bed headloss		196	142	86
Average headloss (cm)		203	147	85
Change in headloss (cm)		13	17	1

[1] *Data calculated from time 0 (start of spike injection) to 360 elapsed minutes*

***Cryptosporidium* and Microsphere Removal Summary:** **Trial 2A**

***Cryptosporidium* Log Removal**

Time	Col 1	Col 2	Col 3
10 min			
20 min	0.00	0.00	0.00
30 min	0.00	0.00	0.00
40 min	0.00	0.00	0.00
50 min	0.00	0.00	0.00
60 min			
70 min			
Avg.[1]	**0.00**	**0.00**	**0.00**

Microsphere Log Removal

Time	Col 1	Col 2	Col 3
10 min	1.12	2.14	0.42
20 min	1.08	2.16	0.38
30 min	1.11	1.92	0.36
40 min	0.97	2.16	0.44
50 min	0.74	1.97	0.33
60 min	-1.64	-1.78	-1.64
70 min	-5.72	-5.26	-4.34
Avg.[1]	**0.99**	**2.03**	**0.38**

[1]*Avgerage denotes time interval from 20 min to 60 min*

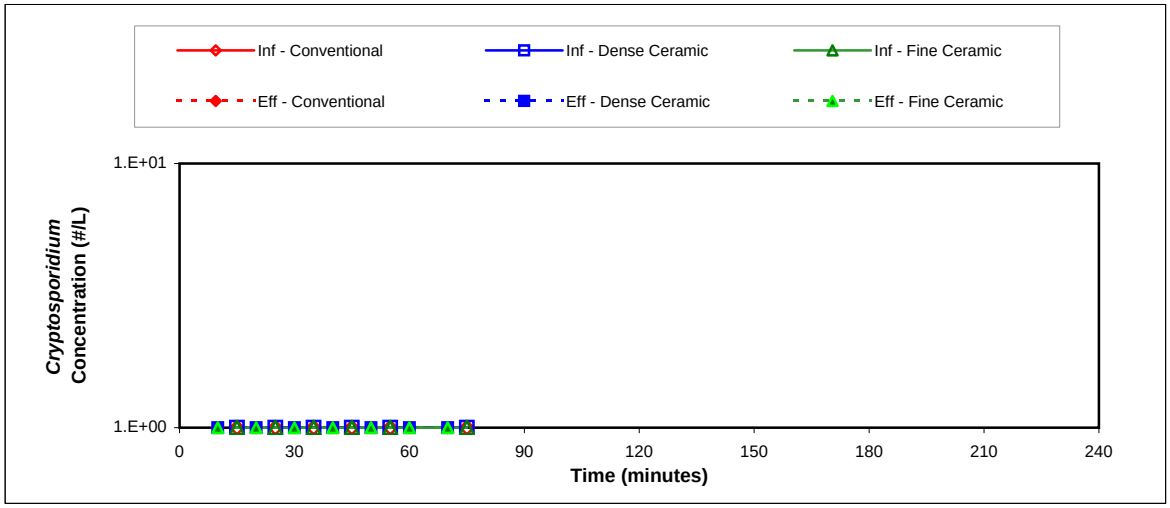

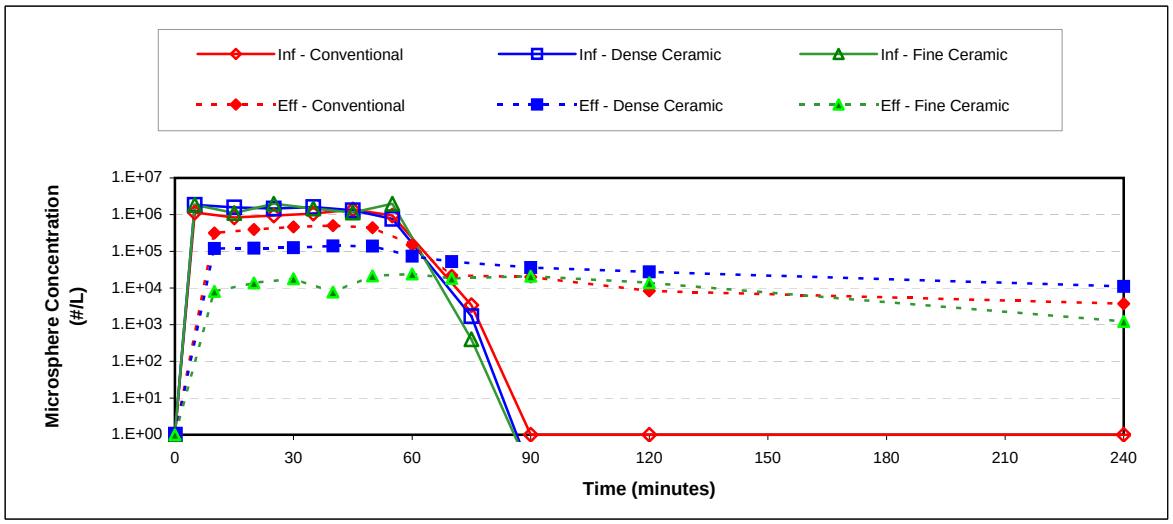

Turbidity Summary: Trial 2A

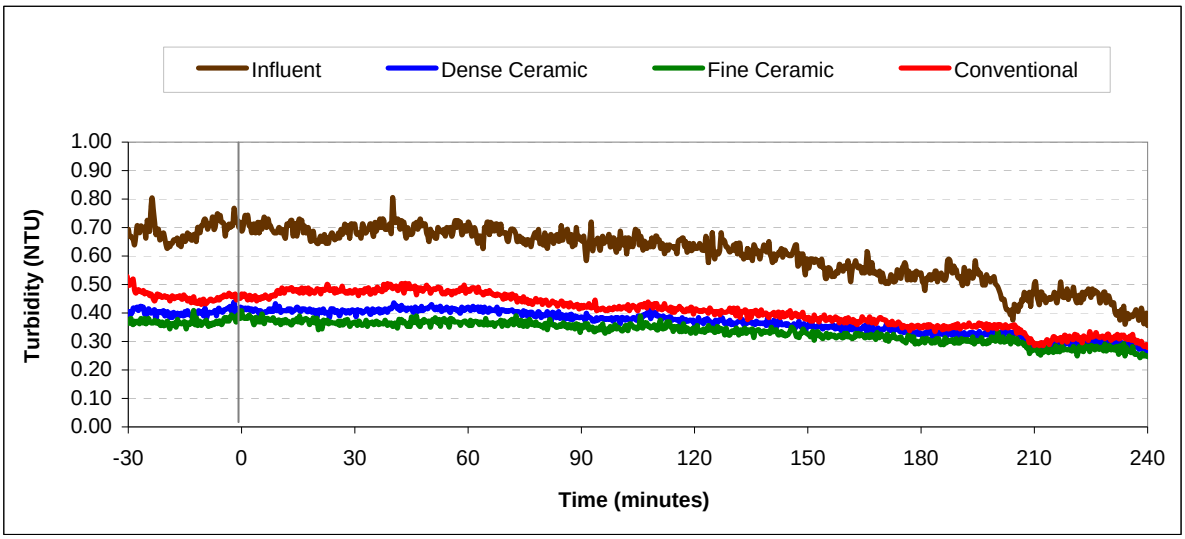

Turbidity Box and Whisker Plots

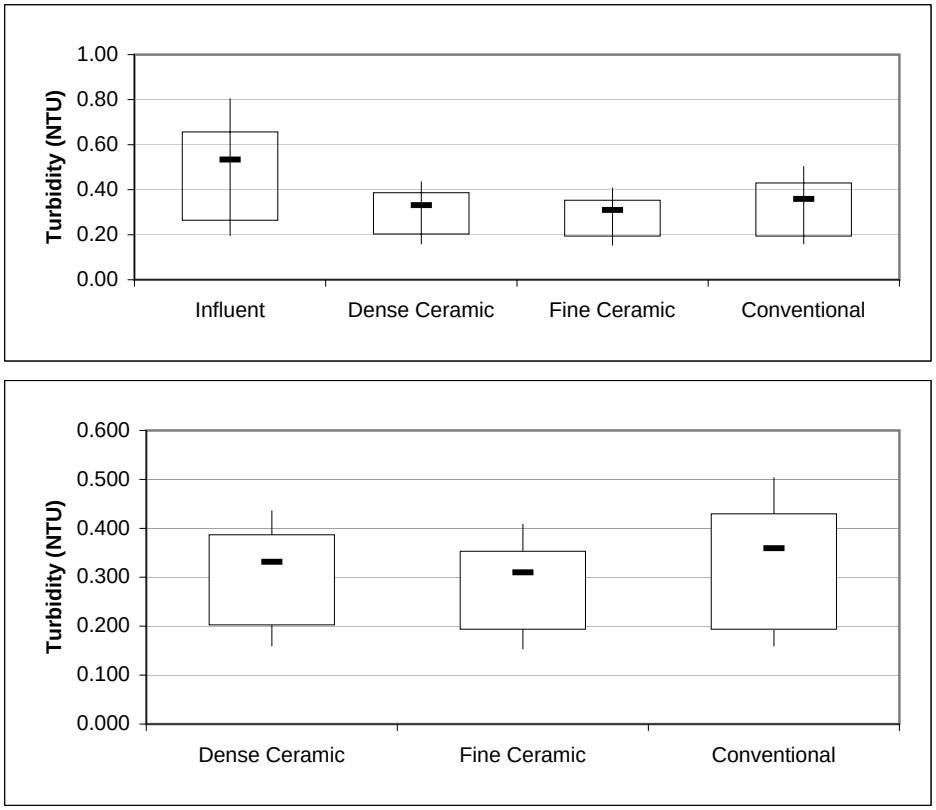

Vertical lines represent maximum and minimum turbidity range. Top and bottom of boxes represent 75th and 25th percentiles of turbidity data. Centre dash represents median turbidity measurement during seeding study.

Particle Count Summary: **Trial 2A**

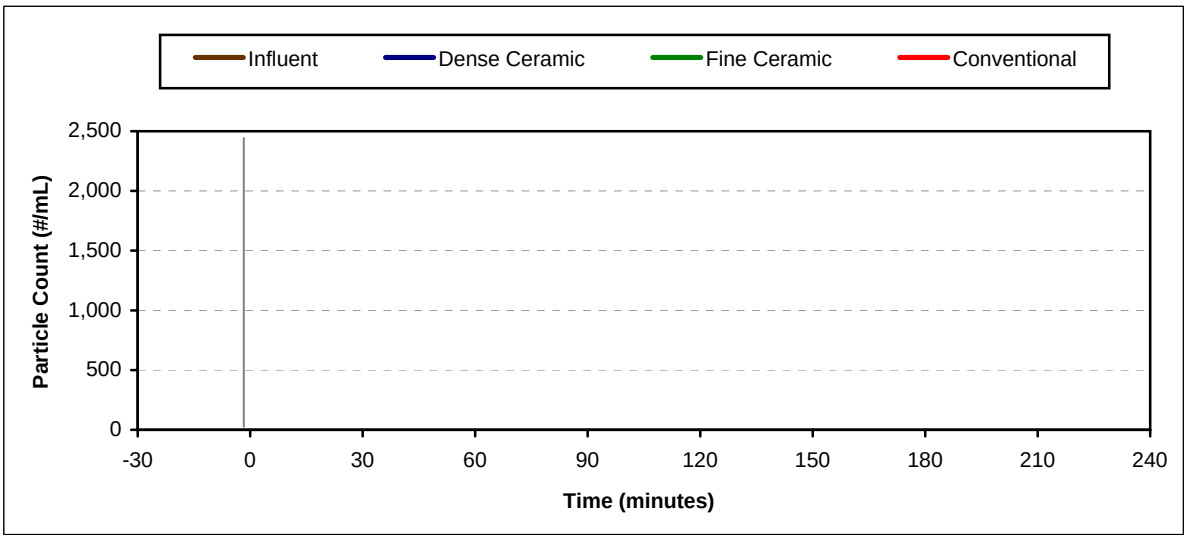

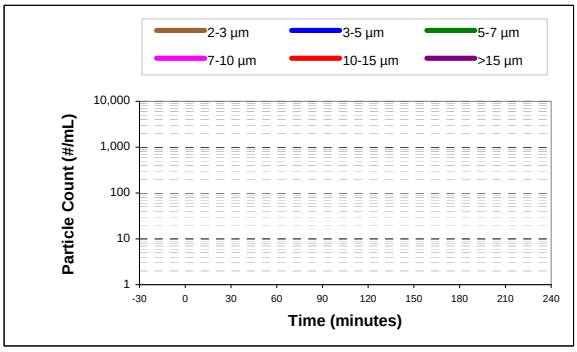

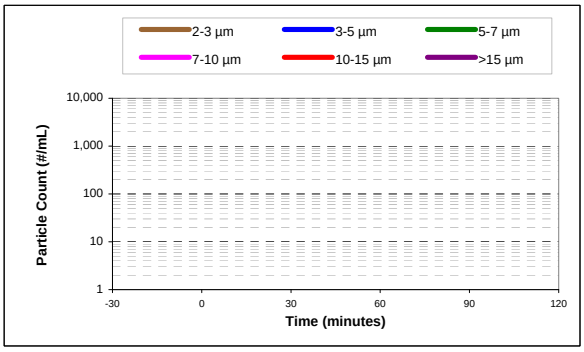

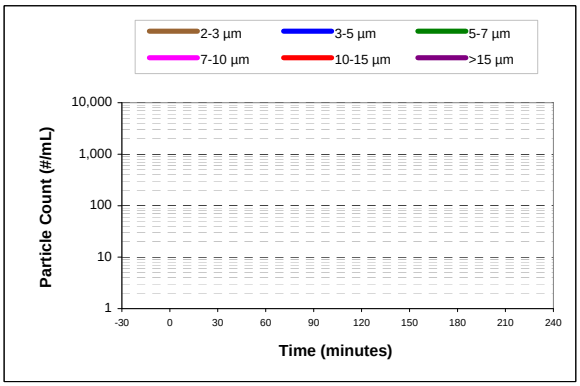

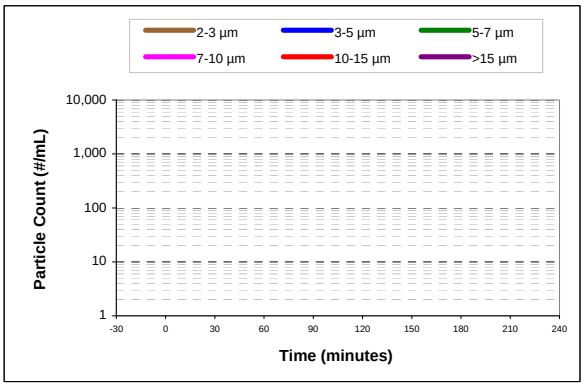

Flow and Headloss Summary: Trial 2A

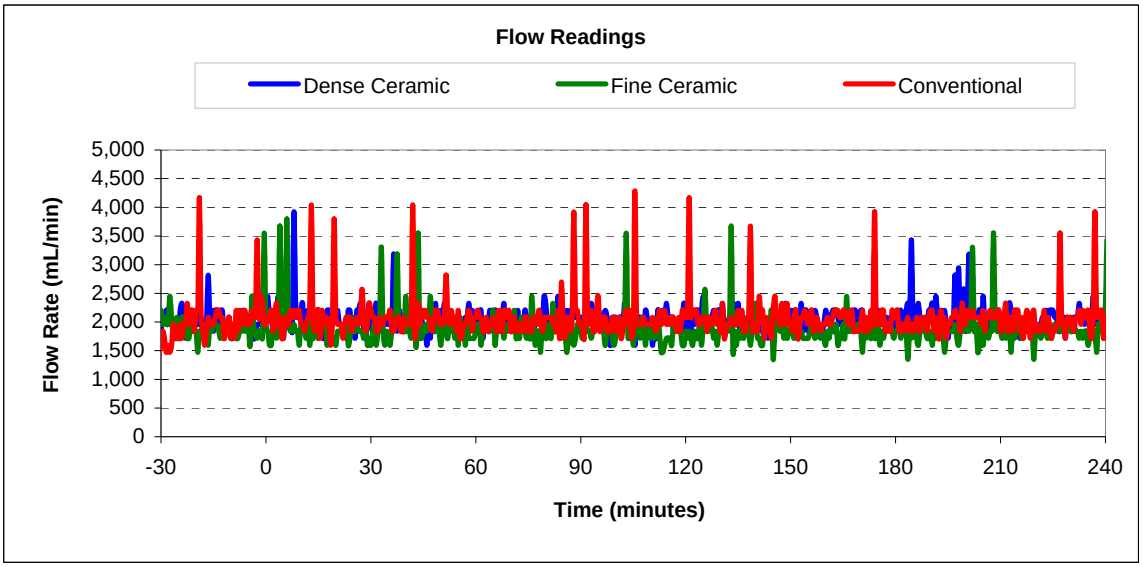

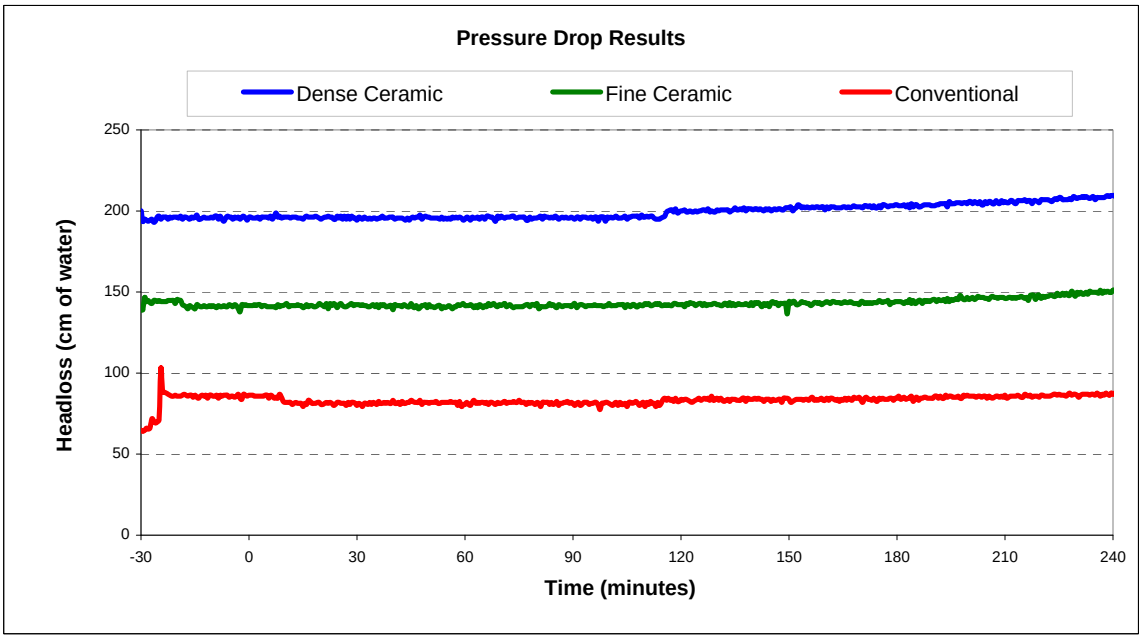

Summary Information for: Trial 2B

Trial Conditions:	
Trial Date	August 11, 2006
Location	Horgan WTP
Water Source	Lake Ontario
Loading Rate	4 GPM/ft^2 (9.8 m/hr)
Coagulation	No Coagulant
Water Temperature	22^{0}C

Filter Media Configuration:

	Column 1	**Column 2**	**Column 3**
	Dense Ceramic	Fine Ceramic	Conventional
Top Layer	45 cm ceramic, ES 0.64 mm	45 cm ceramic, ES 0.96 mm	45 cm anthracite, ES 0.89 mm
Bottom Layer	15 cm ceramic, ES 0.22mm	15 cm ceramic, ES 0.21mm	30 cm sand, ES 0.47 mm
Support Media	20 cm graded gravel bed	20 cm graded gravel bed	20 cm graded gravel bed

Parameter:	**Influent**	**Dense Ceramic**	**Fine Ceramic**	**Conventional**
Log reductions:				
Cryptosporidium		0.00	0.00	0.00
Microspheres		1.87	1.81	0.49
Other Parameters[1]:				
Average turbidity (NTU)	0.573	0.287	0.280	0.355
Turbidity reduction (%)		50	51	38
Average total particle count (#/mL)	na	na	na	na
Particle reduction (%)				
Average flow (mL/min)		784	785	802
Clean bed headloss		67	54	27
Average headloss (cm)		65	52	26
Change in headloss (cm)		0	0	0

[1] *Data calculated from time 0 (start of spike injection) to 360 elapsed minutes*

***Cryptosporidium* and Microsphere Removal Summary:** **Trial 2B**

***Cryptosporidium* Log Removal**

Time	Col 1	Col 2	Col 3
10 min			
20 min	0.00	0.00	0.00
30 min	0.00	0.00	0.00
40 min	0.00	0.00	0.00
50 min	0.00	0.00	0.00
60 min			
70 min			
Avg.[1]	**0.00**	**0.00**	**0.00**

Microsphere Log Removal

Time	Col 1	Col 2	Col 3
10 min	2.19	2.05	0.64
20 min	2.00	1.81	0.49
30 min	1.79	1.84	0.50
40 min	1.71	1.75	0.41
50 min	1.92	1.84	0.53
60 min	1.17	1.26	-0.06
70 min	1.04	1.17	-0.49
Avg.[1]	**1.87**	**1.81**	**0.49**

[1]*Avgerage denotes time interval from 20 min to 60 min*

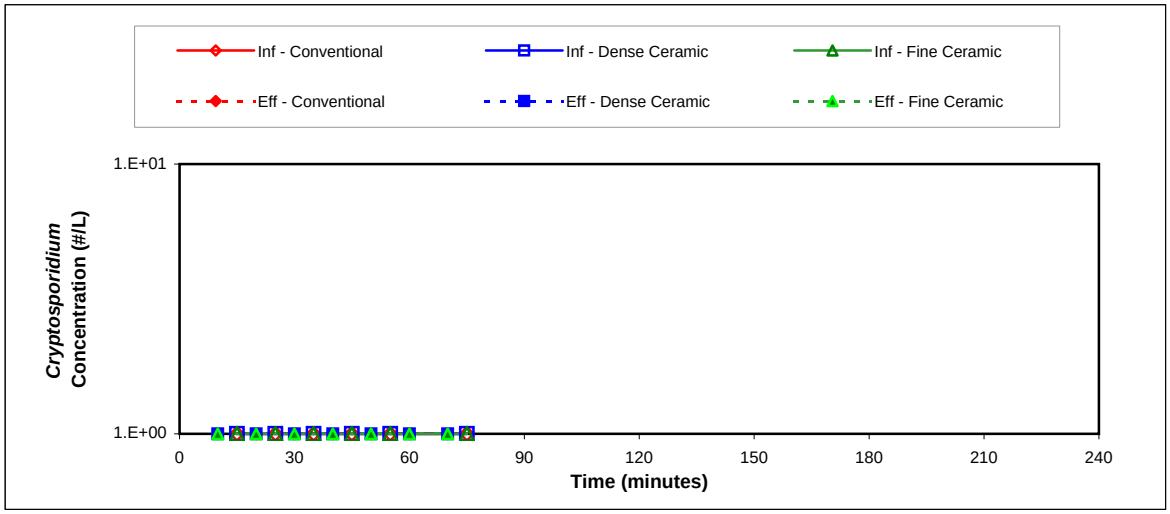

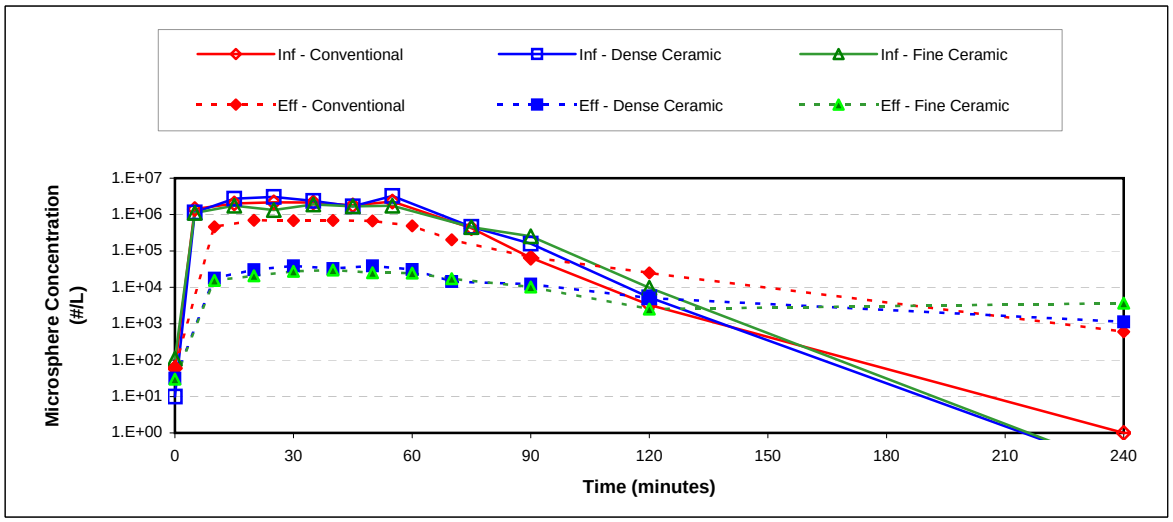

Turbidity Summary: Trial 2B

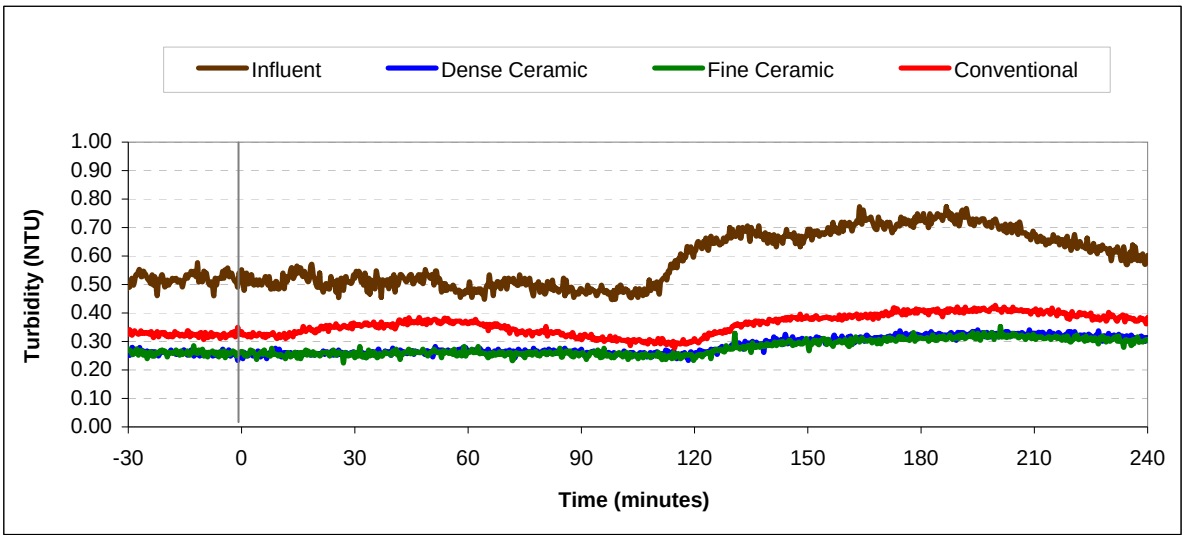

Turbidity Box and Whisker Plots

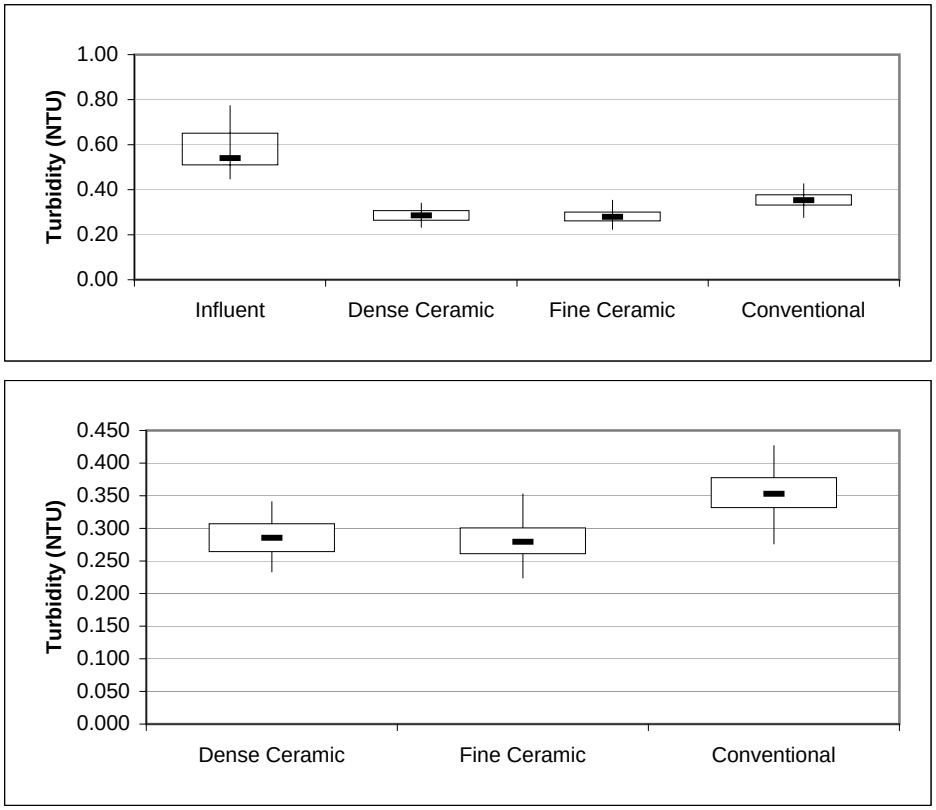

Vertical lines represent maximum and minimum turbidity range. Top and bottom of boxes represent 75th and 25th percentiles of turbidity data. Centre dash represents median turbidity measurement during seeding study.

Particle Count Summary: **Trial 2B**

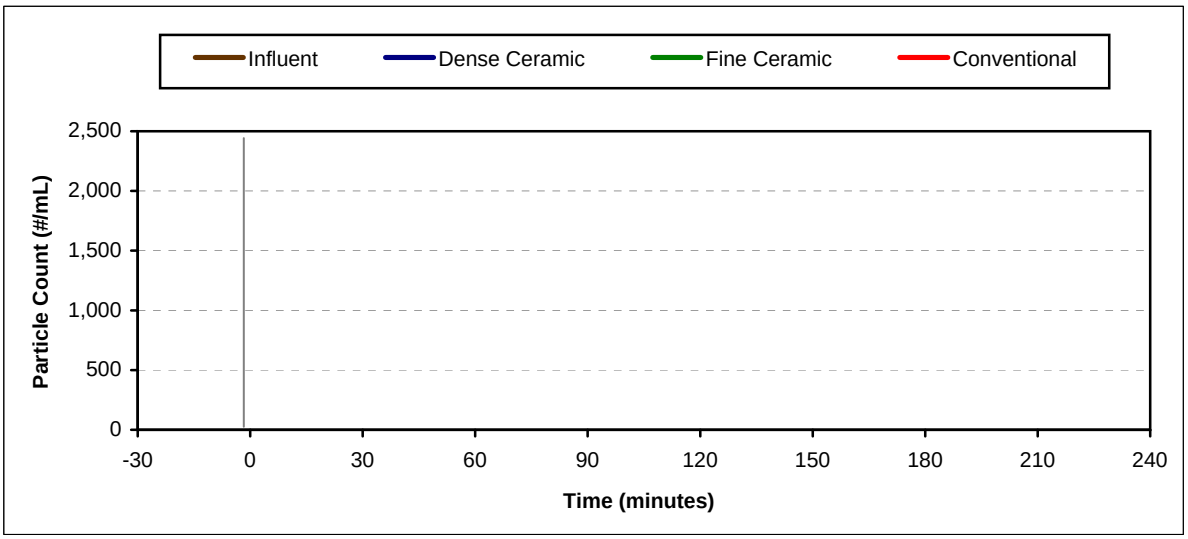

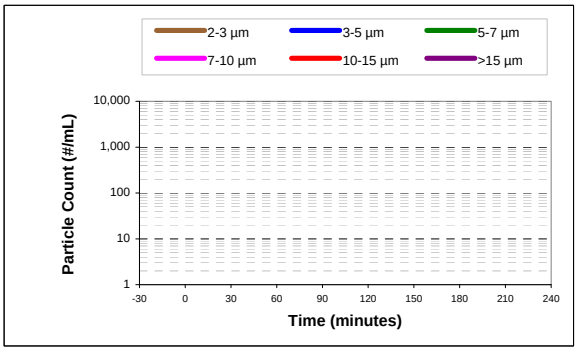

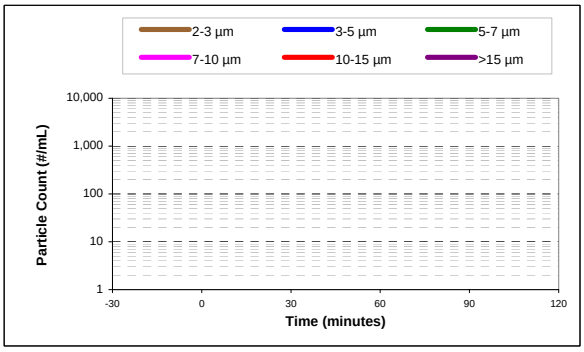

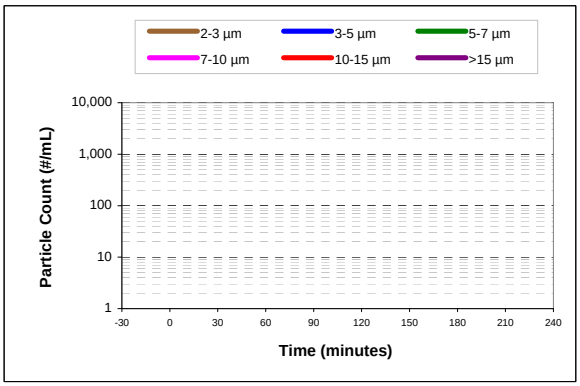

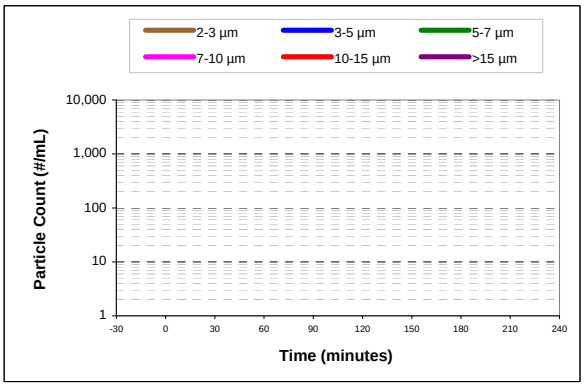

Flow and Headloss Summary: Trial 2B

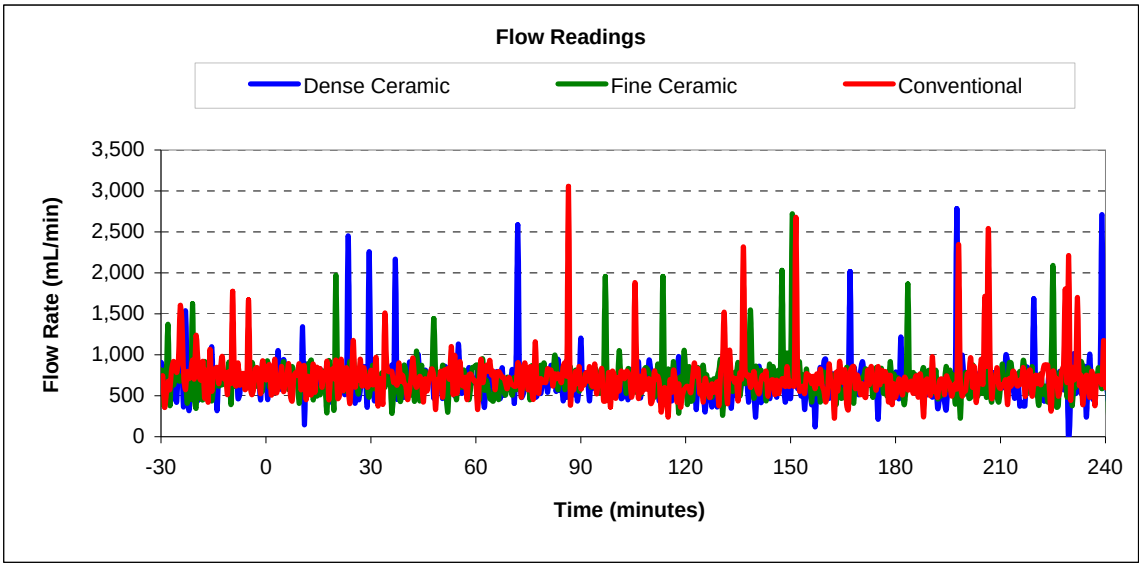

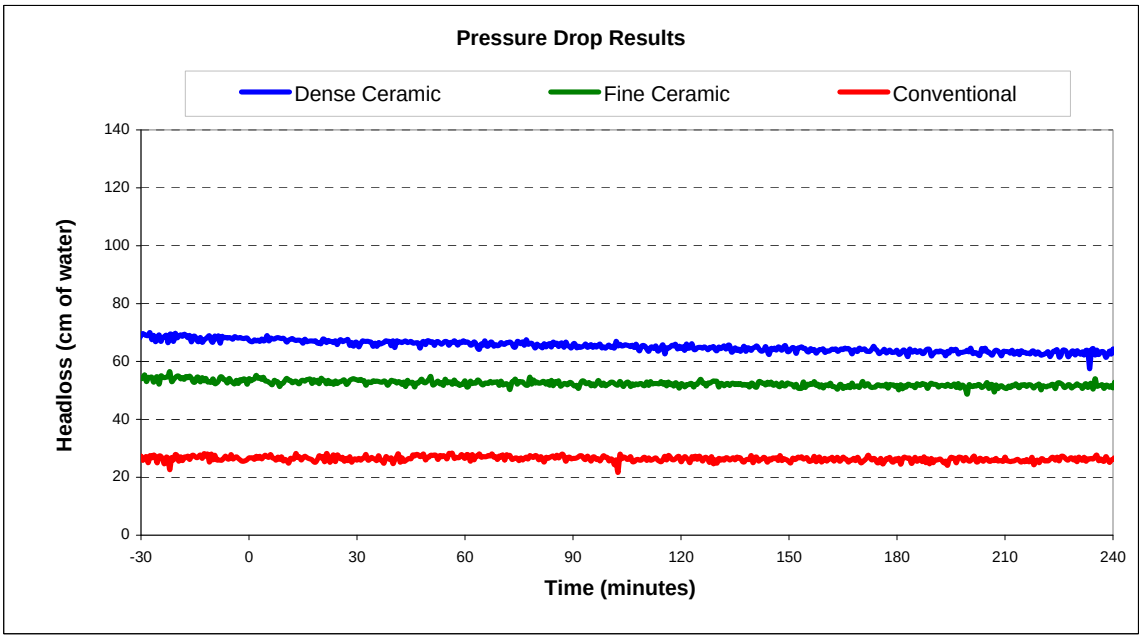

Summary Information for: Trial 2C

Trial Conditions:	
Trial Date	September 6, 2006
Location	Horgan WTP
Water Source	Lake Ontario
Loading Rate	10 GPM/ft^2 (24.4 m/hr)
Coagulation	No Coagulant
Water Temperature	20^{0}C

Filter Media Configuration:

	Column 1	**Column 2**	**Column 3**
	Dense Ceramic	Fine Ceramic	Conventional
Top Layer	45 cm ceramic, ES 0.64 mm	45 cm ceramic, ES 0.96 mm	45 cm anthracite, ES 0.89 mm
Bottom Layer	15 cm ceramic, ES 0.22mm	15 cm ceramic, ES 0.21mm	30 cm sand, ES 0.47 mm
Support Media	20 cm graded gravel bed	20 cm graded gravel bed	20 cm graded gravel bed

Parameter:	**Influent**	**Dense Ceramic**	**Fine Ceramic**	**Conventional**
Log reductions:				
Cryptosporidium		1.17	1.00	1.12
Microspheres		1.12	1.65	0.97
Other Parameters[1]:				
Average turbidity (NTU)	0.730	0.375	0.359	0.504
Turbidity reduction (%)		49	51	31
Average total particle count (#/mL)	6405	2114	1187	2371
Particle reduction (%)		67	81	63
Average flow (mL/min)		2077	1995	2053
Clean bed headloss		193	145	72
Average headloss (cm)		197	149	72
Change in headloss (cm)		4	6	-1

[1] *Data calculated from time 0 (start of spike injection) to 360 elapsed minutes*

***Cryptosporidium* and Microsphere Removal Summary:** **Trial 2C**

***Cryptosporidium* Log Removal**

Time	Col 1	Col 2	Col 3
10 min			
20 min	1.51	1.25	1.77
30 min	1.81	1.62	1.21
40 min	0.96	0.81	0.60
50 min	0.94	0.89	1.42
60 min			
70 min			
Avg.[1]	**1.17**	**1.00**	**1.12**

Microsphere Log Removal

Time	Col 1	Col 2	Col 3
10 min	2.19	2.01	0.90
20 min	1.49	1.90	0.98
30 min	1.44	1.72	0.64
40 min	0.74	1.52	1.04
50 min	1.64	1.58	1.11
60 min	-0.77	-1.28	-1.78
70 min	-1.44	-1.46	0.26
Avg.[1]	**1.12**	**1.65**	**0.97**

[1]*Avgerage denotes time interval from 20 min to 60 min*

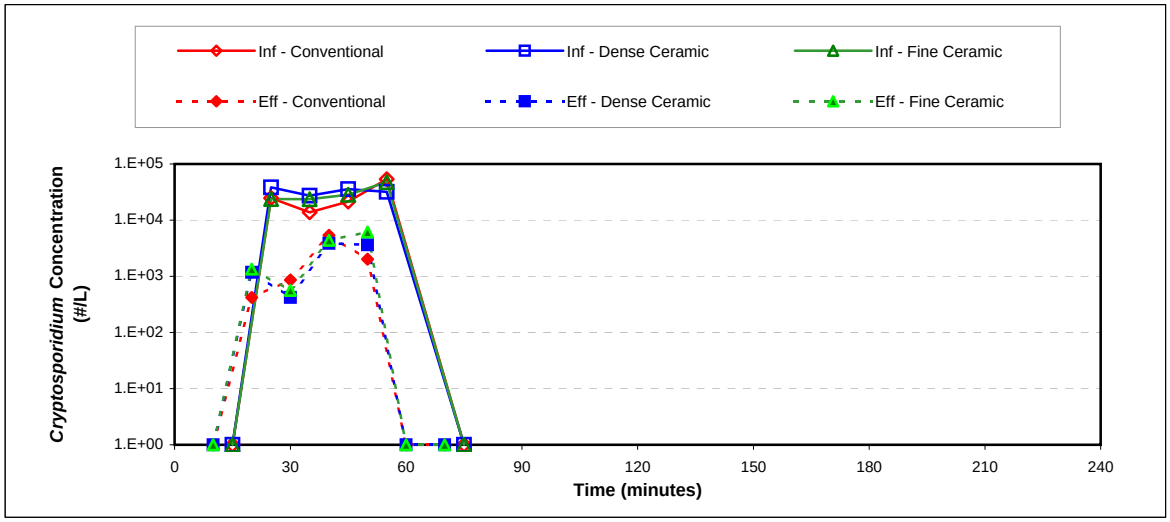

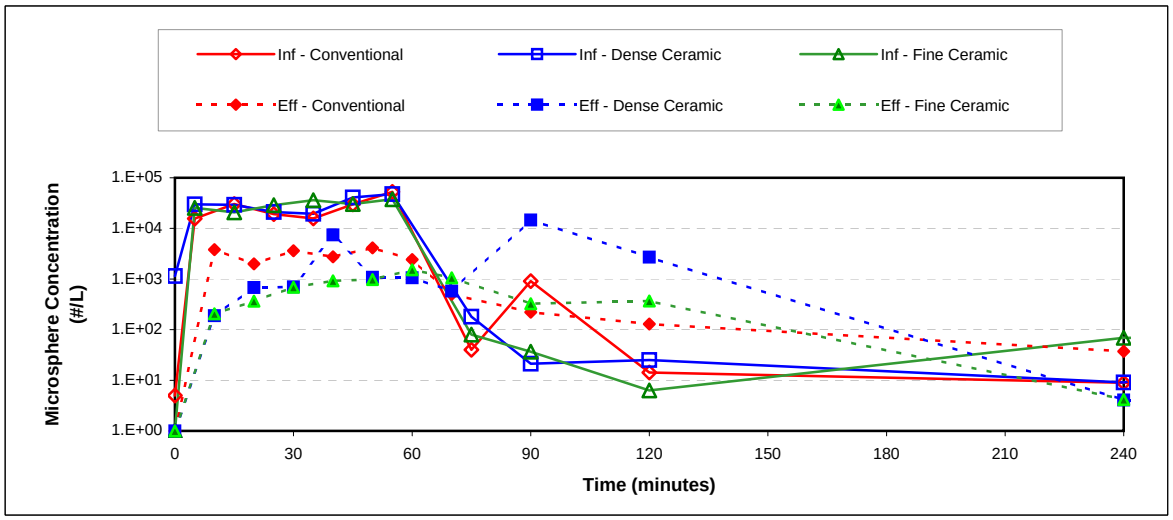

Turbidity Summary: Trial 2C

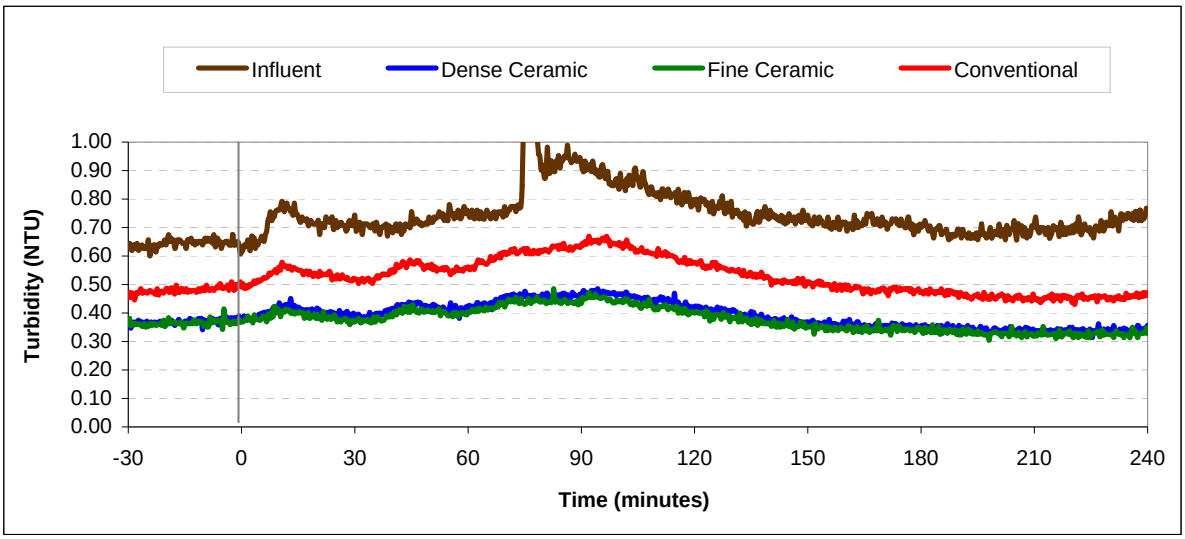

Turbidity Box and Whisker Plots

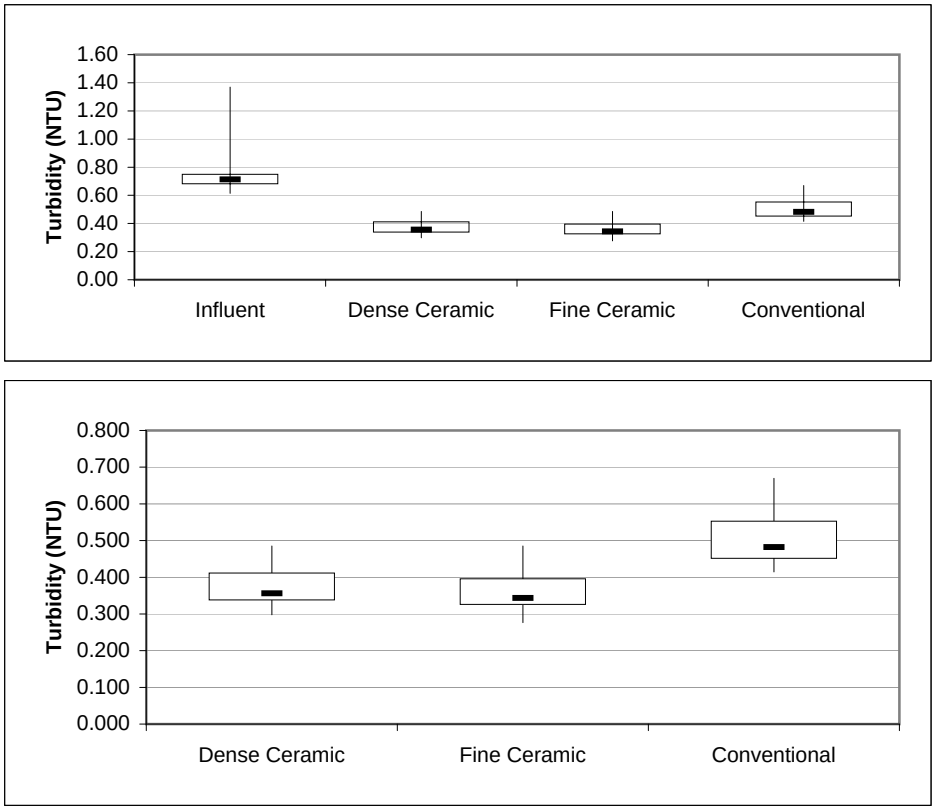

Vertical lines represent maximum and minimum turbidity range. Top and bottom of boxes represent 75th and 25th percentiles of turbidity data. Centre dash represents median turbidity measurement during seeding study.

Particle Count Summary: **Trial 2C**

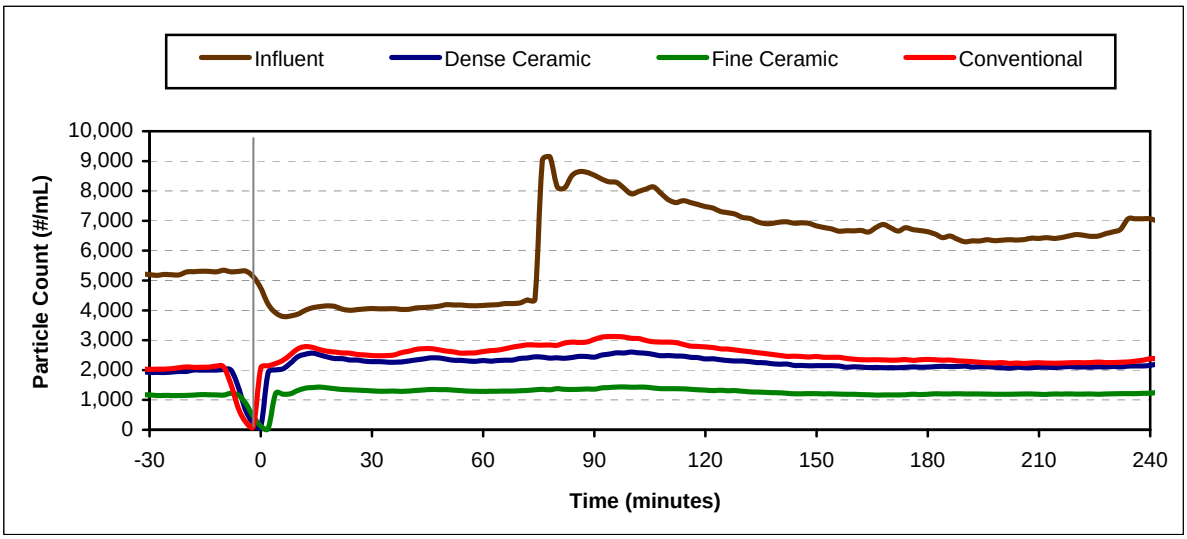

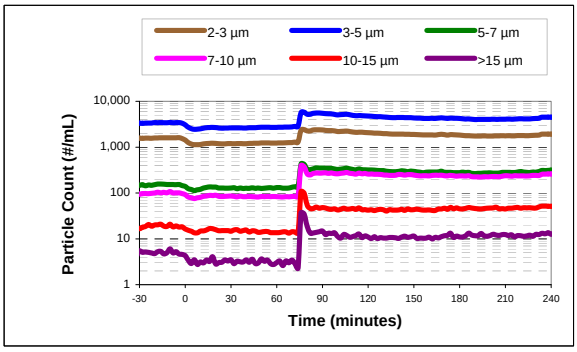

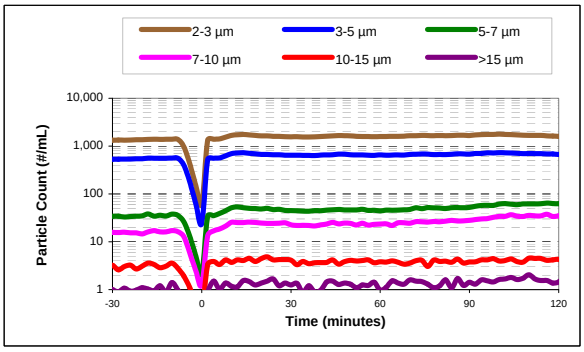

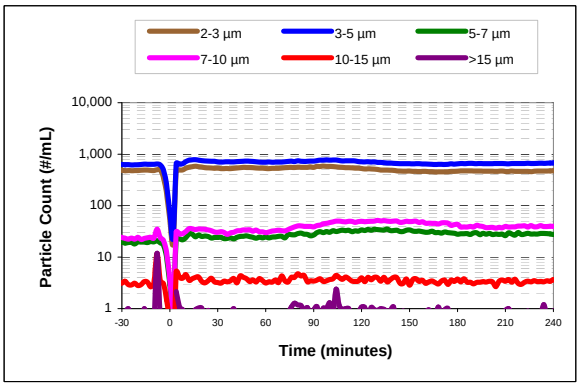

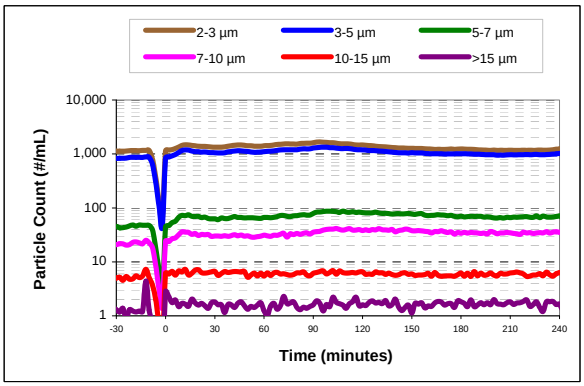

Flow and Headloss Summary: Trial 2C

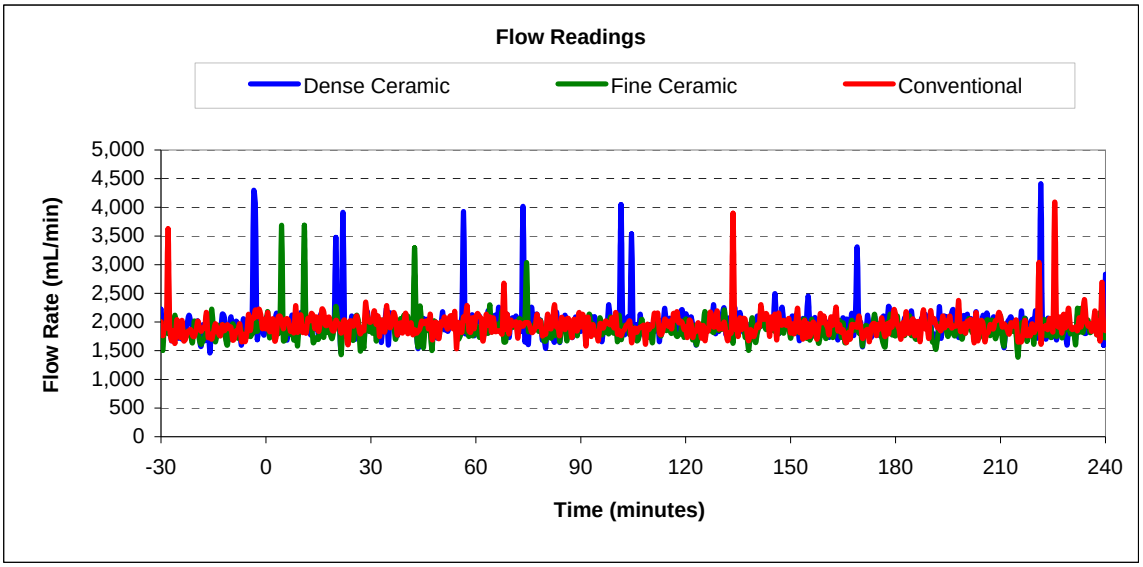

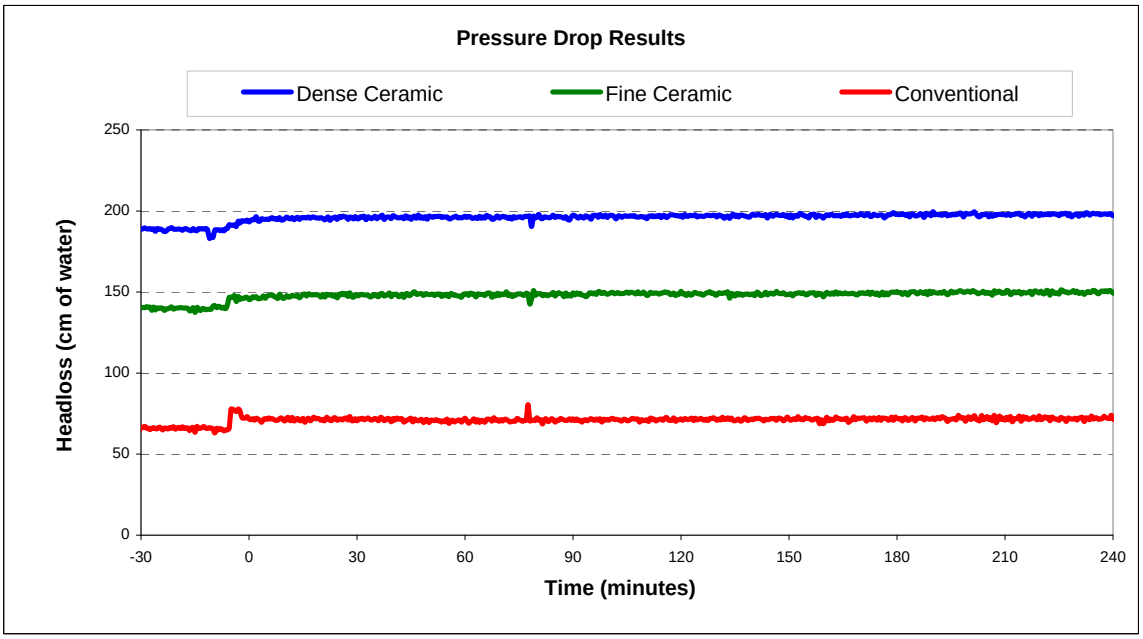

Summary Information for: Trial 2D

Trial Conditions:	
Trial Date	September 11, 2006
Location	Horgan WTP
Water Source	Lake Ontario
Loading Rate	4 GPM/ft^2 (9.8 m/hr)
Coagulation	No Coagulant
Water Temperature	21^{0}C

Filter Media Configuration:

	Column 1	**Column 2**	**Column 3**
	Dense Ceramic	Fine Ceramic	Conventional
Top Layer	45 cm ceramic, ES 0.64 mm	45 cm ceramic, ES 0.96 mm	45 cm anthracite, ES 0.89 mm
Bottom Layer	30 cm ceramic, ES 0.22 mm	15 cm ceramic, ES 0.21mm	30 cm sand, ES 0.47 mm
Support Media	20 cm graded gravel bed	20 cm graded gravel bed	20 cm graded gravel bed

Parameter:	**Influent**	**Dense Ceramic**	**Fine Ceramic**	**Conventional**
Log reductions:				
Cryptosporidium		0.30	0.48	0.60
Microspheres		0.43	0.62	0.42
Other Parameters[1]:				
Average turbidity (NTU)	0.547	0.396	0.380	0.478
Turbidity reduction (%)		28	31	13
Average total particle count (#/mL)	3452	2053	1179	1758
Particle reduction (%)		41	66	49
Average flow (mL/min)		746	763	799
Clean bed headloss		81	73	29
Average headloss (cm)		80	74	28
Change in headloss (cm)		-1	2	-1

[1] *Data calculated from time 0 (start of spike injection) to 360 elapsed minutes*

***Cryptosporidium* and Microsphere Removal Summary:** **Trial 2D**

***Cryptosporidium* Log Removal**

Time	Col 1	Col 2	Col 3
10 min			
20 min	0.59	0.78	0.77
30 min	0.28	0.21	0.43
40 min	-0.04	0.20	1.01
50 min	-0.56	0.31	0.28
60 min			
70 min			
Avg.[1]	**0.30**	**0.48**	**0.60**

Microsphere Log Removal

Time	Col 1	Col 2	Col 3
10 min	1.17	0.78	1.32
20 min	0.02	0.75	0.46
30 min	0.47	0.57	0.33
40 min	0.59	0.73	0.34
50 min	0.48	0.43	0.50
60 min	-0.43	-0.13	-0.38
70 min	-3.84	-1.62	-0.73
Avg.[1]	**0.43**	**0.62**	**0.42**

[1]*Avgerage denotes time interval from 20 min to 60 min*

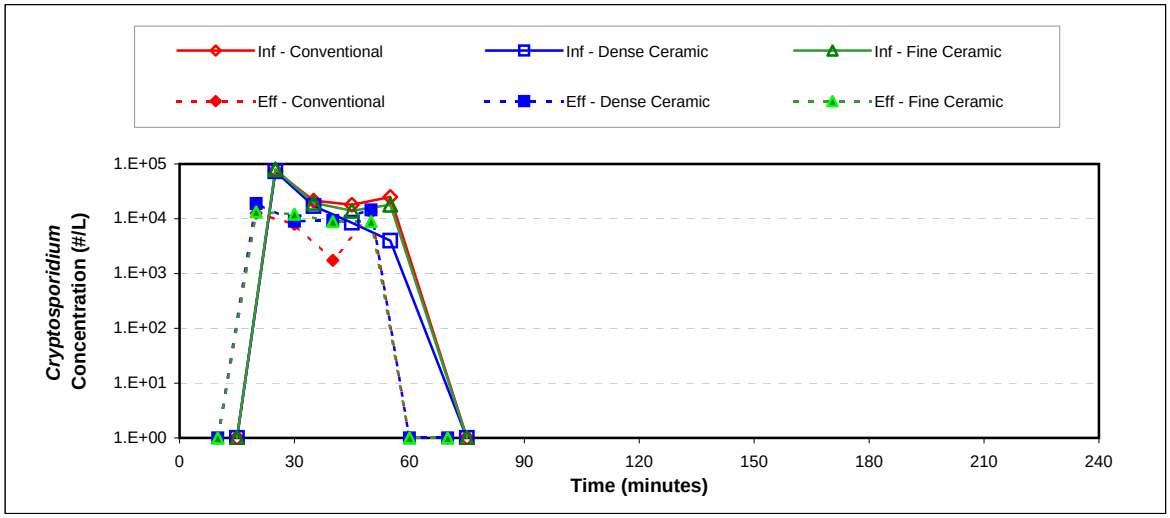

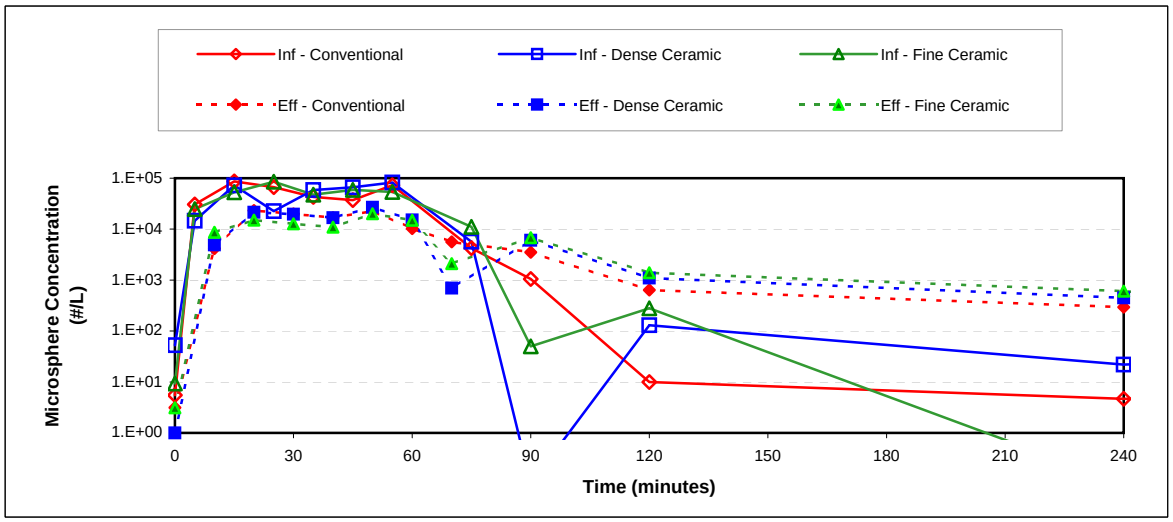

Turbidity Summary: Trial 2D

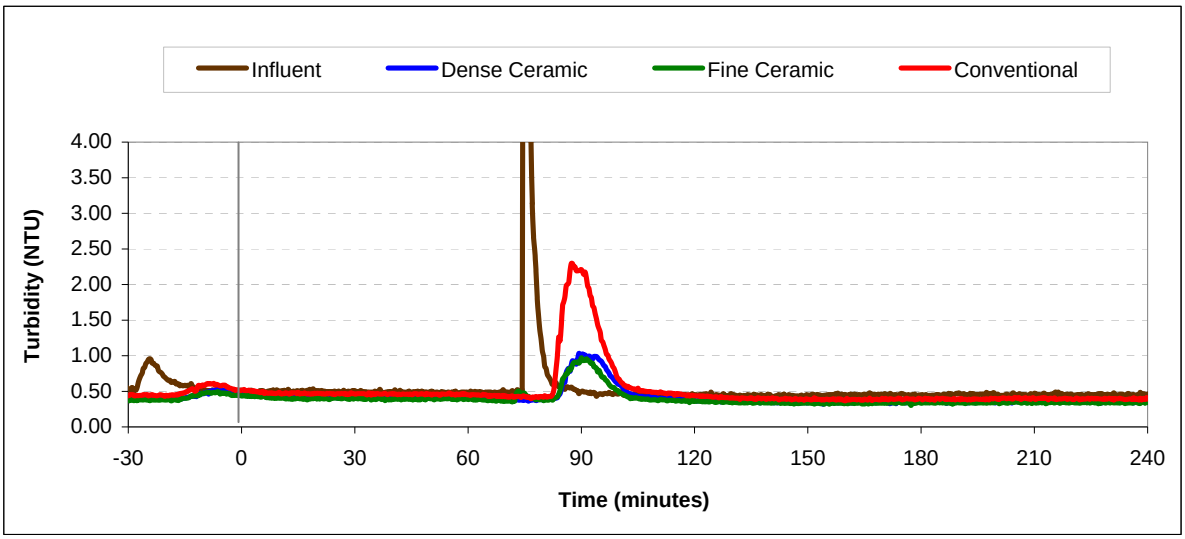

Turbidity Box and Whisker Plots

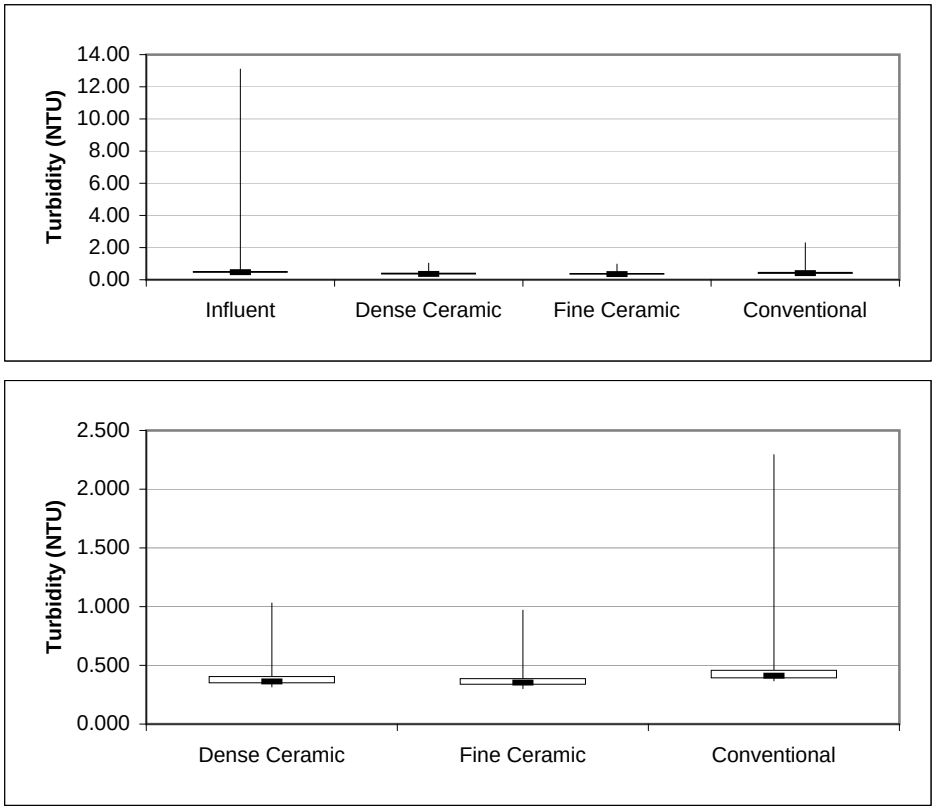

Vertical lines represent maximum and minimum turbidity range. Top and bottom of boxes represent 75th and 25th percentiles of turbidity data. Centre dash represents median turbidity measurement during seeding study.

Particle Count Summary: **Trial 2D**

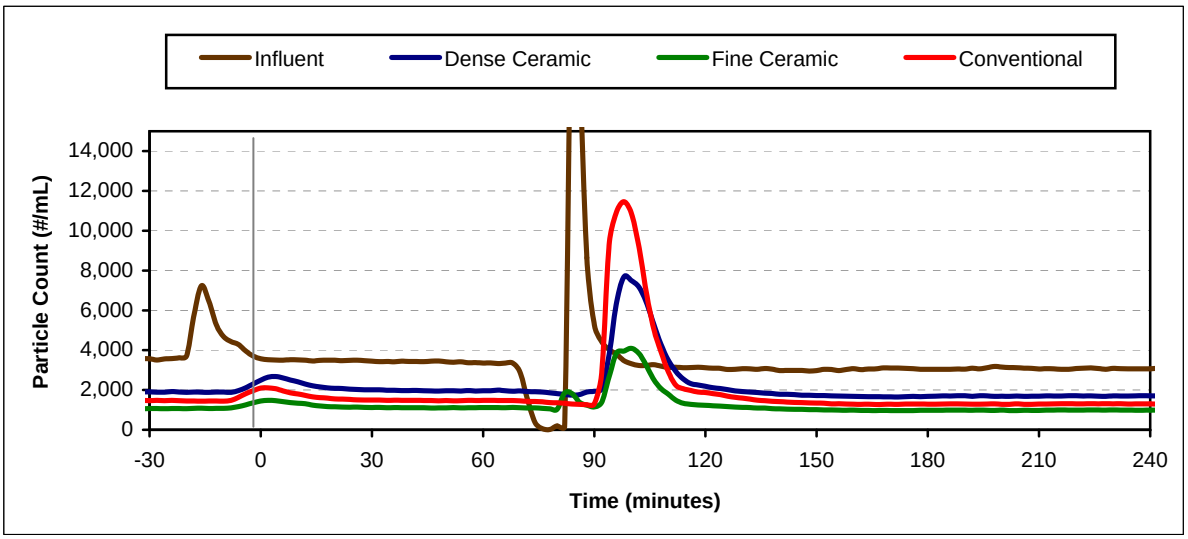

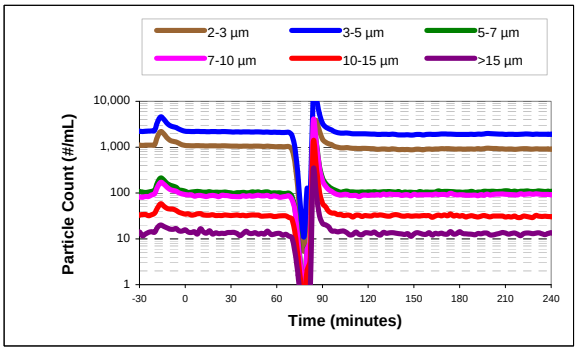

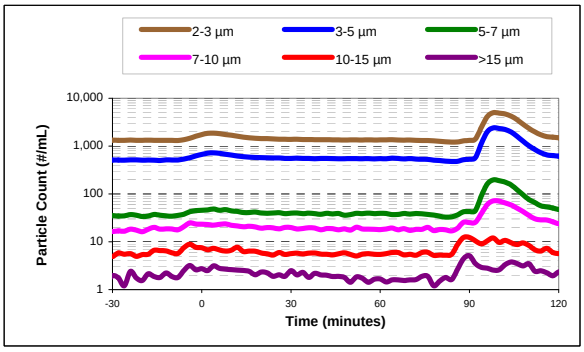

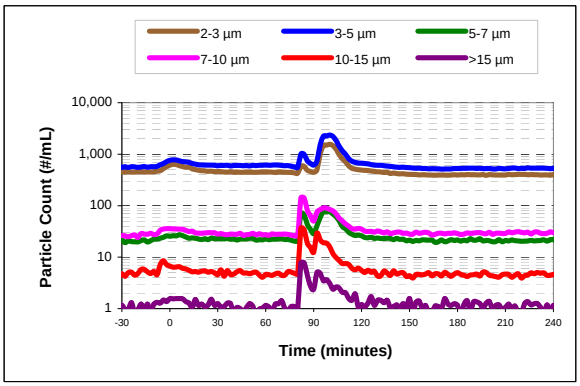

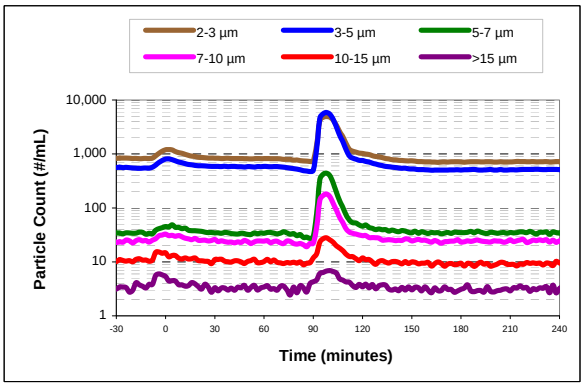

Flow and Headloss Summary: Trial 2D

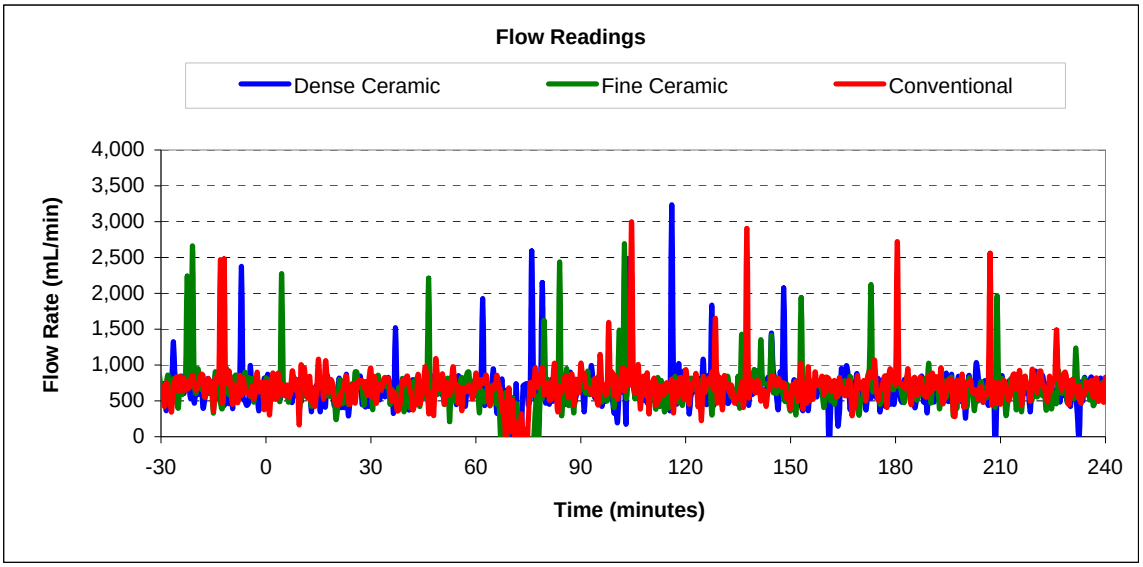

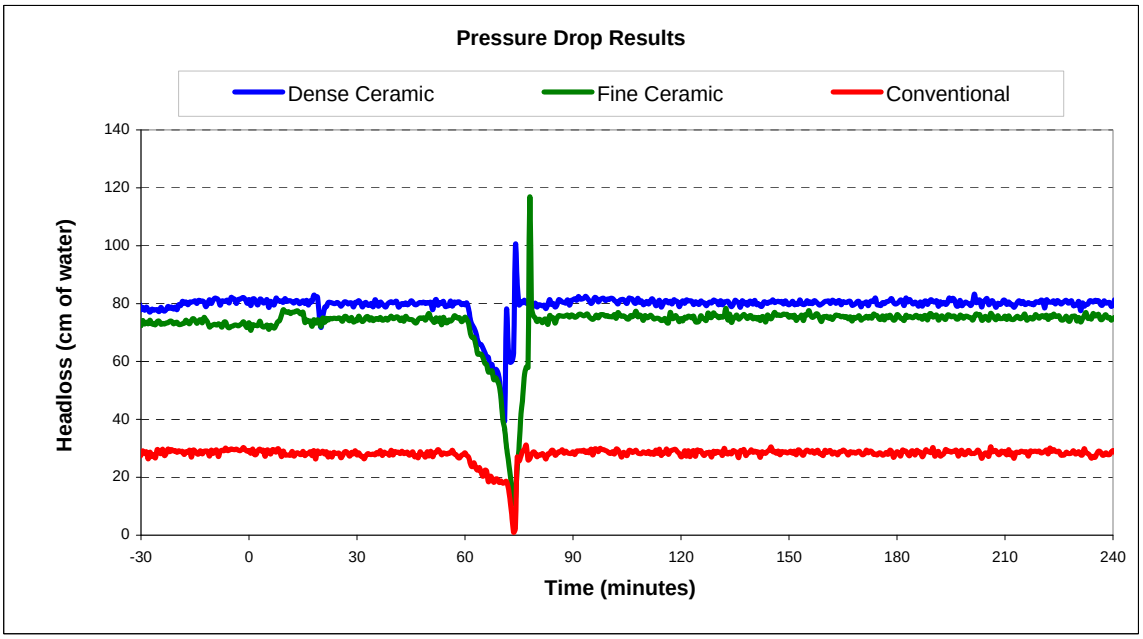

Summary Information for: Trial 2E

Trial Conditions:	
Trial Date	September 12, 2006
Location	Horgan WTP
Water Source	Lake Ontario
Loading Rate	10 GPM/ft^2 (24.4 m/hr)
Coagulation	No Coagulant
Water Temperature	20^{0}C

Filter Media Configuration:

	Column 1	**Column 2**	**Column 3**
	Dense Ceramic	Fine Ceramic	Conventional
Top Layer	45 cm ceramic, ES 0.64 mm	45 cm ceramic, ES 0.96 mm	45 cm anthracite, ES 0.89 mm
Bottom Layer	30 cm ceramic, ES 0.22 mm	15 cm ceramic, ES 0.21mm	30 cm sand, ES 0.47 mm
Support Media	20 cm graded gravel bed	20 cm graded gravel bed	20 cm graded gravel bed

Parameter:	**Influent**	**Dense Ceramic**	**Fine Ceramic**	**Conventional**
Log reductions:				
Cryptosporidium		0.19	-0.04	0.20
Microspheres		0.39	0.76	0.30
Other Parameters[1]:				
Average turbidity (NTU)	0.385	0.279	0.268	0.327
Turbidity reduction (%)		27	30	15
Average total particle count (#/mL)	1958	1131	882	1280
Particle reduction (%)		42	55	35
Average flow (mL/min)		2040	1934	1964
Clean bed headloss		192	136	65
Average headloss (cm)		190	138	65
Change in headloss (cm)		0	2	3

[1] *Data calculated from time 0 (start of spike injection) to 360 elapsed minutes*

***Cryptosporidium* and Microsphere Removal Summary:** **Trial 2E**

***Cryptosporidium* Log Removal**

Time	Col 1	Col 2	Col 3
10 min			
20 min	-0.29	-0.80	-0.31
30 min	0.43	-0.20	0.26
40 min	0.25	0.32	0.51
50 min	0.13	-0.09	-0.03
60 min			
70 min			
Avg.[1]	**0.19**	**-0.04**	**0.20**

[1]*Avgerage denotes time interval from 20 min to 60 min*

Microsphere Log Removal

Time	Col 1	Col 2	Col 3
10 min	-0.24	0.34	4.60
20 min	-0.15	0.28	-0.07
30 min	0.35	1.42	0.08
40 min	0.72	0.87	0.87
50 min	0.71	0.92	0.67
60 min	-2.42	-2.96	-0.15
70 min	-1.18	-1.24	-2.17
Avg.[1]	**0.39**	**0.76**	**0.30**

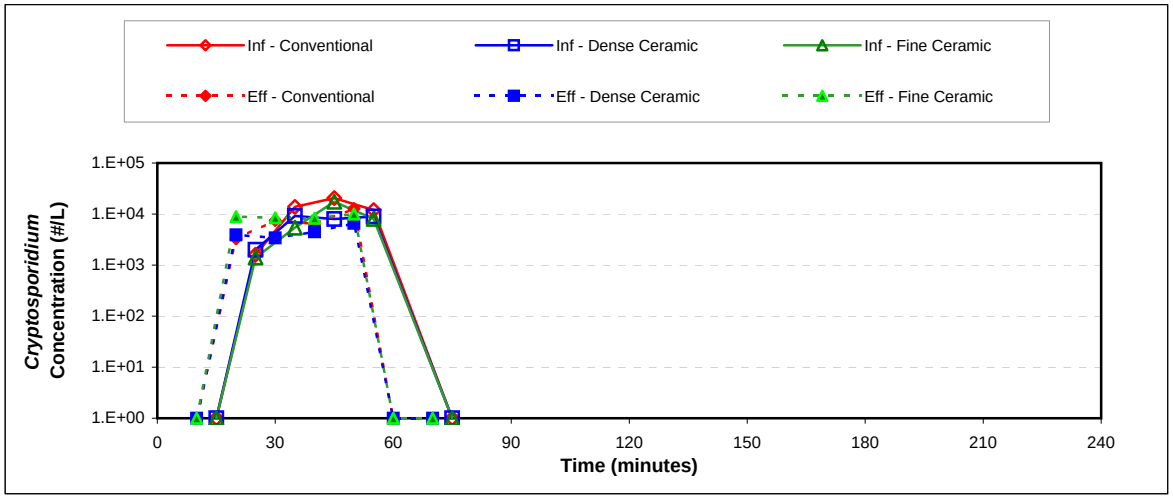

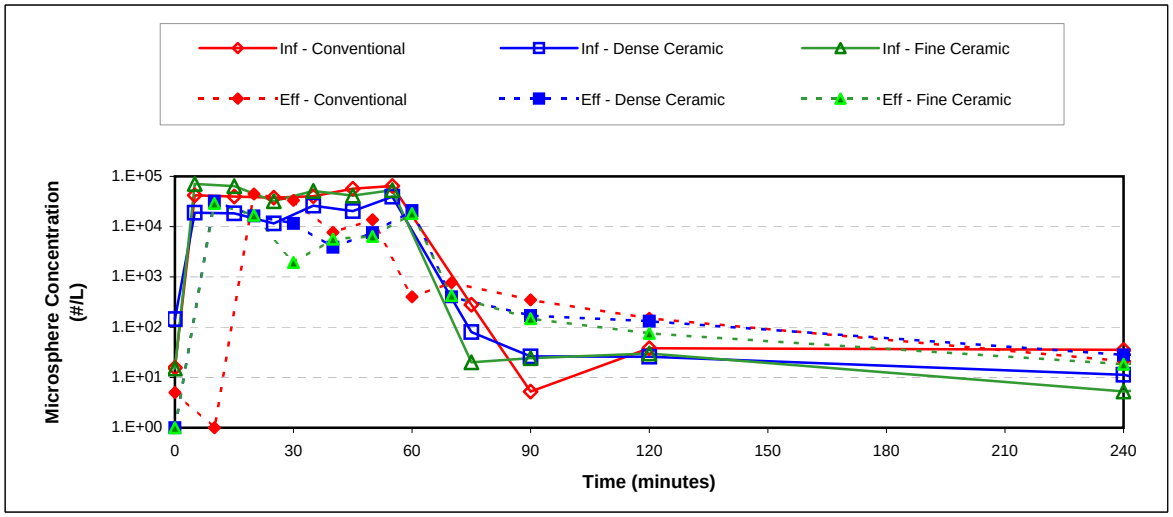

Turbidity Summary: Trial 2E

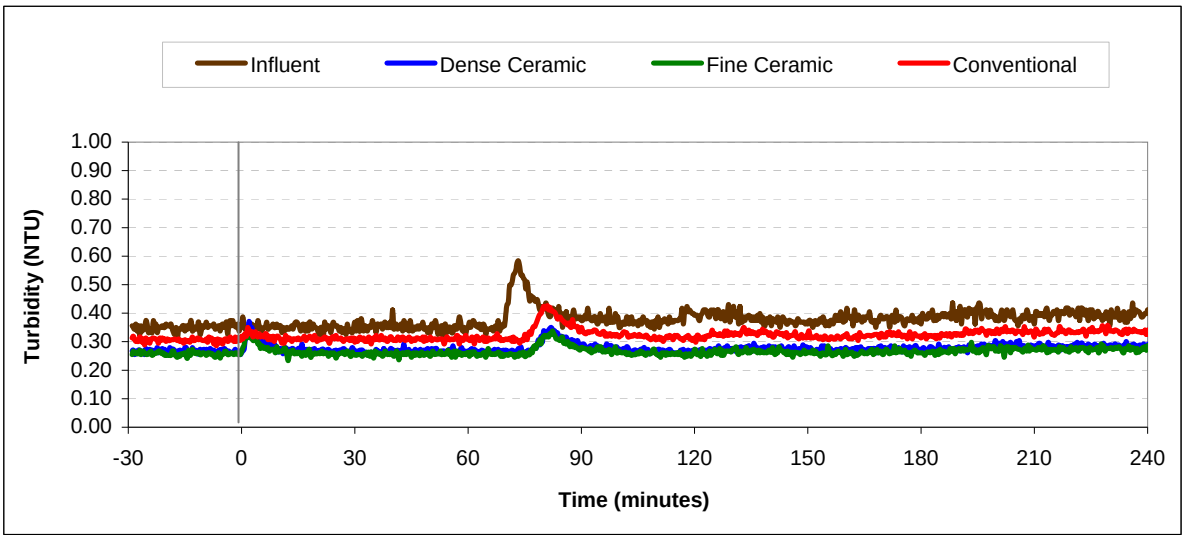

Turbidity Box and Whisker Plots

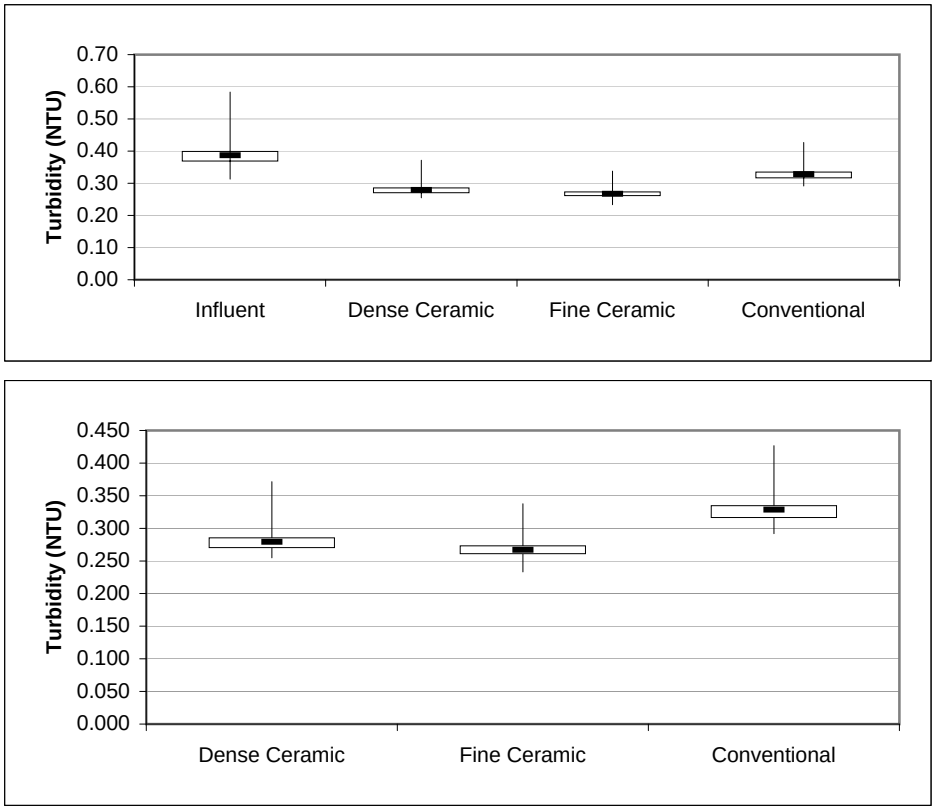

Vertical lines represent maximum and minimum turbidity range. Top and bottom of boxes represent 75th and 25th percentiles of turbidity data. Centre dash represents median turbidity measurement during seeding study.

Particle Count Summary: **Trial 2E**

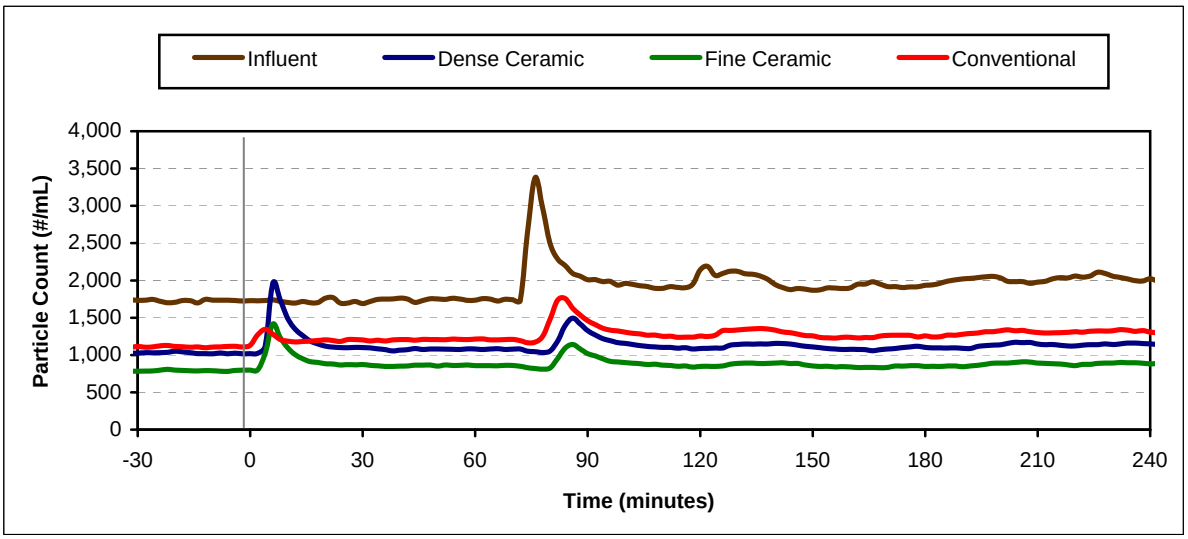

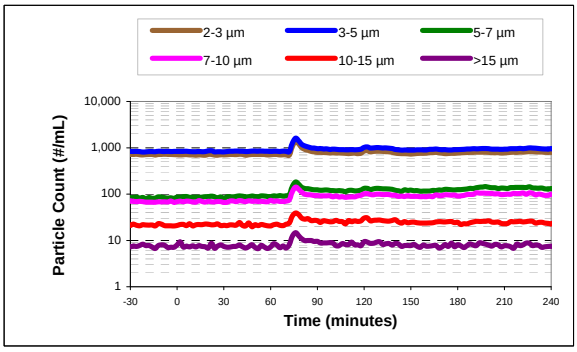

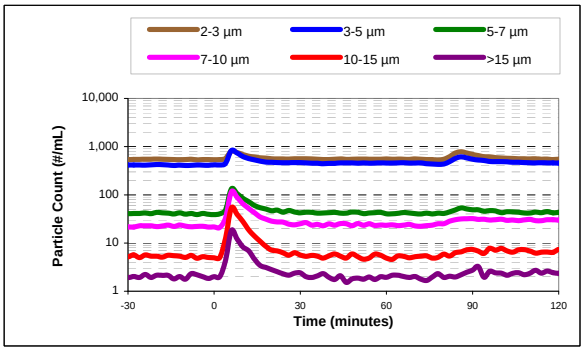

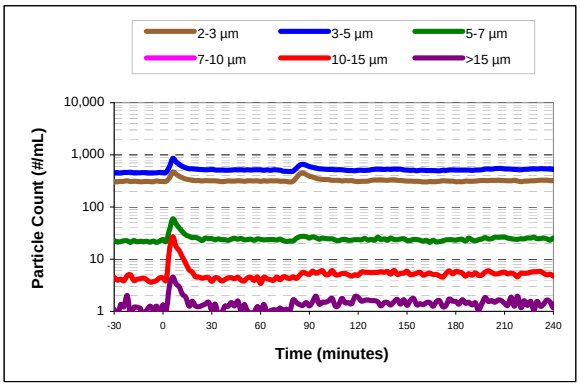

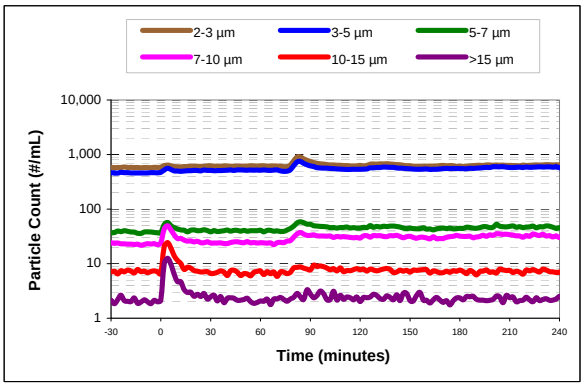

Flow and Headloss Summary: Trial 2E

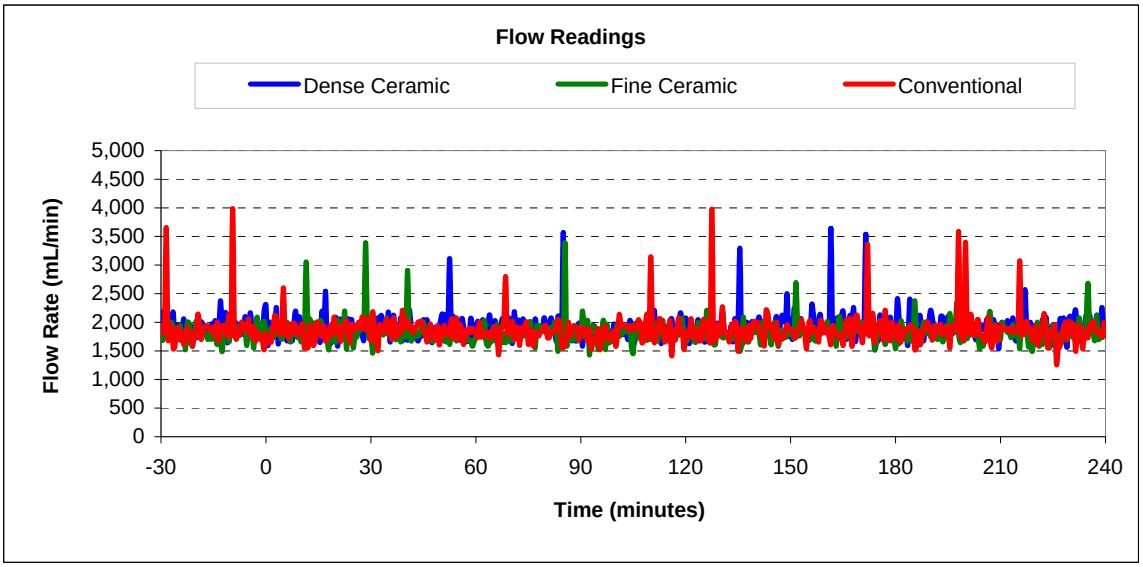

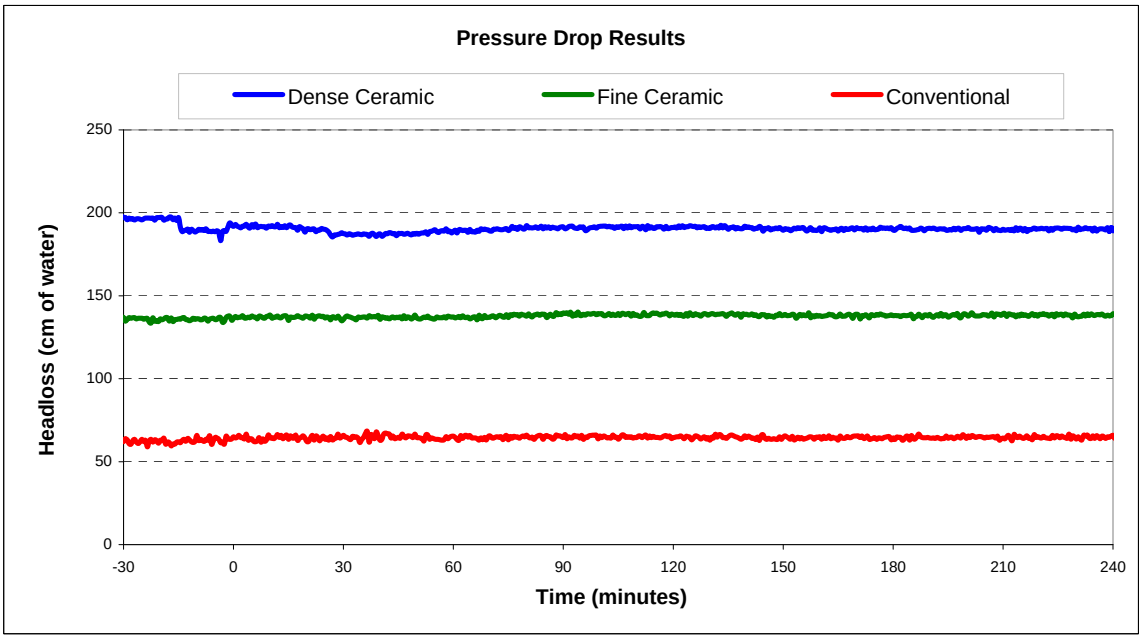

Summary Information for: Trial 2F

Trial Conditions:	
Trial Date	September 25, 2006
Location	Horgan WTP
Water Source	Lake Ontario
Loading Rate	4 GPM/ft^2 (9.8 m/hr)
Coagulation	No Coagulant
Water Temperature	9^{0}C

Filter Media Configuration:

	Column 1	**Column 2**	**Column 3**
	Dense Ceramic	Fine Ceramic	Conventional
Top Layer	45 cm ceramic, ES 0.64 mm	45 cm ceramic, ES 0.96 mm	45 cm anthracite, ES 0.89 mm
Bottom Layer	30 cm ceramic, ES 0.22 mm	15 cm ceramic, ES 0.21mm	30 cm sand, ES 0.47 mm
Support Media	20 cm graded gravel bed	20 cm graded gravel bed	20 cm graded gravel bed

Parameter:	**Influent**	**Dense Ceramic**	**Fine Ceramic**	**Conventional**
Log reductions:				
Cryptosporidium		0.50	0.13	0.07
Microspheres		0.67	0.66	0.40
Other Parameters[1]:				
Average turbidity (NTU)	0.186	0.102	0.095	0.135
Turbidity reduction (%)		45	49	28
Average total particle count (#/mL)	1211	459	358	600
Particle reduction (%)		62	70	50
Average flow (mL/min)		859	806	838
Clean bed headloss		91	79	34
Average headloss (cm)		98	85	34
Change in headloss (cm)		13	10	1

[1] *Data calculated from time 0 (start of spike injection) to 360 elapsed minutes*

***Cryptosporidium* and Microsphere Removal Summary:** **Trial 2F**

***Cryptosporidium* Log Removal**

Time	Col 1	Col 2	Col 3
10 min			
20 min	0.62	0.60	0.11
30 min	0.73	-0.06	0.41
40 min	1.15	0.19	-0.17
50 min	0.06	-0.03	0.16
60 min			
70 min			
Avg.[1]	**0.50**	**0.13**	**0.07**

Microsphere Log Removal

Time	Col 1	Col 2	Col 3
10 min	0.38	0.56	0.59
20 min	0.80	0.63	-0.05
30 min	0.53	0.59	0.34
40 min	0.78	0.69	0.73
50 min	0.67	0.73	0.56
60 min	-0.56	-0.50	-0.77
70 min	-5.39	-2.10	-1.04
Avg.[1]	**0.67**	**0.66**	**0.40**

[1]*Avgerage denotes time interval from 20 min to 60 min*

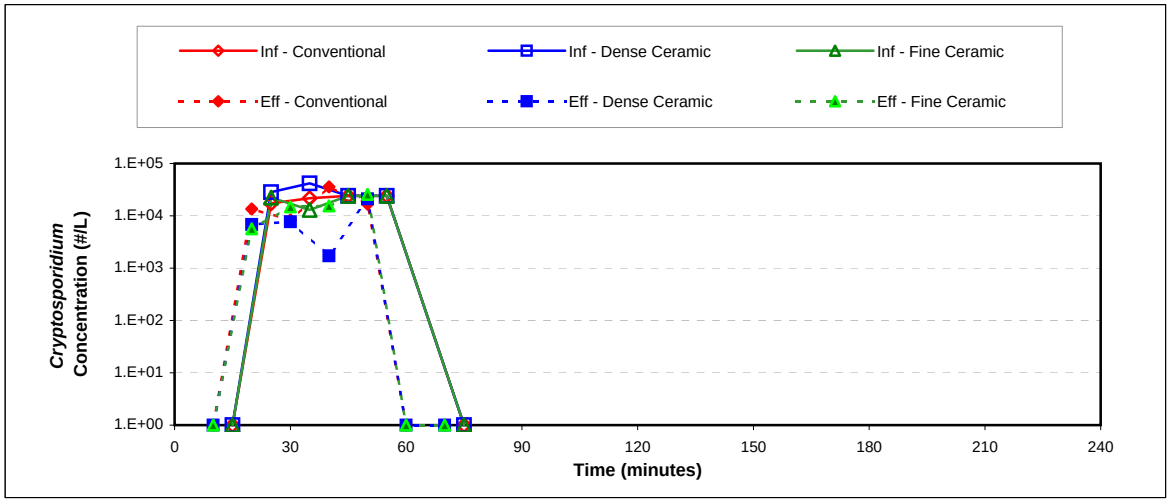

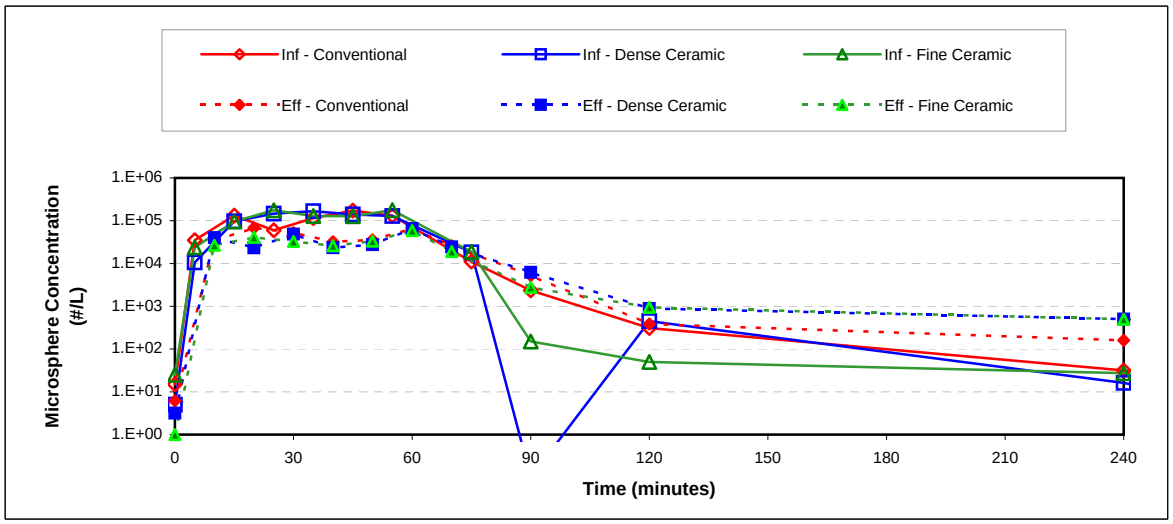

Turbidity Summary: Trial 2F

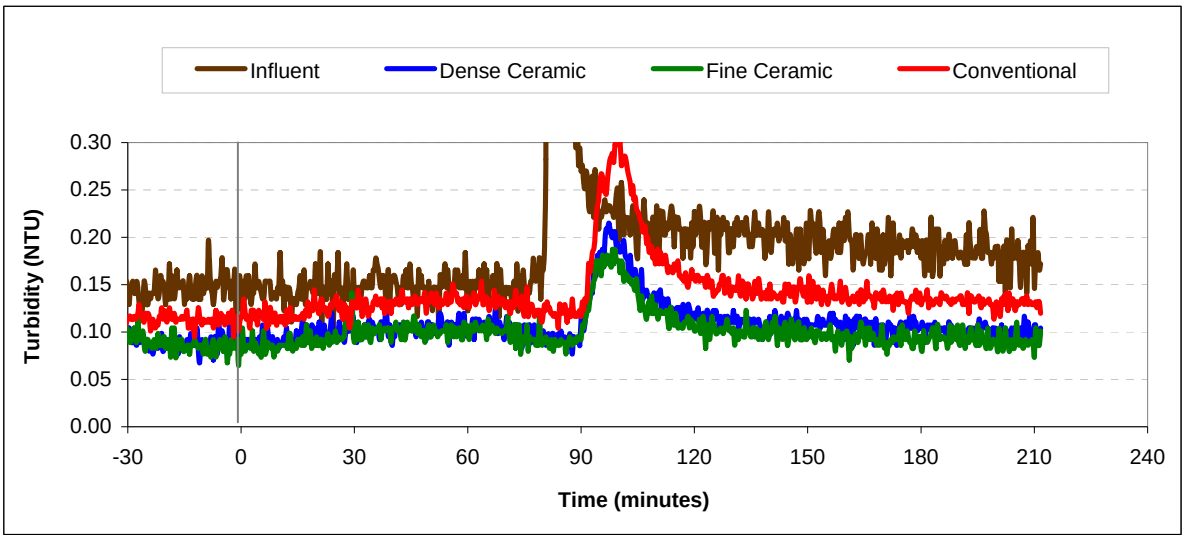

Turbidity Box and Whisker Plots

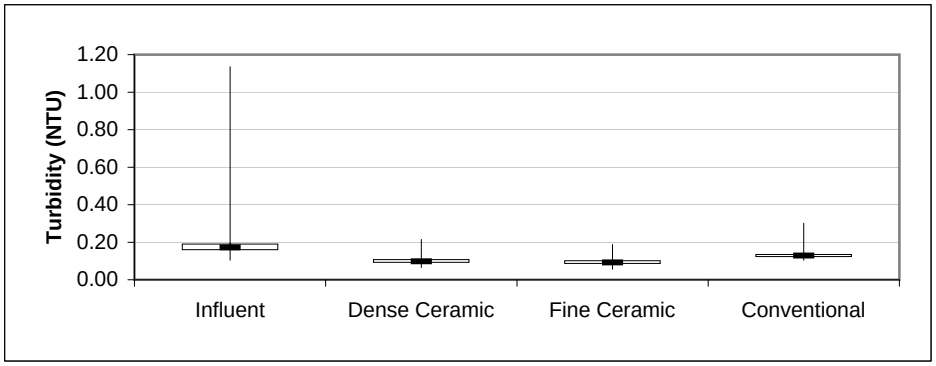

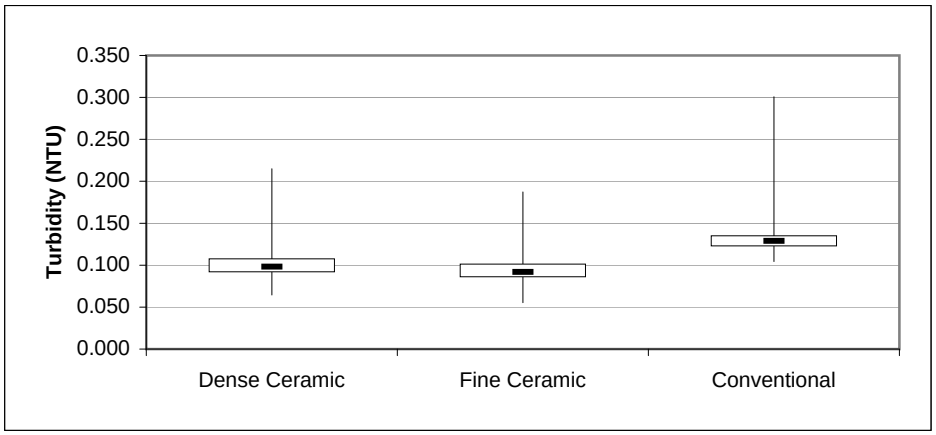

Vertical lines represent maximum and minimum turbidity range. Top and bottom of boxes represent 75th and 25th percentiles of turbidity data. Centre dash represents median turbidity measurement during seeding study.

Particle Count Summary: Trial 2F

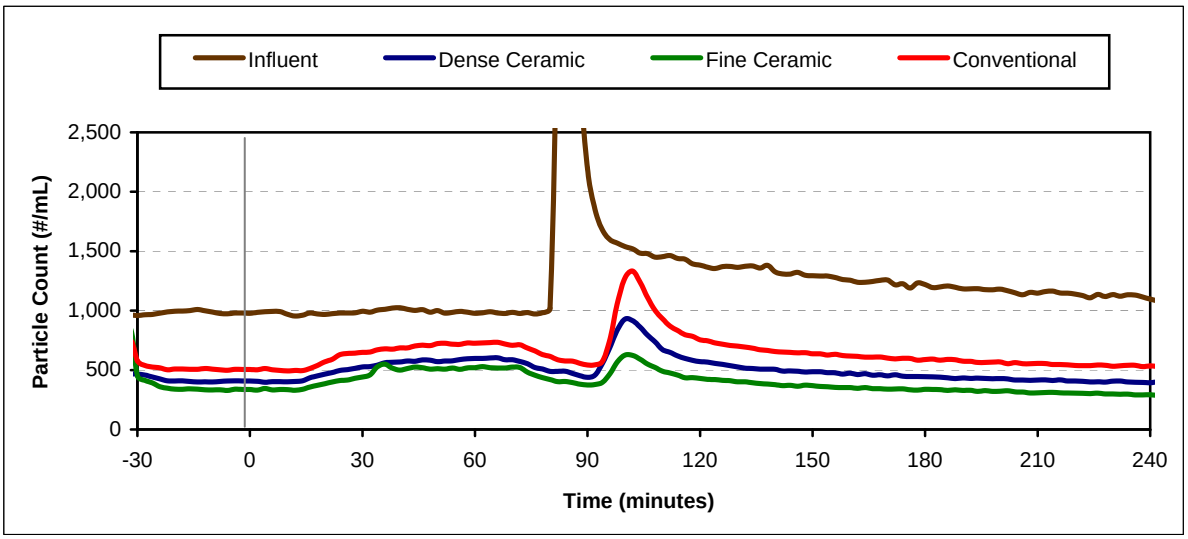

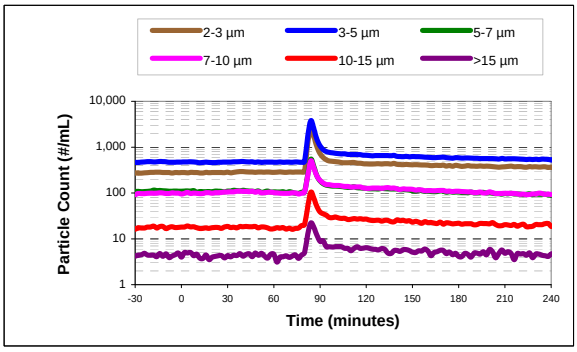

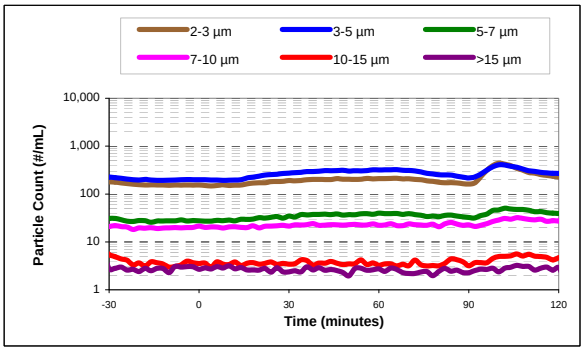

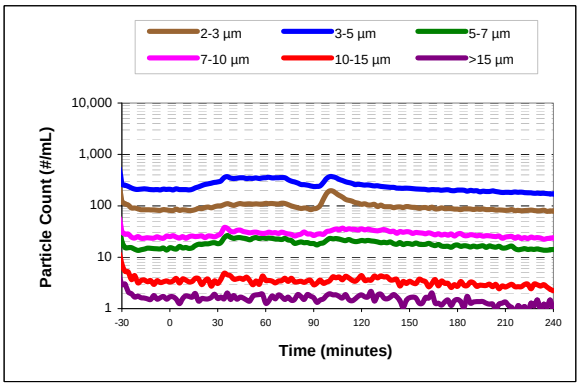

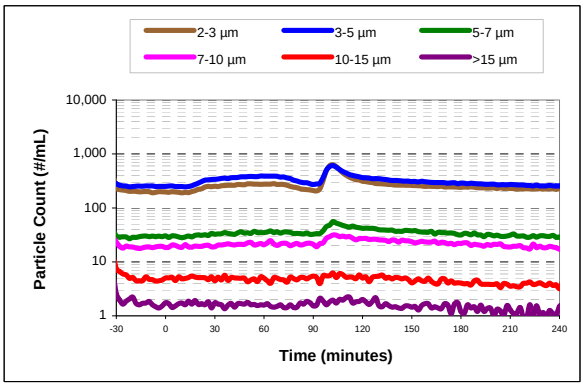

Flow and Headloss Summary: Trial 2F

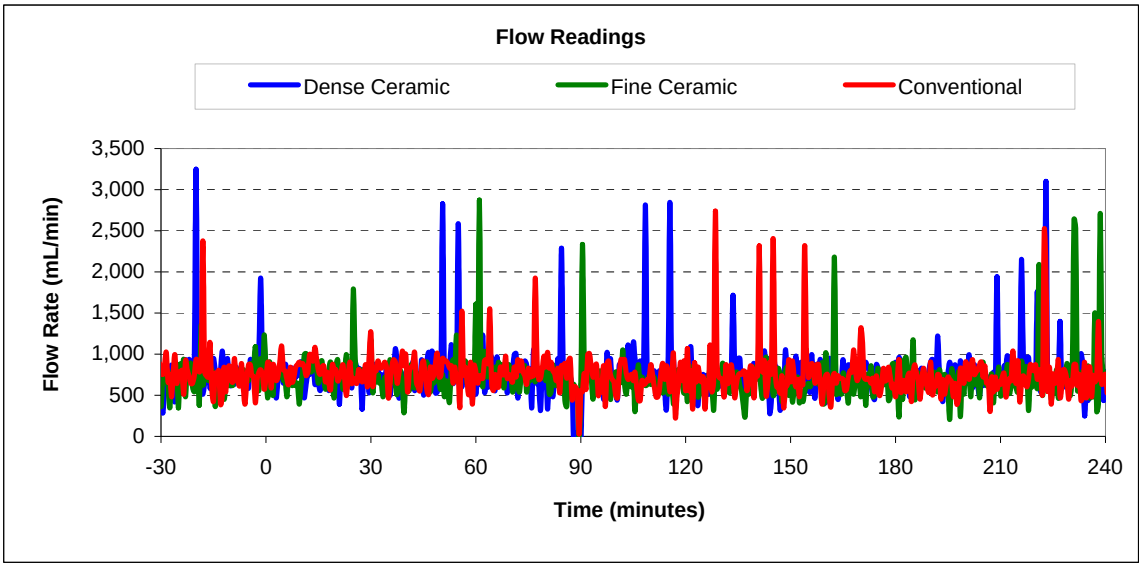

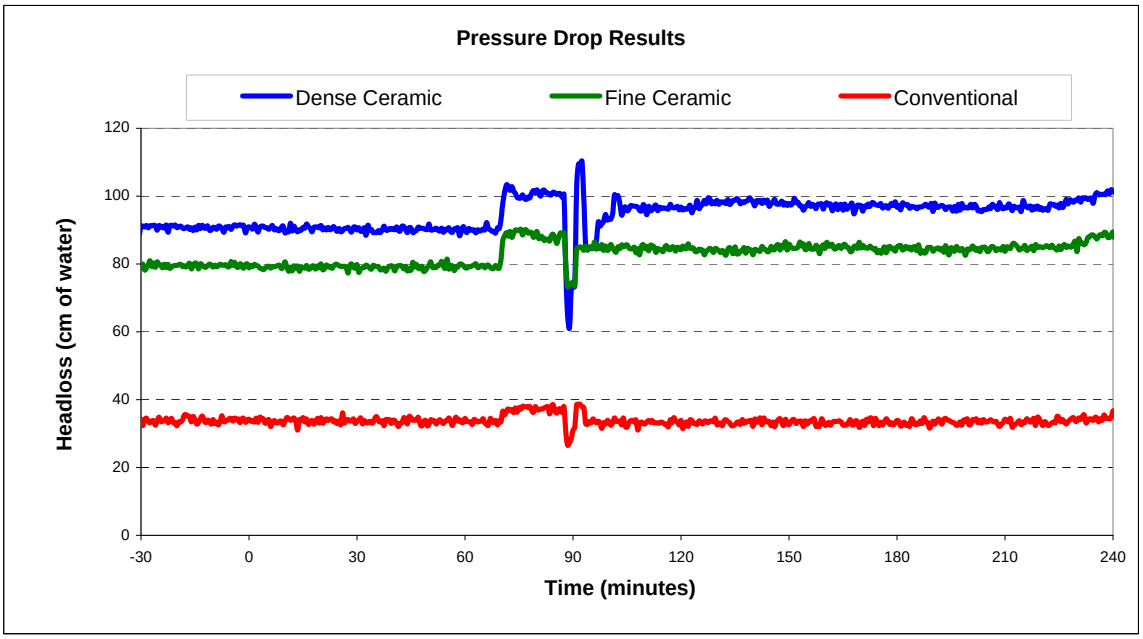

Summary Information for: Trial 3A

Trial Conditions:	
Trial Date	December 11, 2007
Location	Horgan WTP
Water Source	Lake Ontario
Loading Rate	10 GPM/ft^2 (24.4 m/hr)
Coagulation	No Coagulant
Water Temperature	4^0C

Filter Media Configuration:

	Column 1	**Column 2**	**Column 3**
	Matched Ceramic	Fine Ceramic	Conventional
Top Layer	45 cm ceramic, ES 0.89 mm	45 cm ceramic, ES 0.96 mm	45 cm anthracite, ES 0.89 mm
Bottom Layer	30 cm ceramic, ES 0.47 mm	15 cm ceramic, ES 0.21mm	30 cm sand, ES 0.47 mm
Support Media	20 cm graded gravel bed	20 cm graded gravel bed	20 cm graded gravel bed

Parameter:	**Influent**	**Matched Ceramic**	**Fine Ceramic**	**Conventional**
Log reductions:				
Cryptosporidium		-0.03	0.53	0.42
Microspheres		0.28	0.33	0.39
Other Parameters[1]:				
Average turbidity (NTU)	0.194	0.206	0.153	0.190
Turbidity reduction (%)		-6	21	2
Average total particle count (#/mL)	na	na	na	na
Particle reduction (%)				
Average flow (mL/min)		2072	1858	2200
Clean bed headloss		99	204	100
Average headloss (cm)		100	206	100
Change in headloss (cm)		2	2	1

[1] *Data calculated from time 0 (start of spike injection) to 360 elapsed minutes*

***Cryptosporidium* and Microsphere Removal Summary:** **Trial 3A**

***Cryptosporidium* Log Removal**

Time	Col 1	Col 2	Col 3
10 min			
20 min	0.16	0.27	0.27
30 min	-0.38	0.40	0.32
40 min	1.25	0.60	0.81
50 min	0.97	1.29	0.61
60 min			
70 min			
Avg.[1]	**-0.03**	**0.53**	**0.42**

[1]*Avgerage denotes time interval from 20 min to 60 min*

Microsphere Log Removal

Time	Col 1	Col 2	Col 3
10 min	0.44	0.43	-0.21
20 min	-0.01	0.81	0.48
30 min	0.56	0.72	0.34
40 min	0.02	-0.12	0.40
50 min	0.46	0.44	0.36
60 min	1.04	-1.64	-2.21
70 min	1.41	na	-0.24
Avg.[1]	**0.28**	**0.33**	**0.39**

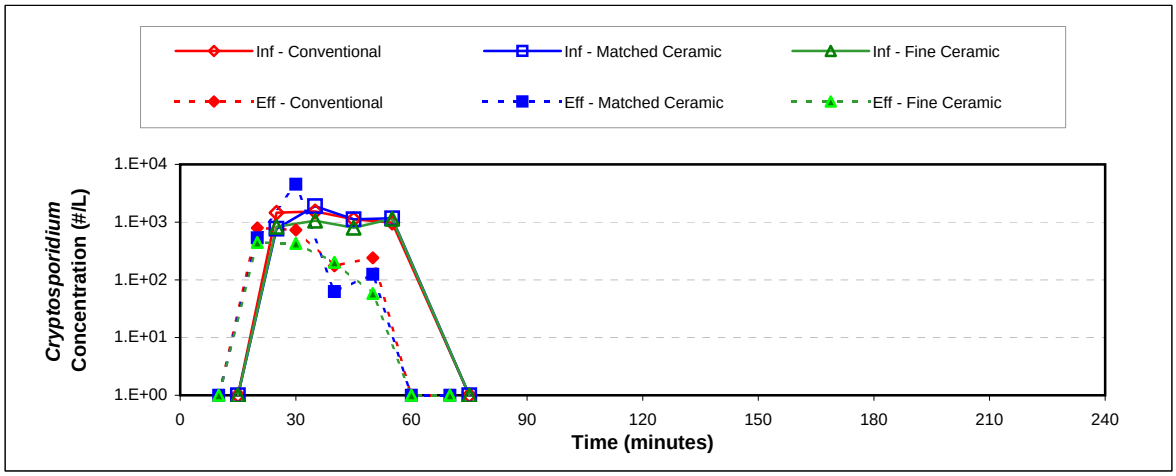

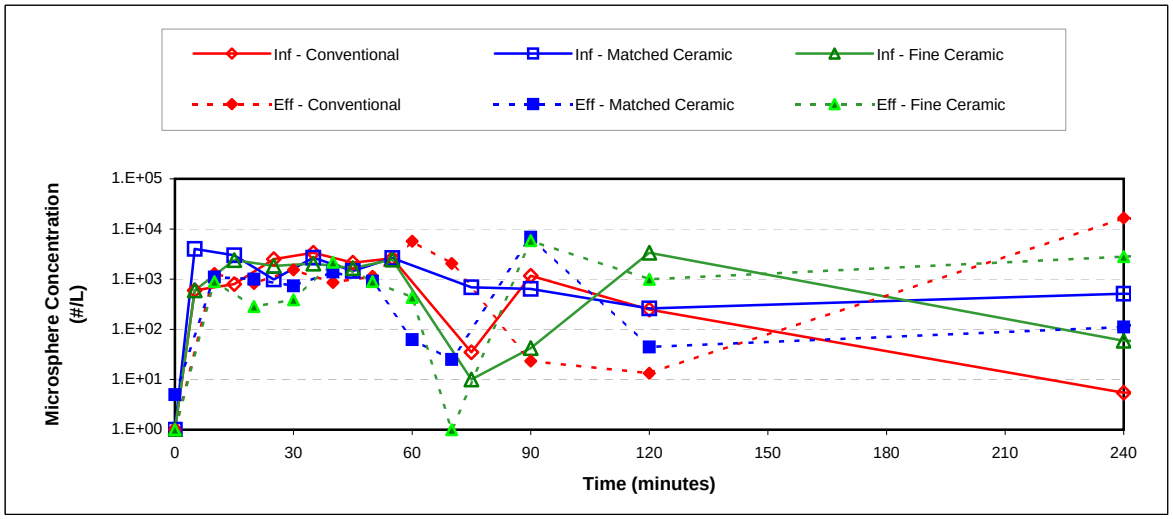

Turbidity Summary: Trial 3A

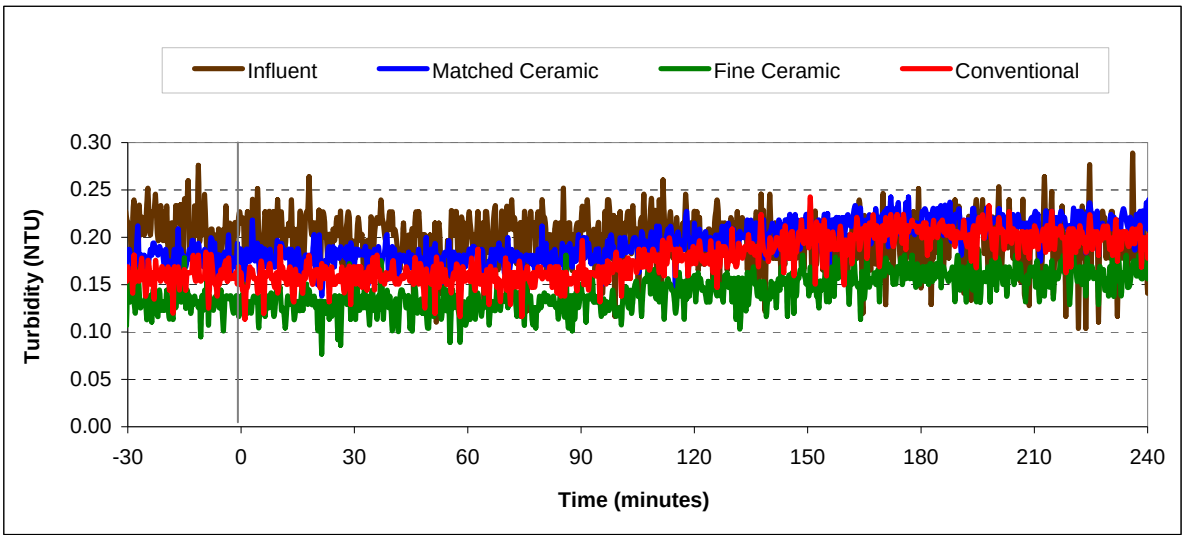

Turbidity Box and Whisker Plots

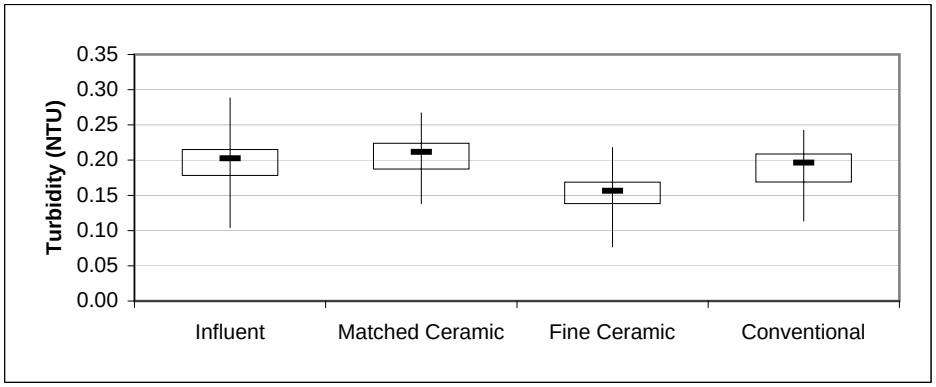

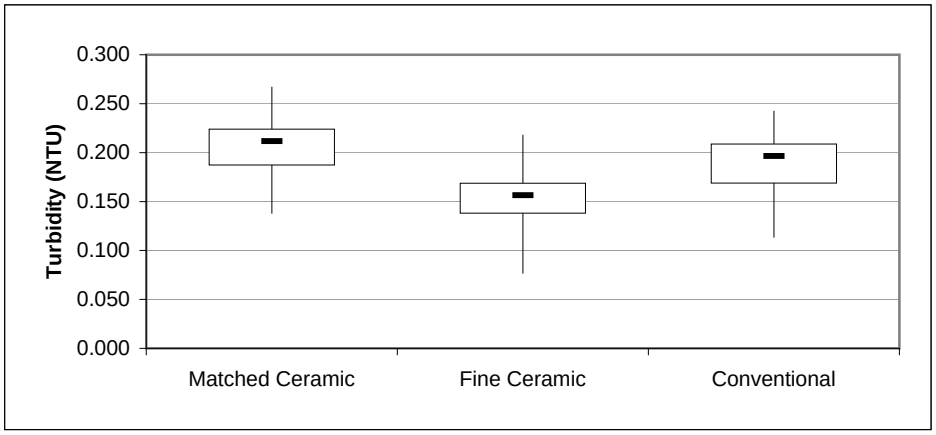

Vertical lines represent maximum and minimum turbidity range. Top and bottom of boxes represent 75th and 25th percentiles of turbidity data. Centre dash represents median turbidity measurement during seeding study.

Particle Count Summary: **Trial 3A**

(particle counters unavailable)

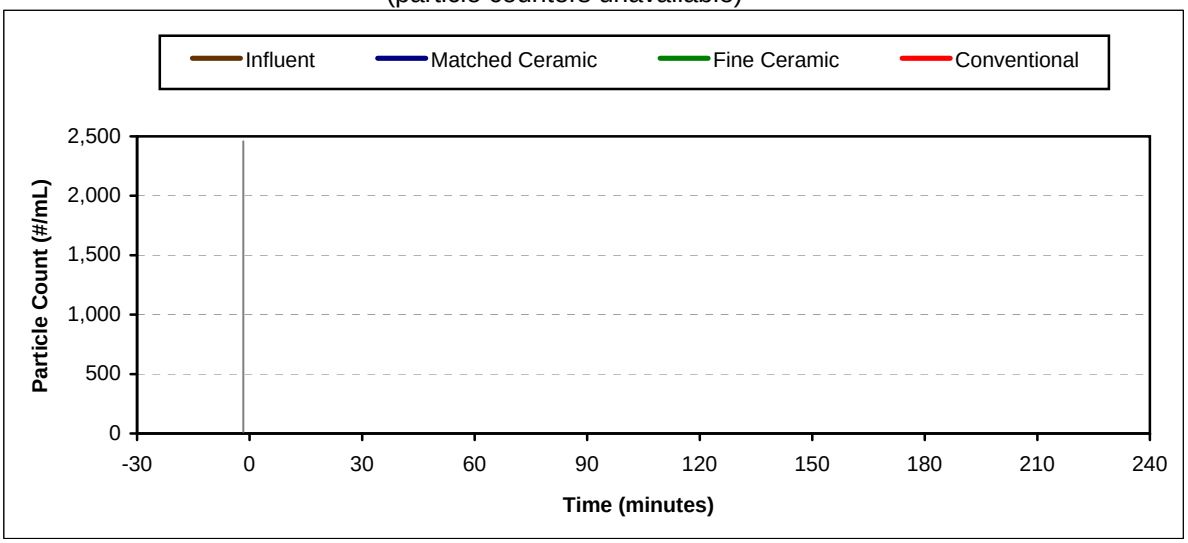

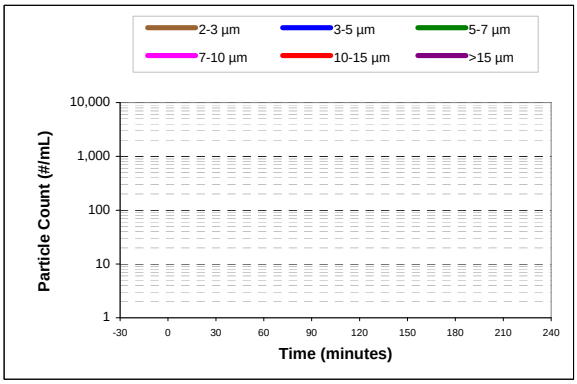

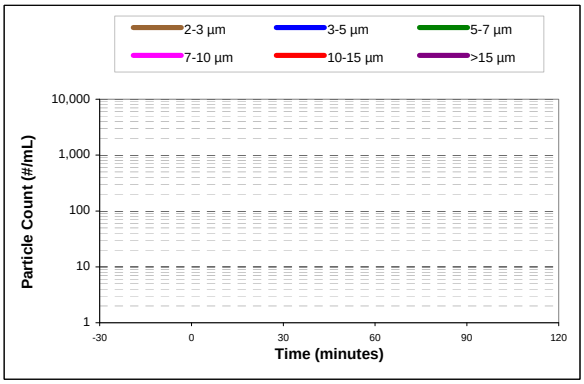

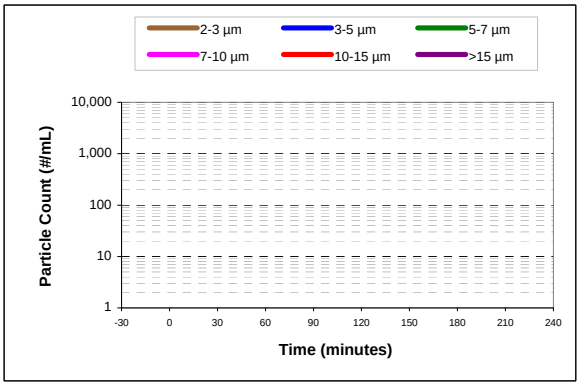

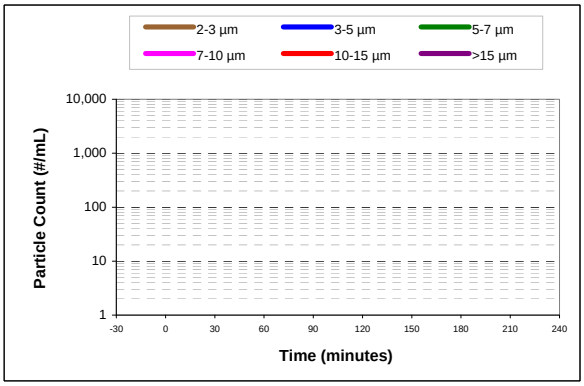

Flow and Headloss Summary: Trial 3A

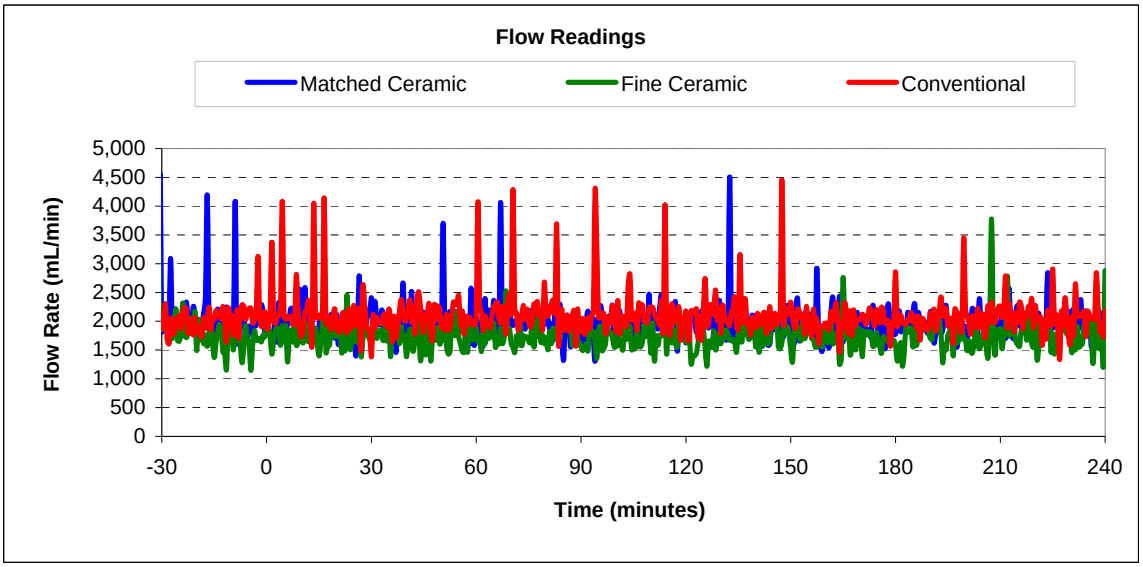

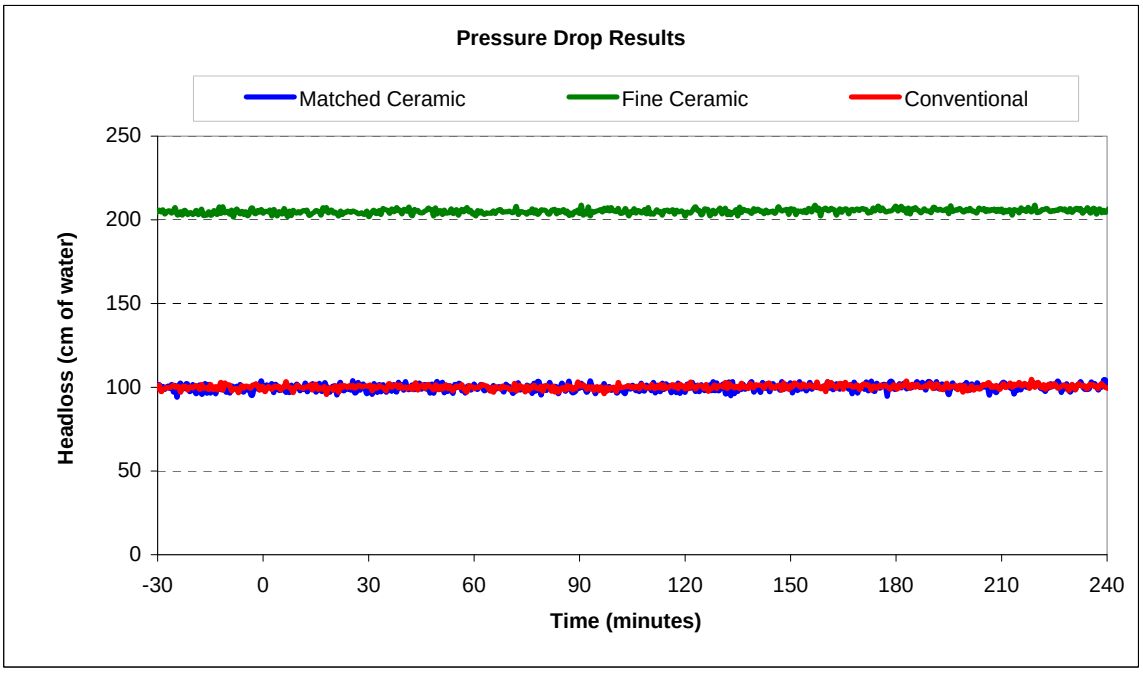

Summary Information for: Trial 3B

Trial Conditions:	
Trial Date	January 29, 2007
Location	Horgan WTP
Water Source	Lake Ontario
Loading Rate	10 GPM/ft^2 (24.4 m/hr)
Coagulation	PACl, 0.8 mg/L
Water Temperature	2^{0}C

Filter Media Configuration:

	Column 1	**Column 2**	**Column 3**
	Matched Ceramic	Fine Ceramic	Conventional
Top Layer	45 cm ceramic, ES 0.89 mm	45 cm ceramic, ES 0.96 mm	45 cm anthracite, ES 0.89 mm
Bottom Layer	30 cm ceramic, ES 0.47 mm	15 cm ceramic, ES 0.21mm	30 cm sand, ES 0.47 mm
Support Media	20 cm graded gravel bed	20 cm graded gravel bed	20 cm graded gravel bed

Parameter:	**Influent**	**Matched Ceramic**	**Fine Ceramic**	**Conventional**
Log reductions:				
Cryptosporidium		5.18	4.82	4.64
Microspheres		5.52	5.40	4.22
Other Parameters[1]:				
Average turbidity (NTU)	0.211	0.055	0.045	0.062
Turbidity reduction (%)		74	79	70
Average total particle count (#/mL)	827	302	408	684
Particle reduction (%)		63	51	17
Average flow (mL/min)		1850	531	1839
Clean bed headloss		114	211	112
Average headloss (cm)		226	287	209
Change in headloss (cm)		224	151	193

[1] *Data calculated from time 0 (start of spike injection) to 360 elapsed minutes*

***Cryptosporidium* and Microsphere Removal Summary:** **Trial 3B**

***Cryptosporidium* Log Removal**

Time	Col 1	Col 2	Col 3
10 min			
20 min	5.62	5.03	4.20
30 min	5.27	5.21	4.82
40 min	4.93	5.62	4.71
50 min	4.76	4.21	5.49
60 min			
70 min			
Avg.[1]	**5.18**	**4.82**	**4.64**

[1]*Avgerage denotes time interval from 20 min to 60 min*

Microsphere Log Removal

Time	Col 1	Col 2	Col 3
10 min	5.28	6.49	5.12
20 min	5.45	5.20	3.97
30 min	5.18	5.49	3.99
40 min	6.53	6.32	5.74
50 min	6.33	6.24	6.23
60 min	2.51	4.91	2.60
70 min	3.65	4.56	2.26
Avg.[1]	**5.52**	**5.40**	**4.22**

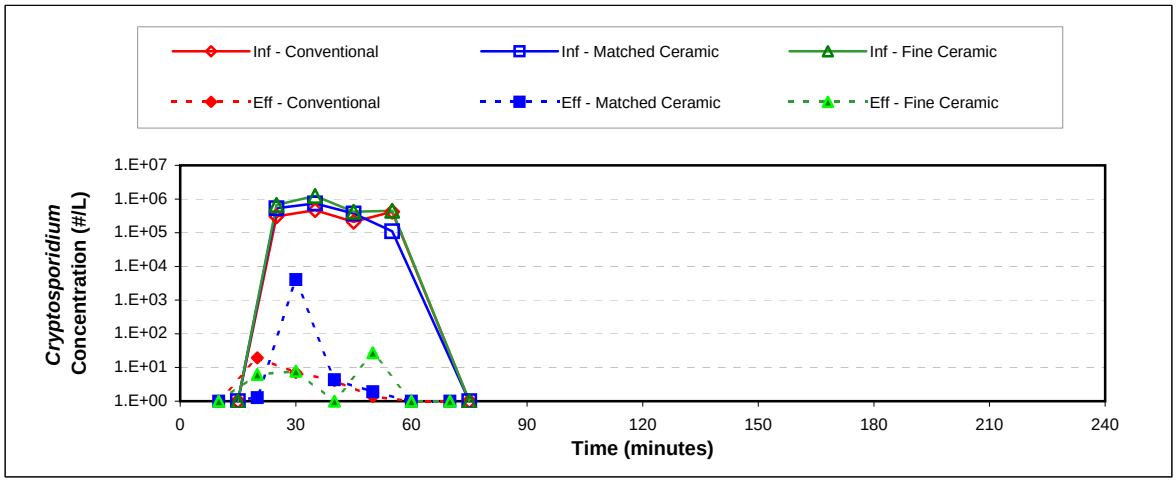

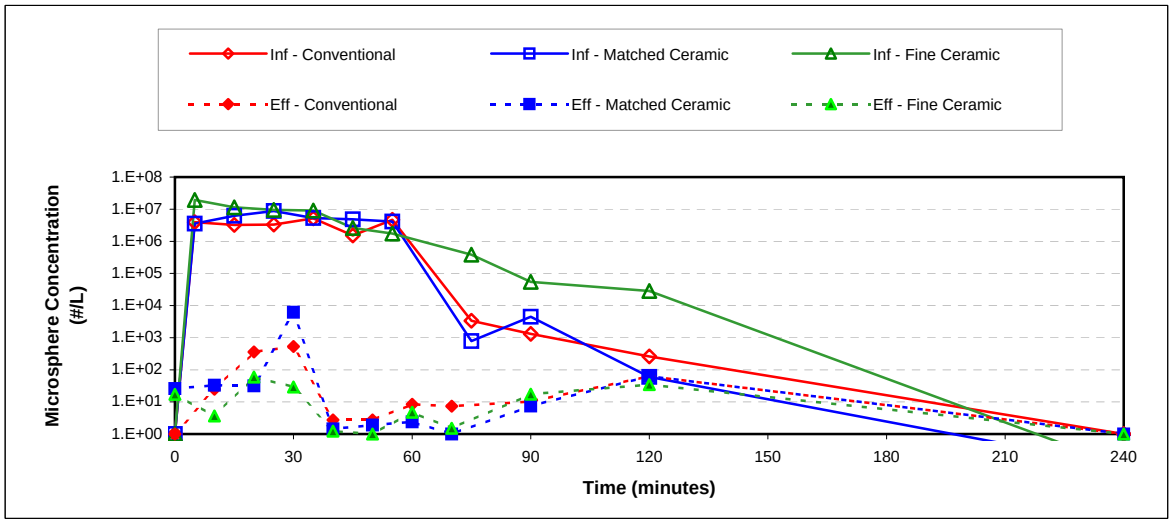

Turbidity Summary: Trial 3B

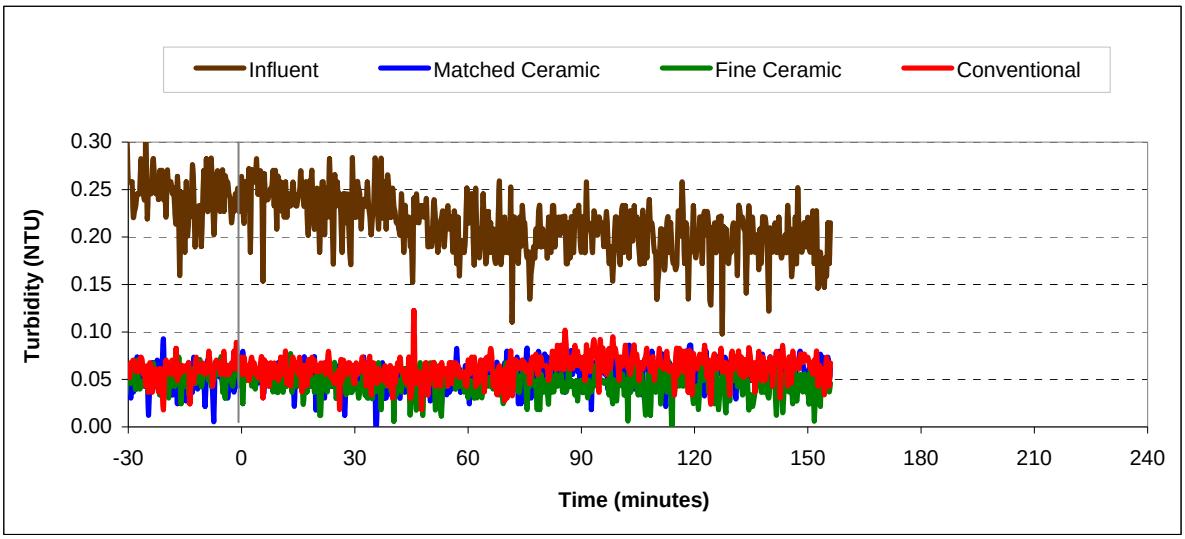

Turbidity Box and Whisker Plots

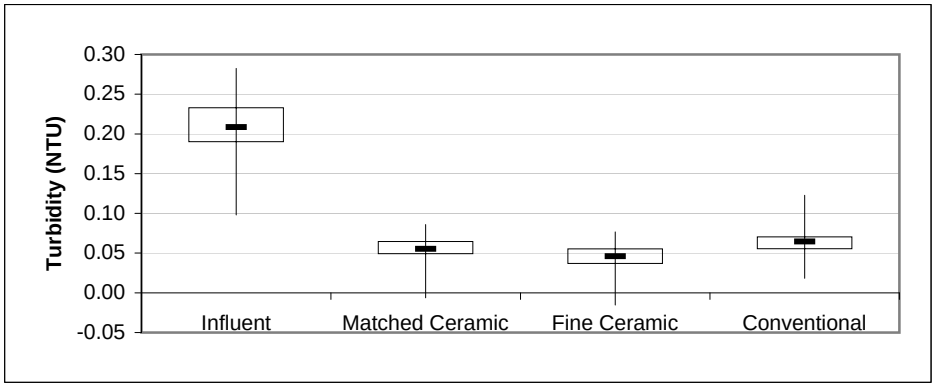

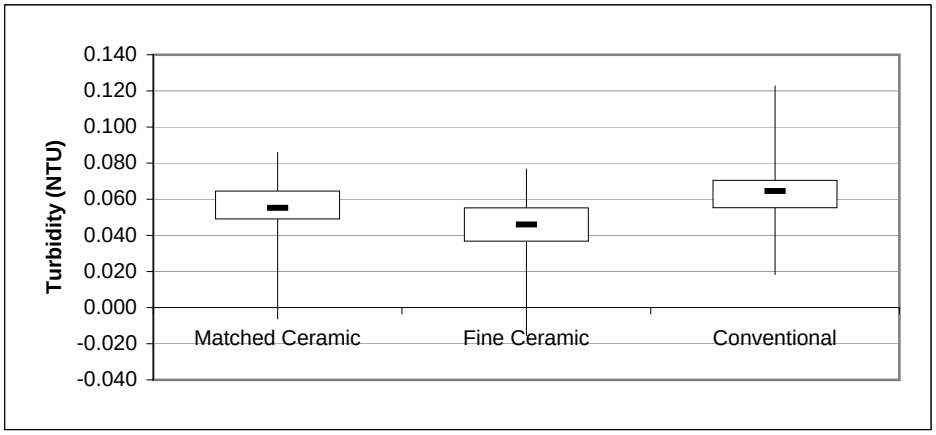

Vertical lines represent maximum and minimum turbidity range. Top and bottom of boxes represent 75th and 25th percentiles of turbidity data. Centre dash represents median turbidity measurement during seeding study.

Particle Count Summary: Trial 3B

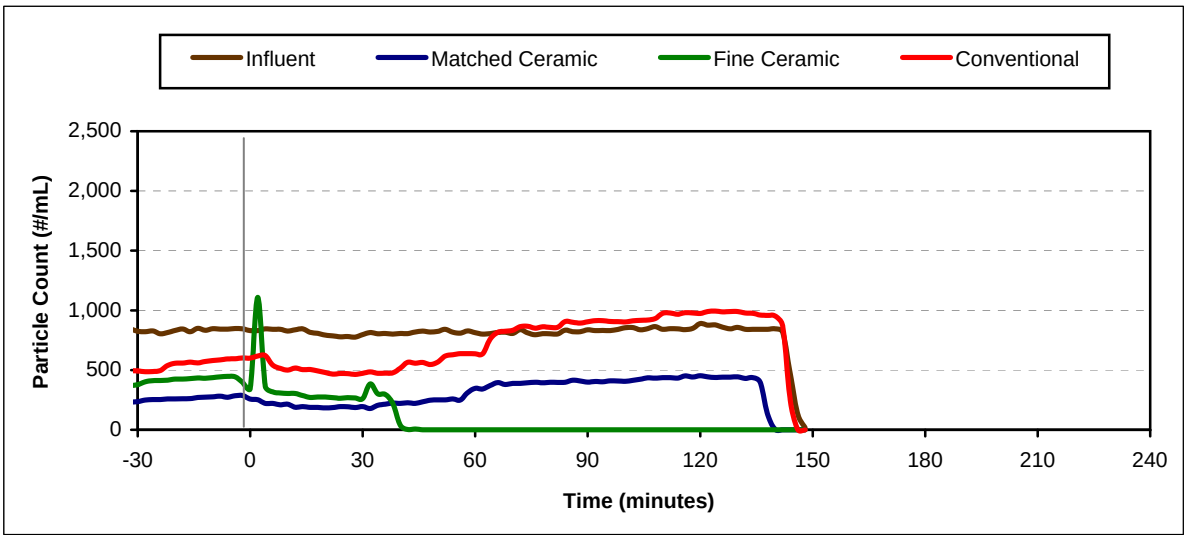

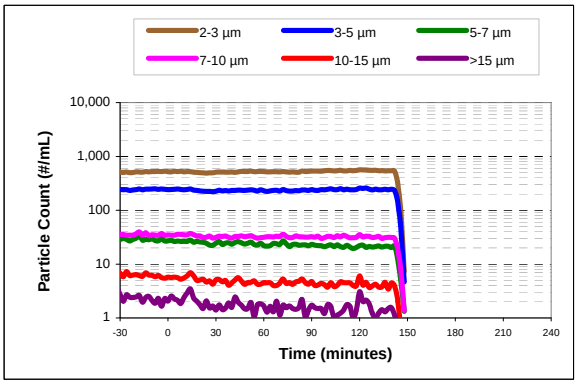

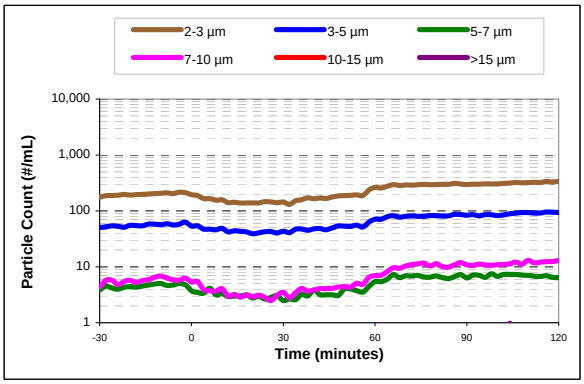

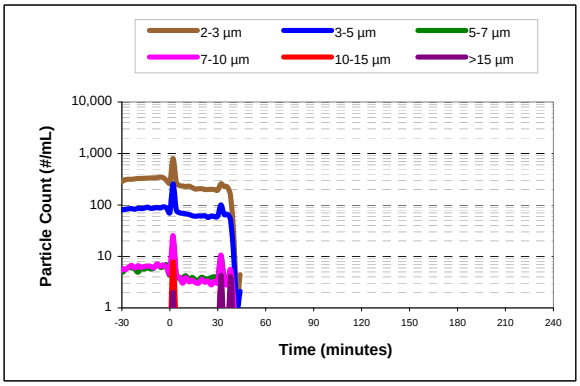

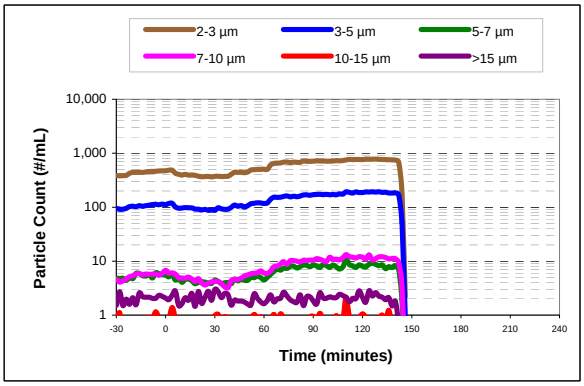

Flow and Headloss Summary: Trial 3B

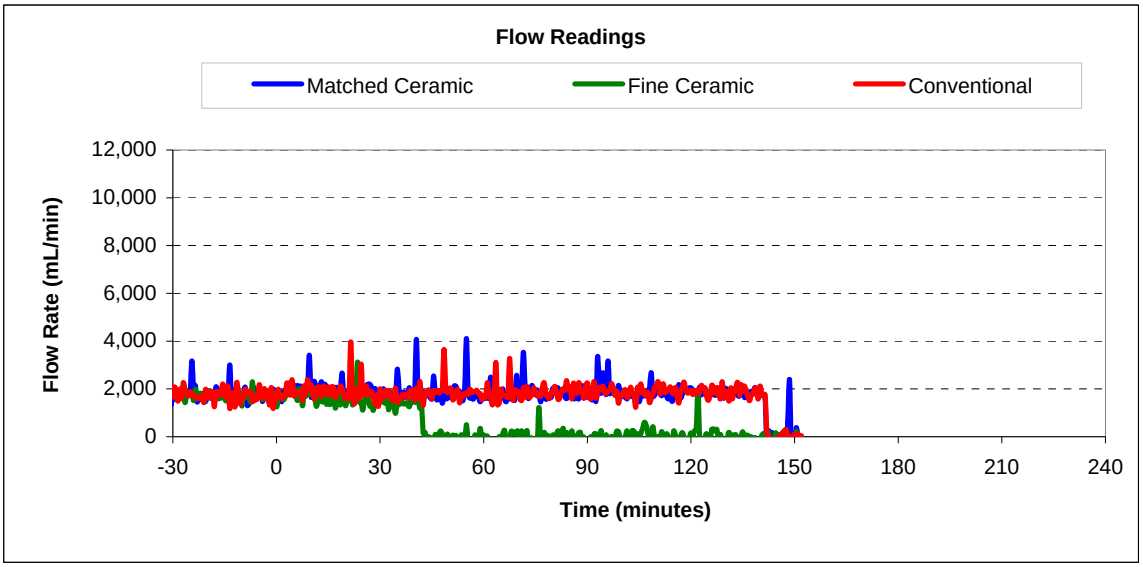

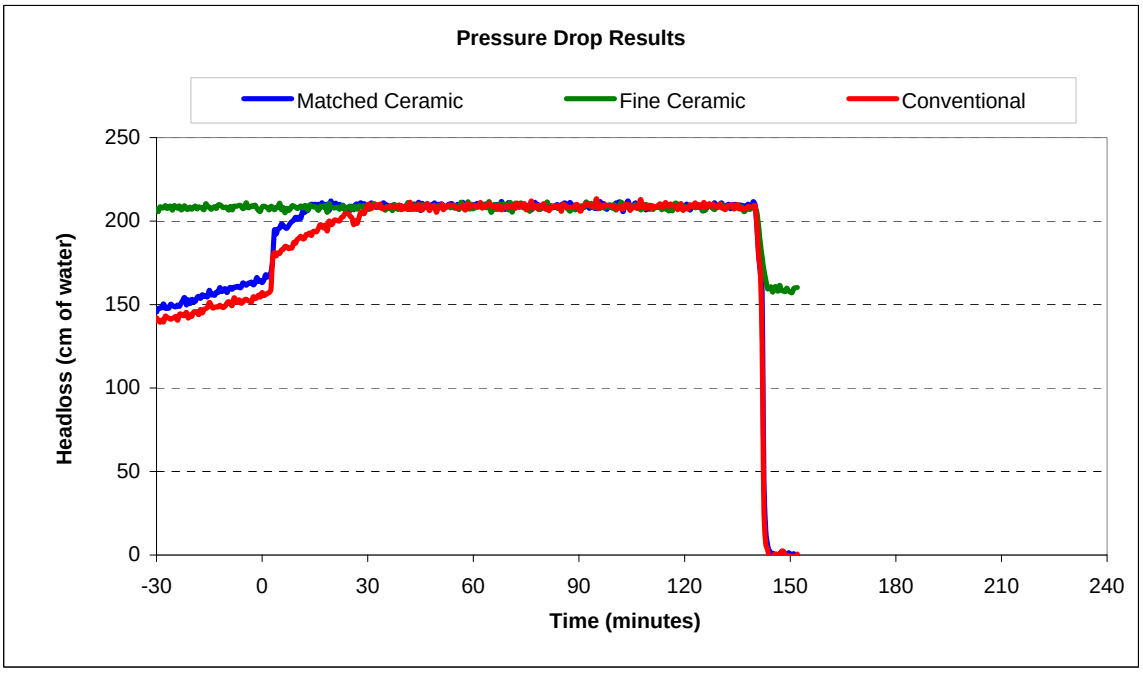

Summary Information for: Trial 3C

Trial Conditions:	
Trial Date	March 28, 2007
Location	Horgan WTP
Water Source	Lake Ontario
Loading Rate	10 GPM/ft^2 (24.4 m/hr)
Coagulation	PACl, 0.6 mg/L
Water Temperature	5.5^{0}C

Filter Media Configuration:

	Column 1	**Column 2**	**Column 3**
	Matched Ceramic	Fine Ceramic	Conventional
Top Layer	45 cm ceramic, ES 0.89 mm	45 cm ceramic, ES 0.96 mm	45 cm anthracite, ES 0.89 mm
Bottom Layer	30 cm ceramic, ES 0.47 mm	15 cm ceramic, ES 0.21mm	30 cm sand, ES 0.47 mm
Support Media	20 cm graded gravel bed	20 cm graded gravel bed	20 cm graded gravel bed

Parameter:	**Influent**	**Matched Ceramic**	**Fine Ceramic**	**Conventional**
Log reductions:				
Cryptosporidium		na	na	na
Microspheres		0.47	0.90	0.67
Other Parameters[1]:				
Average turbidity (NTU)	0.204	0.141	0.118	0.152
Turbidity reduction (%)		31	42	26
Average total particle count (#/mL)	1692	1519	1817	1950
Particle reduction (%)		10	-7	-15
Average flow (mL/min)		2020	1755	1991
Clean bed headloss		124	228	131
Average headloss (cm)		147	328	146
Change in headloss (cm)		41	200	48

[1] *Data calculated from time 0 (start of spike injection) to 360 elapsed minutes*

***Cryptosporidium* and Microsphere Removal Summary:** **Trial 3C**

***Cryptosporidium* Log Removal**

Time	Col 1	Col 2	Col 3
10 min			
20 min	0.00	0.00	0.00
30 min	0.00	0.00	0.00
40 min	0.00	0.00	0.00
50 min	0.00	0.00	0.00
60 min			
70 min			
Avg.[1]	**0.00**	**0.00**	**0.00**

[1]*Avgerage denotes time interval from 20 min to 60 min*

Microsphere Log Removal

Time	Col 1	Col 2	Col 3
10 min	0.37	1.07	0.93
20 min	0.16	0.65	0.70
30 min	0.65	0.91	0.53
40 min	0.32	0.97	0.77
50 min	0.60	1.04	0.68
60 min	-3.24	-3.75	-2.34
70 min	-1.73	-0.21	-1.83
Avg.[1]	**0.47**	**0.90**	**0.67**

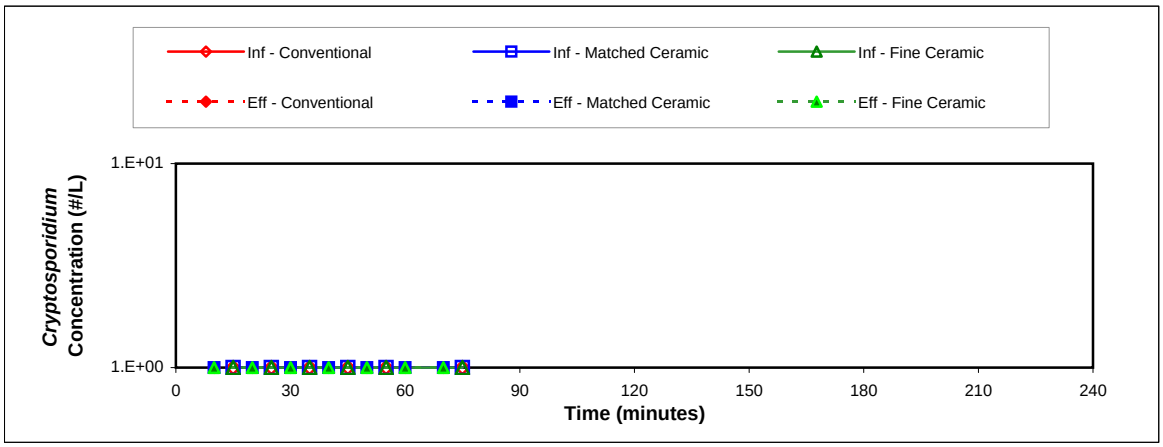

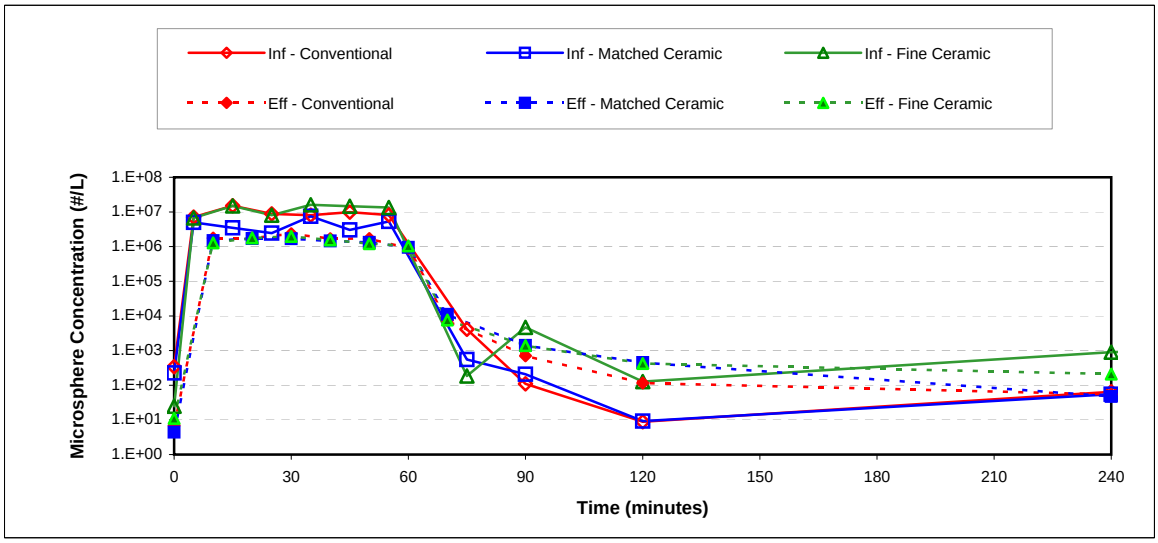

Turbidity Summary: Trial 3C

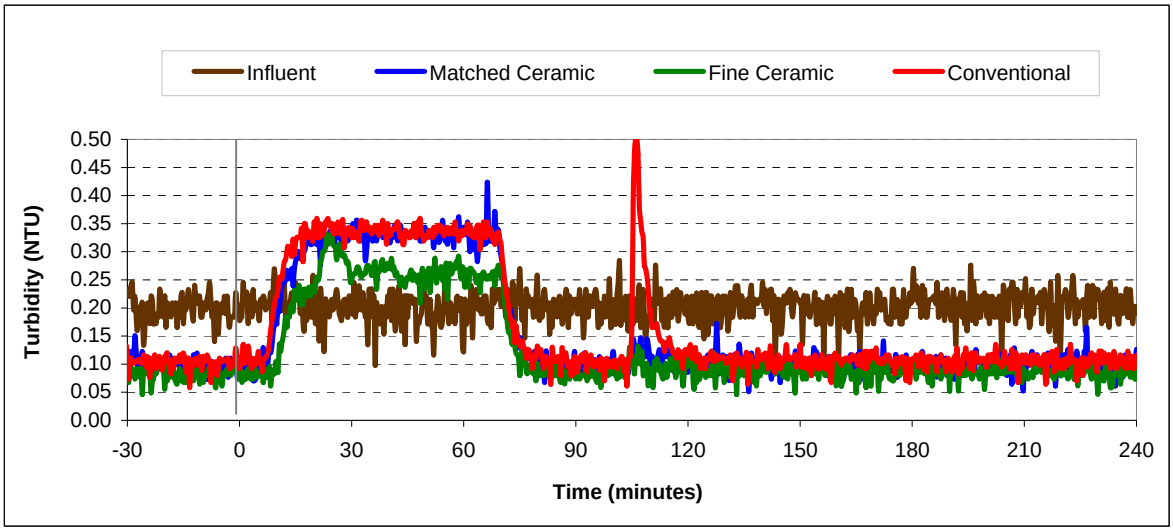

Turbidity Box and Whisker Plots

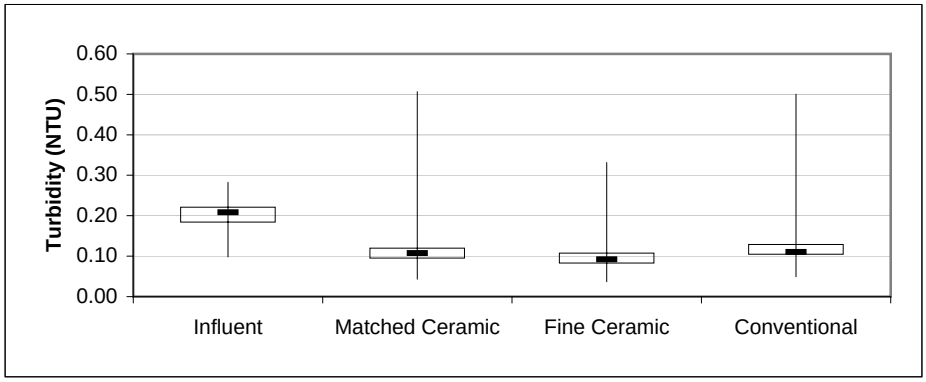

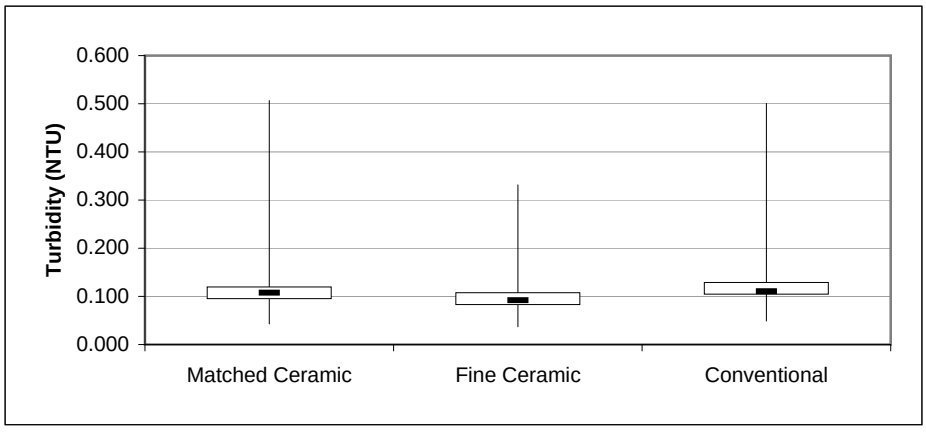

Vertical lines represent maximum and minimum turbidity range. Top and bottom of boxes represent 75th and 25th percentiles of turbidity data. Centre dash represents median turbidity measurement during seeding study.

Particle Count Summary: **Trial 3C**

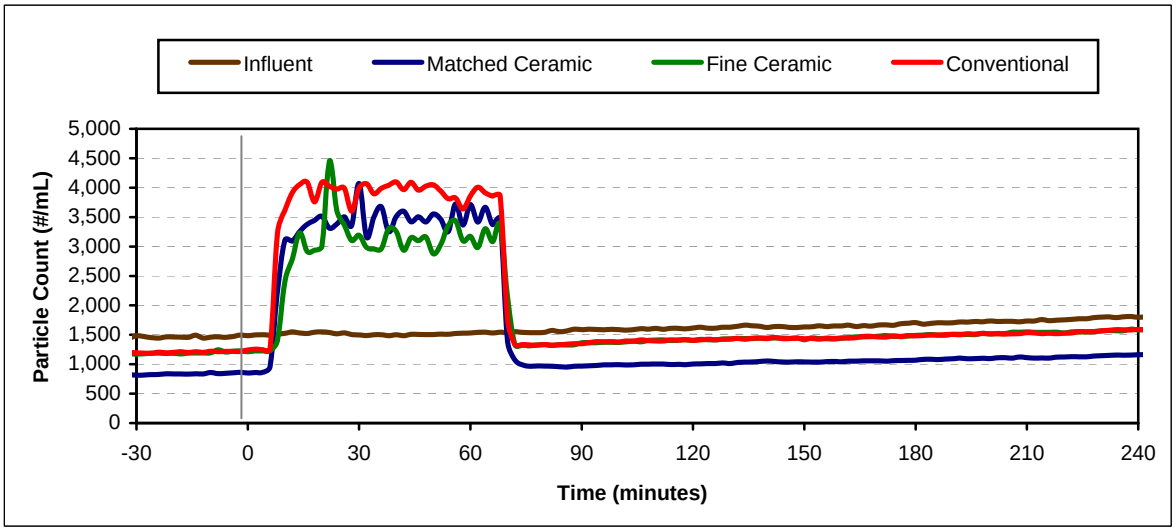

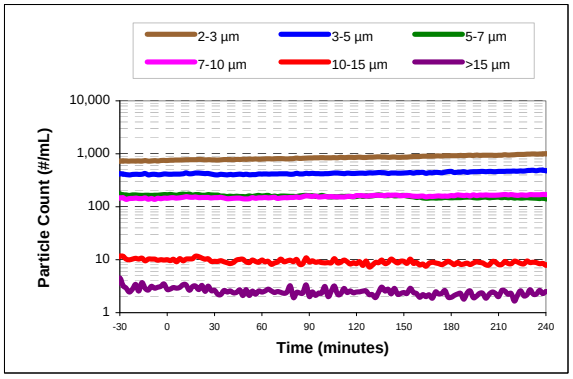

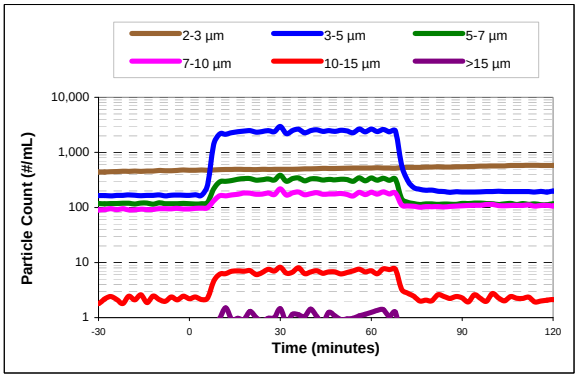

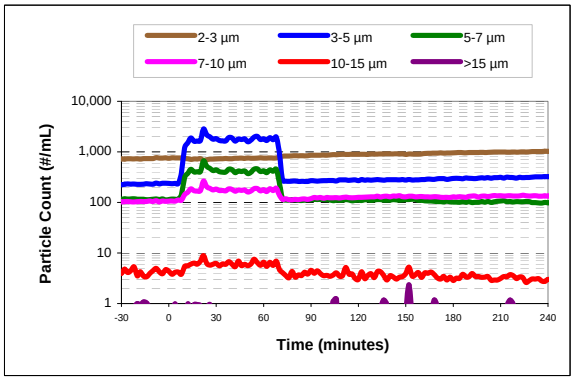

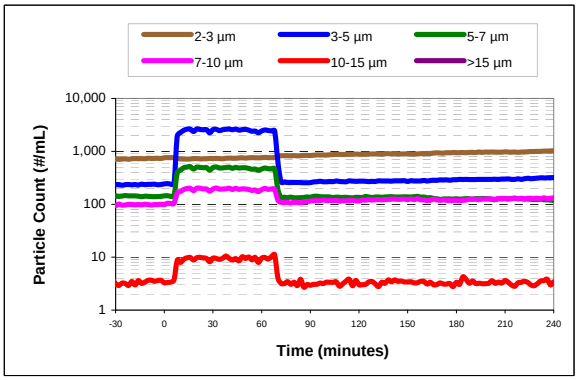

Flow and Headloss Summary: Trial 3C

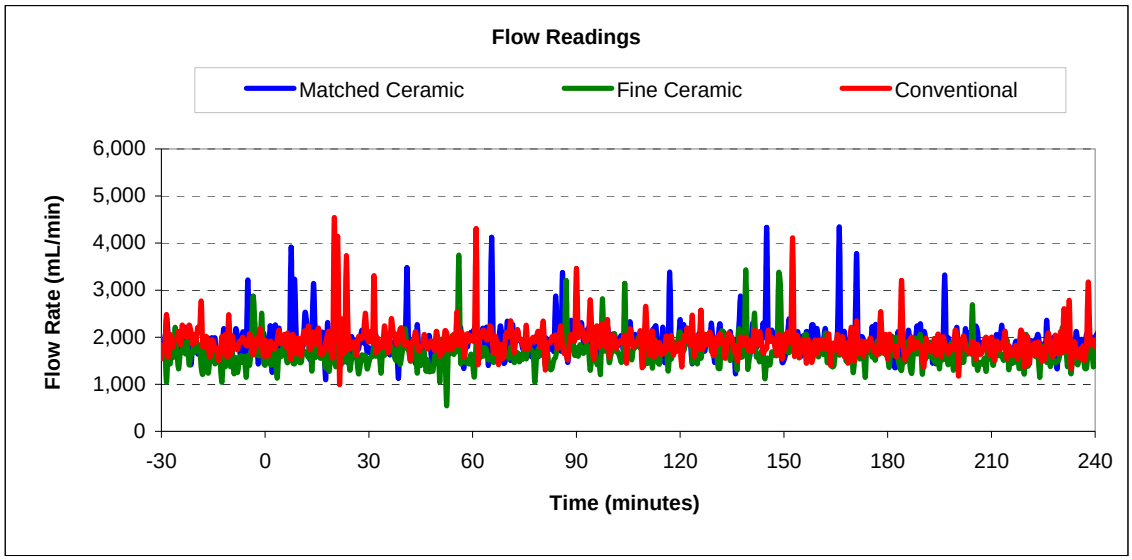

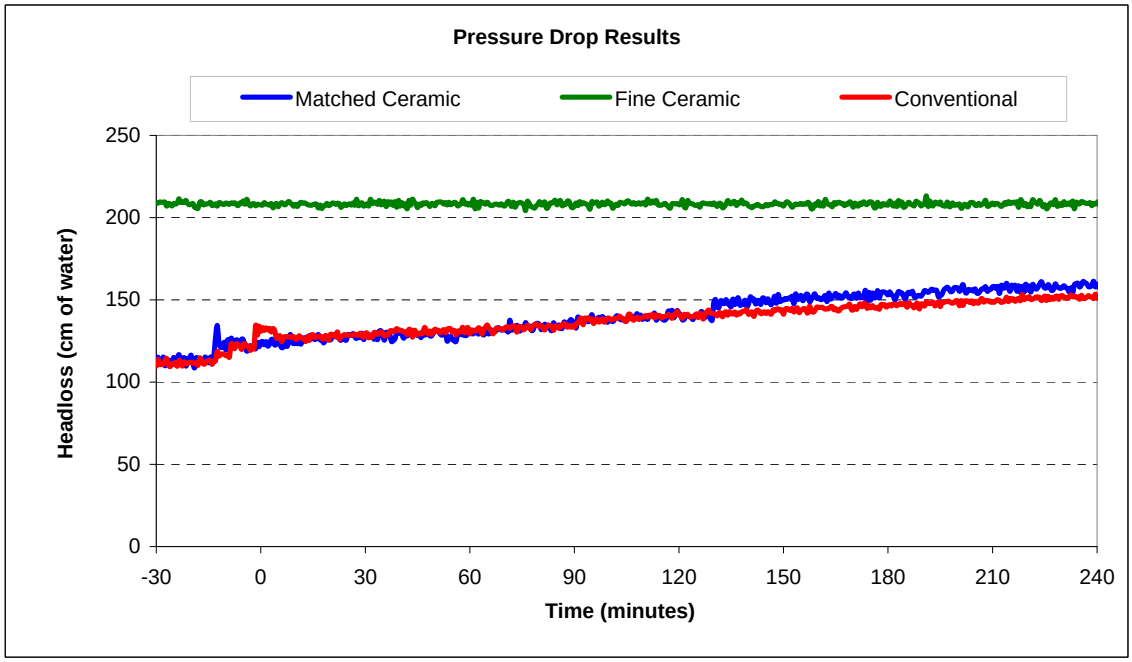

Summary Information for: Trial 3D

Trial Conditions:	
Trial Date	April 2, 2007
Location	Horgan WTP
Water Source	Lake Ontario
Loading Rate	4 GPM/ft^2 (9.8 m/hr)
Coagulation	PACl, 0.6 mg/L
Water Temperature	5.5^{0}C

Filter Media Configuration:

	Column 1	**Column 2**	**Column 3**
	Matched Ceramic	Fine Ceramic	Conventional
Top Layer	45 cm ceramic, ES 0.89 mm	45 cm ceramic, ES 0.96 mm	45 cm anthracite, ES 0.89 mm
Bottom Layer	30 cm ceramic, ES 0.47 mm	15 cm ceramic, ES 0.21mm	30 cm sand, ES 0.47 mm
Support Media	20 cm graded gravel bed	20 cm graded gravel bed	20 cm graded gravel bed

Parameter:	**Influent**	**Matched Ceramic**	**Fine Ceramic**	**Conventional**
Log reductions:				
Cryptosporidium		2.14	2.00	2.12
Microspheres		2.36	1.64	1.99
Other Parameters[1]:				
Average turbidity (NTU)	0.172	0.104	0.108	0.114
Turbidity reduction (%)		40	37	34
Average total particle count (#/mL)	1872	1447	1795	1851
Particle reduction (%)		23	4	1
Average flow (mL/min)		951	874	1006
Clean bed headloss		62	130	51
Average headloss (cm)		61	138	59
Change in headloss (cm)		3	19	16

[1] *Data calculated from time 0 (start of spike injection) to 360 elapsed minutes*

***Cryptosporidium* and Microsphere Removal Summary:** **Trial 3D**

***Cryptosporidium* Log Removal**

Time	Col 1	Col 2	Col 3
10 min			
20 min	1.89	1.90	1.97
30 min	2.34	2.18	2.33
40 min	2.28	1.96	1.97
50 min	1.93	1.98	2.14
60 min			
70 min			
Avg.[1]	**2.14**	**2.00**	**2.12**

[1]*Avgerage denotes time interval from 20 min to 60 min*

Microsphere Log Removal

Time	Col 1	Col 2	Col 3
10 min	2.35	3.04	1.99
20 min	1.96	2.44	1.81
30 min	2.39	0.46	1.88
40 min	2.64	2.98	2.24
50 min	2.20	2.24	2.13
60 min	1.91	2.47	0.38
70 min	1.00	1.56	1.12
Avg.[1]	**2.36**	**1.64**	**1.99**

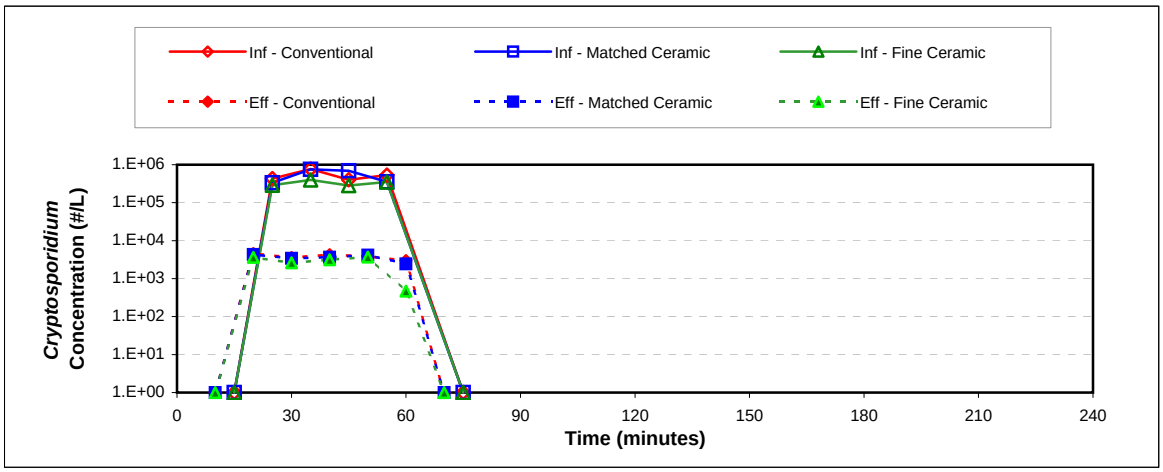

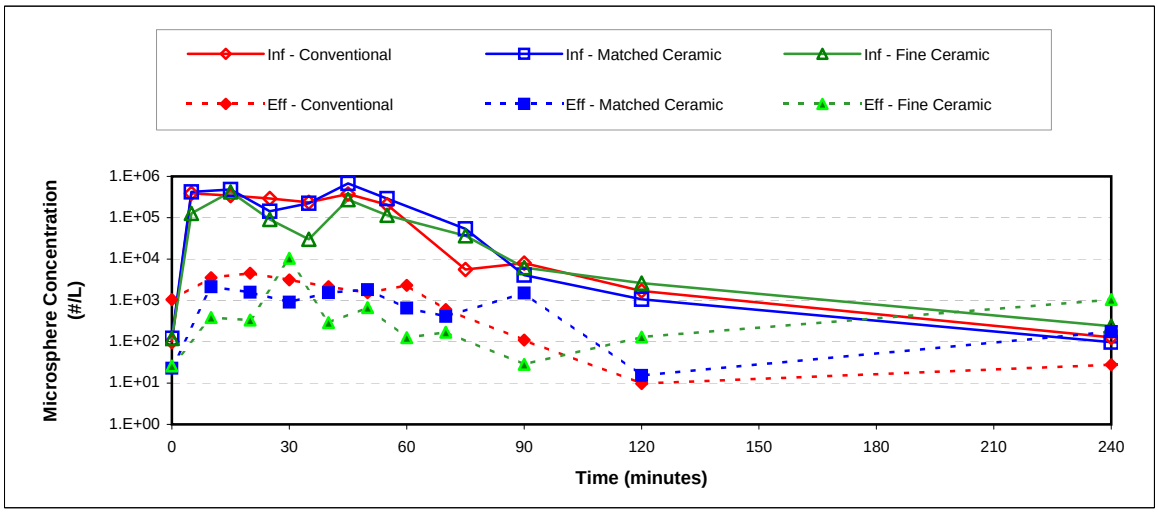

Turbidity Summary: Trial 3D

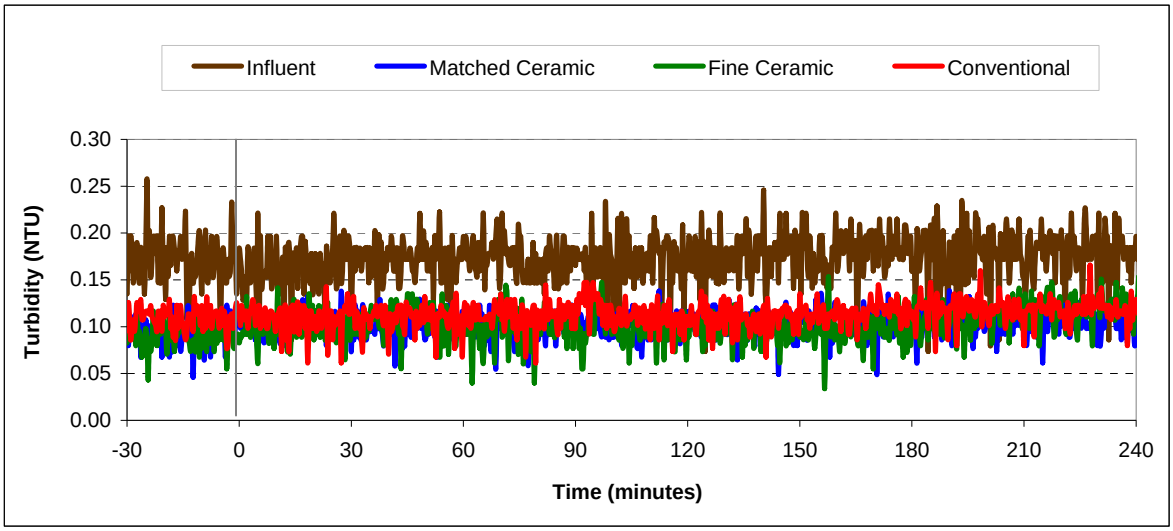

Turbidity Box and Whisker Plots

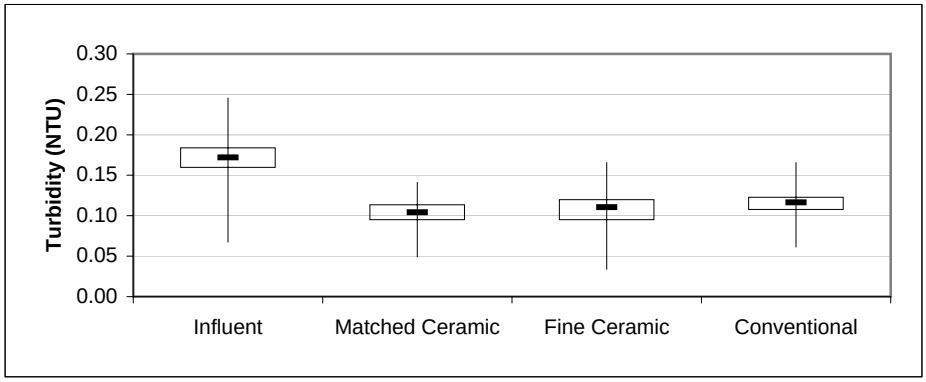

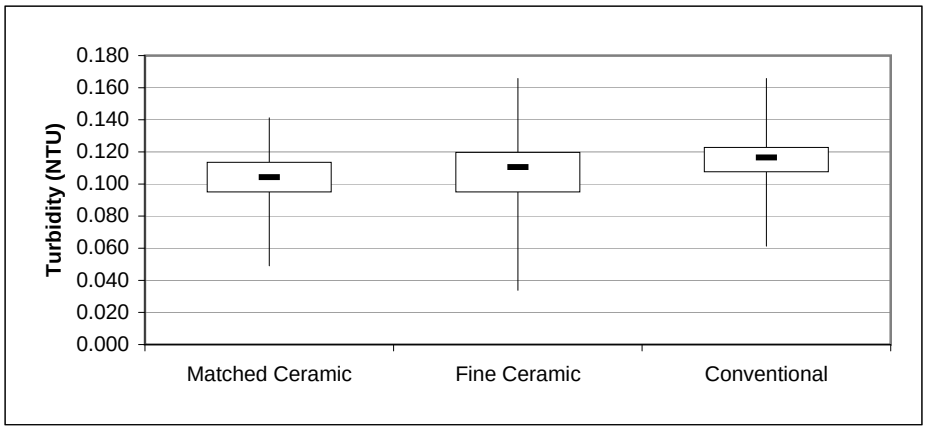

Vertical lines represent maximum and minimum turbidity range. Top and bottom of boxes represent 75th and 25th percentiles of turbidity data. Centre dash represents median turbidity measurement during seeding study.

Particle Count Summary: **Trial 3D**

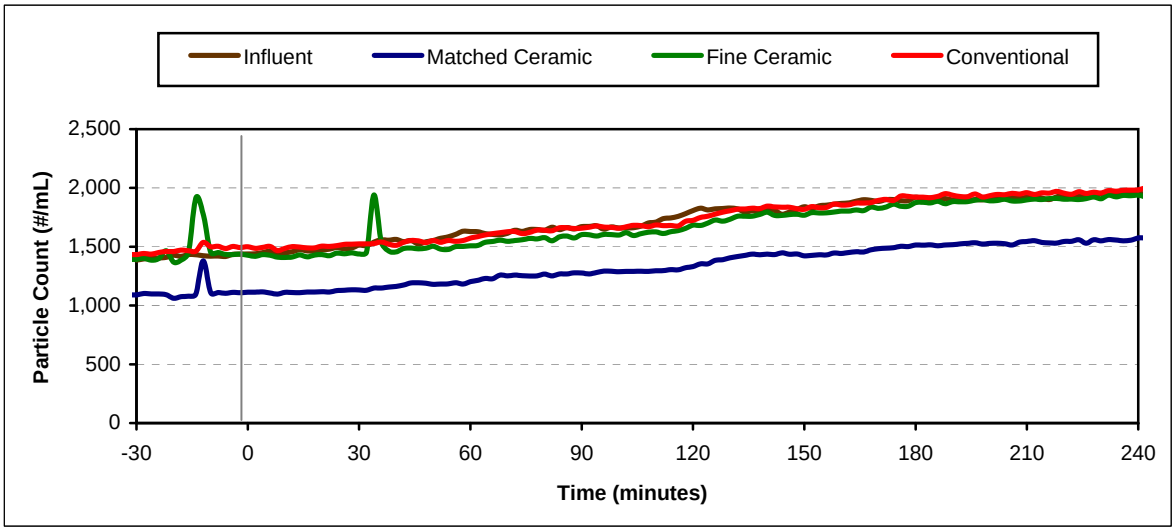

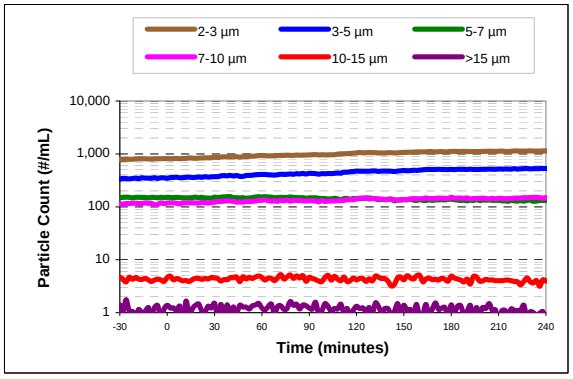

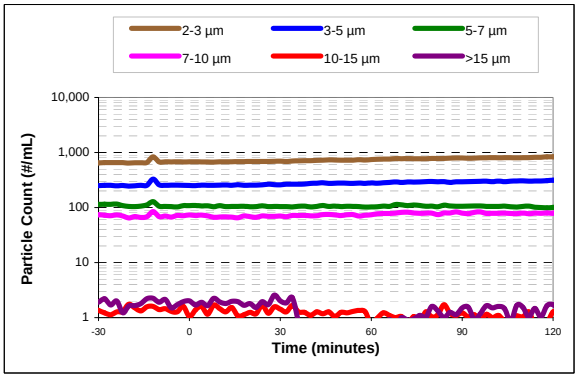

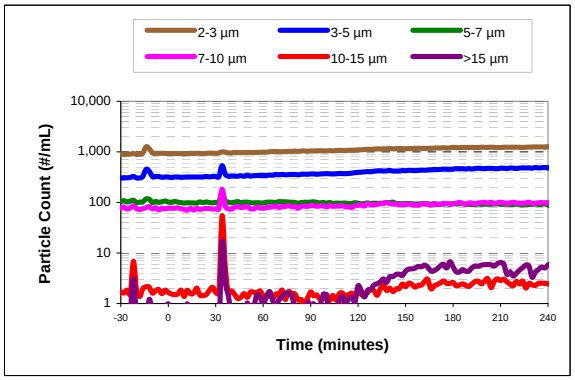

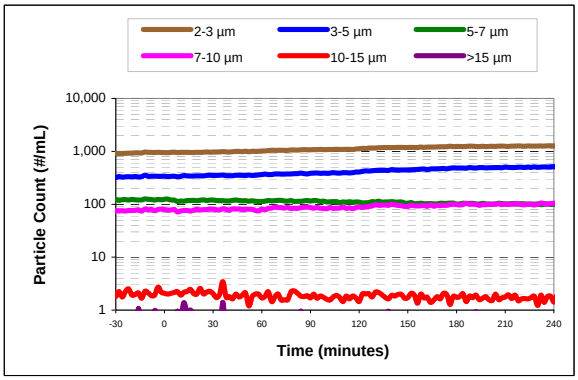

Flow and Headloss Summary: Trial 3D

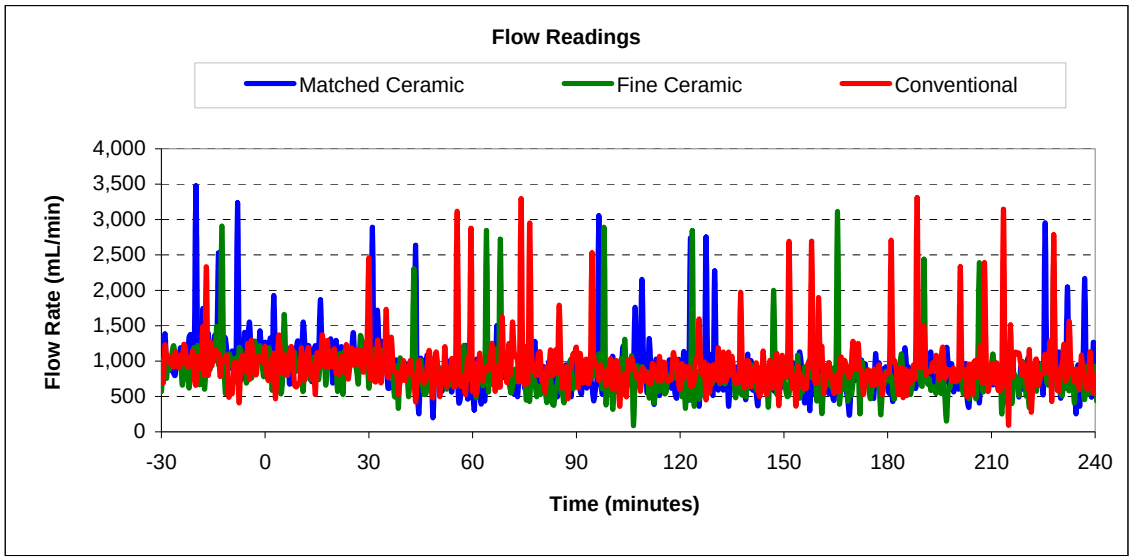

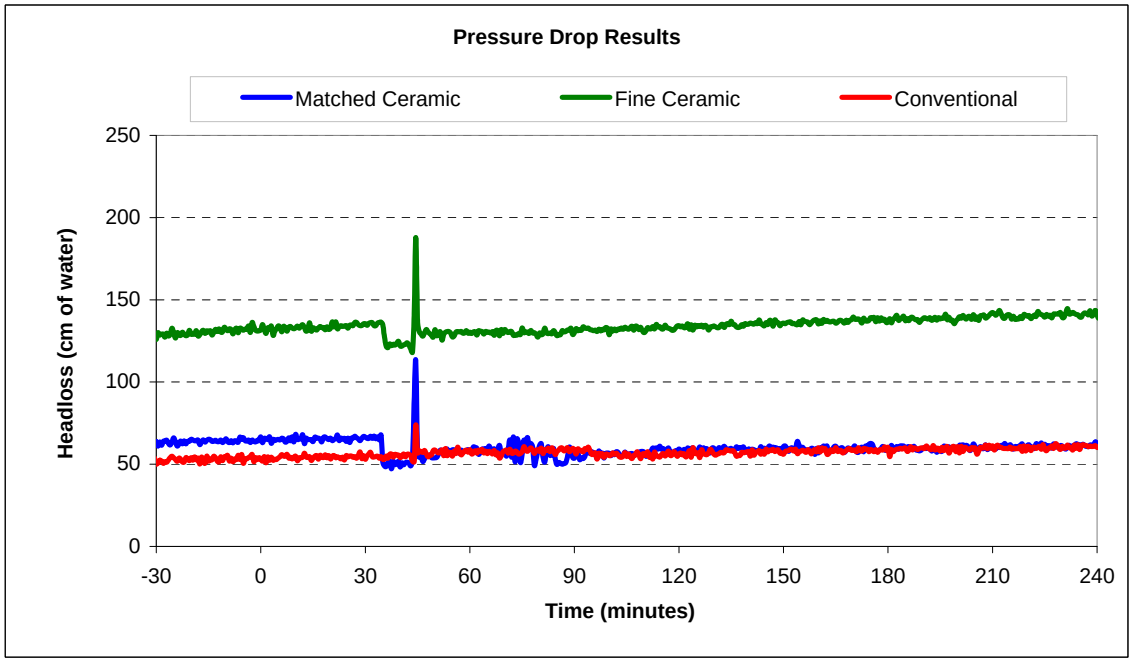

Summary Information for: Trial 3E

Trial Conditions:	
Trial Date	April 6, 2007
Location	Horgan WTP
Water Source	Lake Ontario
Loading Rate	4 GPM/ft2 (9.8 m/hr)
Coagulation	PACl, 0.6 mg/L
Water Temperature	6.5^0C

Filter Media Configuration:

	Column 1	**Column 2**	**Column 3**
	Matched Ceramic	Fine Ceramic	Conventional
Top Layer	45 cm ceramic, ES 0.89 mm	45 cm ceramic, ES 0.96 mm	45 cm anthracite, ES 0.89 mm
Bottom Layer	30 cm ceramic, ES 0.47 mm	15 cm ceramic, ES 0.21mm	30 cm sand, ES 0.47 mm
Support Media	20 cm graded gravel bed	20 cm graded gravel bed	20 cm graded gravel bed

Parameter:	**Influent**	**Matched Ceramic**	**Fine Ceramic**	**Conventional**
Log reductions:				
Cryptosporidium		1.51	2.05	1.64
Microspheres		1.52	1.84	0.80
Other Parameters[1]:				
Average turbidity (NTU)	0.247	0.059	0.060	0.138
Turbidity reduction (%)		76	76	44
Average total particle count (#/mL)	1015	466	490	580
Particle reduction (%)		54	52	43
Average flow (mL/min)		823	747	799
Clean bed headloss		54	126	50
Average headloss (cm)		56	138	56
Change in headloss (cm)		8	24	15

[1] *Data calculated from time 0 (start of spike injection) to 360 elapsed minutes*

***Cryptosporidium* and Microsphere Removal Summary:** **Trial 3E**

***Cryptosporidium* Log Removal**

Time	Col 1	Col 2	Col 3
10 min			
20 min	1.83	2.02	1.76
30 min	2.05	2.04	1.81
40 min	1.79	1.99	1.63
50 min	1.09	2.16	1.51
60 min			
70 min			
Avg.[1]	**1.51**	**2.05**	**1.64**

[1]*Avgerage denotes time interval from 20 min to 60 min*

Microsphere Log Removal

Time	Col 1	Col 2	Col 3
10 min	1.54	1.97	1.41
20 min	1.34	1.84	1.14
30 min	1.42	1.97	0.87
40 min	1.74	1.76	0.77
50 min	1.53	1.71	0.49
60 min	0.76	0.61	-0.26
70 min	1.65	2.05	0.59
Avg.[1]	**1.52**	**1.84**	**0.80**

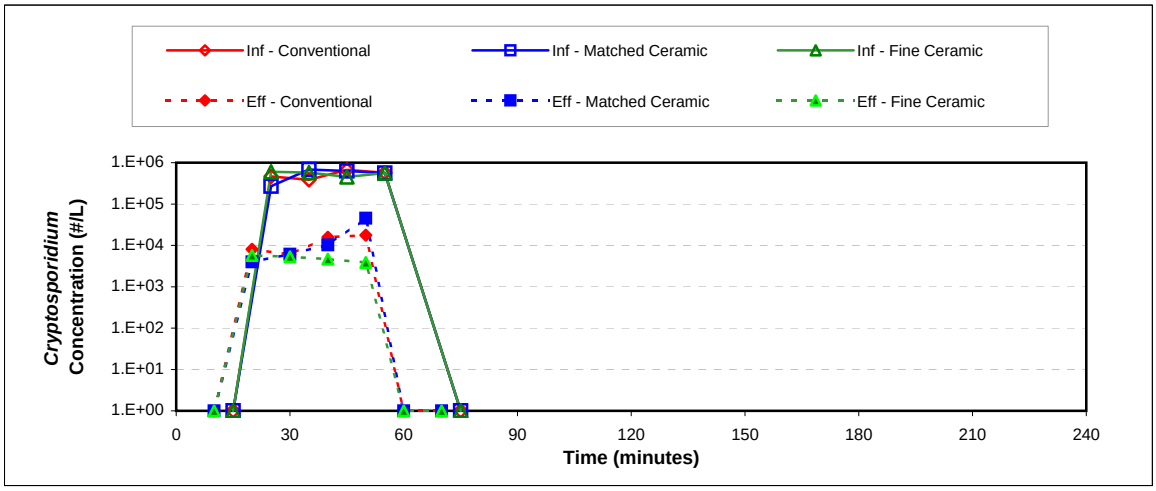

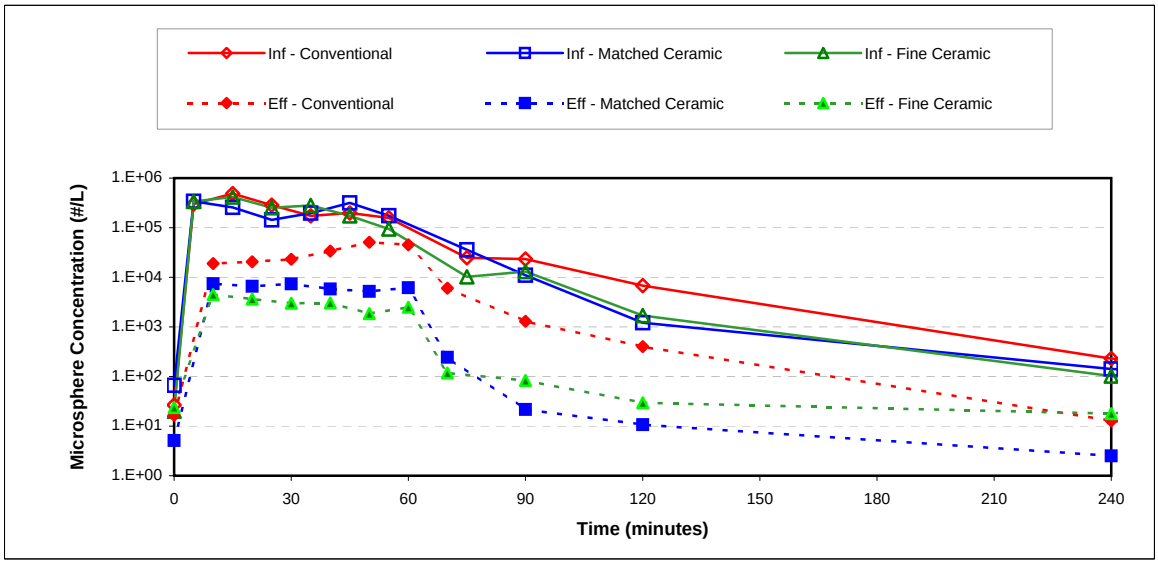

Turbidity Summary: Trial 3E

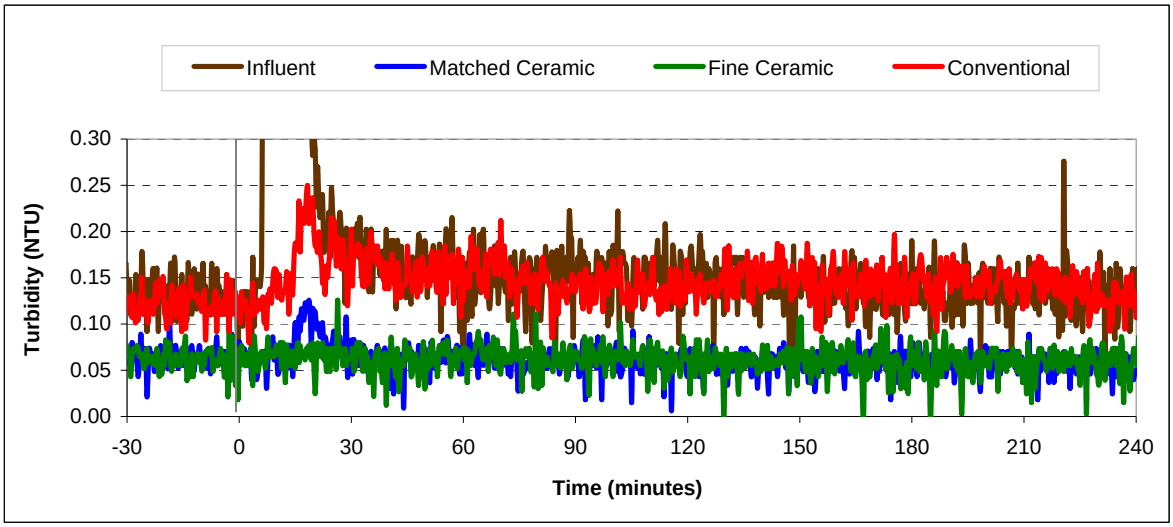

Turbidity Box and Whisker Plots

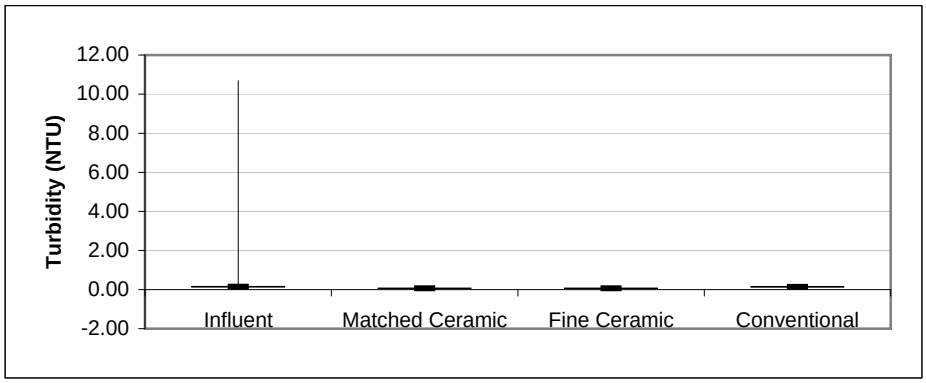

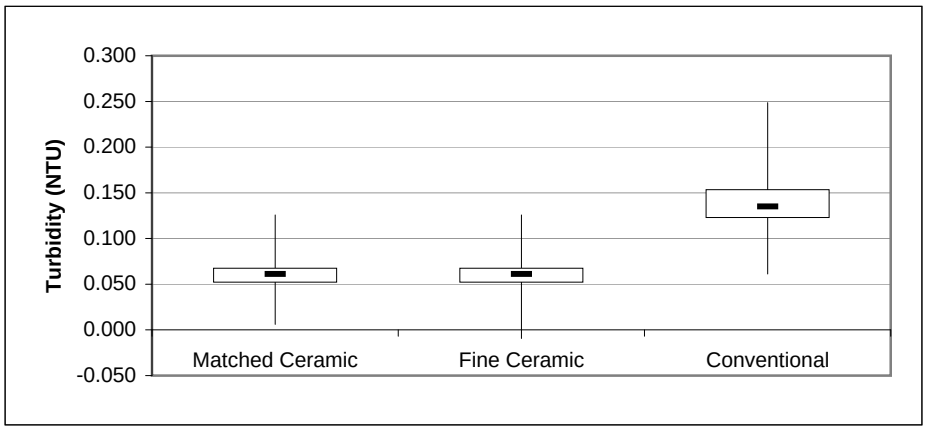

Vertical lines represent maximum and minimum turbidity range. Top and bottom of boxes represent 75th and 25th percentiles of turbidity data. Centre dash represents median turbidity measurement during seeding study.

Particle Count Summary: **Trial 3E**

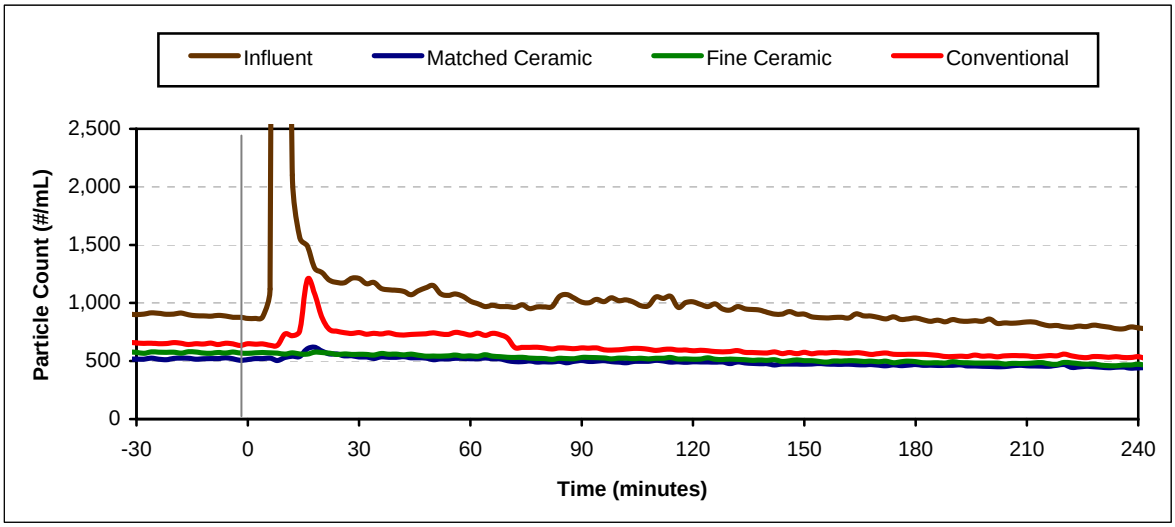

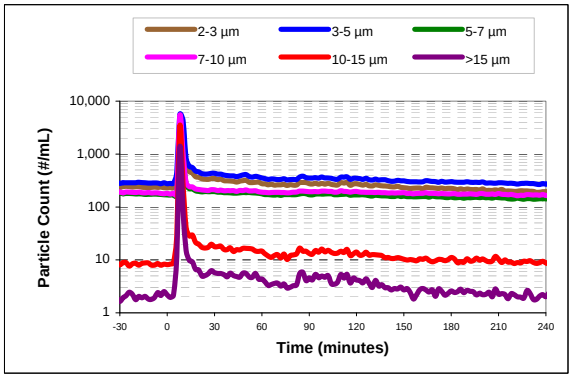

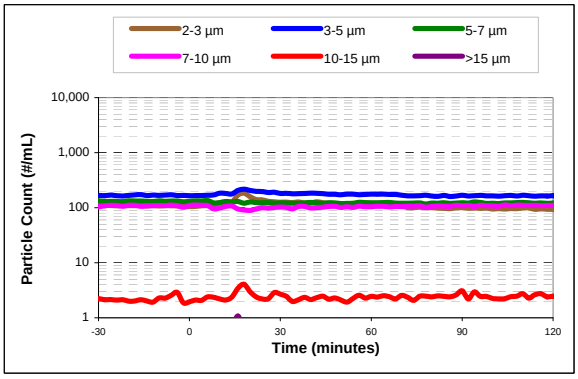

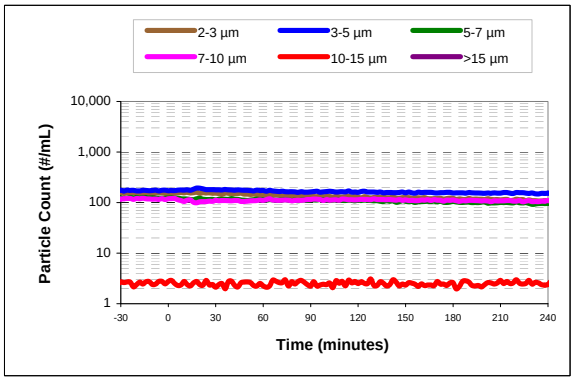

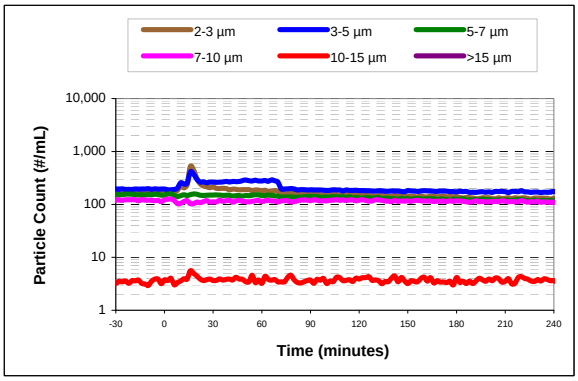

Flow and Headloss Summary: Trial 3E

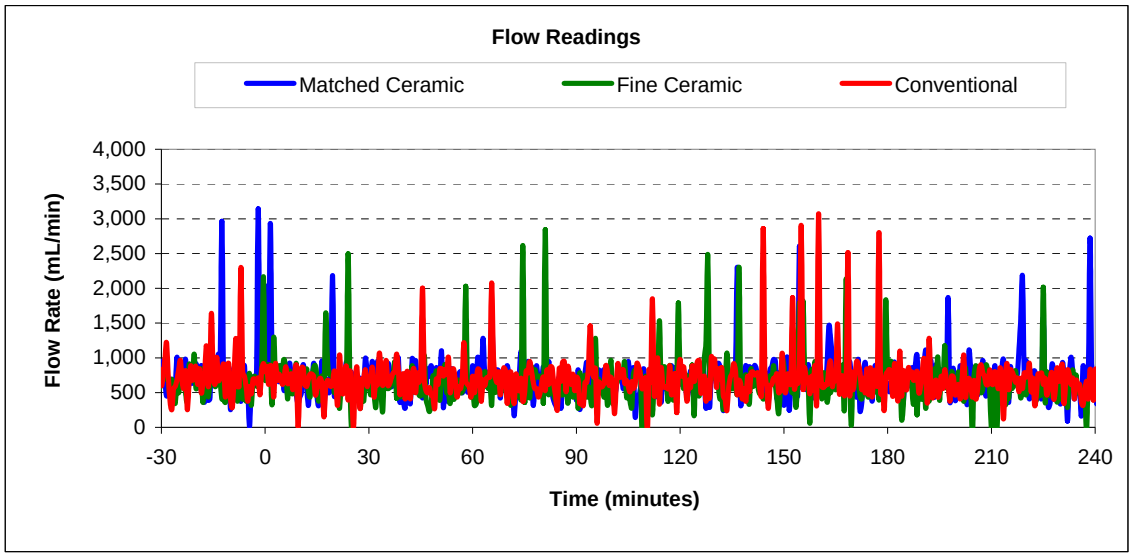

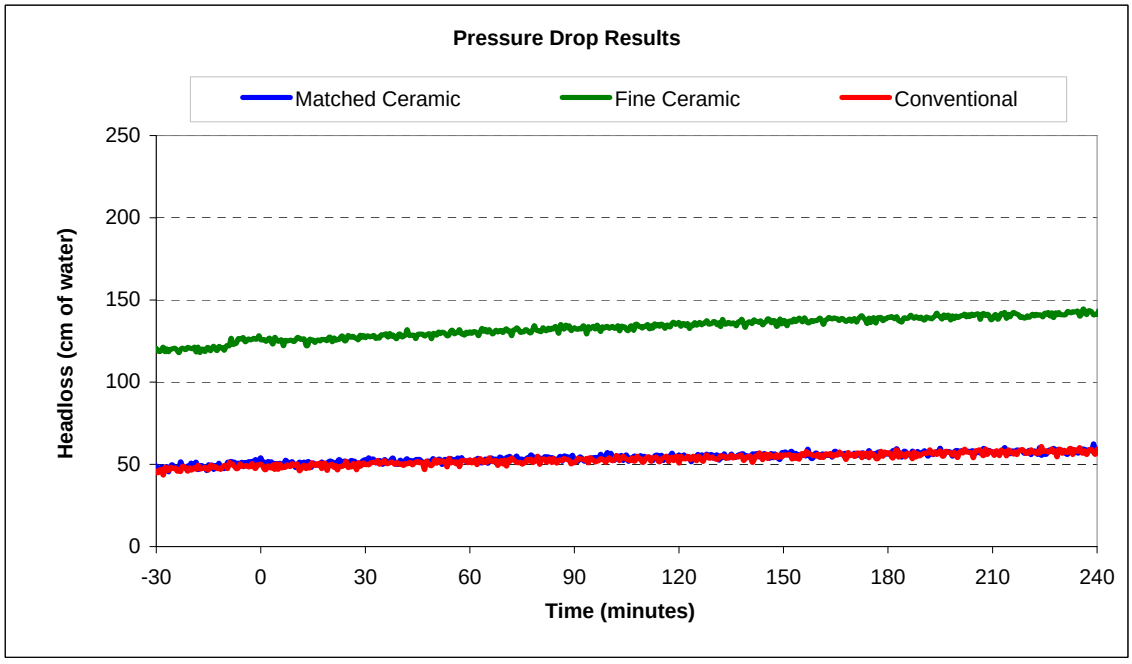

Summary Information for: Trial 3F

Trial Conditions:	
Trial Date	April 11, 2007
Location	Horgan WTP
Water Source	Lake Ontario
Loading Rate	10 GPM/ft^2 (24.4 m/hr)
Coagulation	PACl, 0.6 mg/L
Water Temperature	6.5^{0}C

Filter Media Configuration:

	Column 1	**Column 2**	**Column 3**
	Matched Ceramic	Fine Ceramic	Conventional
Top Layer	45 cm ceramic, ES 0.89 mm	45 cm ceramic, ES 0.96 mm	45 cm anthracite, ES 0.89 mm
Bottom Layer	30 cm ceramic, ES 0.47 mm	15 cm ceramic, ES 0.21mm	30 cm sand, ES 0.47 mm
Support Media	20 cm graded gravel bed	20 cm graded gravel bed	20 cm graded gravel bed

Parameter:	**Influent**	**Matched Ceramic**	**Fine Ceramic**	**Conventional**
Log reductions:				
Cryptosporidium		1.46	1.64	0.99
Microspheres		0.53	0.50	0.35
Other Parameters[1]:				
Average turbidity (NTU)	0.223	0.105	0.090	0.118
Turbidity reduction (%)		53	60	47
Average total particle count (#/mL)	1790	1267	1421	1346
Particle reduction (%)		29	21	25
Average flow (mL/min)		1973	1745	1947
Clean bed headloss		117	209	97
Average headloss (cm)		127	251	113
Change in headloss (cm)		24	108	30

[1] *Data calculated from time 0 (start of spike injection) to 360 elapsed minutes*

***Cryptosporidium* and Microsphere Removal Summary:** **Trial 3F**

***Cryptosporidium* Log Removal**

Time	Col 1	Col 2	Col 3
10 min			
20 min	1.61	1.82	1.42
30 min	1.40	1.71	0.79
40 min	1.36	1.52	0.80
50 min	1.48	1.59	1.06
60 min			
70 min			
Avg.[1]	**1.46**	**1.64**	**0.99**

[1]*Avgerage denotes time interval from 20 min to 60 min*

Microsphere Log Removal

Time	Col 1	Col 2	Col 3
10 min	0.19	0.39	-0.08
20 min	0.66	0.32	0.72
30 min	0.40	0.26	0.33
40 min	0.39	0.53	0.31
50 min	0.66	0.99	0.16
60 min	-2.72	-2.63	-2.47
70 min	0.24	0.27	0.03
Avg.[1]	**0.53**	**0.50**	**0.35**

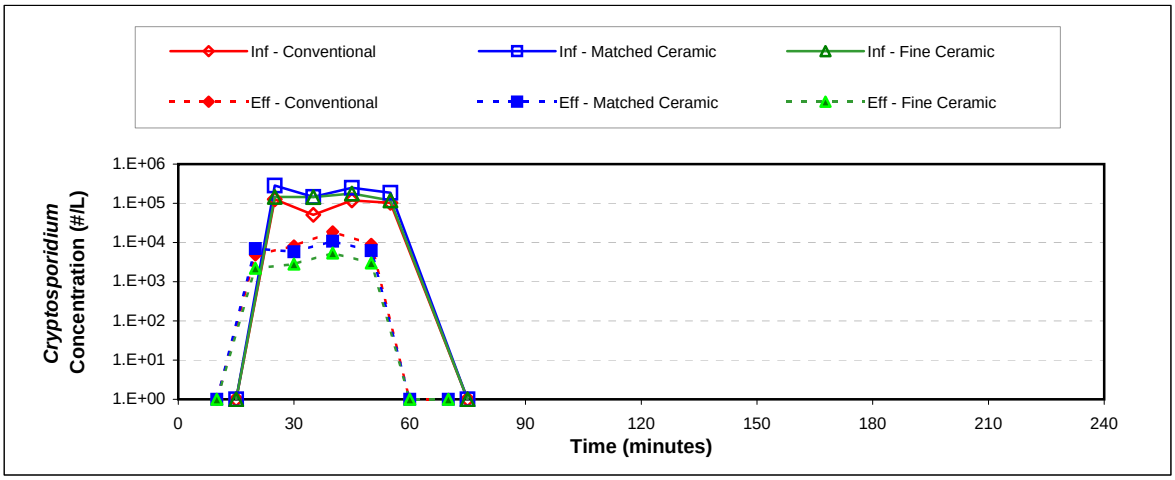

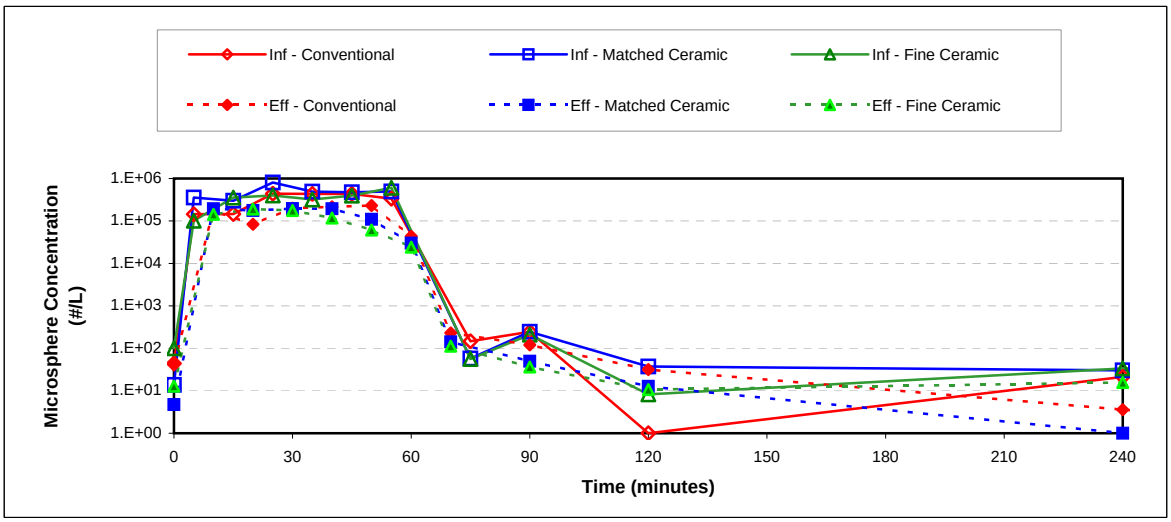

Turbidity Summary: Trial 3F

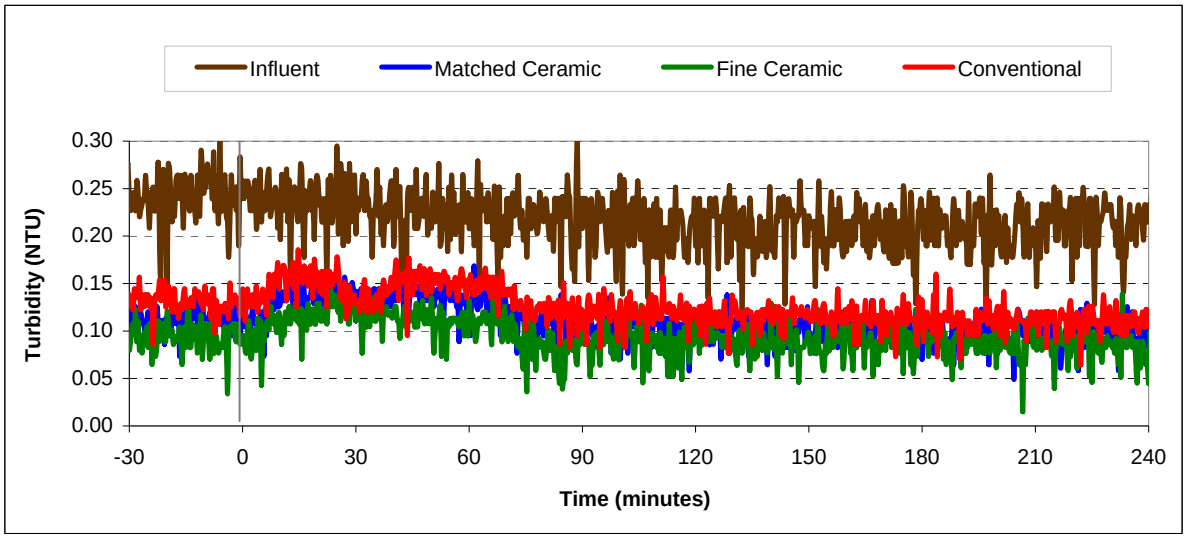

Turbidity Box and Whisker Plots

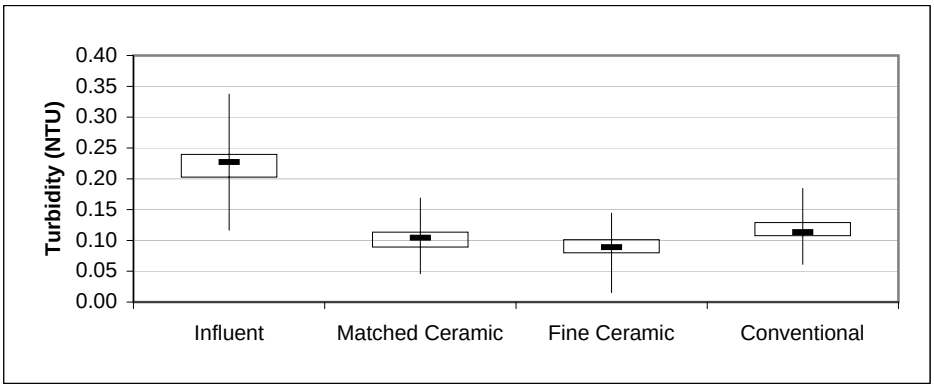

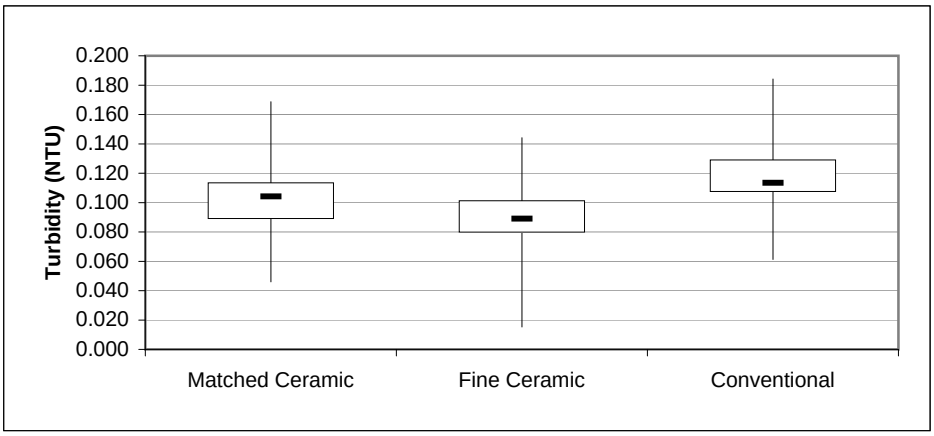

Vertical lines represent maximum and minimum turbidity range. Top and bottom of boxes represent 75th and 25th percentiles of turbidity data. Centre dash represents median turbidity measurement during seeding study.

Particle Count Summary: **Trial 3F**

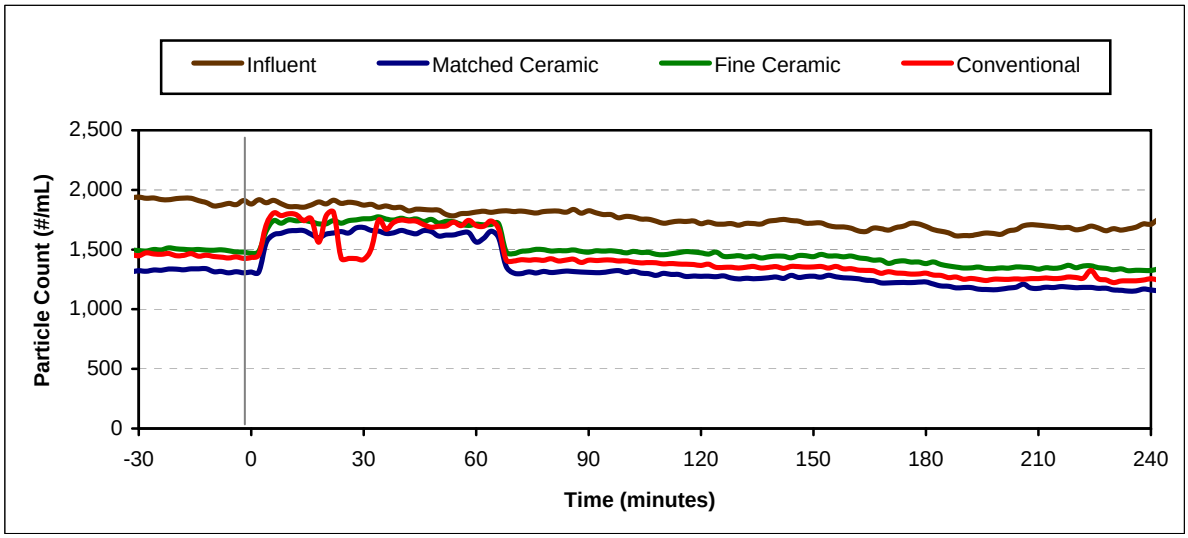

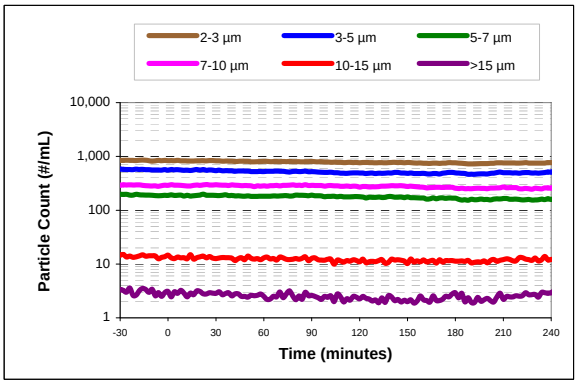

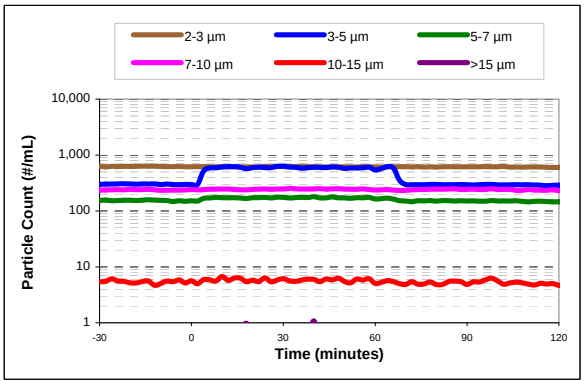

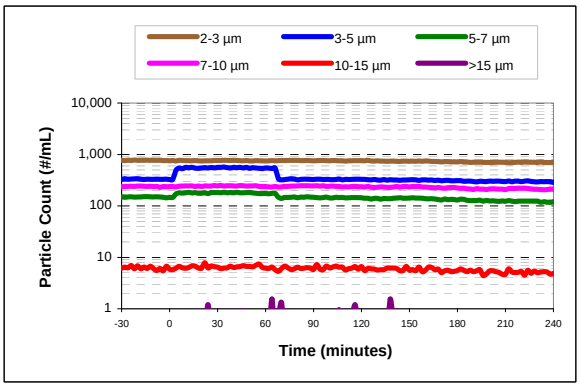

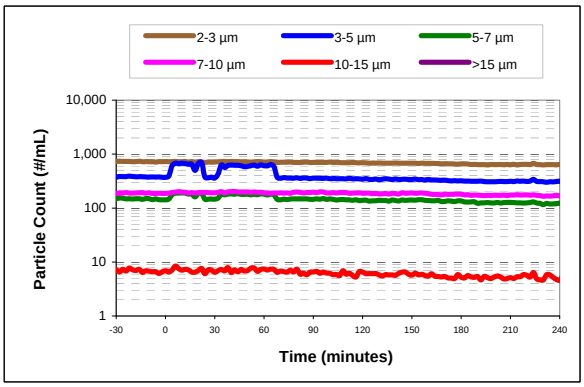

Flow and Headloss Summary: Trial 3F

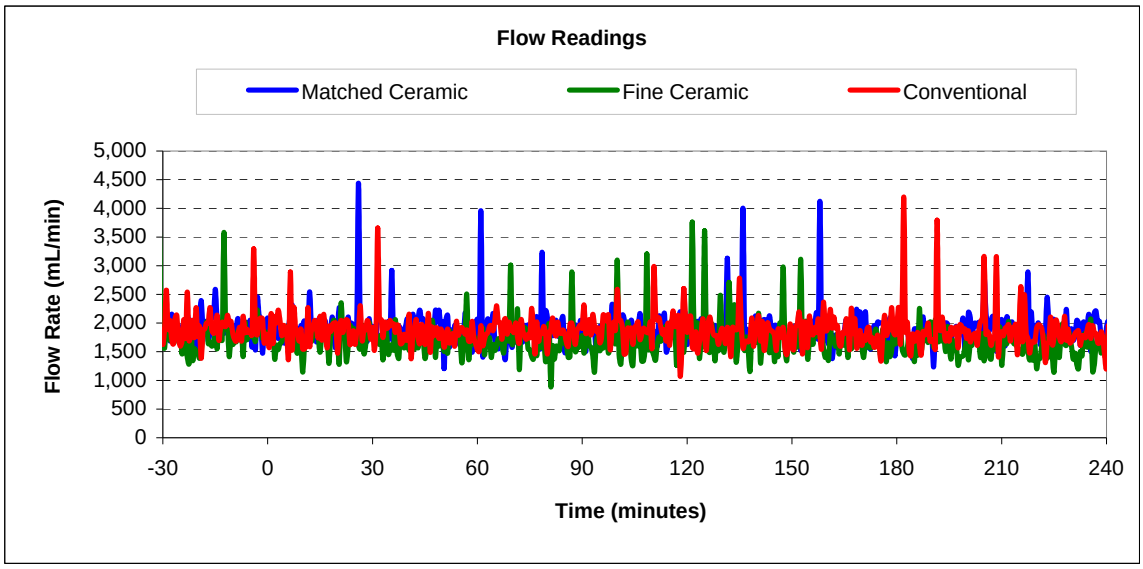

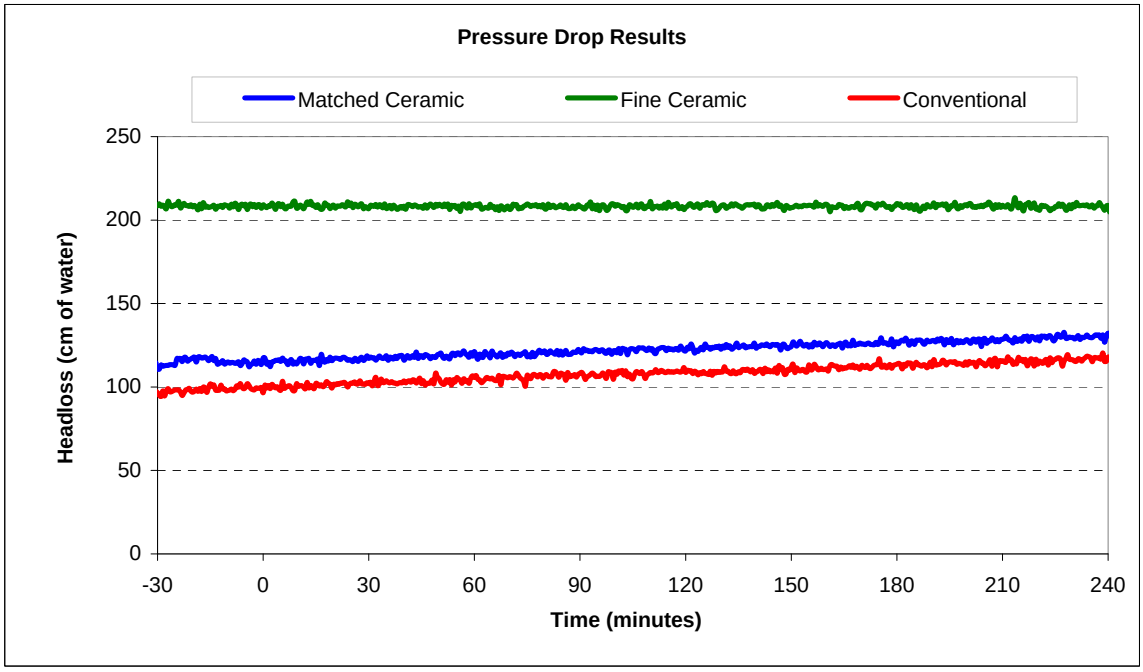

Summary Information for: Trial 3G

Trial Conditions:	
Trial Date	April 16, 2007
Location	Horgan WTP
Water Source	Lake Ontario
Loading Rate	4 GPM/ft^2 (9.8 m/hr)
Coagulation	PACl, 0.6 mg/L
Water Temperature	7^{0}C

Filter Media Configuration:

	Column 1	**Column 2**	**Column 3**
	Matched Ceramic	Fine Ceramic	Conventional
Top Layer	45 cm ceramic, ES 0.89 mm	45 cm ceramic, ES 0.96 mm	45 cm anthracite, ES 0.89 mm
Bottom Layer	30 cm ceramic, ES 0.47 mm	15 cm ceramic, ES 0.21mm	30 cm sand, ES 0.47 mm
Support Media	20 cm graded gravel bed	20 cm graded gravel bed	20 cm graded gravel bed

Parameter:	**Influent**	**Matched Ceramic**	**Fine Ceramic**	**Conventional**
Log reductions:				
Cryptosporidium		1.75	2.07	1.32
Microspheres		0.00	0.00	0.00
Other Parameters[1]:				
Average turbidity (NTU)	0.264	0.083	0.066	0.101
Turbidity reduction (%)		68	75	62
Average total particle count (#/mL)	1332	298	309	381
Particle reduction (%)		78	77	71
Average flow (mL/min)		947	903	931
Clean bed headloss		50	125	52
Average headloss (cm)		51	134	52
Change in headloss (cm)		4	16	1

[1] *Data calculated from time 0 (start of spike injection) to 360 elapsed minutes*

***Cryptosporidium* and Microsphere Removal Summary:** **Trial 3G**

***Cryptosporidium* Log Removal**

Time	Col 1	Col 2	Col 3
10 min			
20 min	1.82	2.20	1.67
30 min	1.48	2.17	1.30
40 min	1.86	2.01	1.12
50 min	1.38	2.01	1.11
60 min			
70 min			
Avg.[1]	**1.75**	**2.07**	**1.32**

[1]*Avgerage denotes time interval from 20 min to 60 min*

Microsphere Log Removal

Time	Col 1	Col 2	Col 3
10 min	0.00	0.00	0.00
20 min	0.00	0.00	0.00
30 min	0.00	0.00	0.00
40 min	0.00	0.00	0.00
50 min	0.00	0.00	0.00
60 min	0.00	0.00	0.00
70 min	0.00	0.00	0.00
Avg.[1]	**0.00**	**0.00**	**0.00**

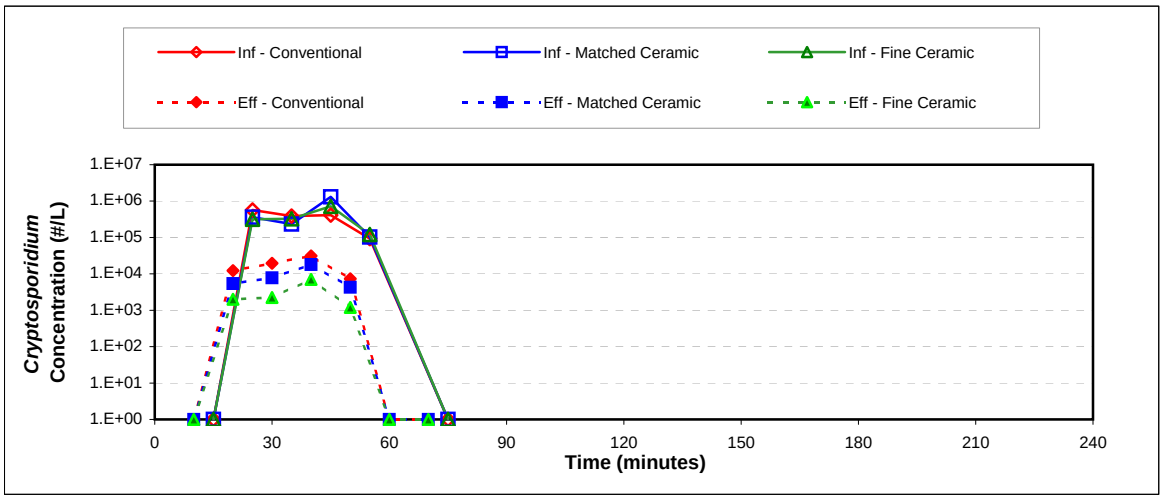

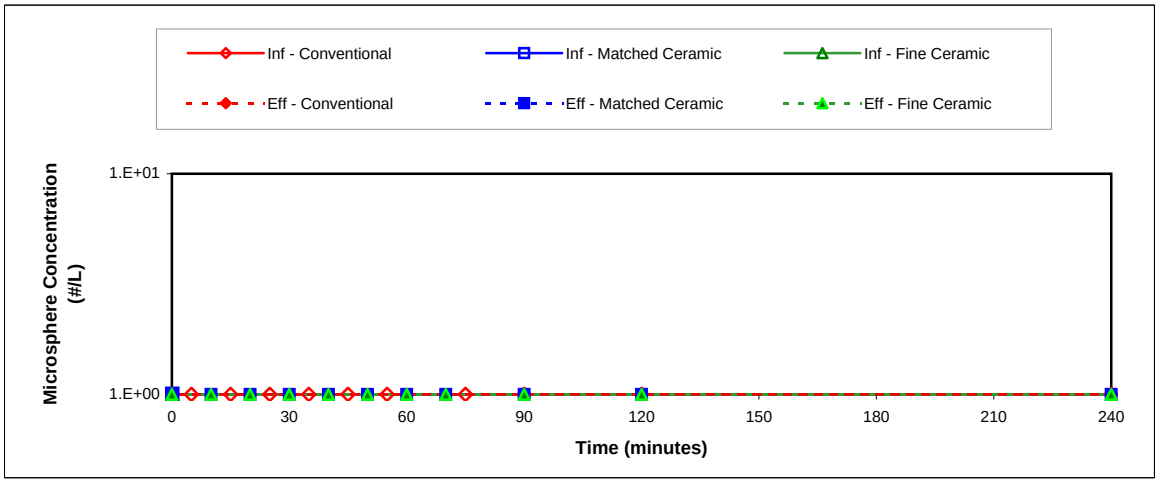

Turbidity Summary: Trial 3G

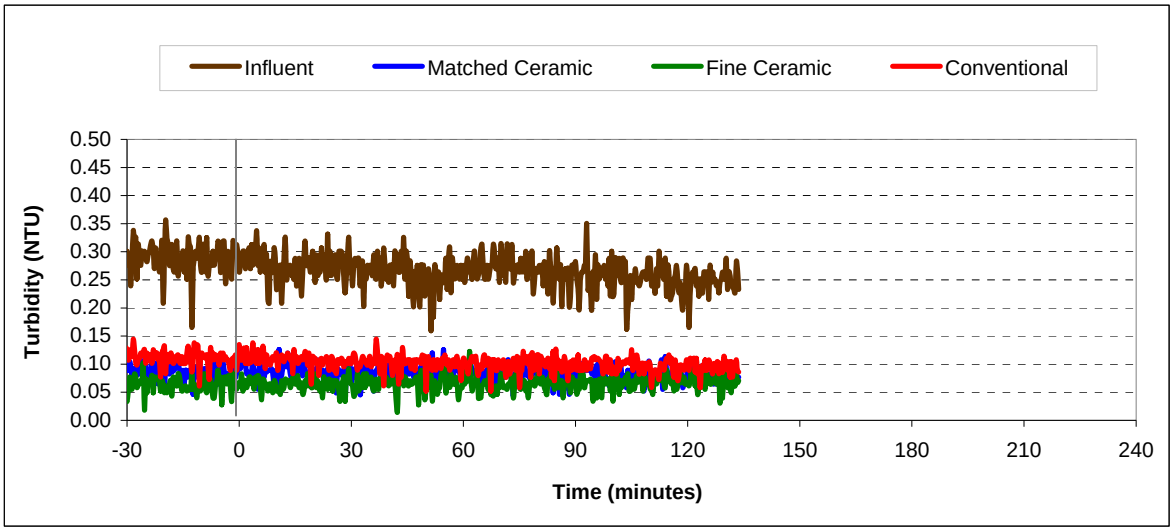

Turbidity Box and Whisker Plots

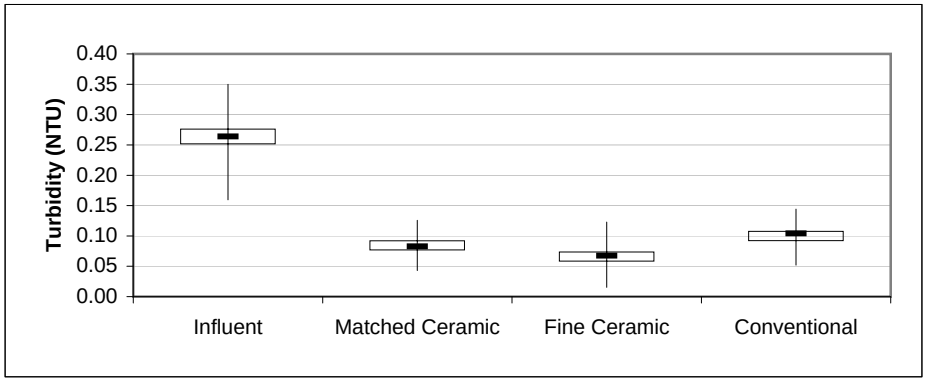

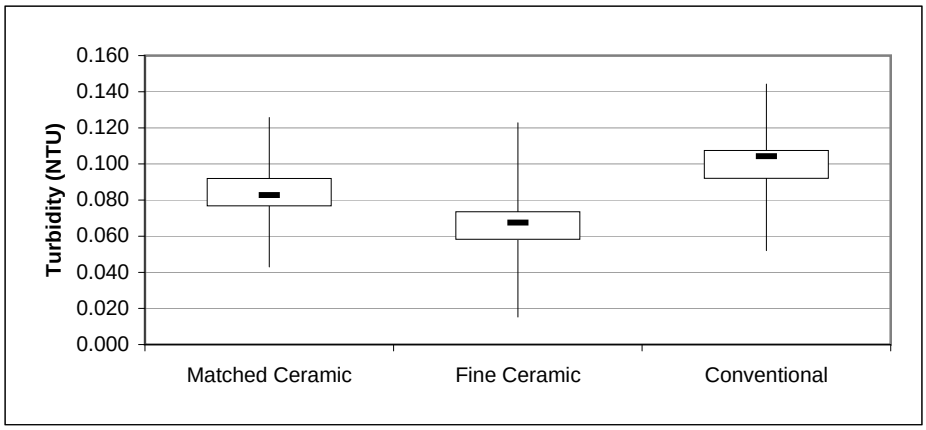

Vertical lines represent maximum and minimum turbidity range. Top and bottom of boxes represent 75th and 25th percentiles of turbidity data. Centre dash represents median turbidity measurement during seeding study.

Particle Count Summary: Trial 3G

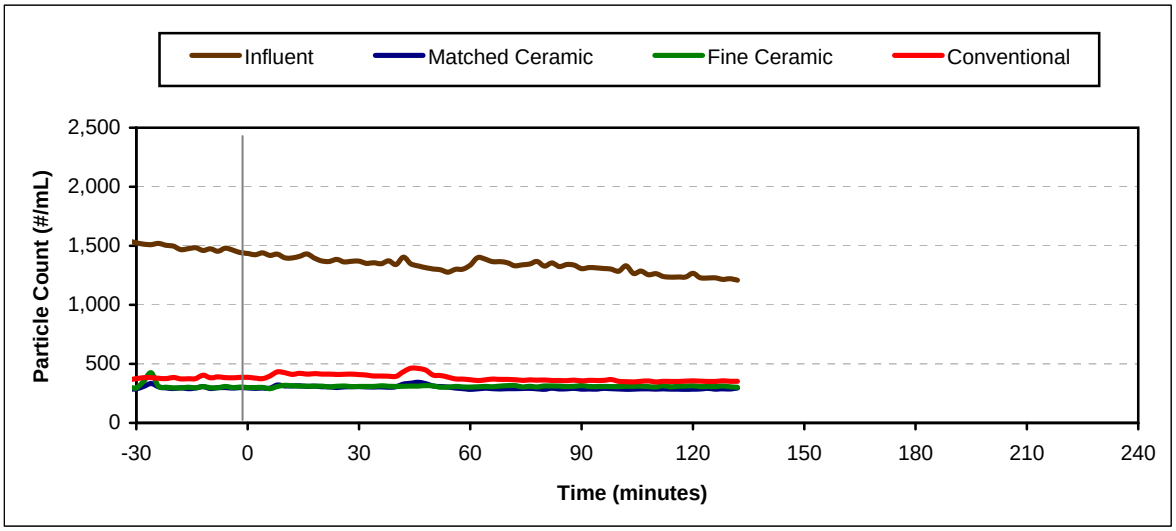

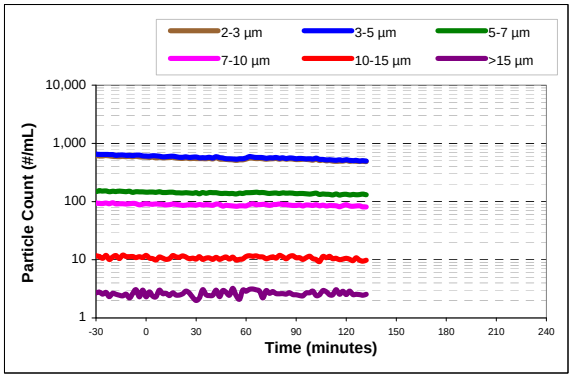

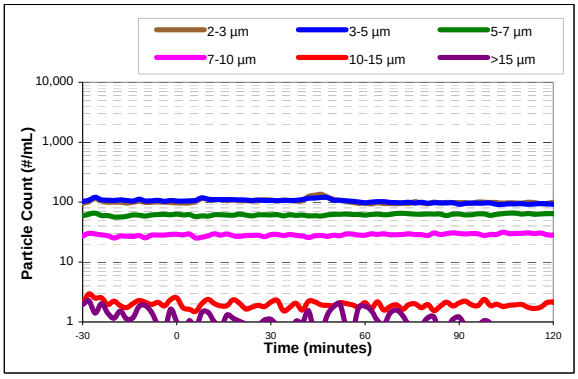

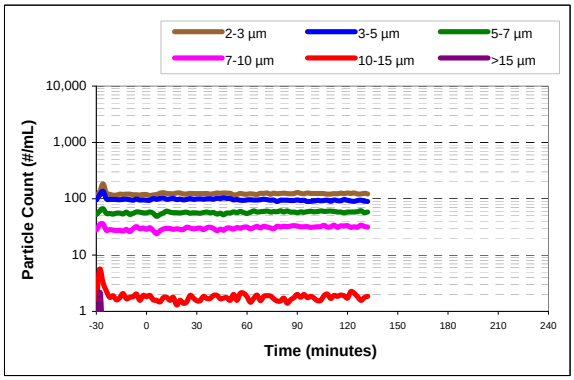

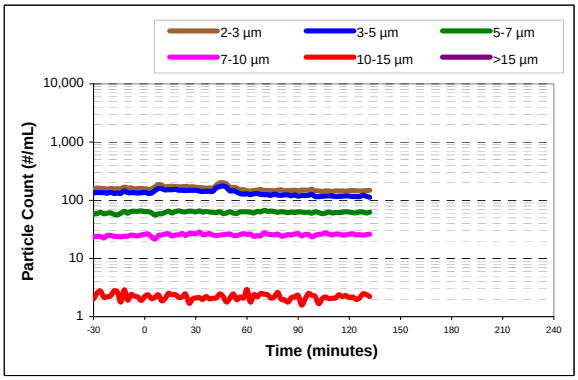

Flow and Headloss Summary: Trial 3G

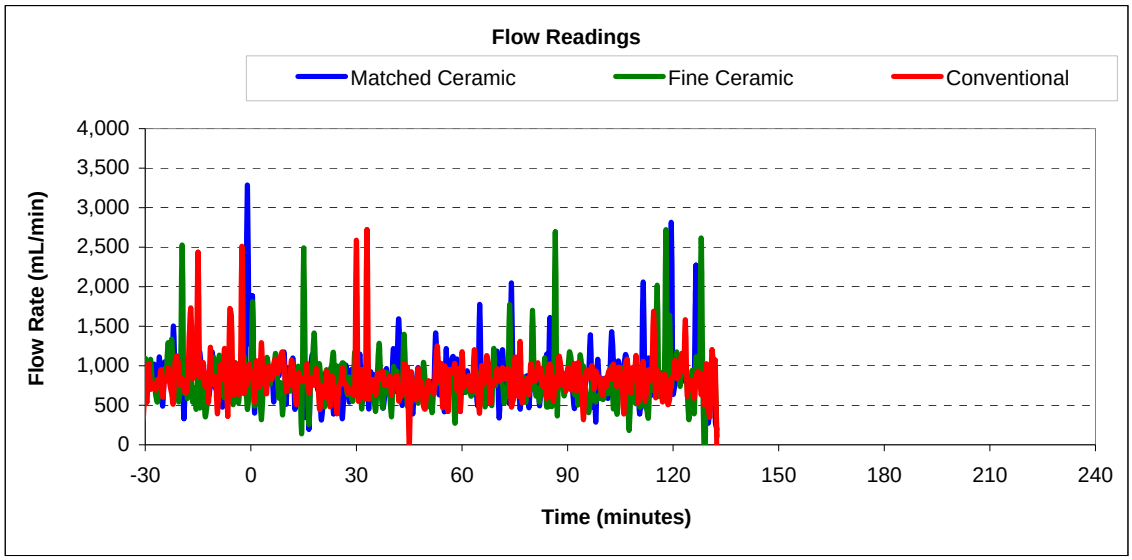

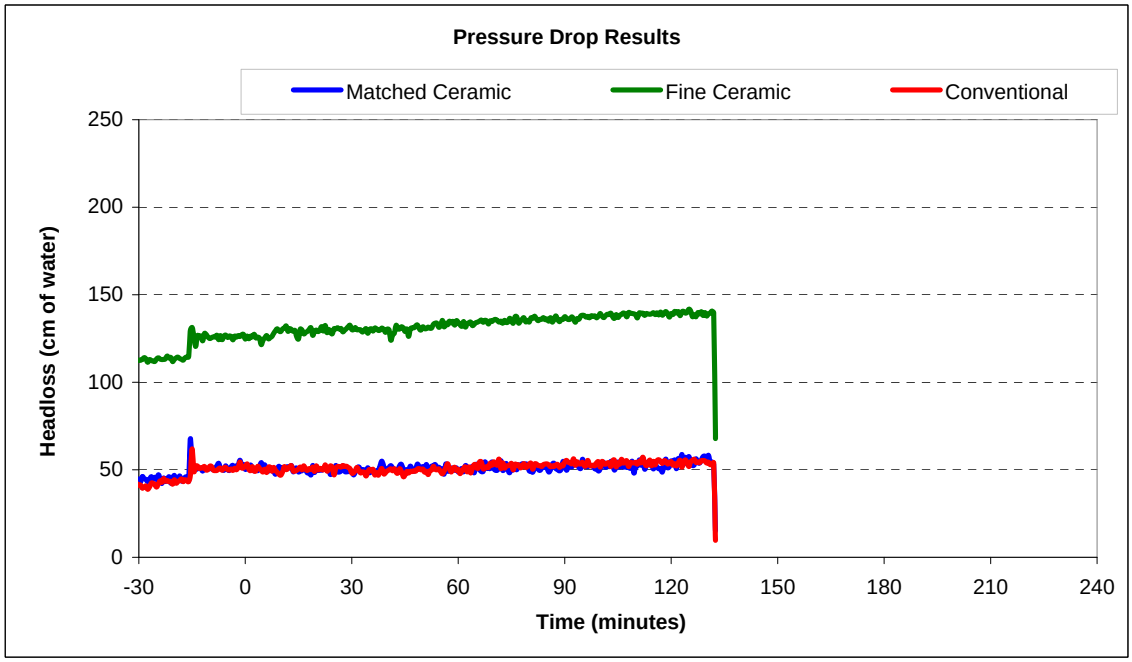

Summary Information for: Trial 3H

Trial Conditions:	
Trial Date	April 20, 2007
Location	Horgan WTP
Water Source	Lake Ontario
Loading Rate	10 GPM/ft2 (24.4 m/hr)
Coagulation	PACl, 0.3mg/L
Water Temperature	6^0C

Filter Media Configuration:

	Column 1	**Column 2**	**Column 3**
	Matched Ceramic	Fine Ceramic	Conventional
Top Layer	45 cm ceramic, ES 0.89 mm	45 cm ceramic, ES 0.96 mm	45 cm anthracite, ES 0.89 mm
Bottom Layer	30 cm ceramic, ES 0.47 mm	15 cm ceramic, ES 0.21mm	30 cm sand, ES 0.47 mm
Support Media	20 cm graded gravel bed	20 cm graded gravel bed	20 cm graded gravel bed

Parameter:	**Influent**	**Matched Ceramic**	**Fine Ceramic**	**Conventional**
Log reductions:				
Cryptosporidium		1.30	1.54	0.89
Microspheres		0.56	0.59	0.45
Other Parameters[1]:				
Average turbidity (NTU)	0.119	0.081	0.076	0.091
Turbidity reduction (%)		32	36	23
Average total particle count (#/mL)	558	517	509	605
Particle reduction (%)		7	9	-8
Average flow (mL/min)		1996	1828	2031
Clean bed headloss		103	210	93
Average headloss (cm)		110	268	100
Change in headloss (cm)		11	84	12

[1] *Data calculated from time 0 (start of spike injection) to 360 elapsed minutes*

***Cryptosporidium* and Microsphere Removal Summary:** **Trial 3H**

***Cryptosporidium* Log Removal**

Time	Col 1	Col 2	Col 3
10 min			
20 min	1.38	1.35	1.15
30 min	1.41	1.87	0.89
40 min	1.11	1.38	0.86
50 min	1.31	1.64	0.67
60 min			
70 min			
Avg.[1]	**1.30**	**1.54**	**0.89**

[1]*Avgerage denotes time interval from 20 min to 60 min*

Microsphere Log Removal

Time	Col 1	Col 2	Col 3
10 min	0.60	0.28	0.34
20 min	0.74	0.60	0.44
30 min	0.67	0.61	0.39
40 min	0.36	0.45	0.91
50 min	0.46	0.76	0.17
60 min	-3.54	-2.54	-2.88
70 min	-0.43	-0.26	-0.70
Avg.[1]	**0.56**	**0.59**	**0.45**

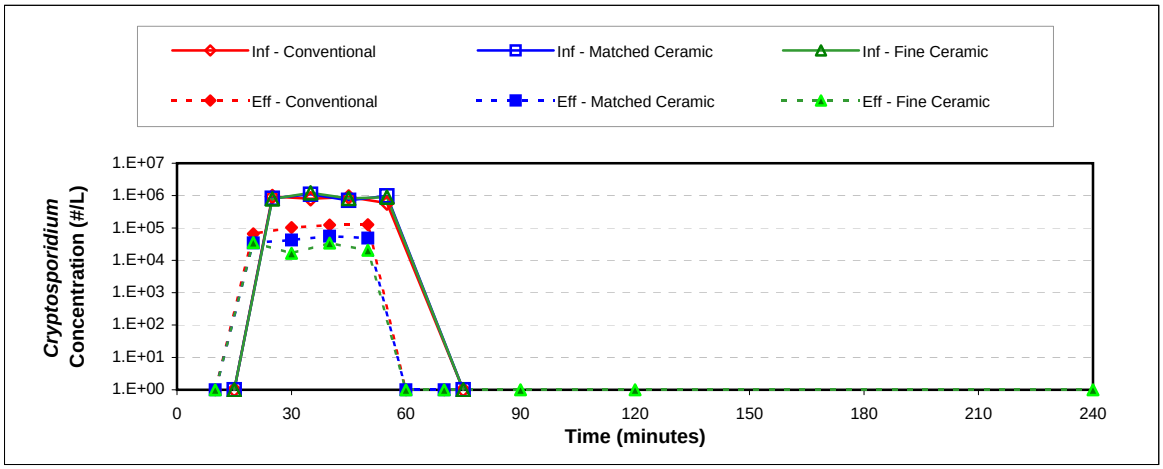

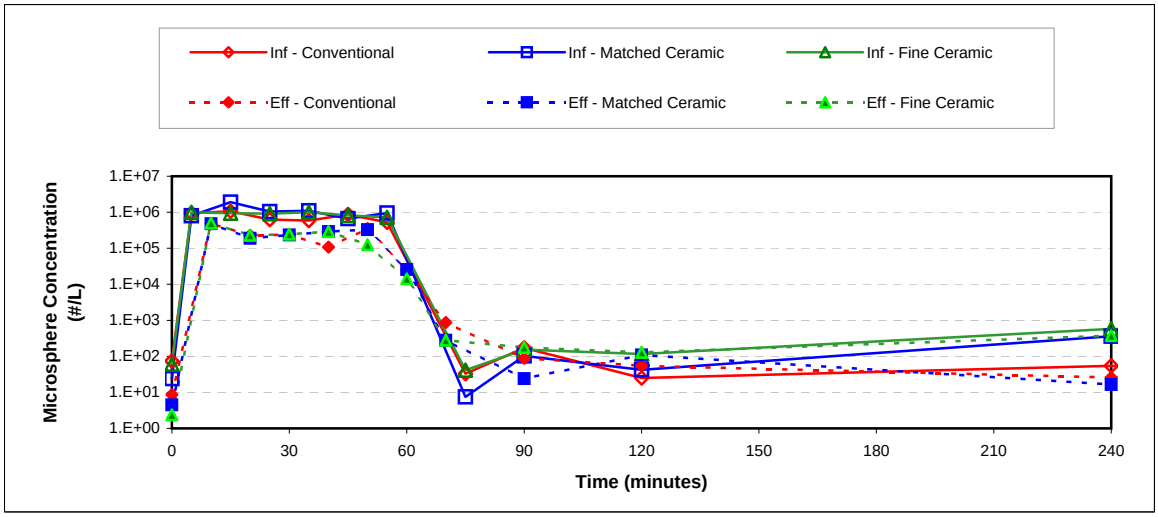

Turbidity Summary: Trial 3H

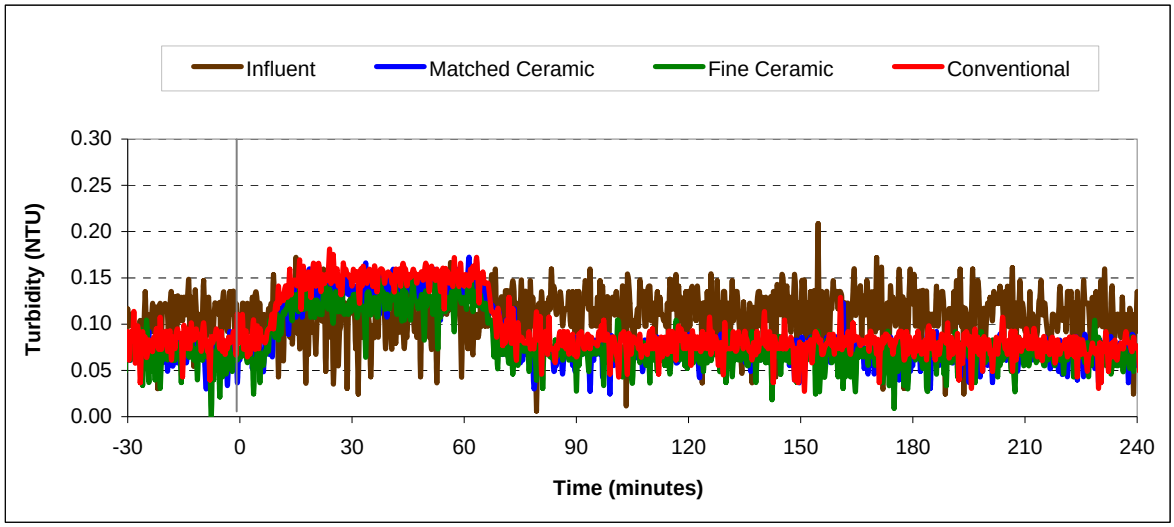

Turbidity Box and Whisker Plots

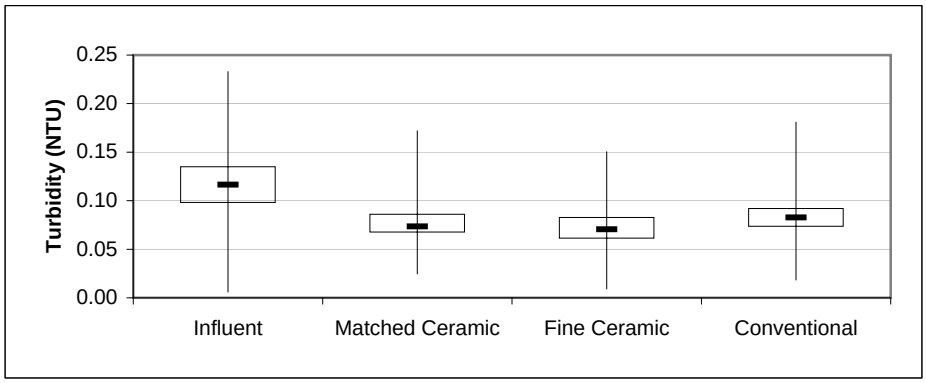

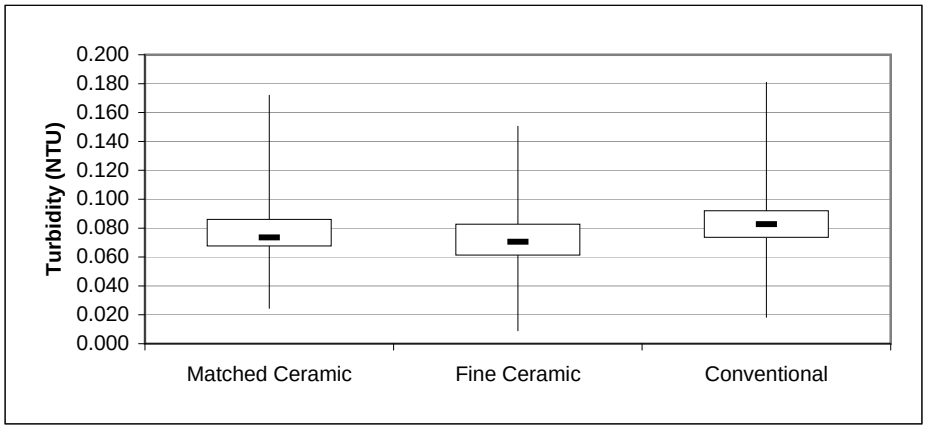

Vertical lines represent maximum and minimum turbidity range. Top and bottom of boxes represent 75th and 25th percentiles of turbidity data. Centre dash represents median turbidity measurement during seeding study.

Particle Count Summary: **Trial 3H**

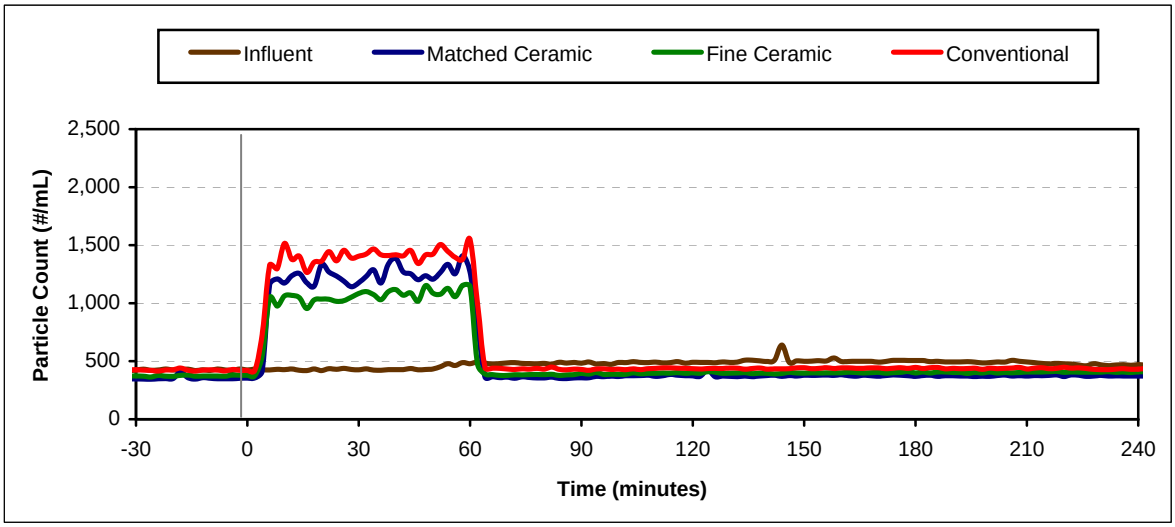

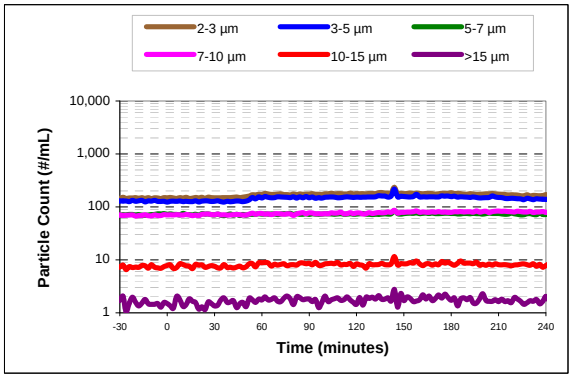

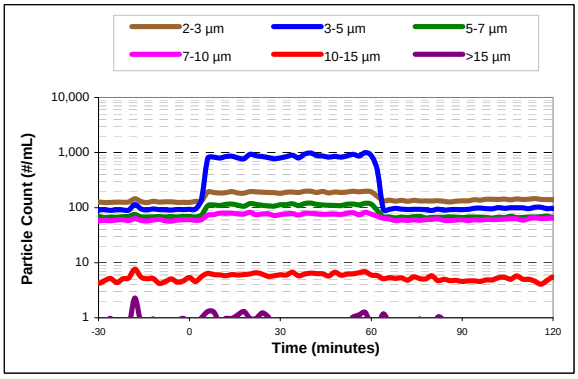

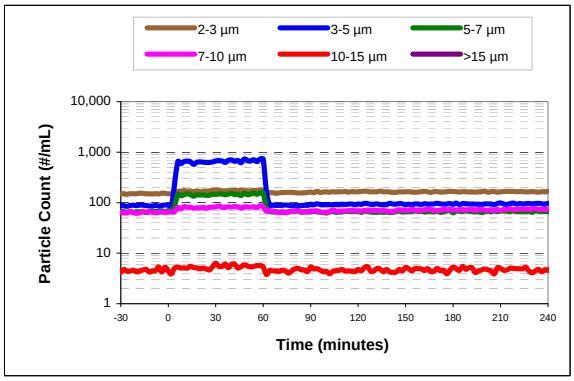

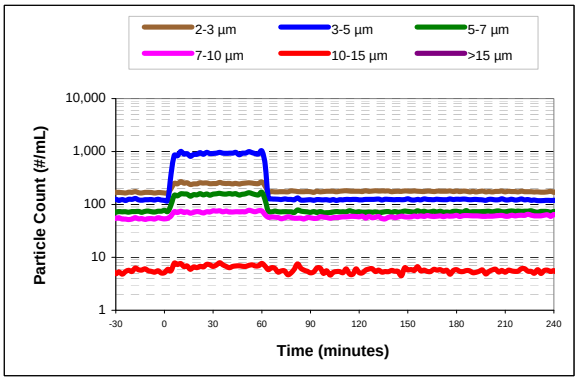

Flow and Headloss Summary: Trial 3H

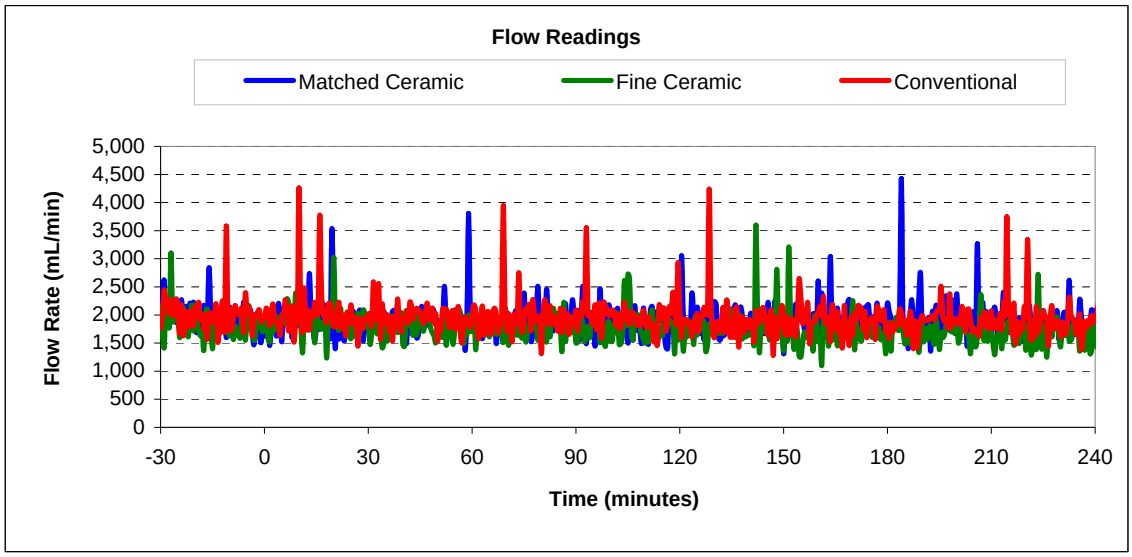

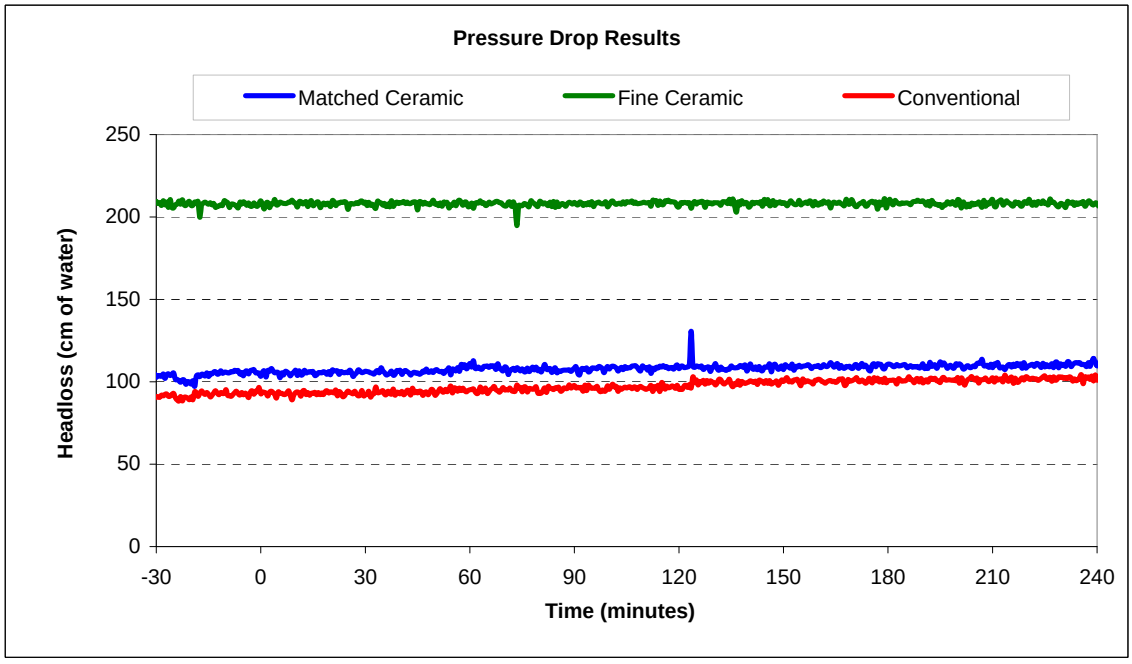

Summary Information for: Trial 3I

Trial Conditions:	
Trial Date	April 20, 2007
Location	Horgan WTP
Water Source	Lake Ontario
Loading Rate	4GPM/ft^2 (9.8 m/hr)
Coagulation	PACl 0.3 mg/L
Water Temperature	6^{0}C

Filter Media Configuration:

	Column 1	**Column 2**	**Column 3**
	Matched Ceramic	Fine Ceramic	Conventional
Top Layer	45 cm ceramic, ES 0.89 mm	45 cm ceramic, ES 0.96 mm	45 cm anthracite, ES 0.89 mm
Bottom Layer	30 cm ceramic, ES 0.47 mm	15 cm ceramic, ES 0.21mm	30 cm sand, ES 0.47 mm
Support Media	20 cm graded gravel bed	20 cm graded gravel bed	20 cm graded gravel bed

Parameter:	**Influent**	**Matched Ceramic**	**Fine Ceramic**	**Conventional**
Log reductions:				
Cryptosporidium		1.17	1.58	1.08
Microspheres		0.42	0.69	0.33
Other Parameters[1]:				
Average turbidity (NTU)	0.130	0.088	0.084	0.104
Turbidity reduction (%)		32	36	20
Average total particle count (#/mL)	714	499	462	659
Particle reduction (%)		30	35	8
Average flow (mL/min)		902	914	909
Clean bed headloss		51	102	46
Average headloss (cm)		44	106	42
Change in headloss (cm)		-9	7	-4

[1] *Data calculated from time 0 (start of spike injection) to 360 elapsed minutes*

***Cryptosporidium* and Microsphere Removal Summary:** **Trial 3I**

***Cryptosporidium* Log Removal**

Time	Col 1	Col 2	Col 3
10 min			
20 min	1.26	1.65	0.88
30 min	1.15	2.03	0.88
40 min	1.25	1.26	2.01
50 min	1.04	1.79	0.92
60 min			
70 min			
Avg.[1]	**1.17**	**1.58**	**1.08**

[1]*Avgerage denotes time interval from 20 min to 60 min*

Microsphere Log Removal

Time	Col 1	Col 2	Col 3
10 min	0.45	0.66	0.20
20 min	0.44	0.89	0.17
30 min	0.32	0.88	0.49
40 min	0.75	0.38	1.07
50 min	0.12	0.82	0.05
60 min	-0.43	0.06	-0.50
70 min	0.00	-0.73	-0.25
Avg.[1]	**0.42**	**0.69**	**0.33**

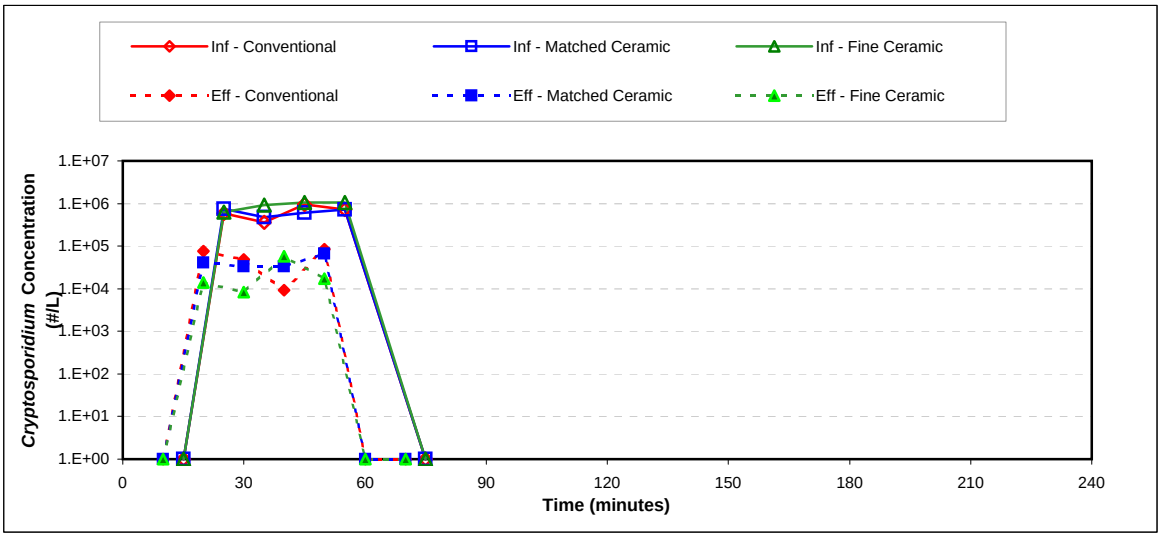

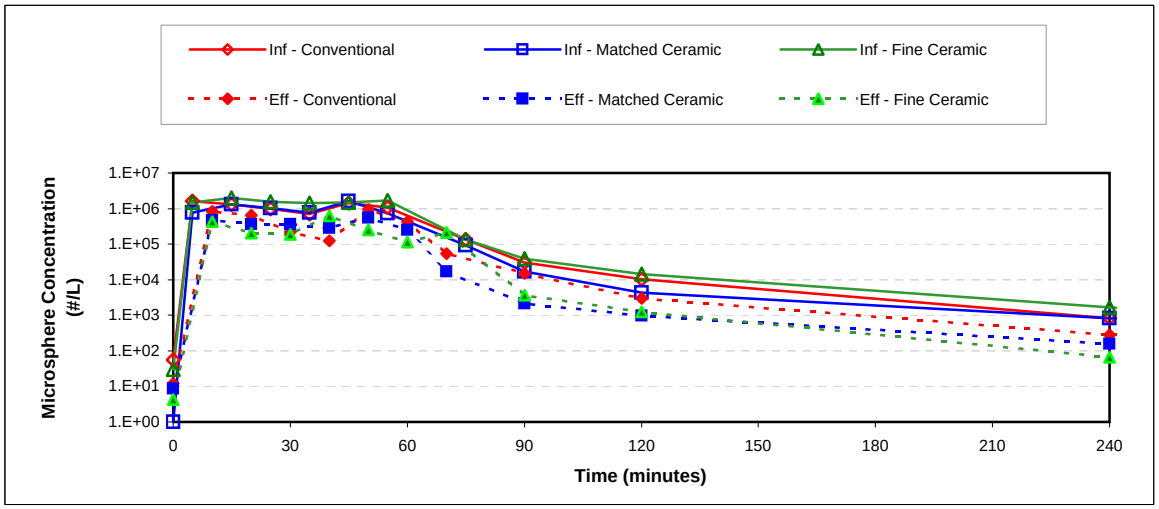

Turbidity Summary: Trial 3I

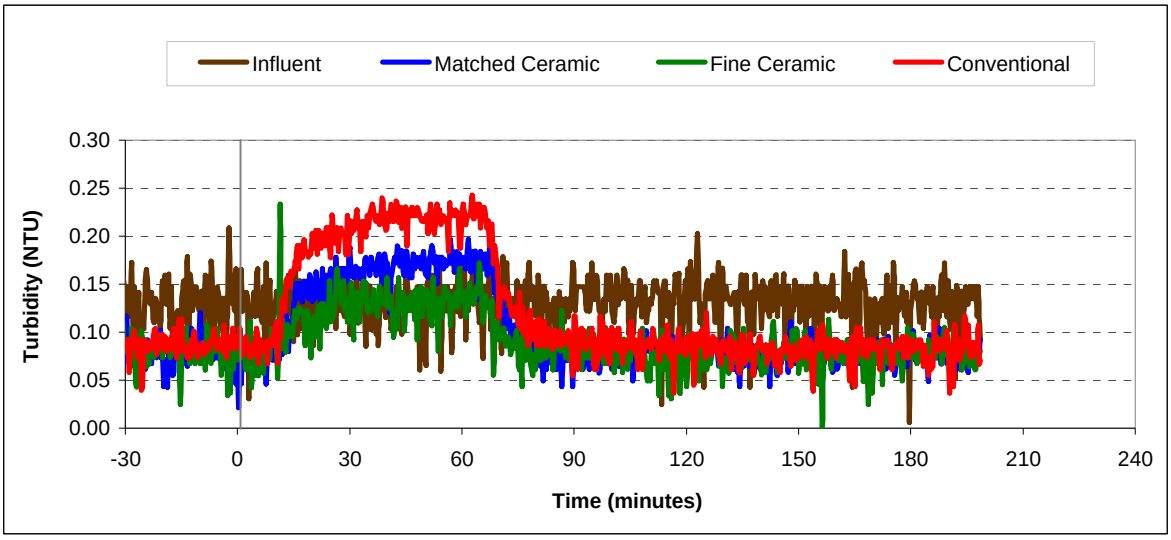

Turbidity Box and Whisker Plots

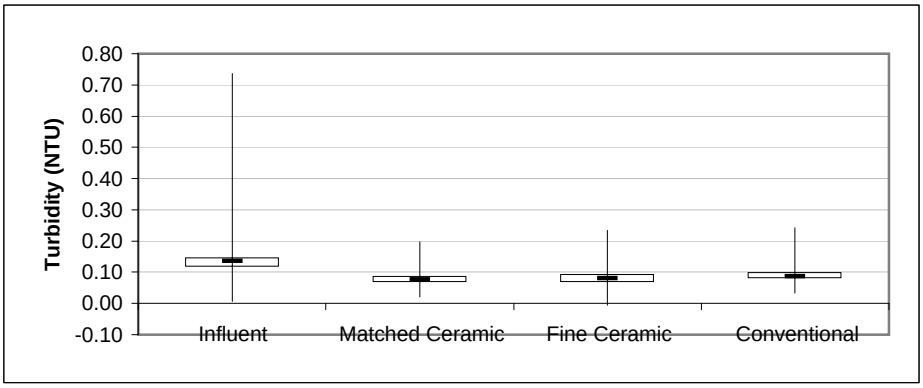

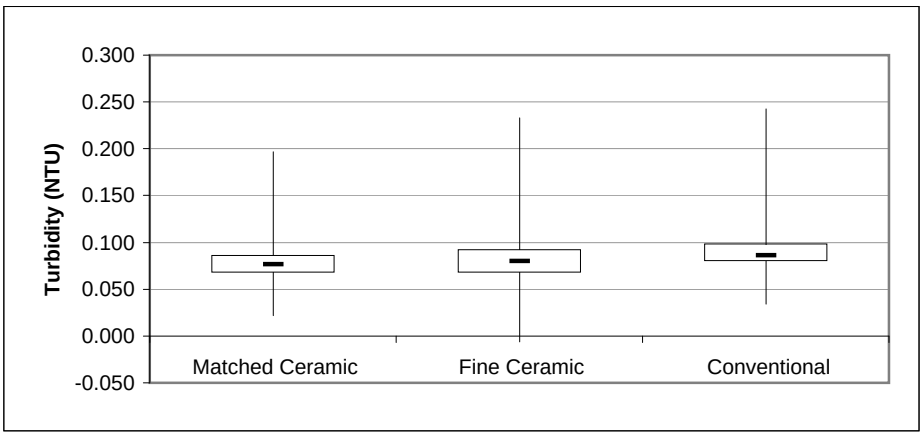

Vertical lines represent maximum and minimum turbidity range. Top and bottom of boxes represent 75th and 25th percentiles of turbidity data. Centre dash represents median turbidity measurement during seeding study.

Particle Count Summary: **Trial 3I**

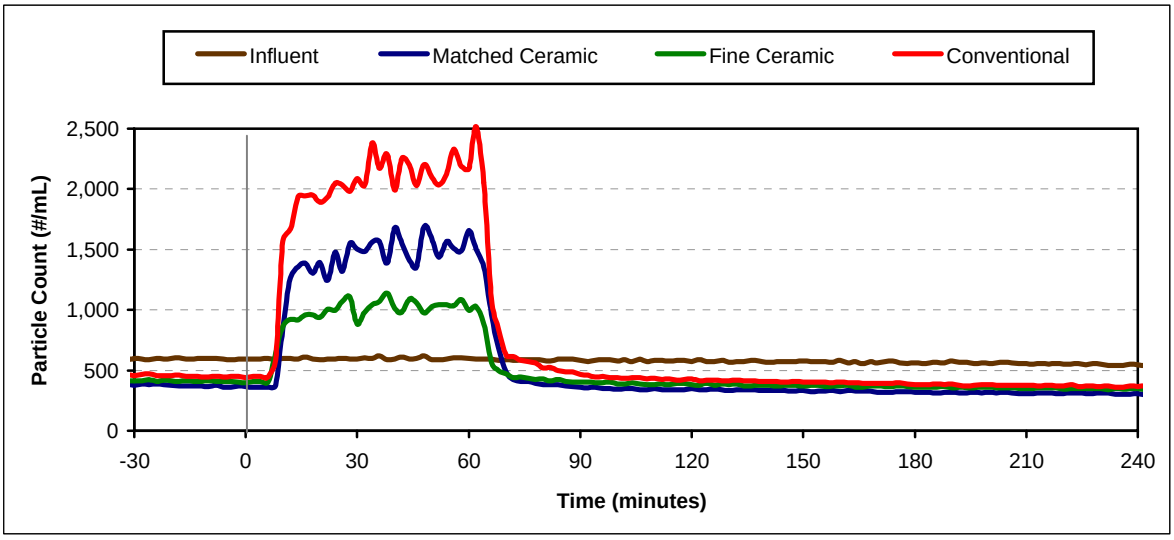

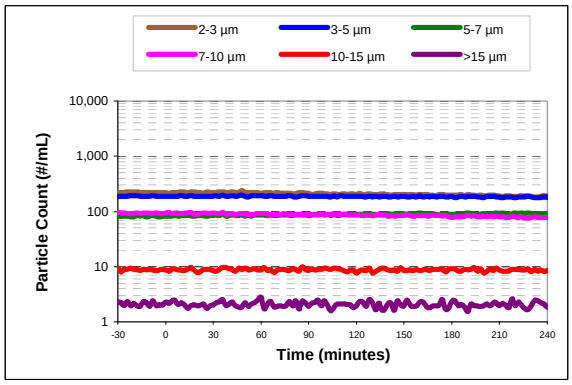

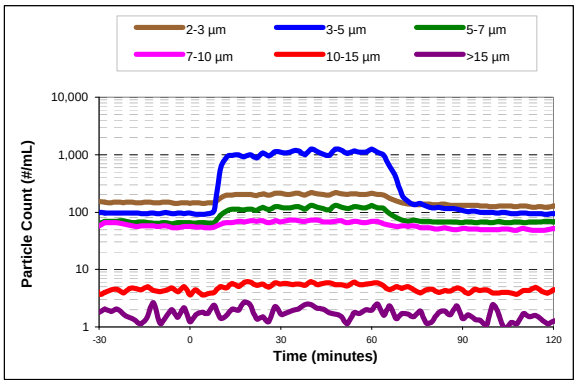

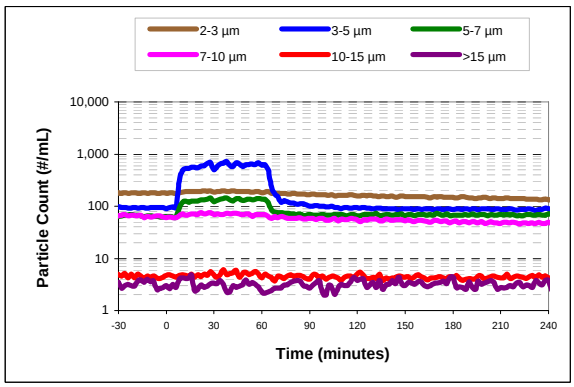

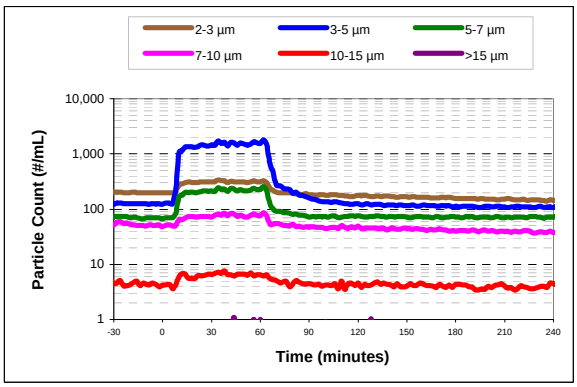

Flow and Headloss Summary: Trial 3I

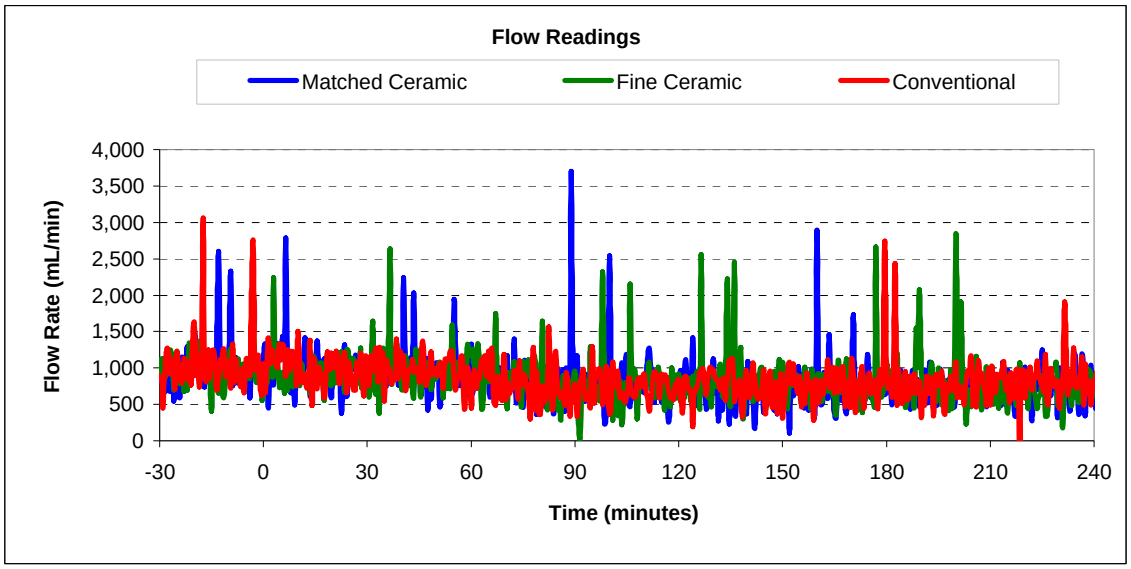

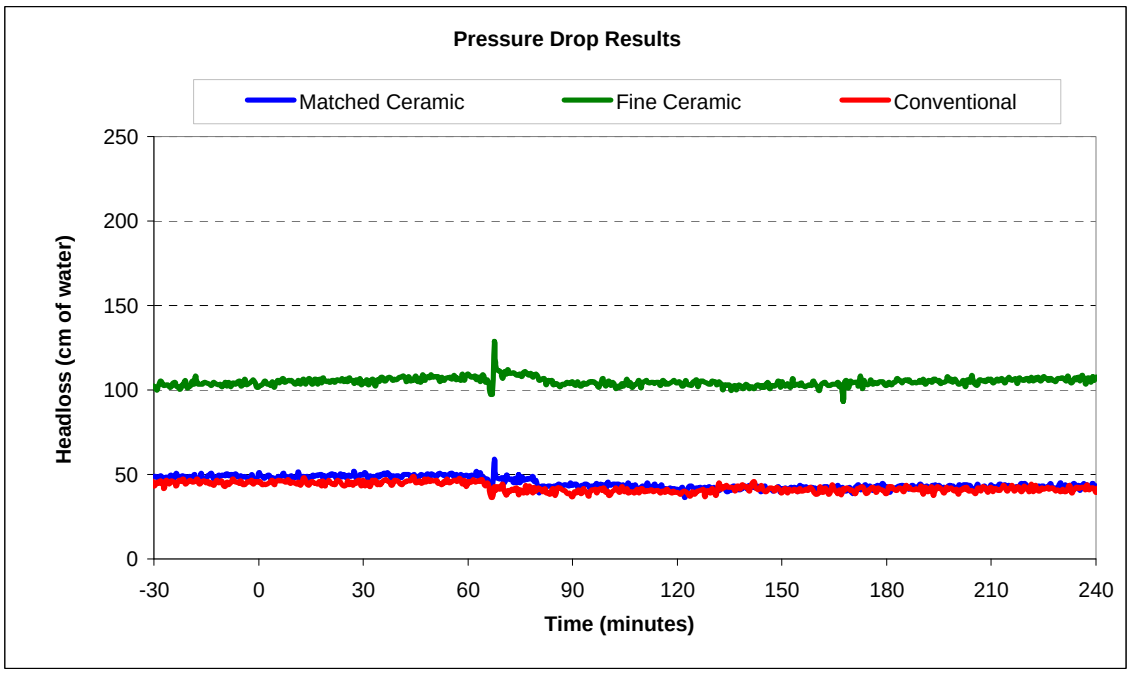

Summary Information for: Trial 3J

Trial Conditions:	
Trial Date	April 24, 2007
Location	Horgan WTP
Water Source	Lake Ontario
Loading Rate	4 GPM/ft^2 (9.8 m/hr)
Coagulation	PACL, 0.3 mg/L
Water Temperature	7^{0}C

Filter Media Configuration:

	Column 1	**Column 2**	**Column 3**
	Matched Ceramic	Fine Ceramic	Conventional
Top Layer	45 cm ceramic, ES 0.89 mm	45 cm ceramic, ES 0.96 mm	45 cm anthracite, ES 0.89 mm
Bottom Layer	30 cm ceramic, ES 0.47 mm	15 cm ceramic, ES 0.21mm	30 cm sand, ES 0.47 mm
Support Media	20 cm graded gravel bed	20 cm graded gravel bed	20 cm graded gravel bed

Parameter:	**Influent**	**Matched Ceramic**	**Fine Ceramic**	**Conventional**
Log reductions:				
Cryptosporidium		0.89	1.59	0.97
Microspheres		0.06	0.82	0.38
Other Parameters[1]:				
Average turbidity (NTU)	0.173	0.106	0.092	0.120
Turbidity reduction (%)		38	47	30
Average total particle count (#/mL)	787	517	514	701
Particle reduction (%)		34	35	11
Average flow (mL/min)		902	824	943
Clean bed headloss		44	104	50
Average headloss (cm)		43	109	51
Change in headloss (cm)		-1	9	1

[1] *Data calculated from time 0 (start of spike injection) to 360 elapsed minutes*

***Cryptosporidium* and Microsphere Removal Summary:** **Trial 3J**

***Cryptosporidium* Log Removal**

Time	Col 1	Col 2	Col 3
10 min			
20 min	0.65	1.58	1.13
30 min	1.10	1.75	0.90
40 min	0.59	1.41	0.64
50 min	1.19	1.57	1.16
60 min			
70 min			
Avg.[1]	**0.89**	**1.59**	**0.97**

[1]*Avgerage denotes time interval from 20 min to 60 min*

Microsphere Log Removal

Time	Col 1	Col 2	Col 3
10 min	0.92	1.35	0.45
20 min	-6.33	1.26	0.70
30 min	-0.01	-5.83	0.40
40 min	0.13	0.27	-0.49
50 min	0.35	1.05	0.46
60 min	-0.16	0.93	-0.08
70 min	0.50	0.97	0.55
Avg.[1]	**0.06**	**0.82**	**0.38**

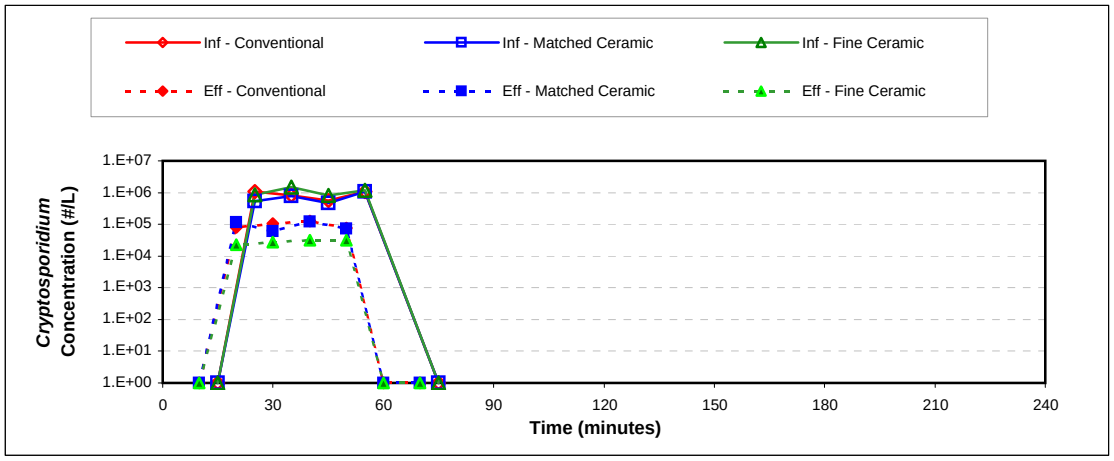

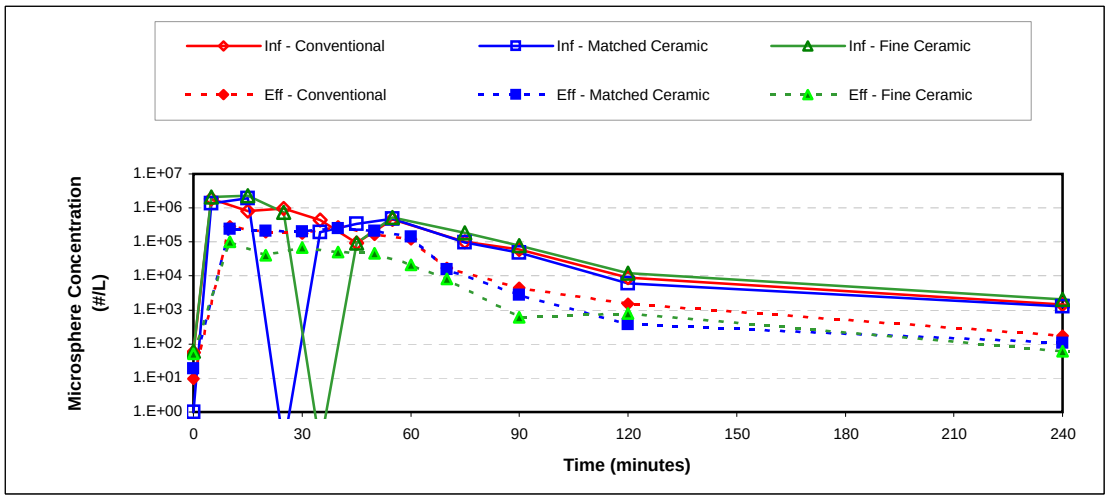

Turbidity Summary: Trial 3J

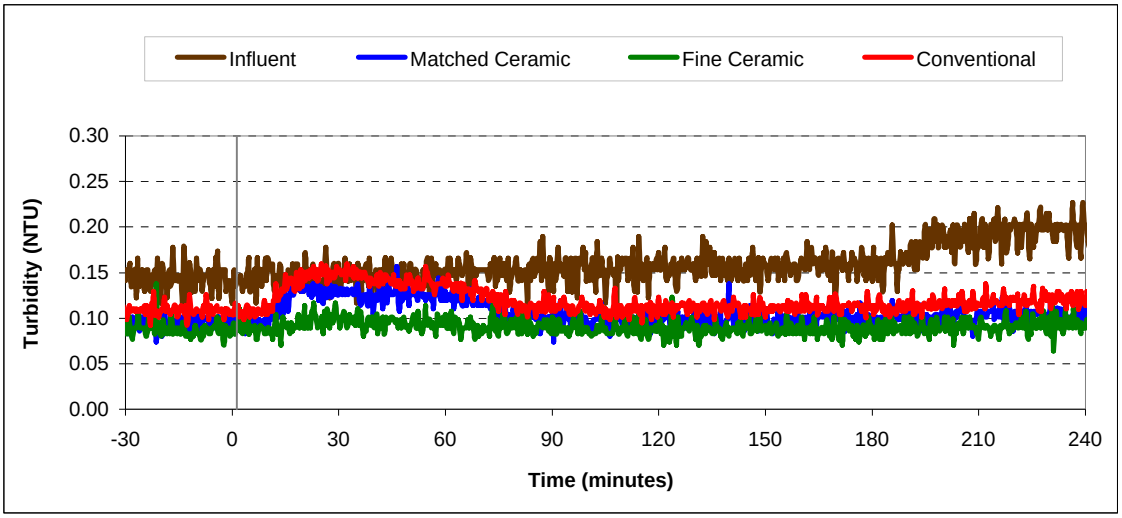

Turbidity Box and Whisker Plots

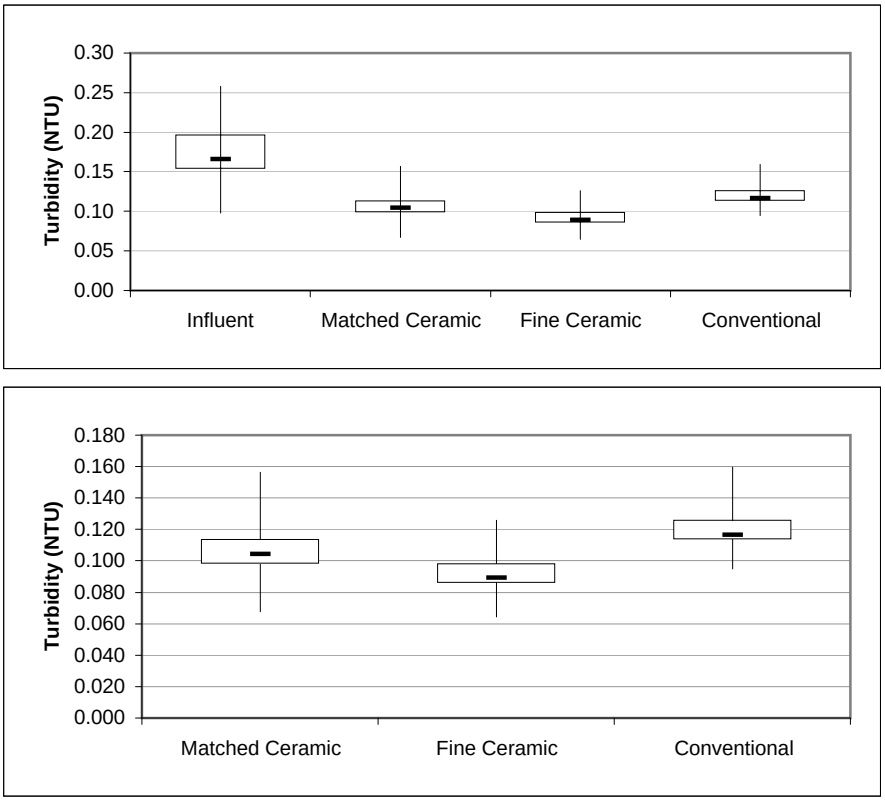

Vertical lines represent maximum and minimum turbidity range. Top and bottom of boxes represent 75th and 25th percentiles of turbidity data. Centre dash represents median turbidity measurement during seeding study.

Particle Count Summary: **Trial 3J**

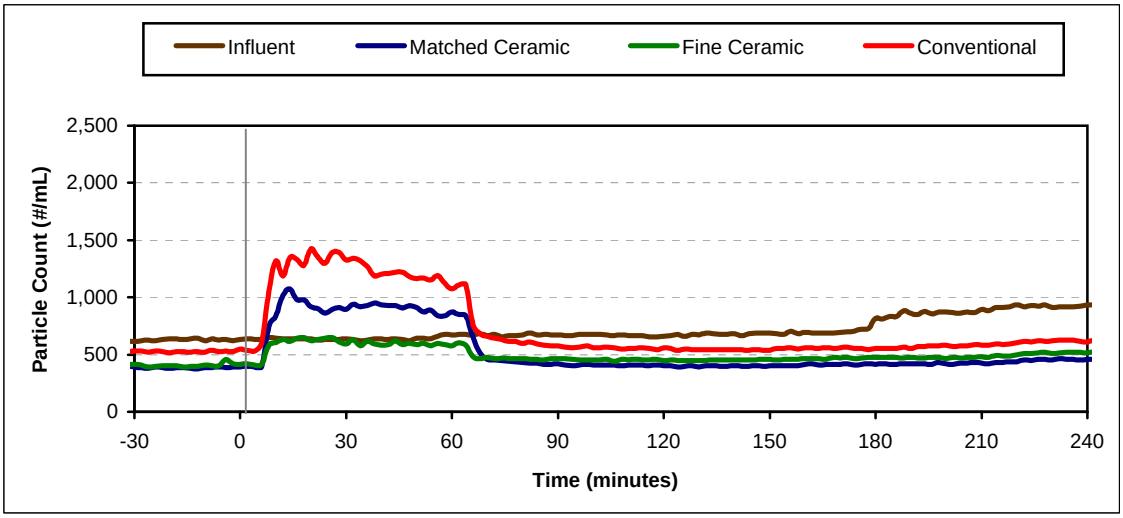

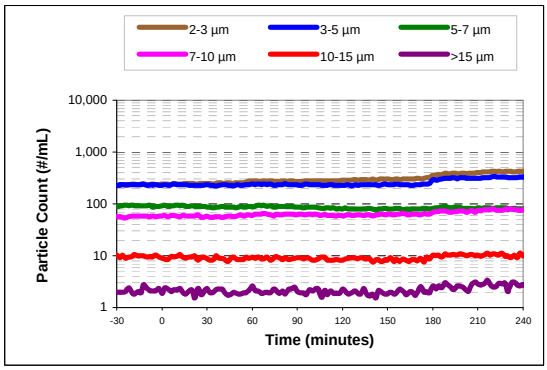

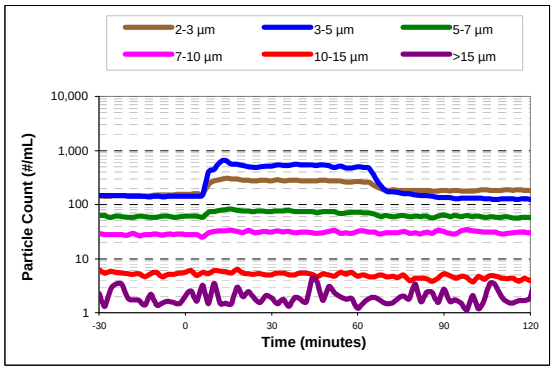

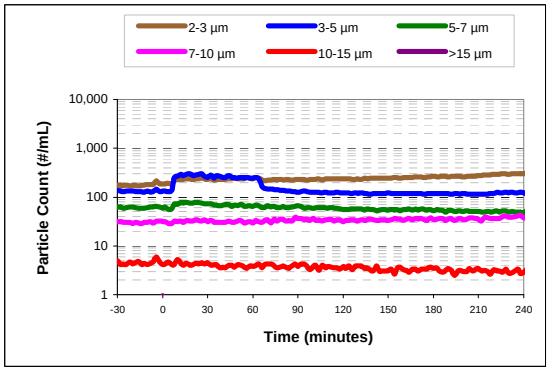

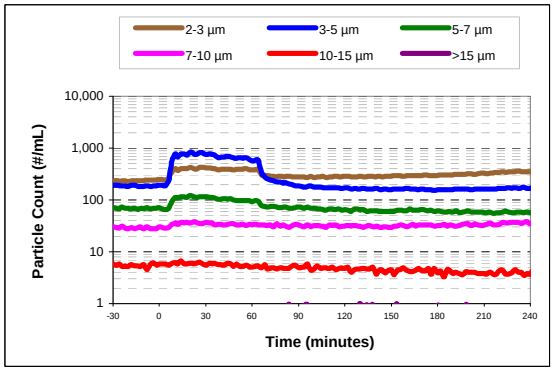

Flow and Headloss Summary: Trial 3J

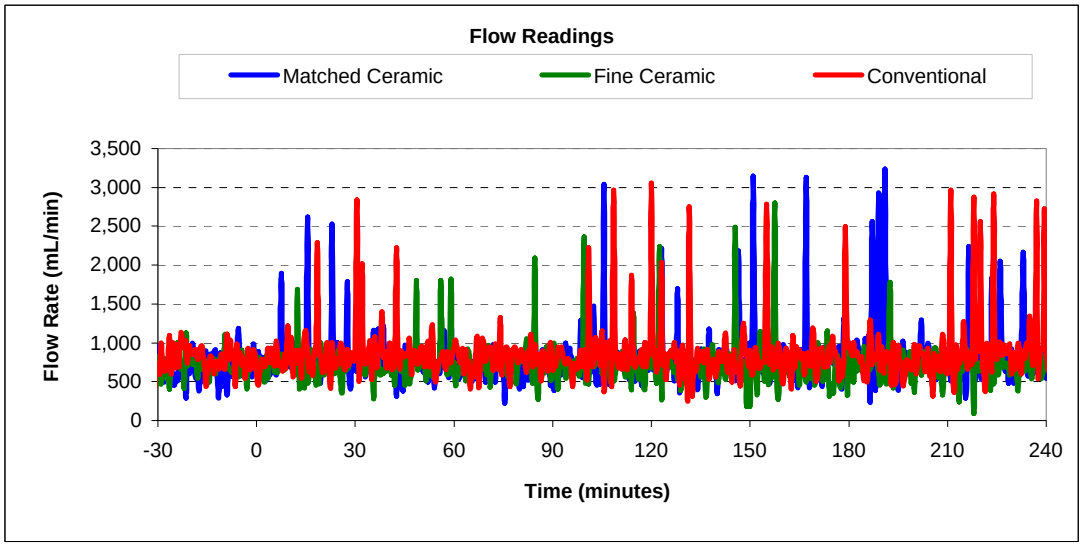

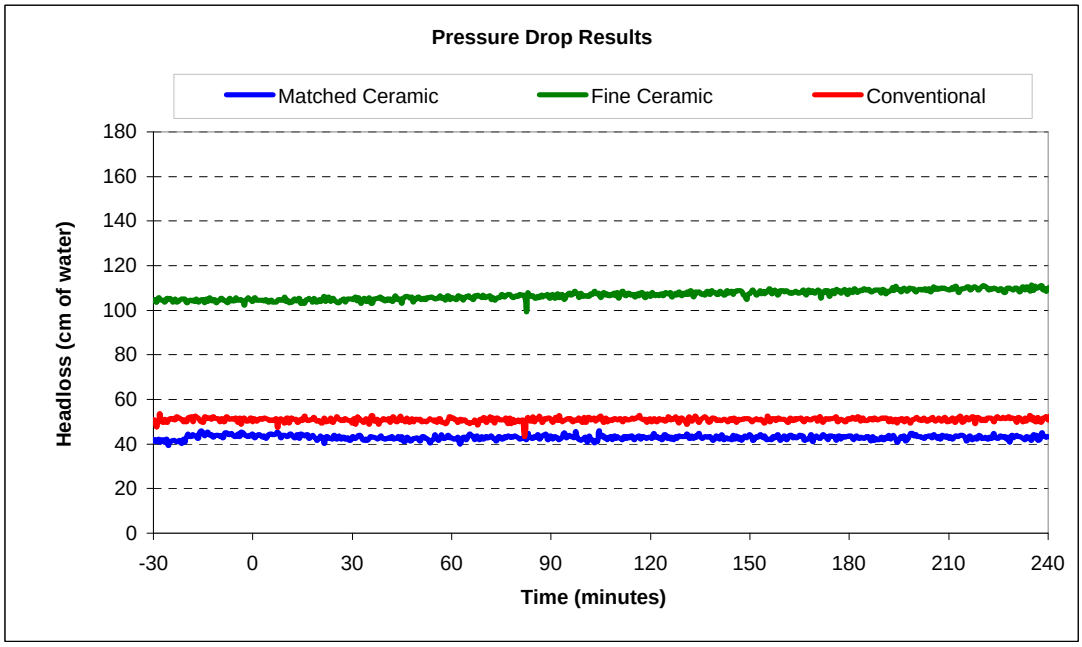

Summary Information for: Trial 3K

Trial Conditions:	
Trial Date	April 26, 2007
Location	Horgan WTP
Water Source	Lake Ontario
Loading Rate	10 GPM/ft^2 (24.4 m/hr)
Coagulation	PACl, 0.3 mg/L
Water Temperature	7^{0}C

Filter Media Configuration:

	Column 1	**Column 2**	**Column 3**
	Matched Ceramic	Fine Ceramic	Conventional
Top Layer	45 cm ceramic, ES 0.89 mm	45 cm ceramic, ES 0.96 mm	45 cm anthracite, ES 0.89 mm
Bottom Layer	30 cm ceramic, ES 0.47 mm	15 cm ceramic, ES 0.21mm	30 cm sand, ES 0.47 mm
Support Media	20 cm graded gravel bed	20 cm graded gravel bed	20 cm graded gravel bed

Parameter:	**Influent**	**Matched Ceramic**	**Fine Ceramic**	**Conventional**
Log reductions:				
Cryptosporidium		4.40	3.92	3.14
Microspheres		3.00	3.46	2.64
Other Parameters[1]:				
Average turbidity (NTU)	0.212	0.110	0.096	0.132
Turbidity reduction (%)		48	55	38
Average total particle count (#/mL)	1191	703	756	895
Particle reduction (%)		41	36	25
Average flow (mL/min)		2176	1998	2130
Clean bed headloss		103	207	90
Average headloss (cm)		106	208	93
Change in headloss (cm)		5	1	5

[1] *Data calculated from time 0 (start of spike injection) to 360 elapsed minutes*

***Cryptosporidium* and Microsphere Removal Summary:** **Trial 3K**

***Cryptosporidium* Log Removal**

Time	Col 1	Col 2	Col 3
10 min			
20 min	4.62	3.72	3.35
30 min	4.25	3.76	2.77
40 min	4.43	4.54	3.77
50 min	4.67	4.56	3.53
60 min			
70 min			
Avg.[1]	**4.40**	**3.92**	**3.14**

[1]*Avgerage denotes time interval from 20 min to 60 min*

Microsphere Log Removal

Time	Col 1	Col 2	Col 3
10 min	3.54	3.65	2.65
20 min	3.07	3.66	2.55
30 min	3.12	3.44	3.08
40 min	2.91	3.30	2.48
50 min	2.85	3.43	2.55
60 min	1.17	-0.84	-1.09
70 min	1.23	-0.39	1.38
Avg.[1]	**3.00**	**3.46**	**2.64**

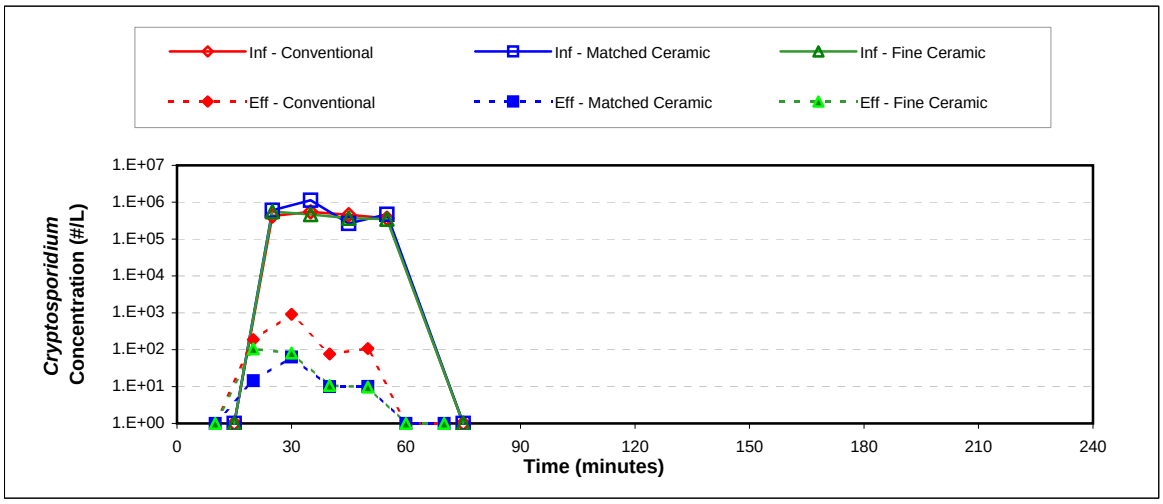

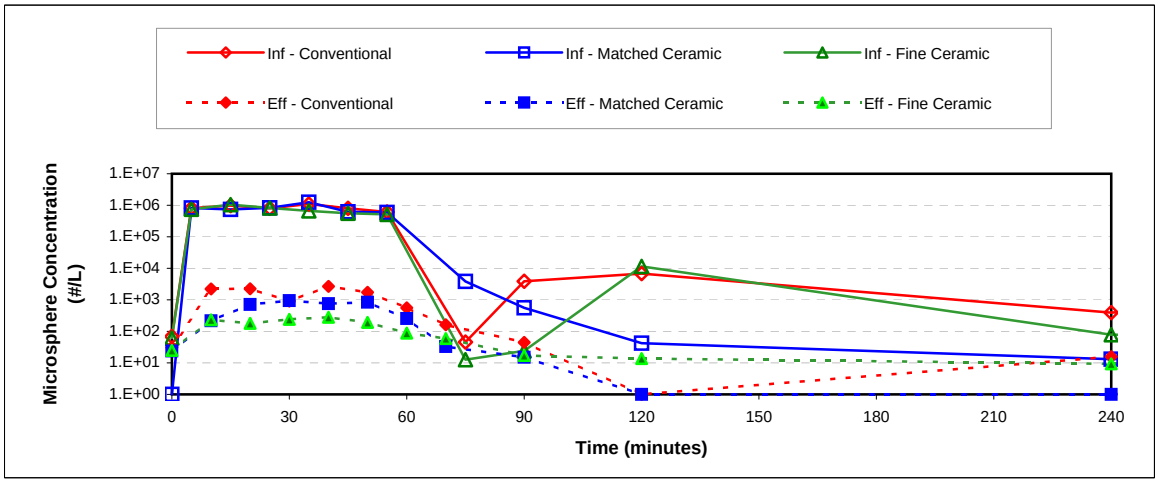

Turbidity Summary: Trial 3K

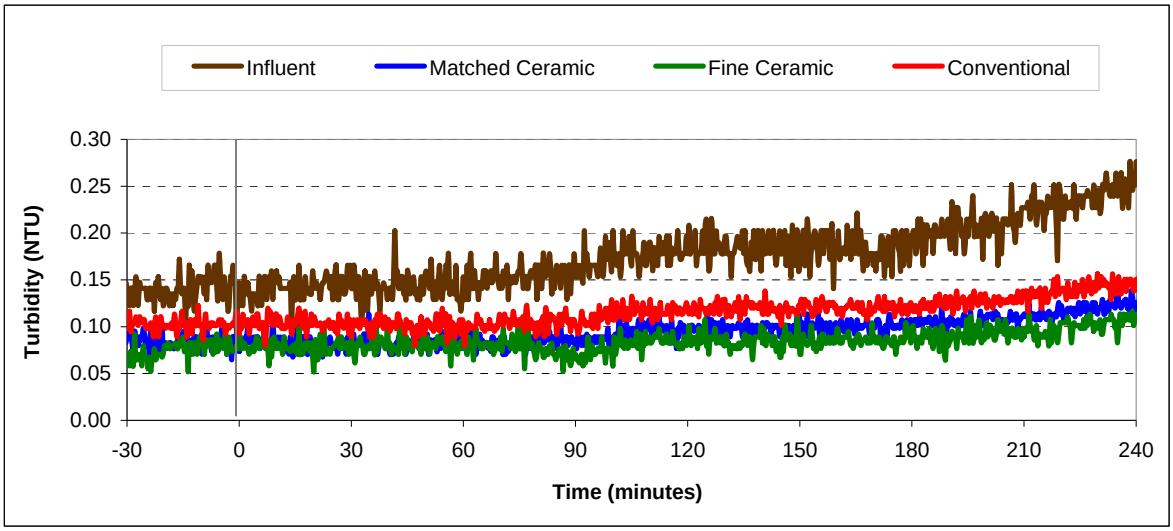

Turbidity Box and Whisker Plots

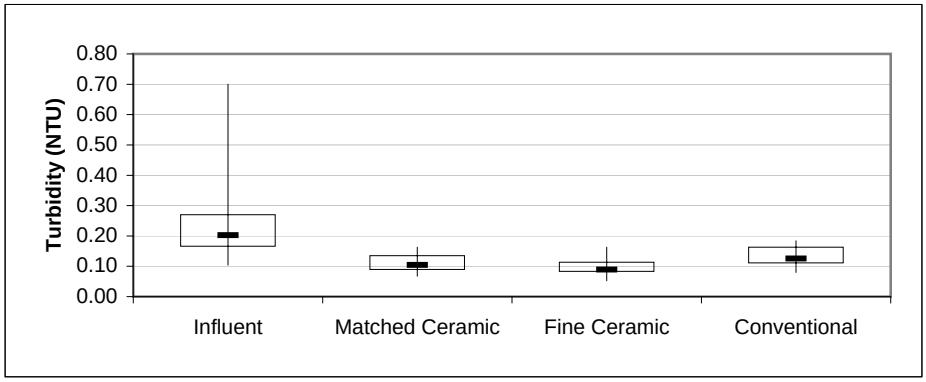

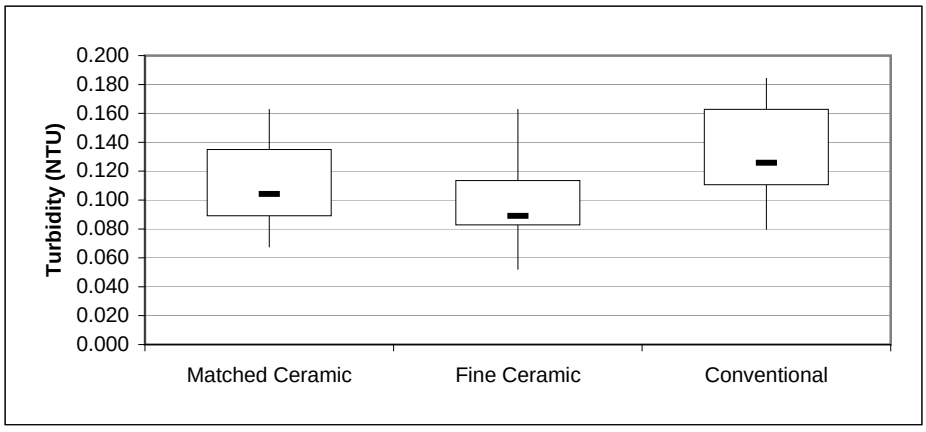

Vertical lines represent maximum and minimum turbidity range. Top and bottom of boxes represent 75th and 25th percentiles of turbidity data. Centre dash represents median turbidity measurement during seeding study.

Particle Count Summary: **Trial 3K**

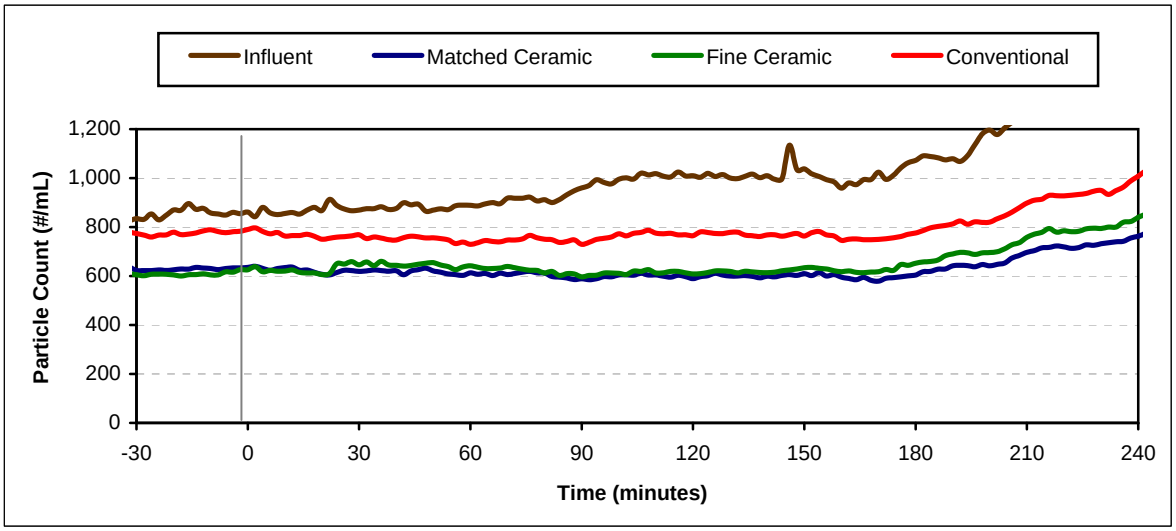

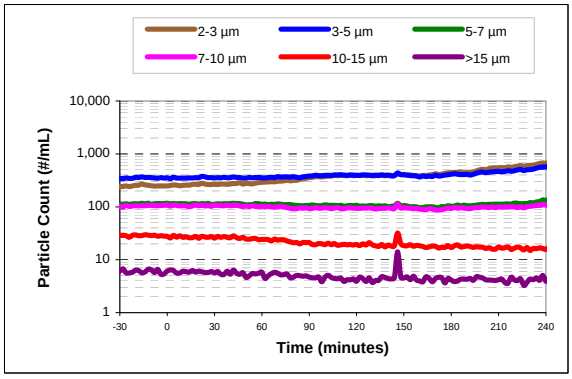

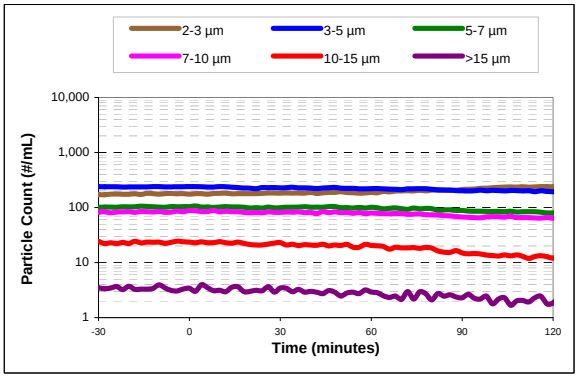

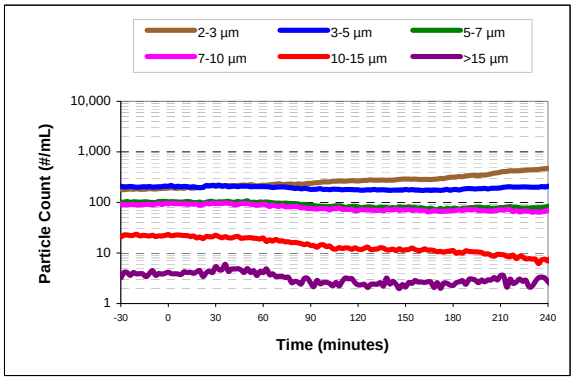

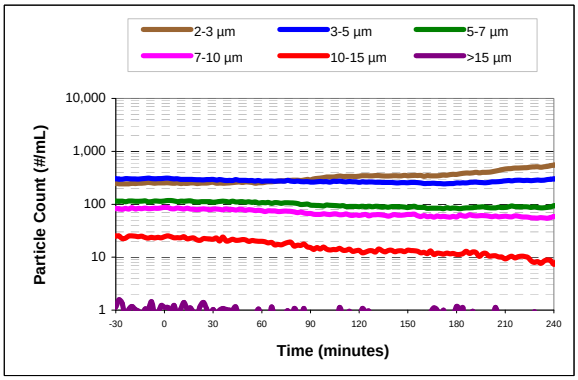

Flow and Headloss Summary: Trial 3K

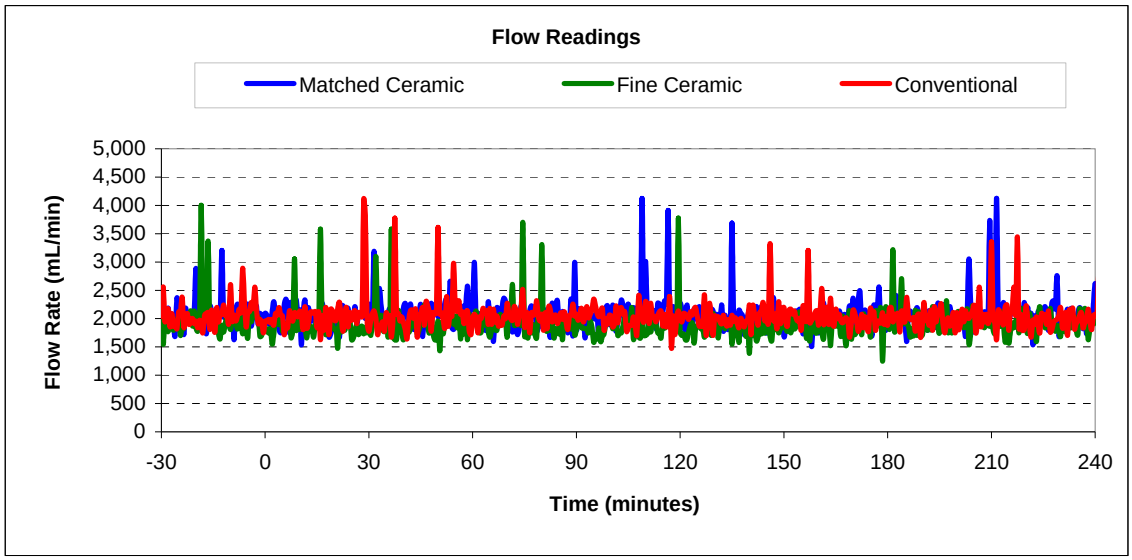

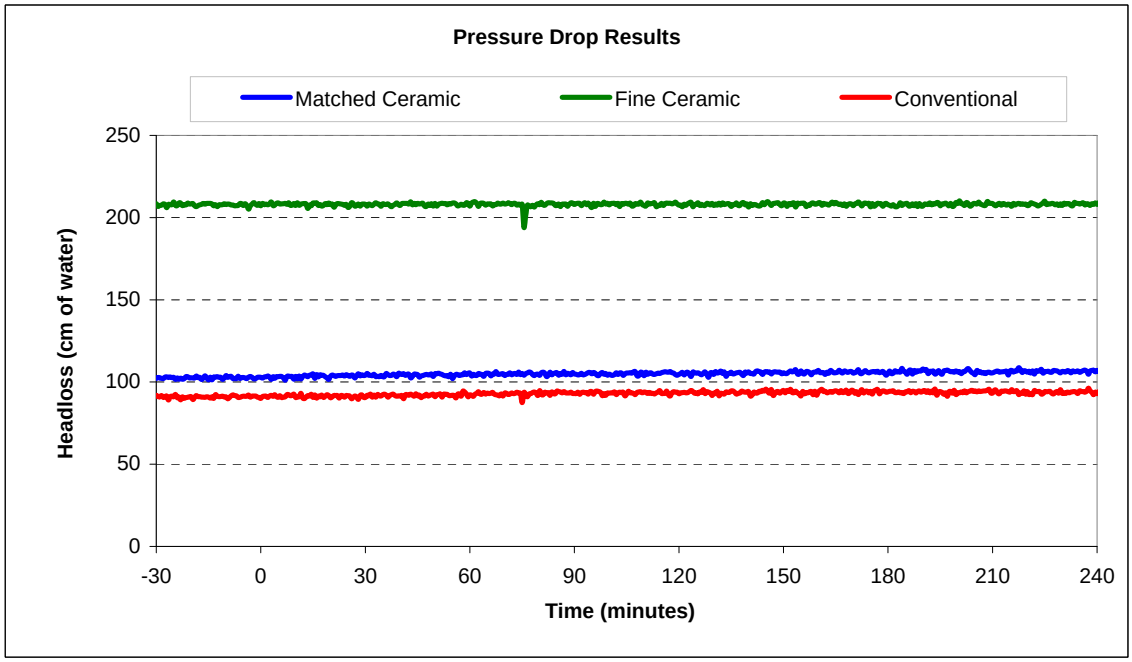

Summary Information for: Trial 3L

Trial Conditions:	
Trial Date	September 12, 2007
Location	Horgan WTP
Water Source	Lake Ontario
Loading Rate	10 GPM/ft^2 (24.4 m/hr)
Coagulation	Alum, 5 mg/L
Water Temperature	22^{0}C

Filter Media Configuration:

	Column 1	**Column 2**	**Column 3**
	Matched Ceramic	Fine Ceramic	Conventional
Top Layer	45 cm ceramic, ES 0.89 mm	45 cm ceramic, ES 0.96 mm	45 cm anthracite, ES 0.89 mm
Bottom Layer	30 cm ceramic, ES 0.47 mm	15 cm ceramic, ES 0.21mm	30 cm sand, ES 0.47 mm
Support Media	20 cm graded gravel bed	20 cm graded gravel bed	20 cm graded gravel bed

Parameter:	**Influent**	**Matched Ceramic**	**Fine Ceramic**	**Conventional**
Log reductions:				
Cryptosporidium		0.28	1.04	0.29
Microspheres		1.86	2.19	0.97
Other Parameters[1]:				
Average turbidity (NTU)	0.349	0.087	0.075	0.107
Turbidity reduction (%)		75	78	69
Average total particle count (#/mL)	1067	306	218	468
Particle reduction (%)		71	80	56
Average flow (mL/min)		1747	1700	1826
Clean bed headloss		76	198	71
Average headloss (cm)		121	253	114
Change in headloss (cm)		134	109	123

[1] *Data calculated from time 0 (start of spike injection) to 360 elapsed minutes*

***Cryptosporidium* and Microsphere Removal Summary:** **Trial 3L**

***Cryptosporidium* Log Removal**

Time	Col 1	Col 2	Col 3
10 min			
20 min	0.35	1.50	0.32
30 min	0.24	0.80	1.10
40 min	-0.13	1.21	-0.19
50 min	0.27	0.40	0.12
60 min			
70 min			
Avg.[1]	**0.28**	**1.04**	**0.29**

[1]*Avgerage denotes time interval from 20 min to 60 min*

Microsphere Log Removal

Time	Col 1	Col 2	Col 3
10 min	2.13	2.36	1.29
20 min	2.04	2.66	1.02
30 min	1.60	2.10	1.56
40 min	1.39	1.96	0.55
50 min	1.85	1.79	0.74
60 min	-0.89	0.39	-0.79
70 min	-0.19	1.46	-0.71
Avg.[1]	**1.86**	**2.19**	**0.97**

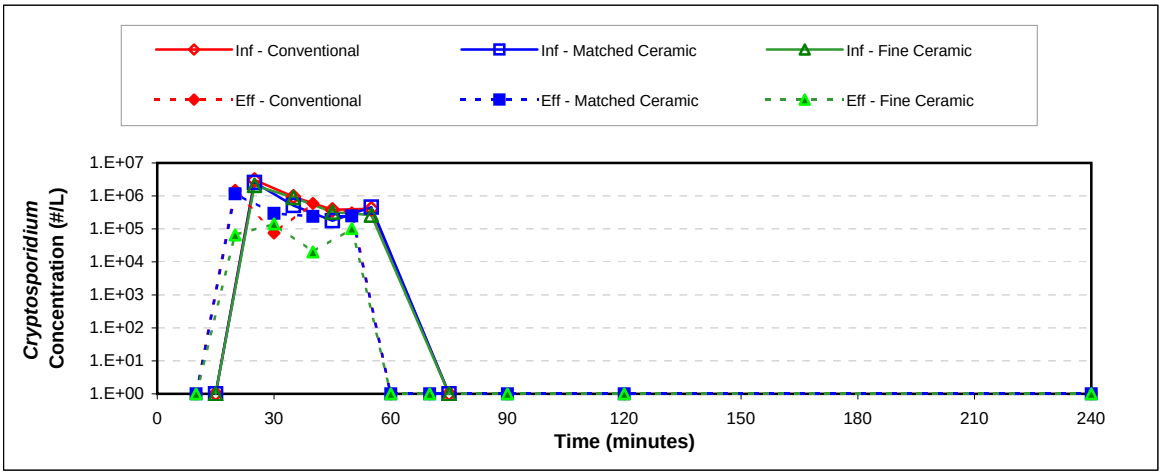

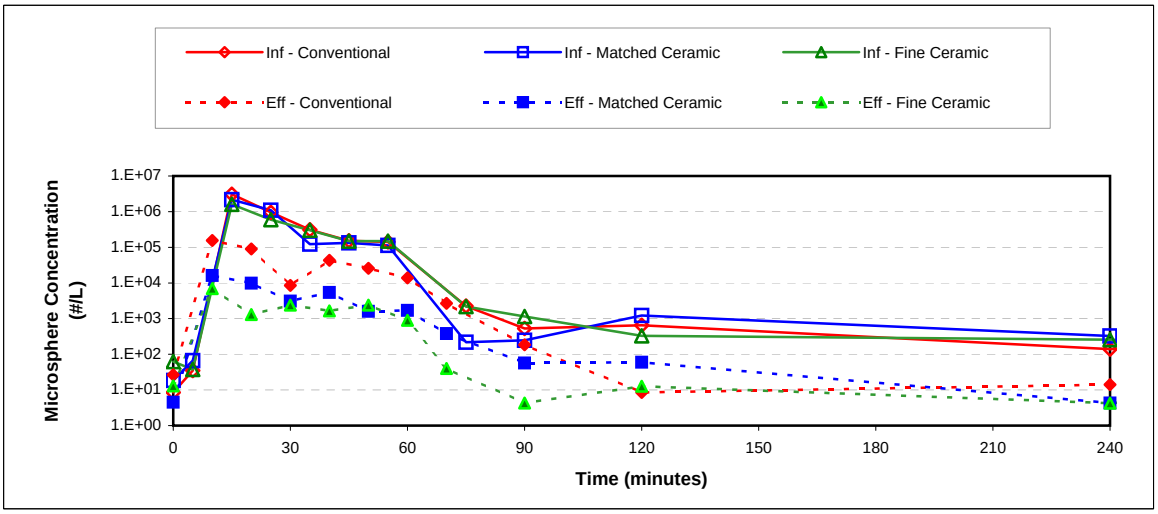

Turbidity Summary: Trial 3L

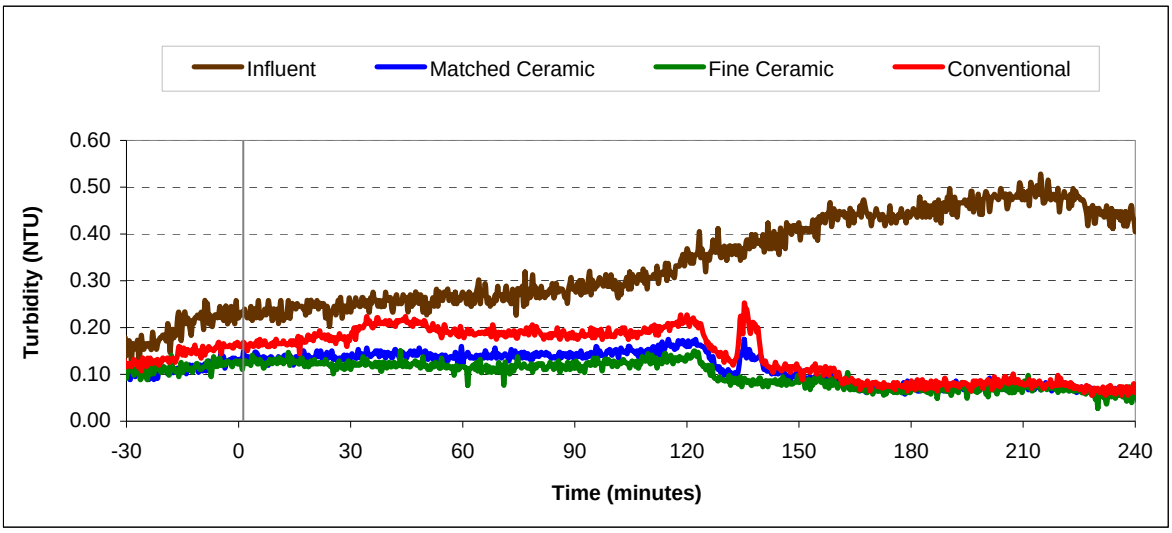

Turbidity Box and Whisker Plots

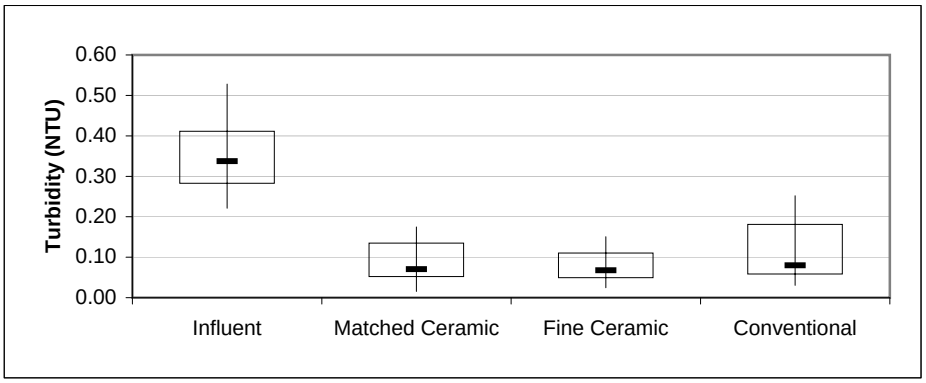

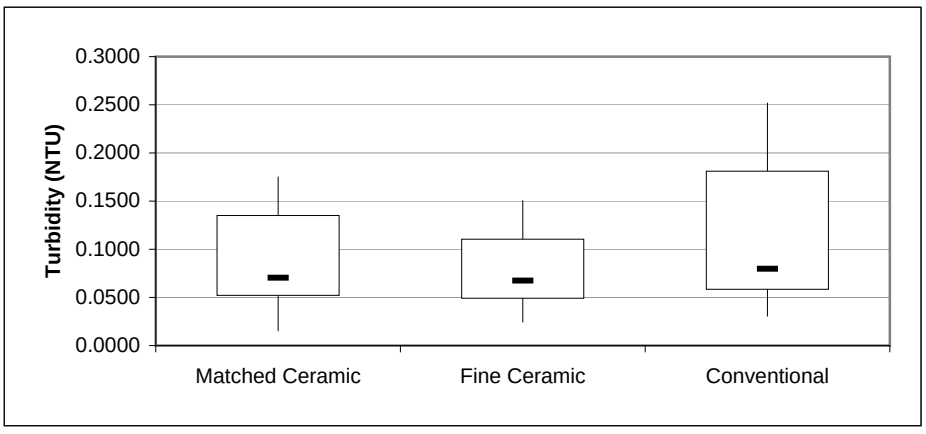

Vertical lines represent maximum and minimum turbidity range. Top and bottom of boxes represent 75th and 25th percentiles of turbidity data. Centre dash represents median turbidity measurement during seeding study.

Particle Count Summary: Trial 3L

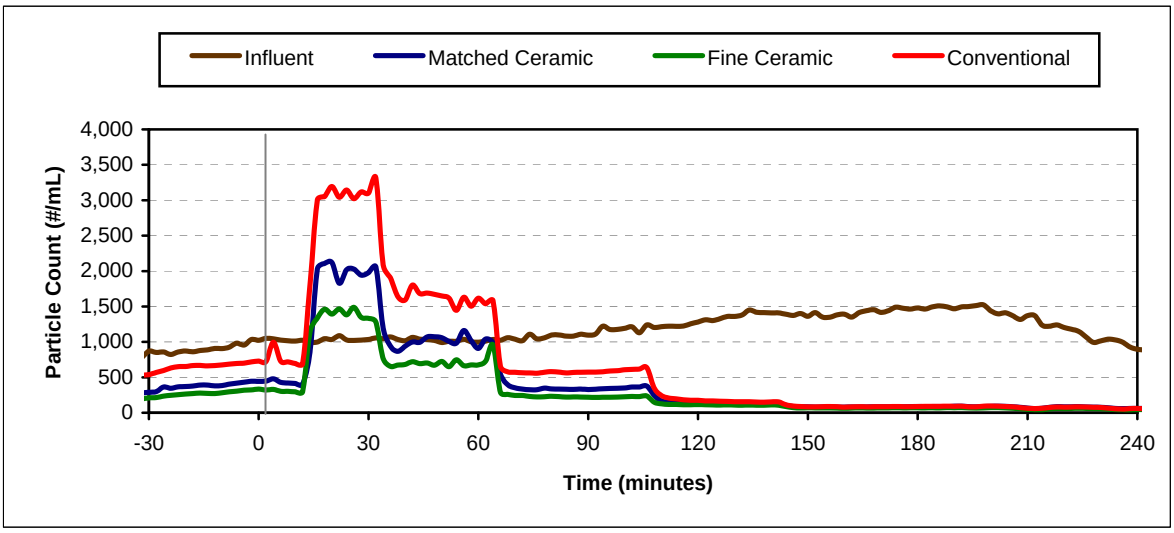

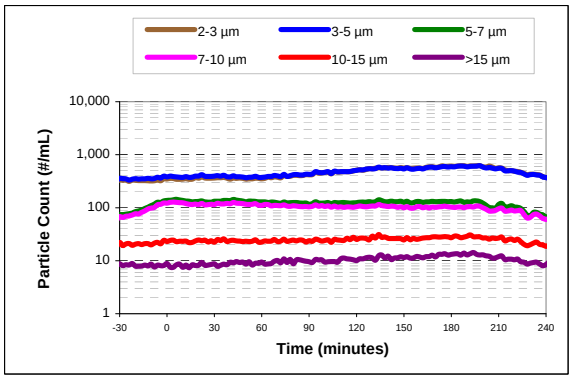

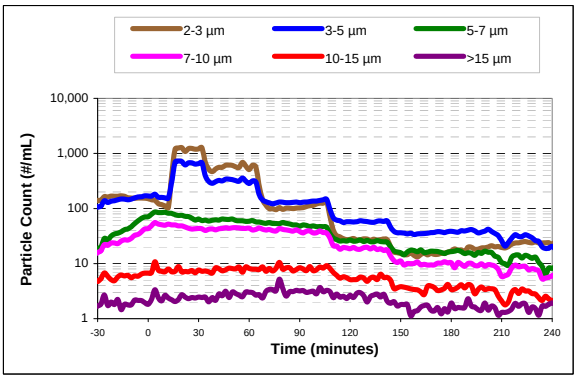

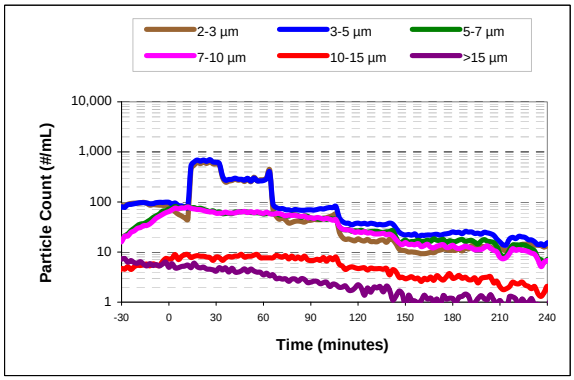

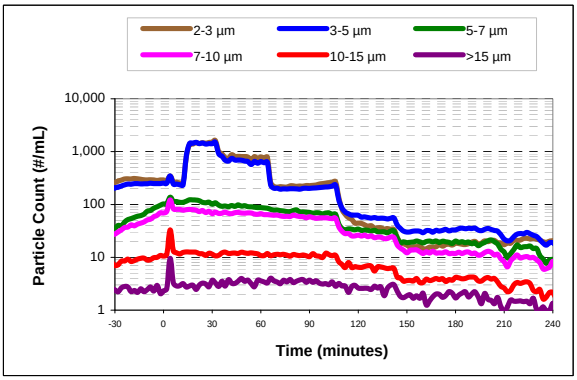

Flow and Headloss Summary: Trial 3L

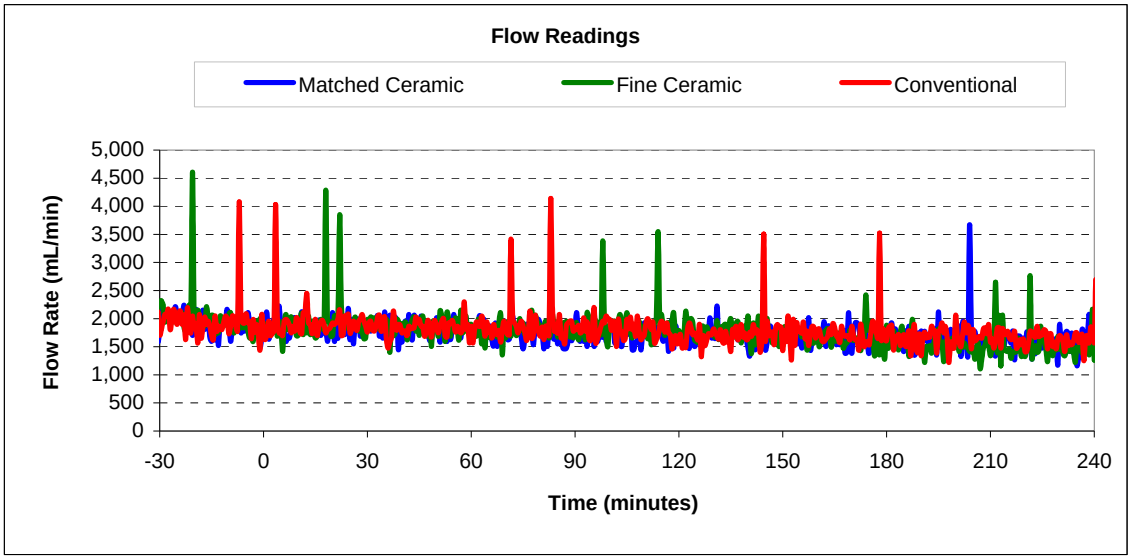

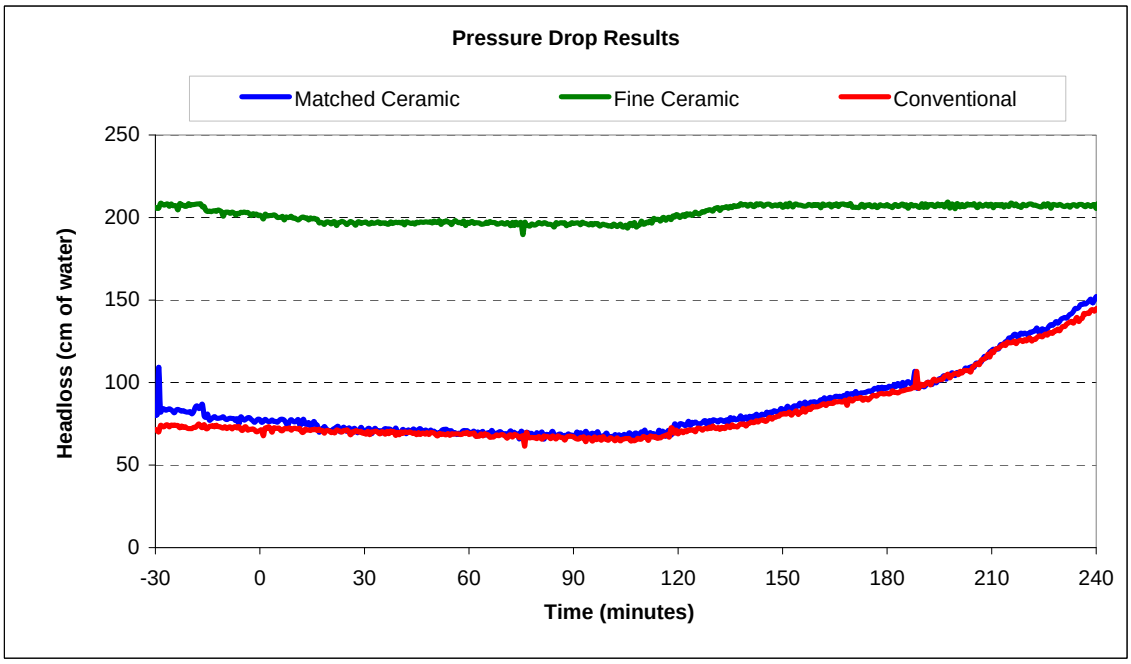

Summary Information for: Trial 3M

Trial Conditions:	
Trial Date	September 13, 2007
Location	Horgan WTP
Water Source	Lake Ontario
Loading Rate	4 GPM/ft^2 (9.8 m/hr)
Coagulation	Alum, 3.7 mg/L
Water Temperature	22^{0}C

Filter Media Configuration:

	Column 1	**Column 2**	**Column 3**
	Matched Ceramic	Fine Ceramic	Conventional
Top Layer	45 cm ceramic, ES 0.89 mm	45 cm ceramic, ES 0.96 mm	45 cm anthracite, ES 0.89 mm
Bottom Layer	30 cm ceramic, ES 0.47 mm	15 cm ceramic, ES 0.21mm	30 cm sand, ES 0.47 mm
Support Media	20 cm graded gravel bed	20 cm graded gravel bed	20 cm graded gravel bed

Parameter:	**Influent**	**Matched Ceramic**	**Fine Ceramic**	**Conventional**
Log reductions:				
Cryptosporidium		1.94	2.54	2.24
Microspheres		3.15	3.58	3.39
Other Parameters[1]:				
Average turbidity (NTU)	0.308	0.056	0.052	0.063
Turbidity reduction (%)		82	83	80
Average total particle count (#/mL)	1115	78	6	91
Particle reduction (%)		93	99	92
Average flow (mL/min)		715	719	859
Clean bed headloss		32	129	62
Average headloss (cm)		65	136	71
Change in headloss (cm)		48	22	23

[1] *Data calculated from time 0 (start of spike injection) to 360 elapsed minutes*

***Cryptosporidium* and Microsphere Removal Summary:** **Trial 3M**

***Cryptosporidium* Log Removal**

Time	Col 1	Col 2	Col 3
10 min			
20 min	1.99	2.42	1.66
30 min	1.84	2.28	2.86
40 min	1.75	2.69	2.02
50 min	2.17	2.91	2.61
60 min			
70 min			
Avg.[1]	**1.94**	**2.54**	**2.24**

[1]*Avgerage denotes time interval from 20 min to 60 min*

Microsphere Log Removal

Time	Col 1	Col 2	Col 3
10 min	3.37	3.29	2.31
20 min	3.24	3.41	2.66
30 min	2.74	3.45	3.57
40 min	3.17	3.50	3.53
50 min	3.58	3.85	3.78
60 min	3.04	4.28	2.82
70 min	2.28	4.45	2.63
Avg.[1]	**3.15**	**3.58**	**3.39**

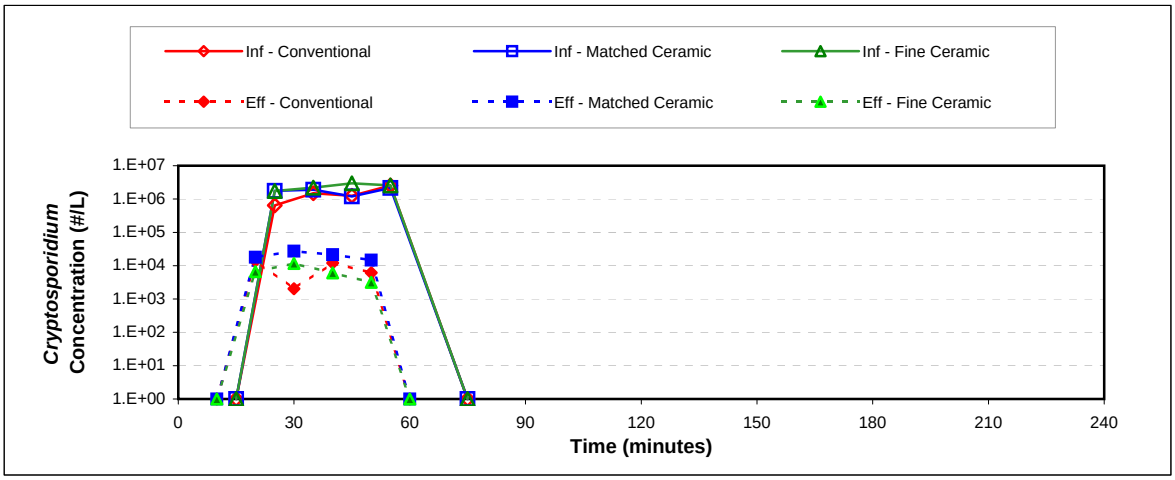

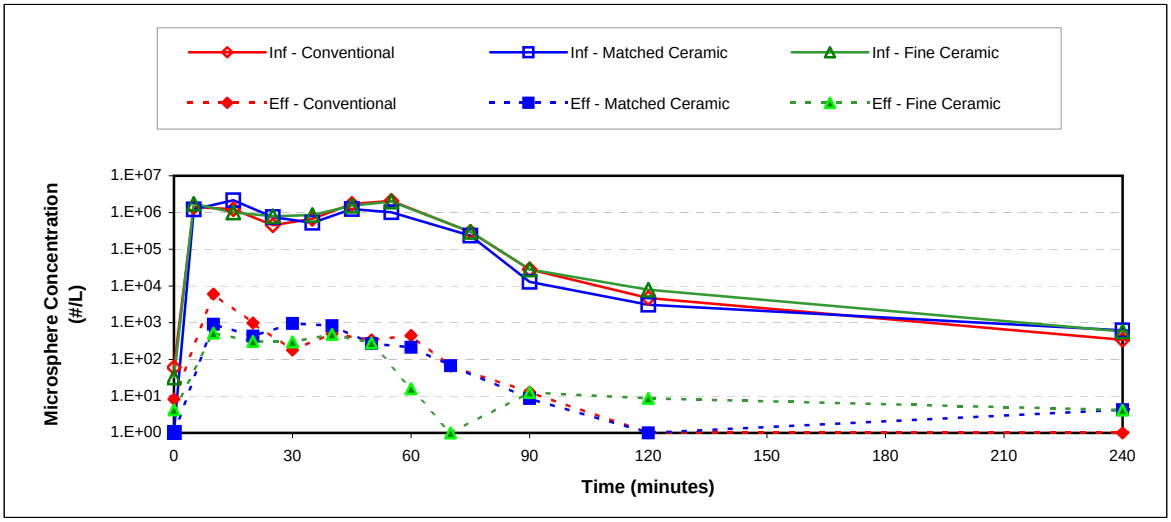

Turbidity Summary: Trial 3M

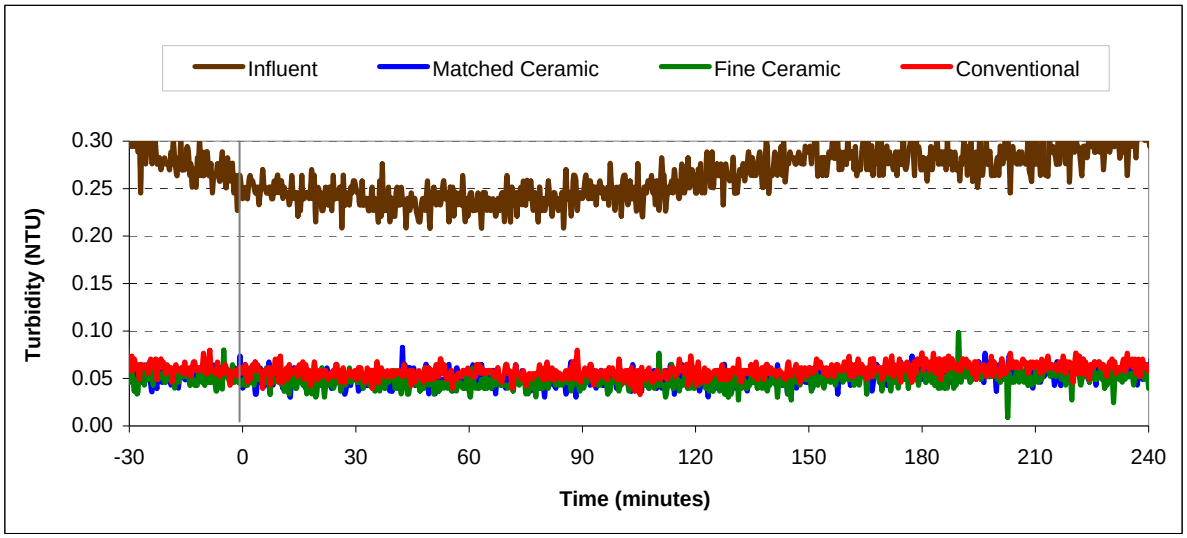

Turbidity Box and Whisker Plots

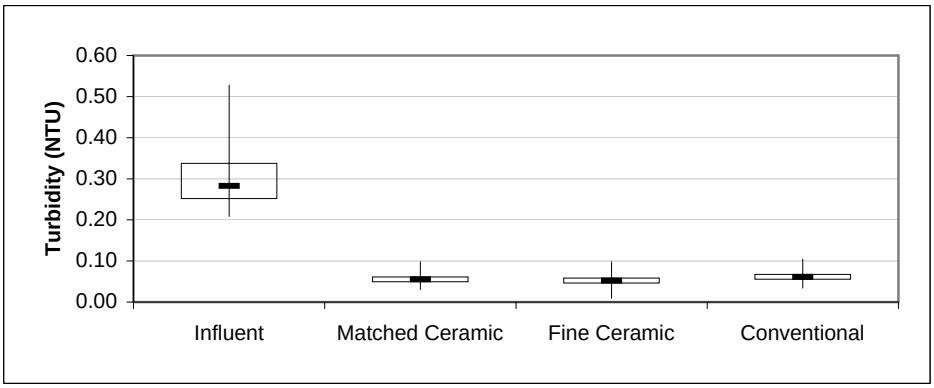

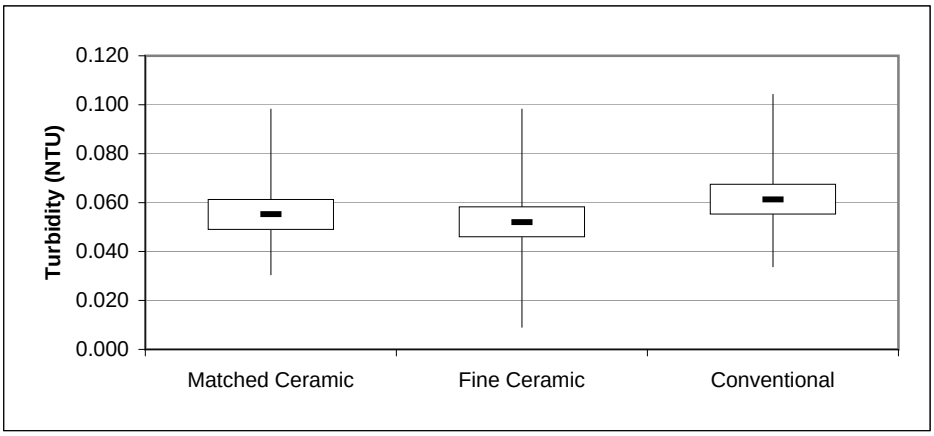

Vertical lines represent maximum and minimum turbidity range. Top and bottom of boxes represent 75th and 25th percentiles of turbidity data. Centre dash represents median turbidity measurement during seeding study.

Particle Count Summary: **Trial 3M**

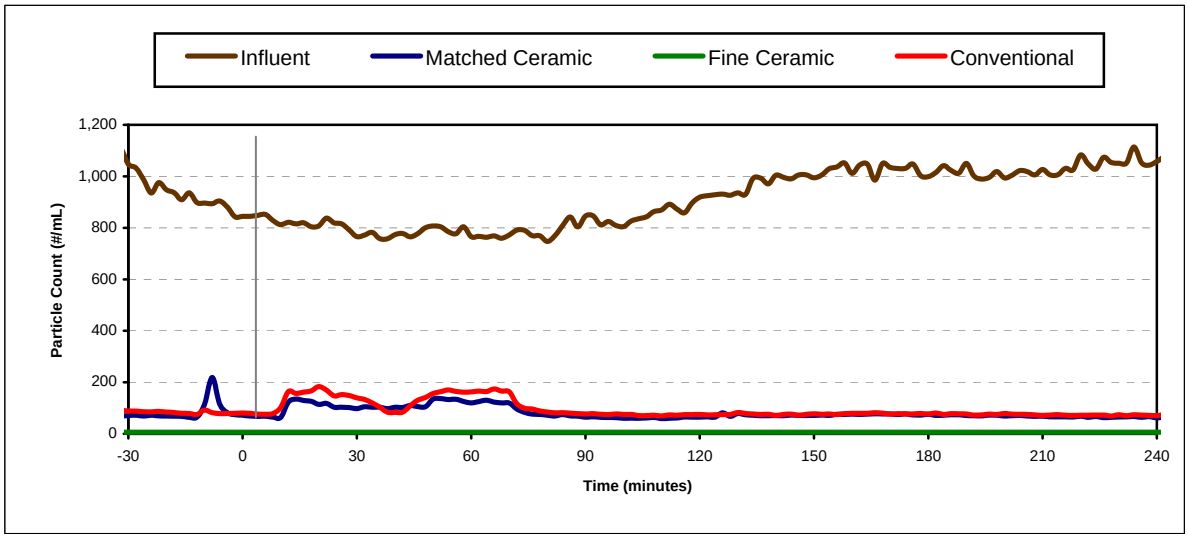

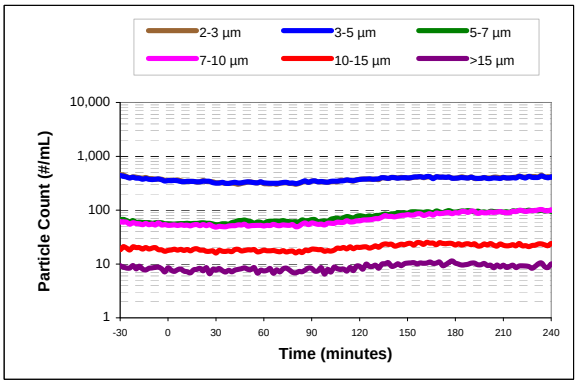

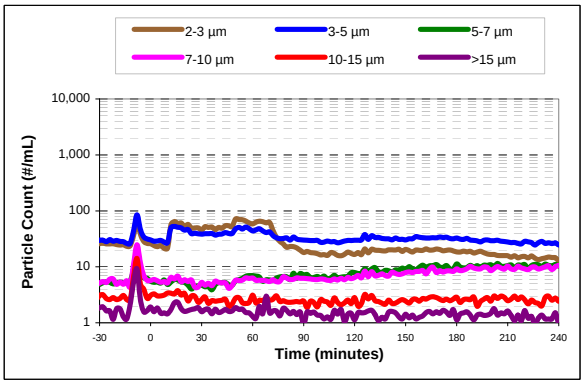

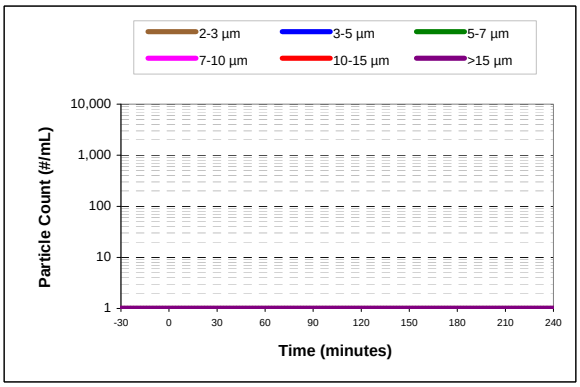

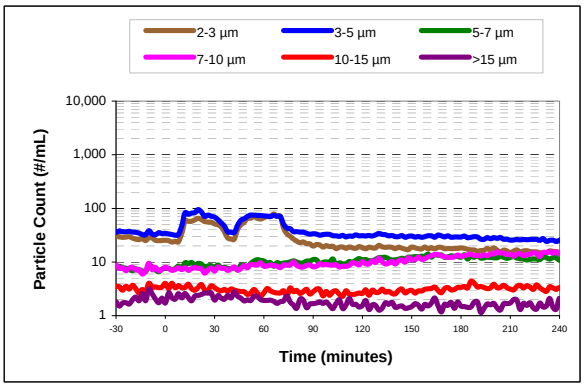

Flow and Headloss Summary: Trial 3M

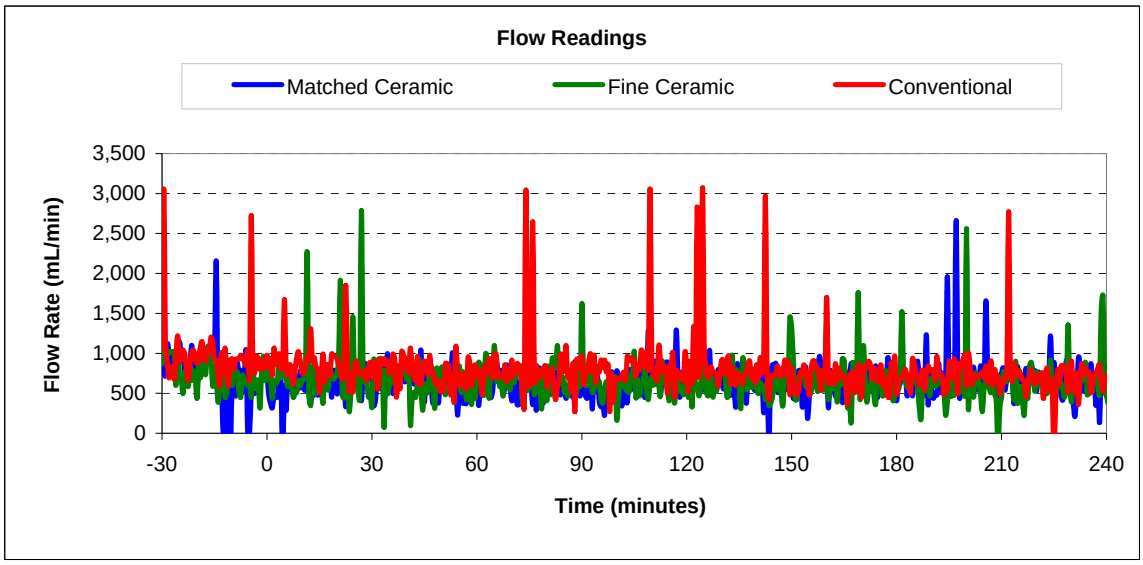

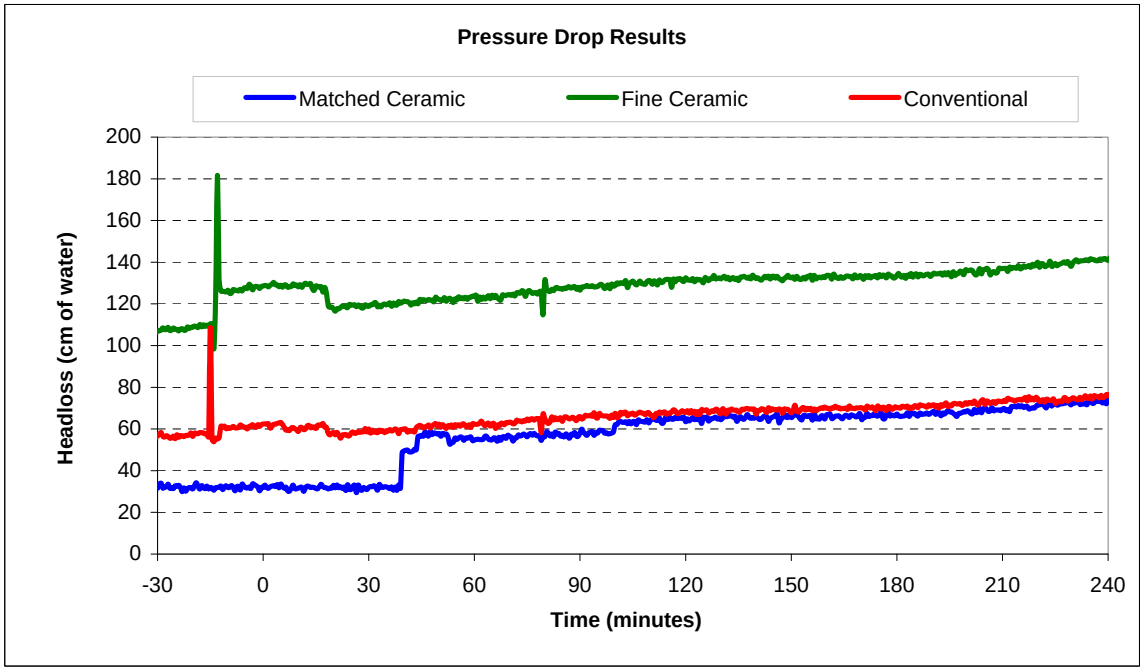

References

Aboytes, R., Di Giovanni, G. D., Abrams, F. A., Rheinecker, C., McElroy, W., Shaw, N., et al. (2004). Detection of infectious *Cryptosporidium* in filtered drinking water. Journal American Water Works Association, 96(9), 88-98.

Adamczyk, Z., Czarnecki, J., & Warszynski, P. (1985). The effect of fluctuations of the energy barrier on colloid stability. Journal of Colloid and Interface Science, 106(2), 299-306.

Aksogan, S., Basturk, A., Yuksel, E., & Akgiray, O. (2003). On the use of crushed shells of apricot stones as the upper layer in dual media filters. Water Science and Technology, 48(11-12), 497-503.

Albinger, O., Biesemeyer, B. K., Arnold, R. G., & Logan, B. E. (1994). Effect of bacterial heterogeneity on adhesion to uniform collectors by monoclonal populations. FEMS Microbiology Letters, 124(3), 321-326.

Allen, M. J., Clancy, J. L., & Rice, E. W. (2000). The plain, hard truth about pathogen monitoring. Journal American Water Works Association, 92(9), 64-76.

Alvarez, A. C., Hime, G., Marchesin, D., & Bedrikovetsky, P. G. (2007). The inverse problem of determining the filtration function and permeability reduction in flow of water with particles in porous media. Transport in Porous Media, 70(1), 43-62.

Amburgey, J. E. (2005). Optimization of the extended terminal subfluidization wash (ETSW) filter backwashing procedure. Water Research, 39(2-3), 314-330.

Amburgey, J. E., & Amirtharajah, A. (2005). Strategic filter backwashing techniques and resulting particle passage. Journal of Environmental Engineering-Asce, 131(4), 535-547.

Amburgey, J. E., Amirtharajah, A., Brouckaert, B. M., & Spivey, N. C. (2003). An enhanced backwashing technique for improved filter ripening. Journal American Water Works Association, 95(12), 81-94.

Amburgey, J. E., Amirtharajah, A., York, M. T., Brouckaert, B. M., Spivey, N. C., & Arrowood, M. J. (2005). Comparison of conventional and biological filter performance for *Cryptosporidium* and microsphere removals. Journal American Water Works Association, 97(12), 77-+.

Angus, K. W. (1983). Cryptosporidiosis in man, domestic-animals and birds - a review. Journal of the Royal Society of Medicine, 76(1), 62-70.

Bai, R., & Tien, C. (1999). Particle deposition under unfavorable surface interactions. Journal of Colloid and Interface Science, 218(2), 488-499.

Bai, R., & Tien, C. (2000). Effect of deposition in deep-bed filtration: Determination and search of rate parameters. Journal of Colloid and Interface Science, 231(2), 299-311.

Bandyopadhyay, K., Kellar, K. L., Moura, I., Cristina, M., Carollo, C., Graczyk, T. K., et al. (2007). Rapid microsphere assay for identification of *Cryptosporidium* hominis and *Cryptosporidium* parvum in stool and environmental samples. Journal of Clinical Microbiology, 45(9), 2835-2840.

Barton, J. W., & Ford, R. M. (1997). Mathematical model for characterization of bacterial migration through sand cores. Biotechnology and Bioengineering, 53(5), 487-496.

Batra, A., Paria, S., Manohar, C., & Khilar, K. C. (2001). Removal of surface adhered particles by surfactants and fluid motions. AICHE Journal, 47(11), 2557-2565.

Bergendahl, J. A., & Grasso, D. (2003). Mechanistic basis for particle detachment from granular media. Environmental Science & Technology, 37(10), 2317-2322.

Bergendahl, J., & Grasso, D. (1998). Colloid generation during batch leaching experiments: Mechanics of disaggregation. Colloids and Surfaces A: Physicochemical and Engineering Aspects, 135(1-3), 193-205.

Bhattacharjee, S., Chen, J. Y., & Elimelech, M. (2000). DLVO interaction energy between spheroidal particles and a fiat surface. Colloids and Surfaces A-Physicochemical and Engineering Aspects, 165(1-3), 143-156.

Bhattacharjee, S., & Elimelech, M. (1997). Prediction of DLVO interaction energy and particle deposition rates for rough surfaces. Abstracts of Papers of the American Chemical Society, 214, 40-COLL.

Bhattacharjee, S., & Elimelech, M. (2000). Particle deposition dynamics in a bed of spherical collectors: Beyond random sequential adsorption. Abstracts of Papers of the American Chemical Society, 220, U228-U228.

Bhattacharjee, S., Elimelech, M., & Borkovec, M. (1998). DLVO interaction between colloidal particles: Beyond Derjaguin's approximation. Croatica Chemica Acta, 71(4), 883-903.

Bhattacharjee, S., Ko, C. H., & Elimelech, M. (1998). DLVO interaction between rough surfaces. Langmuir, 14(12), 3365-3375.

Bhattacharjee, S., Nazemifard, N., & Masliyah, J. (2005). Particle deposition onto micro-patterned charged heterogeneous substrates. Abstracts of Papers of the American Chemical Society, 229, U647-U647.

Biswas, N., Arbuckle, W. B., & Hajra, M. G. (2003). Polyurethane foam filter. Journal American Water Works Association, 95(5), 183-188.

Bodley-Tickell, A. T., Kitchen, S. E., & Sturdee, A. P. (2002). Occurrence of *Cryptosporidium* in agricultural surface waters during an annual farming cycle in lowland UK. Water Research, 36(7), 1880-1886.

Bradford, S. A., & Bettahar, M. (2005). Straining, attachment, and detachment of *Cryptosporidium* oocysts in saturated porous media. Journal of Environmental Quality, 34(2), 469-478.

Bradford, S. A., Bettahar, M., Simunek, J., & van Genuchten, M. T. (2004). Straining and attachment of colloids in physically heterogeneous porous media. Vadose Zone Journal, 3(2), 384-394.

Bradford, S. A., Simunek, J., Bettahar, M., Tadassa, Y. F., van Genuchten, M. T., & Yates, S. R. (2005). Straining of colloids at textural interfaces. Water Resources Research, 41(10), W10404.

Bradford, S. A., Simunek, J., Bettahar, M., Van Genuchten, M. T., & Yates, S. R. (2003). Modeling colloid attachment, straining, and exclusion in saturated porous media. Environmental Science & Technology, 37(10), 2242-2250.

Bradford, S. A., Simunek, J., Bettahar, M., van Genuchten, M. T., & Yates, S. R. (2006). Significance of straining in colloid deposition: Evidence and implications. Water Resources Research, 42(12), W12S15.

Bradford, S. A., Torkzaban, S., & Walker, S. L. (2007). Coupling of physical and chemical mechanisms of colloid straining in saturated porous media. Water Research, 41(13), 3012-3024.

Bradford, S., Torkzaban, S., & Walker, S. (2007). Coupling of physical and chemical mechanisms of colloid straining in saturated porous media. Water Research, 41(13), 3012-3024.

Brown, D. G., & Jaffe, P. R. (2001). Effects of nonionic surfactants on bacterial transport through porous media. Environmental Science & Technology, 35(19), 3877-3883.

Brown, D. G., & Jaffe, P. R. (2006). Effects of nonionic surfactants on the cell surface hydrophobicity and apparent Hamaker constant of a sphingomonas sp. Environmental Science & Technology, 40(1), 195-201.

Burenbaatar, B., Bakheit, M. A., Plutzer, J., Suzuki, N., Igarashi, I., Ongerth, J., et al. (2008). Prevalence and genotyping of *Cryptosporidium* species from farm animals in Mongolia. Parasitology Research, 102(5), 901-905.

Bustamante, H. A., Shanker, S. R., Pashley, R. M., & Karaman, M. E. (2001). Interaction between *Cryptosporidium* oocysts and water treatment coagulants. Water Research, 35(13), 3179-3189.

Byrd, T. L., & Walz, J. Y. (2007). Investigation of the interaction force between *Cryptosporidium* parvum oocysts and solid surfaces. Langmuir, 23(14), 7475-7483.

Caliskaner, O., & Tchobanoglous, G. (2005). Modeling depth filtration of activated sludge effluent using a compressible medium filter. Water Environment Research, 77(7), 3080-3091.

Caliskaner, O., Tchobanoglous, G., & Carolan, A. (1999). High-rate filtration with a synthetic compressible media. Water Environment Research, 71(6), 1171-1177.

Carey, C. M., Lee, H., & Trevors, J. T. (2004). Biology, persistence and detection of *Cryptosporidium* parvum and *Cryptosporidium* hominis oocyst. Water Research, 38(4), 818-862.

Carreno, R. A., Martin, D. S., & Barta, J. R. (1999). *Cryptosporidium* is more closely related to the gregarines than to coccidia as shown by phylogenetic analysis of apicomplexan parasites inferred using small-subunit ribosomal RNA gene sequences. Parasitology Research, 85(11), 899-904.

Chen, J. N., Truesdail, S., Lu, F. H., Zhan, G. G., Belvin, C., Koopman, B., et al. (1998). Long-term evaluation of aluminum hydroxide-coated sand for removal of bacteria from wastewater. Water Research, 32(7), 2171-2179.

Chitikela, S., Dentel, S. K., & Allen, H. E. (1995). Modified method for the analysis of anionic surfactants as methylene-blue active substances. Analyst, 120(7), 2001-2004.

Clancy, J. L., Bukhari, Z., McCuin, R. M., Matheson, Z., & Fricker, C. R. (1999). USEPA method 1622. Journal American Water Works Association, 91(9), 60-68.

Clean Washington Centre. (1998). Evaluation of recycled crushed glass sand media for high-rate sand filtration. Report No. GL-98-1

Colton, J. F., Hillis, P., & Fitzpatrick, C. S. B. (1996). Filter backwash and start-up strategies for enhanced particulate removal. Water Research, 30(10), 2502-2507.

Connell, K., Clancy, J., Regli, S., Messner, M., Rodgers, C., Fricker, C., et al. (2001). Discussion of: "evaluation of USEPA method 1622 for detection of *Cryptosporidium* oocysts in stream waters". Journal American Water Works Association, 93(3), 106-108.

Considine, R. F., Dixon, D. R., & Drummond, C. J. (2002). Oocysts of *Cryptosporidium* parvum and model sand surfaces in aqueous solutions: An atomic force microscope (AFM) study. Water Research, 36(14), 3421-3428.

Considine, R. F., & Drummond, C. J. (2001). Surface roughness and surface force measurement: A comparison of electrostatic potentials derived from atomic force microscopy and electrophoretic mobility measurements. Langmuir, 17(25), 7777-7783.

Considine, R. F., Drummond, C. J., & Dixon, D. R. (2001). Force of interaction between a biocolloid and an inorganic oxide: Complexity of surface deformation, roughness, and brush like behavior. Langmuir, 17(20), 6325-6335.

Coupe, S., Delabre, K., Pouillot, R., Houdart, S., Santillana-Hayat, M., & Derouin, F. (2006). Detection of *Cryptosporidium*, giardia and enterocytozoon bieneusi in surface water, including recreational areas: A one-year prospective study. FEMS Immunology and Medical Microbiology, 47(3), 351-359.

Craun, G. F., Calderon, R. L., & Craun, M. F. (2005). Outbreaks associated with recreational water in the United States. International Journal of Environmental Health Research, 15(4), 243-262.

Cushing, R. S., & Lawler, D. F. (1998). Depth filtration: Fundamental investigation through three dimensional trajectory analysis. Environmental Science & Technology, 32(23), 3793-3801.

Czarnecki, J. (1986). The effects of surface inhomogeneities on the interactions in colloidal systems and colloid stability. Advances in Colloid and Interface Science, 24(4), 283-319.

Czarnecki, J., & Dabros, T. (1980). Attenuation of the van der Waals attraction energy in the particle semi-infinite medium system due to the roughness of the particle surface. Journal of Colloid and Interface Science, 78(1), 25-30.

Czarnecki, J., & Itschenskij, V. (1984). van der Waals attraction energy between unequal rough spherical-particles. Journal of Colloid and Interface Science, 98(2), 590-591.

Czarnecki, J., & Warszynski, P. (1987). The evaluation of tangential forces due to surface inhomogeneities in the particle deposition process. Colloids and Surfaces, 22(2-4), 207-214.

Czarnecki, J. (1985). The effects of surface inhomogeneities on the interactions in colloidal systems and colloid stability. Advances in Colloid and Interface Science, 24, 283-319.

Darby, J. L., & Lawler, D. F. (1990). Ripening in depth filtration: Effect of particle size on removal and head loss. Environmental Science & Technology, 24(7), 1069-1079.

Dawson, D. J., Samuel, C. M., Scrannage, V., & Atherton, C. J. (2004). Survival of *Cryptosporidium* species in environments relevant to foods and beverages. Journal of Applied Microbiology, 96(6), 1222-1229.

Dietrich, J., Loge, F., Ginn, T., & Başagˇaogˇlu, H. (2007). Inactivation of particle-associated microorganisms in wastewater disinfection: Modeling of ozone and chlorine reactive diffusive transport in polydispersed suspensions. Water Research, 41(10), 2189-2201.

Duval, J. F. L., Leermakers, F. A. M., & van Leeuwen, H. P. (2004). Electrostatic interactions between double layers: Influence of surface roughness, regulation, and chemical heterogeneities. Langmuir, 20(12), 5052-5065.

Duval, J. F. L., Leermakers, F. A. M., & vanLeeuwen, H. P. (2004). Electrostatic interactions between double layers: Influence of surface roughness, regulation, and chemical heterogeneities. Langmuir, 20(12), 5052-5065.

Eichenlaub, S., Gelb, A., & Beaudoin, S. (2004). Roughness models for particle adhesion. Journal of Colloid and Interface Science, 280(2), 289-298.

Eichenlaub, S., Kumar, G., & Beaudoin, S. (2006). A modeling approach to describe the adhesion of rough, asymmetric particles to surfaces. Journal of Colloid and Interface Science, 299(2), 656-664.

Eichenlaub, S., Gelb, A., & Beaudoin, S. (2004). Roughness models for particle adhesion. Journal of Colloid and Interface Science, 280(2), 289-298.

Eikebrokk, B., & Saltnes, T. (2002). NOM removal from drinking water by chitosan coagulation and filtration through lightweight expanded clay aggregate filters. Journal of Water Supply Research and Technology-Aqua, 51(6), 323-332.

Elimelech, M. (1994). Effect of particle-size on the kinetics of particle deposition under attractive double-layer interactions (vol. 164, pg 190, 1994). Journal of Colloid and Interface Science, 166(1), 266-266.

Elimelech, M., Chen, J. Y., & Kuznar, Z. A. (2003). Particle deposition onto solid surfaces with micropatterned charge heterogeneity: The "hydrodynamic bump" effect. Langmuir, 19(17), 6594-6597.

Elimelech, M., Kuznar, Z. A., & Chen, J. Y. (2003). Deposition of colloidal particles on chemically heterogeneous surfaces: Role of microscopic surface charge heterogeneity. Abstracts of Papers of the American Chemical Society, 226, U479-U479.

Elimelech, M., Nagai, M., Ko, C. -., & Ryan, J. N. (2000). Relative insignificance of mineral grain zeta potential to colloid transport in geochemically heterogeneous porous media. Environmental Science & Technology, 34(11), 2143-2148.

Elimelech, M., & Omelia, C. R. (1990). Kinetics of deposition of colloidal particles in porous-media. Environmental Science & Technology, 24(10), 1528-1536.

Elliott, R. W. (2001). Evaluation of the use of crushed recycled glass as a filter medium: Part 1. Water-Engineering & Management, 148(7), 13-+.

Elliott, R. W. (2001). Evaluation of the use of crushed recycled glass as a filter medium: Part 2. Water-Engineering & Management, 148(8), 17-20.

Emelko, M. B. (2003). Removal of viable and inactivated *Cryptosporidium* by dual- and tri-media filtration. Water Research, 37(12), 2998-3008.

Emelko, M.B. and Brown, T.J. Chitosan Coagulation at Low, Cost-Effective Dosages: Impacts on Filtration of Particles and Pathogens. In Proc. of the 11th International Gothenburg Symposium on Chemical Treatment, 2004.

Emelko, M. B., & Huck, P. M. (2004). Microspheres as surrogates for *Cryptosporidium* filtration. Journal American Water Works Association, 96(3), 94-105.

Emelko, M. B., Huck, P. M., & Coffey, B. M. (2005). A review of *Cryptosporidium* Oocyst Removal by granular media filtration. Journal American Water Works Association, 97(12), 101-+.

Emelko, M. B., Huck, P. M., & Douglas, I. P. (2003). *Cryptosporidium* and microsphere removal during late in-cycle filtration. Journal American Water Works Association, 95(5), 173-182.

Fall, A., Thompson, R. C. A., Hobbs, R. P., & Morgan-Ryan, U. (2003). Morphology is not a reliable tool for delineating species within *Cryptosporidium*. Journal of Parasitology, 89(2), 399-402.

Farizoglu, B., Nuhoglu, A., Yildiz, E., & Keskinler, B. (2003/4). The performance of pumice as a filter bed material under rapid filtration conditions. Filtration & Separation, 40(3), 41-47.

Fayer, R. (2004). *Cryptosporidium*: A water-borne zoonotic parasite. Veterinary Parasitology, 126(1-2), 37-56.

Fayer, R., & Ungar, B. L. P. (1986). *Cryptosporidium* spp and cryptosporidiosis. Microbiological Reviews, 50(4), 458-483.

Fitzpatrick, C. S. B. (1998). Instrumentation for investigating and optimising filter backwashing. Filtration & Separation, 35(1), 69-72.

Fletcher, P., Stephenson, T., & Judd, S. (1994). The use of an applied electric-field for the filtration of particles from a low conductivity aqueous suspension. Chemical Engineering Science, 49(14), 2371-2378.

Frisby, H. R., Addiss, D. G., Reiser, W. J., Hancock, B., Vergeront, J. M., Hoxie, N. J., et al. (1997). Clinical and epidemiologic features of a massive waterborne outbreak of cryptosporidiosis in persons with HIV infection. Journal of Acquired Immune Deficiency Syndromes and Human Retrovirology, 16(5), 367-373.

Frost, F. J., Roberts, M., Kunde, T. R., Craun, G., Tollestrup, K., Harter, L., et al. (2005). How clean must our drinking water be: The importance of protective immunity. Journal of Infectious Diseases, 191(5), 809-814.

Frost, R. J., Muller, T., Craun, G. F., Lockwood, W. B., & Calderon, R. L. (2002). Serological evidence of endemic waterborne *Cryptosporidium* infections. Annals of Epidemiology, 12(4), 222-227.

Gaillard, J. F., Chen, C., Stonedahl, S. H., Lau, B. L. T., Keane, D. T., & Packman, A. I. (2007). Imaging of colloidal deposits in granular porous media by X-ray difference micro-tomography. Geophysical Research Letters, 34(18), L18404.

Gatei, W., Das, P., Dutta, P., Sen, A., Cama, V., Lal, A. A., et al. (2007). Multilocus sequence typing and genetic structure of *Cryptosporidium* hominis from children in Kolkata, India. Infection Genetics and Evolution, 7(2), 197-205.

Gimbel, R., & Nahrstedt, A. (1997). Removal of different kinds of particles in deep bed filters consisting of permeable synthetic collectors (PSC). Water Science and Technology, 36(4), 249-258.

Ginn, T. R., Wood, B. D., Nelson, K. E., Scheibe, T. D., Murphy, E. M., & Clement, T. P. (2002). Processes in microbial transport in the natural subsurface. Advances in Water Resources, 25(8-12), 1017-1042.

Gross, M. J., & Logan, B. E. (1995). Influence of different chemical treatments on transport of alcaligenes paradoxus in porous-media. Applied and Environmental Microbiology, 61(5), 1750-1756.

Hahn, M. W., Abadzic, D., & O'Melia, C. R. (2004). Aquasols: On the role of secondary minima. Environmental Science & Technology, 38(22), 5915-5924.

Hahn, M. W., & O'Melia, C. R. (2004). Deposition and reentrainment of brownian particles in porous media under unfavorable chemical conditions: Some concepts and applications. Environmental Science & Technology, 38(1), 210-220.

Hancock, C. M., Rose, J. B., & Callahan, M. (1998). *C. parvum* and giardia in US groundwater. Journal American Water Works Association, 90(3), 58-61.

Hansen, J. S., & Ongerth, J. E. (1991). Effects of time and watershed characteristics on the concentration of *Cryptosporidium* oocysts in river water. Applied and Environmental Microbiology, 57(10), 2790-2795.

Harrington, G. W., Xagoraraki, I., Assavasilavasukul, P., & Standridge, J. H. (2003). Effect of filtration conditions on removal of emerging waterborne pathogens. Journal American Water Works Association, 95(12), 95-104.

Harris, J. R., & Petry, F. (1999). *Cryptosporidium* parvum: Structural components of the oocyst wall. Journal of Parasitology, 85(5), 839-849.

Herman, M. C., & Papadopoulos, K. D. (1990). Effects of asperities on the van der Waals and electric double-layer interactions of 2 parallel flat plates. Journal of Colloid and Interface Science, 136(2), 385-392.

Herman, M., & Papadopoulos, K. (1990). Effects of asperities on the van der Waals and electric double-layer interactions of two parallel flat plates. Journal of Colloid and Interface Science, 136(2), 385-392.

Herzig, J. P., Leclerc, D. M., & Goff, P. L. (1970). Flow of suspensions through porous Media—Application to deep filtration. Industrial & Engineering Chemistry, 62(5), 8-35.

Hoek, E. M. V., Bhattacharjee, S., & Elimelech, M. (2003). Effect of membrane surface roughness on colloid-membrane DLVO interactions. Langmuir, 19(11), 4836-4847.

Hoek, E. M. V., & Agarwal, G. K. (2006). Extended DLVO interactions between spherical particles and rough surfaces. Journal of Colloid and Interface Science, 298(1), 50-58.

Hoxie, N. J., Davis, J. P., Vergeront, J. M., Nashold, R. D., & Blair, K. A. (1997). Cryptosporidiosis-associated mortality following a massive waterborne outbreak in Milwaukee, Wisconsin. American Journal of Public Health, 87(12), 2032-2035.

Huck, P. M., Coffey, B. M., Emelko, M. B., Maurizio, D. D., Slawson, R. M., Anderson, W. B., et al. (2002). Effects of filter operation on *Cryptosporidium* Removal. Journal American Water Works Association, 94(6), 97-111.

Hull, M., & Kitchener, J. (1969). Interaction of spherical colloidal particles with planar surfaces. Transactions of the Faraday Society, 65(563P), 3093-&.

Humby, M. S., & Fitzpatrick, C. S. B. (1996). Attrition of granular filter media during backwashing with combined air and water. Water Research, 30(2), 291-294.

Hunt, J. R., Hwang, B. C., & McDowell-Boyer, L. M. (1993). Solids accumulation during deep bed filtration. Environmental Science & Technology, 27(6), 1099-1107.

Jittapalapong, S., Pinyopanuwat, N., Chimnoi, W., Siripanth, C., & Stich, R. W. (2006). Prevalence of *Cryptosporidium* among dairy cows in Thailand. Impact of Emerging Zoonotic Diseases on Animal Health, 1081, 328-335.

Johnson, W. P., Li, X., & Yal, G. (2007). Colloid retention in porous media: Mechanistic confirmation of wedging and retention in zones of flow stagnation. Environmental Science & Technology, 41(4), 1279-1287.

Karaman, M. E., Pashley, R. M., Bustamante, H., & Shanker, S. R. (1999). Microelectrophoresis of *Cryptosporidium* parvum oocysts in aqueous solutions of inorganic and surfactant cations. Colloids and Surfaces A-Physicochemical and Engineering Aspects, 146(1-3), 217-225.

Kasuga, I., Shimazaki, D., & Kunikane, S. (2007). Influence of backwashing on the microbial community in a biofilm developed on biological activated carbon used in a drinking water treatment plant. Water Science and Technology, 55(8-9), 173-180.

Kau, S. M., & Lawler, D. F. (1995). Dynamics of deep-bed filtration - velocity, depth, and media. Journal of Environmental Engineering-Asce, 121(12), 850-859.

Kaur, P., Fitzpatrick, C. S. B., & Kerr, C. (2003). Biofilm formation in granular-bed filters. Journal of the Chartered Institution of Water and Environmental Management, 17(3), 145-148.

Kemps, J. A. L., & Bhattacharjee, S. (2005). Interactions between a solid spherical particle and a chemically heterogeneous planar substrate. Langmuir, 21(25), 11710-11721.

Kim, J., Nason, J. A., & Lawler, D. F. (2006). Zeta potential distributions in particle treatment processes. Journal of Water Supply Research and Technology-Aqua, 55(7-8), 461-470.

Kinetico Incorporated. (1994). Material safety data sheet for macrolite ceramic spheres. Newbury OH: Kinetico Incorporated.

Kinetico Incorporated. (2008). Macrolite.http://international.kinetico.com/Kinetico/EN/Municipal/Products/Filtration/Macrolite/

Kistemann, T., Classen, T., Koch, C., Dangendorf, F., Fischeder, R., Gebel, J., et al. (2002). Microbial load of drinking water reservoir tributaries during extreme rainfall and runoff. Applied and Environmental Microbiology, 68(5), 2188-2197.

Ko, C. H., Bhattacharjee, S., & Elimelech, M. (1999). The "shadow effect" in colloid transport and deposition dynamics in granular porous media: Measurements and mechanisms. Abstracts of Papers of the American Chemical Society, 217, U731-U731.

Ko, C. H., & Elimelech, M. (2000). The "shadow effect" in colloid transport and deposition dynamics in granular porous media: Measurements and mechanisms. Environmental Science & Technology, 34(17), 3681-3689.

Kuznar, Z. A., & Elimelech, M. (2004). Adhesion kinetics of viable *Cryptosporidium* parvum oocysts to quartz surfaces. Environmental Science & Technology, 38(24), 6839-6845.

Kuznar, Z. A., & Elimelech, M. (2004). Deposition kinetics of *Cryptosporidium* parvum oocysts onto quartz surfaces. Abstracts of Papers of the American Chemical Society, 228, U633-U633.

Kuznar, Z. A., & Elimelech, M. (2005). Role of surface proteins in the deposition kinetics of *Cryptosporidium* parvum oocysts. Langmuir, 21(2), 710-716.

Kuznar, Z. A., & Elimelech, M. (2006). *Cryptosporidium* oocyst surface macromolecules significantly hinder oocyst attachment. Environmental Science & Technology, 40(6), 1837-1842.

Kuznar, Z. A., & Elimelech, M. (2007). Direct microscopic observation of particle deposition in porous media: Role of the secondary energy minimum. Colloids and Surfaces A-Physicochemical and Engineering Aspects, 294(1-3), 156-162.

Lang, J. S., Giron, J. J., Hansen, A. T., Trussell, R. R., & Hodges, W. E.,Jr. (1993). Investigating filter performance as a function of the ratio of filter size to media size. Journal of the American Water Works Association, 85(10), 122-130.

Lang, S. (2002). Biological amphiphiles (microbial biosurfactants). Current Opinion in Colloids and Interface Science, 7(1-2), 12-20.

Lawler, D. F. (1997). Particle size distributions in treatment processes: Theory and practice. Water Science and Technology, 36(4), 15-23.

Lawler, D. F., & Nason, J. A. (2006). Granular media filtration: Old process, new thoughts. Water Science and Technology, 53(7), 1-7.

Leoni, F., Mallon, M. E., Smith, H. V., Tait, A., & McLauchlin, J. (2007). Multilocus analysis of *Cryptosporidium* hominis and *Cryptosporidium* parvum isolates from sporadic and outbreak-related human cases and C-parvum isolates from sporadic livestock cases in the united kingdom. Journal of Clinical Microbiology, 45(10), 3286-3294.

Li, L. J., & Haas, C. N. (2004). Inactivation of *Cryptosporidium* parvum with ozone in treated drinking water. Journal of Water Supply Research and Technology-Aqua, 53(5), 287-297.

Li, Q., & Logan, B. E. (1999). Enhancing bacterial transport for bioaugmentation of aquifers using low ionic strength solutions and surfactants. Water Research, 33(4), 1090-1100.

Li, S. Y., Goodrich, J. A., Owens, J. H., Willeke, G. E., Schaefer, F. W., & Clark, R. M. (1997). Reliability of surrogates for determining *Cryptosporidium* Removal. Journal American Water Works Association, 89(5), 90-99.

Li, X. D., Brasseur, P., Agnamey, P., Ballet, J. J., & Clemenceau, C. (2004). Time and temperature effects on the viability and infectivity of *Cryptosporidium* parvum oocysts in chlorinated tap water. Archives of Environmental Health, 59(9), 462-466.

Litton, G. M., & Olson, T. M. (1993). Colloid deposition rates on silica bed media and artifacts related to collector surface preparation methods. Environmental Science & Technology, 27(1), 185-193.

Logsdon, G. S., Neden, D. G., Ferguson, A. M. D., & Labonde, S. D. (1993). Testing direct-filtration for the treatment of high-turbidity water. Journal American Water Works Association, 85(12), 39-46.

Loveland, J. P., Amy, G. L., & Ryan, J. N. (1994). Effect of chemical perturbations on virus attachment and detachment - relating kinetics to intersurface potential energies. Abstracts of Papers of the American Chemical Society, 207, 172-ENVR.

Lukasik, J., Cheng, Y. F., Lu, F. H., Tamplin, M., & Farrah, S. R. (1999). Removal of microorganisms from water by columns containing sand coated with ferric and aluminum hydroxides. Water Research, 33(3), 769-777.

Marshall, J. K., & Kitchener, J. A. (1966). The deposition of colloidal particles on smooth solids. Journal of Colloid and Interface Science, 22(4), 342-351.

Maurice Tchio, Boniface Koudjonou, Raymond Desjardins, Alain Gadbois, & Michele Prevost. (2003). Evaluation of the impact of design and operation parameters on direct filtration. Journal of Environmental Engineering and Science, 2(5), 343-353.

Maxit Group. (2008). www.filtralite.com

Mcdowell-Boyer, L. M., Hunt, J. R., & Sitar, N. (1986). Particle transport through porous media. Water Resources Research, 22(13), 1901.

McDowell-Boyer, L. (1992). Chemical mobilization of micron-sized particles in saturated porous media under steady flow conditions. Environmental Science & Technology, 26(3), 586-593.

Media Process and Technology Inc. (1995). Enhancement of macrolite for particle removal, phase II final report. Kinetico Inc.

Mehta, D., & Hawley, M. C. (1969). Wall effect in packed columns. Industrial & Engineering Chemistry Process Design and Development, 8(2), 280-&.

Melin, E. S., Bohne, R. A., Sjovold, F., & Odegaard, H. (2000). Treatment of ozonated water in biofilters containing different media. Water Science and Technology, 41(4-5), 57-60.

Montgomery, J. M. I. (1985). Water treatment principles and design. New York: Wiley-Interscience.

Montgomery, J. M., & Consulting Engineers Inc. (2005). Water treatment principles and design. New York: John Wiley and Sons, Inc.

Moran, D. C., Moran, M. C., Cushing, R. S., & Lawler, D. F. (1993). Particle behavior in deep-bed filtration .1. ripening and breakthrough. Journal American Water Works Association, 85(12), 69-81.

Morgan-Ryan, U. M., Fall, A., Ward, L. A., Hijjawi, N., Sulaiman, I., Fayer, R., et al. (2002). *Cryptosporidium* hominis n. sp (apicomplexa : Cryptosporidiidae) from homo sapiens. Journal of Eukaryotic Microbiology, 49(6), 433-440.

Moulton-Hancock, C., Rose, J. B., Vasconcelos, G. J., Harris, S. I., Klonicki, P. T., & Sturbaum, G. D. (2000). Giardia and *Cryptosporidium* occurrence in groundwater. Journal American Water Works Association, 92(9), 117-123.

Nanduri, J., Williams, S., Aji, T., & Flanigan, T. P. (1999). Characterization of an immunogenic glycocalyx on the surfaces of *Cryptosporidium* parvum oocysts and sporozoites. Infection and Immunity, 67(4), 2022-2024.

Nelson, K. E., & Ginn, T. R. (2005). Colloid filtration theory and the happel sphere-in-cell model revisited with direct numerical simulation of colloids. Langmuir, 21(6), 2173-2184.

Nieminski, E. C., Bellamy, W. D., & Moss, L. R. (2000). Using surrogates to improve plant performance. Journal American Water Works Association, 92(3), 67-+.

Nieminski, E. C., & Ongerth, J. E. (1995). Removing *giardia* and *Cryptosporidium* by conventional treatment and direct-filtration. Journal American Water Works Association, 87(9), 96-106.

Nime, F. A., Burek, J. D., Page, D. L., Holscher, M. A., & Yardley, J. H. (1976). Acute enterocolitis in a human being infected with protozoan *Cryptosporidium*. Gastroenterology, 70(4), 592-598.

Nordin, J. S., Tsuchiya, H. M., & Fredrick.Ag. (1967). Interfacial phenomena governing adhesion of chlorella to glass surfaces. Biotechnology and Bioengineering, 9(4), 545-&.

NSF International. (2001). Physical removal of *giardia* cysts and *Cryptosporidium* oocysts in drinking water, Kinetico Incorporated CPS100CPT Coagulation and Filtration System

NSF International. (2001). Removal of arsenic in drinking water, Kinetico Incorporated Macrolite Coagulation and Filtration System, model CPS100CPT No. NSF 01/23/EPADW395)NSF International.

O'Melia, C. R., & Hahn, M. W. (2003). Deposition and reentrainment of brownian particles in porous media under unfavorable chemical conditions. Abstracts of Papers of the American Chemical Society, 226, U479-U479.

OMelia, C. R., Hahn, M. W., & Chen, C. T. (1997). Some effects of particle size in separation processes involving colloids. Water Science and Technology, 36(4), 119-126.

Ongerth, J. E., & Pecoraro, J. P. (1995). Removing *Cryptosporidium* using multimedia filters. Journal American Water Works Association, 87(12), 83-89.

Ongerth, J. E., & Pecoraro, J. P. (1996). Electrophoretic mobility of *Cryptosporidium* oocysts and giardia cysts. Journal of Environmental Engineering-Asce, 122(3), 228-231.

Palmer, J., Flint, S., & Brooks, J. (2007). Bacterial cell attachment, the beginning of a biofilm. Journal of Industrial Microbiology & Biotechnology, 34(9), 577-588.

Philpotts, A. R. (1990). Principles of igneous and metamorphic petrology. Englewood Cliffs, NJ USA: Prentice Hall.

Raccurt, C. P., Brasseur, P., Verdier, R. I., Li, X. D., Eyma, E., Stockman, C. P., et al. (2006). Human cryptosporidiosis and *Cryptosporidium* spp. in Haiti. Tropical Medicine & International Health, 11(6), 929-934.

Rajagopalan, R., & Tien, C. (1976). Trajectory analysis of deep-bed filtration with sphere-in-cell porous-media model. AICHE Journal, 22(3), 523-533.

Rajagopalan, R., & Tien, C. (2005). Comment on "correlation equation for predicting single-collector efficiency in physicochemical filtration in saturated porous media". Environmental Science & Technology, 39(14), 5494-5495.

Redman, J. A., Walker, S. L., & Elimelech, M. (2004). Bacterial adhesion and transport in porous media: Role of the secondary energy minimum. Environmental Science & Technology, 38(6), 1777-1785.

Reynolds, D. T., Slade, R. B., Sykes, N. J., Jonas, A., & Fricker, C. R. (1999). Detection of *Cryptosporidium* oocysts in water: Techniques for generating precise recovery data. Journal of Applied Microbiology, 87(6), 804-813.

Rizwan, T., & Bhattacharjee, S. (2005). Initial deposition of colloidal particles on a rough nanofiltration (NF) membrane. Abstracts of Papers of the American Chemical Society, 229, U658-U658.

Robertson, D. C. Controlled cycled solids screening

Ruecker, N. J., Bounsombath, N., Wallis, P., Ong, C. S. L., Isaac-Renton, J. L., & Neumann, N. F. (2005). Molecular forensic profiling of *Cryptosporidium* species and genotypes in raw water. Applied and Environmental Microbiology, 71(12), 8991-8994.

Ruecker, N. J., Braithwaite, S. L., Topp, E., Edge, T., Lapen, D. R., Wilkes, G., et al. (2007). Tracking host sources of *Cryptosporidium* spp. in raw water for improved health risk assessment. Applied and Environmental Microbiology, 73(12), 3945-3957.

Ruecker, N. J., & Neumann, N. F. (2006). Re-assessing the public health risk associated with the waterborne transmission of *Cryptosporidium* spp. Reviews in Medical Microbiology, 17(1), 1-9.

Ryan, J. N., & Gschwend, P. M. (1992). Effect of iron diagenesis on the transport of colloidal clay in an unconfined sand aquifer. Geochimica Et Cosmochimica Acta, 56(4), 1507-1521.

Saiers, J. E., & Ryan, J. N. (2005). Colloid deposition on non-ideal porous media: The influences of collector shape and roughness on the single-collector efficiency. Geophysical Research Letters, 32(21), L21406.

Saltnes, T., Eikebrokk, B., & Odegaard, H. (2002). Coagulation optimisation for NOM removal by direct filtration in clay aggregate filters. Journal of Water Supply Research and Technology-Aqua, 51(2), 125-134.

Scholz, M., & Xu, J. (2002). Performance comparison of experimental constructed wetlands with different filter media and macrophytes treating industrial wastewater contaminated with lead and copper. Bioresource Technology, 83(2), 71-79.

Shellenberger, K., & Logan, B. E. (2002). Effect of molecular scale roughness of glass beads on colloidal and bacterial deposition. Environmental Science & Technology, 36(2), 184-189.

Shin, J. Y., & O'Melia, C. R. (2006). Pretreatment chemistry for dual media filtration: Model simulations and experimental studies. Water Science and Technology, 53(7), 167-175.

Simoes, M., Cleto, S., Pereira, M. O., & Viera, M. J. (2007). Influence of biofilm composition on the resistance to detachment. Water Science and Technology, 55(8-9), 473-480.

Simoes, M., Simoes, L. C., Machado, I., Pereira, M. O., & Vieira, M. J. (2006). Control of flow-generated biofilms with surfactants - evidence of resistance and recovery. Food and Bioproducts Processing, 84(C4), 338-345.

Smith, D. M. (2007). Cryptosporidiosis: Still a problem. Aids Reader, 17(8), 381-+.

Song, L., Johnson, P., & Elimelech, M. (1994). Kinetics of colloid deposition onto heterogeneously charged surfaces in porous media. Environmental Science & Technology, 28(6), 1164-1171.

Stevenson, D. G. (1997). Flow and filtration through granular media - the effect of grain and particle size dispersion. Water Research, 31(2), 310-322.

Sturdee, A., Foster, I., Bodley-Tickell, A. T., & Archer, A. (2007). Water quality and *Cryptosporidium* distribution in an upland water supply catchment, cumbria, UK. Hydrological Processes, 21(7), 873-885.

Sunnotel, O., Lowery, C. J., Moore, J. E., Dooley, J. S. G., Xiao, L., Millar, B. C., et al. (2006). *Cryptosporidium*. Letters in Applied Microbiology, 43(1), 7-16.

Swanton, S. W. (1995). Modeling colloid transport in groundwater - the prediction of colloid stability and retention behavior. Advances in Colloid and Interface Science, 54, 129-208.

Swertfeger, J., Metz, D. H., DeMarco, J., Braghetta, A., & Jacangelo, J. G. (1999). Effect of filter media on cyst and oocyst removal. Journal American Water Works Association, 91(9), 90-100.

Tabor, D. (1977). Surface forces and surface interactions. Journal of Colloid and Interface Science, 58(1), 2-13.

Talsania, S. K., Wang, Y., Rajagopalan, R., & Mohanty, K. K. (1997). Monte Carlo simulations for micellar encapsulation. Journal of Colloid and Interface Science, 190(1), 92-103.

Tamai, H., Nagai, Y., & Suzawa, T. (1983). Latex deposition on fibers. VI. deposition state and interaction energy. Journal of Colloid and Interface Science, 91(2), 464-471.

Tate, C. H., & Trussell, R. R. (1980). Recent developments in direct-filtration. Journal American Water Works Association, 72(3), 165-169.

Tchio, M., Koudjonou, B., Desjardins, R., Gadbois, A., & Prevost, M. (2003). Evaluation of the impact of design and operation parameters on direct filtration. Journal of Environmental Engineering and Science, 2(5), 343-353.

Tien, C. (1989). Granular filtration of aerosols and hydrosols. Boston: Butterworths.

Tobiason, J. E., & Vigneswaran, B. (1994). Evaluation of a modified-model for deep bed filtration. Water Research, 28(2), 335-342.

Tong, M., & Johnson, W. P. (2006). Excess colloid retention in porous media as a function of colloid size, fluid velocity, and grain angularity. Environmental Science & Technology, 40(24), 7725-7731.

Tong, M., & Johnson, W. P. (2007). Colloid population heterogeneity drives hyperexponential deviation from classic filtration theory. Environmental Science & Technology, 41(2), 493-499.

Torkzaban, S., Bradford, S. A., & Walker, S. L. (2007). Resolving the coupled effects of hydrodynamics and DLVO forces on colloid attachment in porous media. Langmuir, 23(19), 9652-9660.

Trussell, R. R., Trussell, A. R., Lang, J. S., & Tate, C. H. (1980). Recent developments in filtration system-design. Journal American Water Works Association, 72(12), 705-710.

Tufenkji, N. (2007). Modeling microbial transport in porous media: Traditional approaches and recent developments. Advances in Water Resources, 30(6-7), 1455-1469.

Tufenkji, N., & Elimelech, M. (2004). Correlation equation for predicting single-collector efficiency in physicochemical filtration in saturated porous media. Environmental Science & Technology, 38(2), 529-536.

Tufenkji, N., & Elimelech, M. (2004). Deviation from colloid filtration theory in the presence of repulsive electrostatic interactions: Implications to microbial transport. Abstracts of Papers of the American Chemical Society, 228, U605-U606.

Tufenkji, N., & Elimelech, M. (2004). Deviation from the classical colloid filtration theory in the presence of repulsive DLVO interactions. Langmuir, 20(25), 10818-10828.

Tufenkji, N., & Elimelech, M. (2005). Breakdown of colloid filtration theory: Role of the secondary energy minimum and surface charge heterogeneities. Langmuir, 21(3), 841-852.

Tufenkji, N., & Elimelech, M. (2005). Reply to comment on breakdown of colloid filtration theory: Role of the secondary energy minimum and surface charge heterogeneities. Langmuir, 21(23), 10896-10897.

Tufenkji, N., & Elimelech, M. (2005). Response to comment on "correlation equation for predicting single-collector efficiency in physicochemical filtration in saturated porous media". Environmental Science & Technology, 39(14), 5496-5497.

Tufenkji, N., & Elimelech, M. (2005). Spatial distributions of *Cryptosporidium* oocysts in porous media: Evidence for dual mode deposition. Environmental Science & Technology, 39(10), 3620-3629.

Tufenkji, N., Miller, G. F., Ryan, J. N., Harvey, R. W., & Elimelech, M. (2004). Transport of *Cryptosporidium* oocysts in porous media: Role of straining and physicochemical filtration. Environmental Science & Technology, 38(22), 5932-5938.

Tufenkji, N., Dixon, D., Considine, R., & Drummond, C. (2006). Multi-scale *Cryptosporidium*/sand interactions in water treatment. Water Research, 40(18), 3315-3331.

Turan, M., Sabah, E., Gulsen, H., & Celik, M. S. (2003). Influence of media characteristics on energy dissipation in filter backwashing. Environmental Science & Technology, 37(18), 4288-4292.

Tyzzer, E. E. (1908). A sporozoan found in the peptic glands of the common mouse. Proceedings of the Society for Experimental Biology and Medicine, 5, 12-13.

Valdes, J. R., & Liang, S. H. (2006). Stress-controlled filtration with compressible particles. Journal of Geotechnical and Geoenvironmental Engineering, 132(7), 861-868.

J. Van den Oever, 2006, personal communication.

Walker, Douglas and Cohen, Harvey, Geoscience Handbook: The AGI Data Sheets, 4th Edition. American Geological Institute, Alexandria, VA 2006.

Walker, S. L., Redman, J. A., & Elimelech, M. (2005). Influence of growth phase on bacterial deposition: Interaction mechanisms in packed-bed column and radial stagnation point flow systems. Environmental Science & Technology, 39(17), 6405-6411.

Warszynski, P., & Czarnecki, J. (1989). Transfer of particles over a randomly fluctuating energy barrier. Journal of Colloid and Interface Science, 128(1), 137-145.

Wilkinson, K. J., Negre, J., & Buffle, J. (1997). Coagulation of colloidal material in surface waters: The role of natural organic matter. Journal of Contaminant Hydrology, 26(1-4), 229-243.

Williams, G. J., Sheikh, B., Holden, R. B., Kouretas, T. J., & Nelson, K. L. (2007). The impact of increased loading rate on granular media, rapid depth filtration of wastewater. Water Research, 41(19), 4535-4545.

Xagoraraki, I., & Harrington, G. W. (2004). Zeta potential, dissolved organic carbon, and removal of *Cryptosporidium* oocysts by coagulation and sedimentation. Journal of Environmental Engineering-Asce, 130(12), 1424-1432.

Xagoraraki, I., Harrington, G. W., Assavasilavasukul, P., & Standridge, J. H. (2004). Removal of emerging waterborne pathogens and pathogen indicators by pilot-scale conventional treatment. Journal American Water Works Association, 96(5), 102-113.

Xiao, L. H., Fayer, R., Ryan, U., & Upton, S. J. (2007). Response to the newly proposed species *Cryptosporidium* pestis. Trends in Parasitology, 23(2), 41-42.

Xu, S. P., Gao, B., & Saiers, J. E. (2006). Straining of colloidal particles in saturated porous media. Water Resources Research, 42(12), W12S216.

Yao, K., Habibian, M. T., & O'Melia, C. R. (1971). Water and waste water filtration. concepts and applications. Environmental Science & Technology, 5(11), 1105-1112.

Young, P. L., & Komisar, S. J. (2005). Impacts of viability and purification on the specific gravity of *Cryptosporidium* oocysts. Water Research, 39(14), 3349-3359.

Youssef, N. H., Duncan, K. E., Nagle, D. P., Savage, K. N., Knapp, R. M., & McInerney, M. J. (2004). Comparison of methods to detect biosurfactant production by diverse microorganisms. Journal of Microbiological Methods, 56(3), 339-347.

Zembala, M. (2004). Electrokinetics of heterogeneous interfaces. Advances in Colloid and Interface Science, 112(1-3), 59-92.